APPENDIX G

Oil Spill Modelling (RPS 2017)

This page has been intentionally left blank for double-sided printing

Trajectory Modelling in Support of the Nexen Energy ULC Flemish Pass Exploration Drilling Project (2018-2028)

Prepared for: Nexen Energy ULC

Project Number:
2017-657

Date Submitted:
1/26/2018

Version:
Final Report

Project Manager
Matthew Horn, Ph.D.

RPS
55 Village Square Dr.
South Kingstown, RI USA
02879-8248

Release	File Name	Date Submitted	Notes
Draft	Nexen – RPS Technical Report_20180126.docx	1/26/2018	RPS final version of report following review by Wood plc and Nexen Energy ULC
Draft	Nexen – RPS Technical Report_20171222.docx	12/22/2017	RPS Draft version of final report following senior technical review
Draft	Nexen – RPS Technical Report_20171220.docx	12/20/2017	RPS Draft version of report for internal senior technical review

List of Contributors

Matthew Horn, PhD – Project Lead and Senior Scientist

matt.horn@rpsgroup.com

Emily Skeehan – Project coordination and report preparation

Lisa McStay – Oil spill modeller and report preparation

Matthew Frediani – Oil Spill modeller and report preparation

Steven Tadros – Oil Spill modeller and report preparation

Jenna Ducharme – GIS Specialist, figure generation

Jeremy Fontenault –Senior GIS Specialist, report preparation

Deborah Crowley – Modeller

Tayebeh Bakhsh – Hydrodynamics

Deborah French McCay – Report review

Cheryl Morse – Programmer / Developer

Timothy Giguere – Programmer/Developer

Executive Summary

Oil spill trajectory and fate modelling were performed to support an Environmental Impact Statement for the Nexen Energy ULC's Flemish Pass Exploration Drilling Project (2018-2028). The Project Area includes the Exploration Licenses EL 1144 and EL 1150, with the western edge approximately 400 km offshore, buffered by 20 km on all sides to accommodate the location and extent of ancillary activities that may be carried out in support of such drilling activities. The Project Area includes portions of the Flemish Cap and Flemish Pass. Stochastic modelling was performed at representative sites that were located approximately 420-460 km east of the Newfoundland Coast, where exploratory drilling is anticipated in waters that range in depth from 330 m to 1,200 m.

Hypothetical releases were modelled as continuous unmitigated subsurface blowouts with scenarios of Bay du Nord crude oil (BdN) at two representative example well site locations within the Exploration Licenses: EL 1144 and EL 1150. In addition, a third site was modelled to include a supply vessel collision and complete loss of marine diesel at a location approximately halfway between St. John's, Newfoundland and the Project Area. The water depths for the two example well sites are approximately 1,137 m for EL 1144 and 378 m for EL 1150, which are representative examples of the range of expected water depths where exploration may take place. In addition, the EL 1144 release location was an example a deeper Jurassic well, while EL 1150 was an example of a shallower Cretaceous well. The Jurrasic and Cretaceous reservoirs have different properties. Modelled release rates and associated total volumes discharged varied by location. Unmitigated 30-day subsurface blowouts of BdN were simulated for 60 days at EL 1144 and EL 1150 example wells. The larger release was modelled at the EL 1144 example well site with a blowout rate of 184,000 bpd, totaling 5,520,000 bbl over the 30-day release duration. A smaller release was modelled at the EL 1150 example well site with a blowout rate of 44,291 bpd totaling 1,329,000 bbl for the 30-day release. These scenarios represent the range of water depths, release rates, and the potential time that is expected to be required to contain a release through the use of a "Capping Stack" and/or other containment equipment. In addition, "batch spills" were modelled as instantaneous unmitigated surface releases of 100 and 1,000 L of marine diesel at the EL 1144 example well sitefor 30 days. The example well site at EL 1144 was selected as the hypothetical release location was closer to shore than the EL 1150 example well site. Finally, a large volume release of marine diesel (750,000 L) was simulated for 30 days at the vessel collision location (VCL) between St. John's and the Project Area to represent a vessel collision and complete loss of cargo and fuel from a supply vessel.

In order to reproduce the dynamic and complex processes associated with deep subsea blowout releases, two models were used. The near-field model OILMAPDeep was used to characterize the dynamics of the jet and buoyant-plume phases of a subsurface blowout. It contains two sub-models, a

plume model and a droplet size model. The plume model predicts the evolution of plume position, geometry, centerline velocity, and oil and gas concentrations until the plume either surfaces or reaches a terminal height, at which point the plume is trapped. The droplet size model was used to characterize the size and distribution of oil droplets, including the associated mass of oil being released at specific water depths, where the plume became neutrally buoyant. The output data from OILMAPDeep was then used to initialize the SIMAP model, which simulated the far-field trajectory, fate, and potential exposure in the marine environment following a release.

Geographical data including habitat mapping and shoreline identification and classification were obtained from multiple data sources. For Canadian areas, data from the New Brunswick , Nova Scotia, and Newfoundland Departments of Natural Resources and Environment and Climate Change Canada were used. For the U.S. shoreline, the U.S. National Oceanic and Atmospheric Administration's Environmental Sensitivity Index and Maine Department of Environmental Protection's Environmental Vulnerability Index were used. Bathymetry was characterized using databases provided by NOAA National Geophysical Data Center and GEBCO.

Currents for the North Atlantic region were acquired from the U.S. Navy Global HYCOM (HYbrid Coordinate Ocean Model) circulation model. Wind data for this study were obtained from the U.S. National Centers for Environmental Prediction Climate Forecast System Reanalysis (CFSR) model. All data was acquired, processed, and used for the period between 2006 and 2010.

A stochastic analysis was conducted for each release location, consisting of 119 individual model runs per scenario. Each run was initialized with a different start date/time between 2006-2010 to sample a range of environmental conditions. The dates and times were selected randomly from within 14 day intervals spanning the entire five years of data. Results of the stochastic analysis included probability footprints above specified thresholds and minimum time to oil exposure. Because the runs spanned five full years and included all of the associated seasonal variability, the complete set was referred to as annual summaries. To investigate seasonality, individual runs within the stochastic analysis were classified as either summer or winter, depending on whether the majority of the days within the modelled 60-day period had the presence (winter) or absence (summer) of ice cover.

Representative deterministic scenarios (i.e., single trajectory) were identified from each set of stochastic subsurface blowout results. Individual scenarios were selected based upon the size of the surface oil footprint, the mass of oil on shorelines, and the concentration of dissolved hydrocarbons in the water column, based upon a set of highly conservative socio-economic thresholds:

- Surface oil average thickness >0.04 µm
- Shore oil average concentration >1.0 g/m^2
- Subsurface (within the water column) dissolved hydrocarbon concentrations >1.0 µg/L

The selected scenarios included the 95th and 99th percentile runs for surface oil footprint, shoreline oil length, and water column contamination were identified for both release locations when appropriate. Because there was no oil predicted on the shoreline in the 95th percentile case, the 99th percentile scenario for shoreline oil mass was used in the investigation. In addition to these five deterministic scenarios, three surface releases of marine diesel were modelled, including two release volumes (100 L and 1,000L) at the EL 1144 example well site and a full volume release of a supply vessel fuel tank (750,000 L) between St. John's and the Project Area.

It is important to note that although large footprints of oil contamination are depicted for stochastic analyses, they are not the expected distribution of oil from any single release. These maps do not provide any information on the quantity of oil in a given area. They simply denote the probability of oil exceeding the given threshold passing through each grid cell location in the model domain over the entire model duration (60 days), based on the entire ensemble of runs (119 individual releases for all runs). Only probabilities of 1% or greater were included in the map output, as lesser probabilities represent random noise in each set of 119 trajectories. Stochastic maps of water column contamination of dissolved hydrocarbons depict the likelihood that concentration will exceed the identified threshold at any depth within the water column, but do not specify the depth at which this occurs and do not imply that the entire water column (i.e., from surface to bottom) will experience a concentration above the threshold.

Stochastic results are useful in planning for oil spill response, as they characterize the probability that regions may experience contamination above specified thresholds, taking into account the environmental variability that is expected from many potentially-different release scenarios over time. Stochastic footprints for potential surface oil exceeding a thickness of 0.04 µm were between 1,783,000 - 1,942,000 km^2 for the annual 30-day release results. These footprints depict areas with the highest predicted likelihood of potential oil contamination to the east of the release sites, with a much lower probability (1-10% and 10-25%) for oil to be transported to the west towards Canadian waters. While these areas are quite large, most of this footprint represents a relatively low probability (<10%) of surface oil thickness >0.04 µm. Footprints depicting higher probability contours (90%) yield only a fraction of the total footprint, ranging from 16,750 – 56,100 km^2 for the annual 30-day release results, depending on the scenario.

Seasonal variations were evaluated yielding different predicted surface oil results for summer versus winter scenarios. For the releases at the EL 1144 and EL 1150 example well sites, larger surface oil footprints associated with >90% probability contours were predicted for summer scenarios at both sites indicating more coherency in the release.

The highest predicted potential (<3%) for oil to make contact with shorelines exceeding 1 g/m^2 occurred only in the winter scenarios from the EL 1144 example well releases, with oil reaching Sable Island. Modelled oil from these subsurface releases had a higher potential to be transport to the west and southwest prior to surfacing, where surface currents and winds typically carried releases further offshore. No oil contact with shorelines was predicted in summer scenarios. For the releases at the EL 1150 example well site, oil was not predicted to reach the shore within 60 days from any scenario. The oil that was predicted to make it to shorelines was expected to be highly weathered, patchy, and discontinuous, as minimum time estimates for first shoreline oil exposure ranged from approximately 52-53 days from the EL 1144 example well site.

Individual trajectories of interest were identified and selected from the stochastic ensemble of results for deterministic analysis. The identified simulations represented the 95th percentile for exposure area to surface oil and mass of oil in the water column, and the 99th percentile length of shoreline contacted. For most representative deterministic scenarios, the amount of oil on sediments at the end of the 60-day simulation was less than one percent. Entrainment into the water column ranged between 20% and 27% after 60 days. There was very little surface oil (<6%) and shoreline oil (<0.01%) predicted at the end of each representative 60-day simulation. Shoreline contact was minimal for these modelled simulations, where even the 99th percentile shoreline contact case was predicted to have less than 0.01% of the total volume of released oil reaching shore.

The amount of evaporation and degradation was relatively consistent between model runs. Approximately 35-42% of the releases were predicted to evaporate and another 32-38% to degrade by the end of the 60-day simulation. Most of the variability in the mass balances was associated with the amount of oil found either on the surface or entrained within the water column.

Accidental discharges from small volume (100 and 1,000 L) instantaneous “batch spills” of marine diesel were predicted to result in little contamination with patchy and discontinuous colorless and silver sheens <0.0001 mm (0.1 µm) predicted over limited distances. The cumulative area of average surface oil thickness >0.04 µm was <1 km^2 for the 100 L release and approximately 8 km^2 for the 1,000 L release. Total hydrocarbon concentrations were not predicted to exceed 1 µg/L for the 100 L release and the vertical maximum THC concentrations for the 1,000 L release were only predicted to reached 2 µg/L within about 5 km of the release site. By the end of the 30-day release simulations, 63-76% of the released diesel was predicted to evaporate, while 8-11% was predicted to remain entrained in the water

column and 16-26% degrade. A small portion of highly weathered diesel may continue to be transported at levels comparable to a colorless or silver sheen at the surface or in the water column for some distance. None of the "batch spills" were predicted to reach any shoreline.

The 750,000 L vessel collision was predicted to result in more extensive surface oil, when compared to the modelled "batch spills." The release would be predicted to result in patchy and discontinuous surface sheens, although the large release volume would likely result in a rainbow sheen for approximately 40 km before transitioning to the colorless and silver sheen that was predicted for the "batch spills." Unlike the "batch spills," ecological thresholds were predicted to be exceeded for surface oil and socioeconomic thresholds were predicted to be exceeded for water column contamination. The predicted exposure area for surface oil from the vessel collision was 925 km^2 for the lower 0.04 µm socioeconomic threshold and 13 km^2 for the higher 10 µm ecological threshold.

The hypothetical releases modelled in this study are not intended to predict a specific future event, but rather to be used as a tool in environmental assessments, contingency planning for oil spill response, and well containment planning. These studies are not intended to predict a similar event. The results presented in this document demonstrate that there are a range of potential trajectories and fates that could result if a release of crude oil or a batch spill of marine diesel were to occur, and those trajectories and fates vary based upon the environmental conditions occurring at the time. While each oil release is unique and therefore uncertainties exist, the results of this modelling study suggest that if oil were to be released in the Project Area, it has the highest likelihood of moving away from shore to the east.

Document Summary

This report includes an introduction describing the region, the modelling approach, the methodology, and finally the results of the study. The model results are summarized in figures and tables in the main body of this document, describing the potential for oil contamination within the water column, on the water surface, and along shorelines. This document is broken down into several sections. Section 1 includes an introduction to the modelling study. Section 2 includes a description of project area, modelling approach with the OILMAPDeep and SIMAP models, scenarios, and uncertainty. Section 3 contains a description of the model input data. Section 4 summarizes the stochastic and deterministic oil trajectory and fate model results. Section 5 summarizes conclusions and discussion points. Section 6 contains the references cited. Appendix A has been provided to include details on the OILMAPDeep and SIMAP model background, theory, inputs, algorithms, and outputs. Appendix B has been provided to include higher resolution results figures to those found in this Technical Report. Each figure is provided as a full page with no modifications or additions.

Table of Contents

List of Figures

List of Tables

List of Acronyms and Abbreviations

3D: Three dimensional, referring to the vertical and horizontal, as in x, y, and z directions

AL: Aliphatic portion of the total hydrocarbon, which is modelled as a volatile but insoluble fraction within the SIMAP model and can therefore evaporate.

AR: Aromatic portion of the total hydrocarbon, which is modelled as a volatile and soluble fraction within the SIMAP model and can therefore evaporate and dissolve.

BAOAC: Bonn Agreement Oil Appearance Code

BdN: Bay du Nord crude oil

BTEX: Benzene, toluene, ethylbenzene, and xylene

CERCLA: The U.S. Superfund or Comprehensive Environmental Response, Compensation, and Liability Act of 1980

EIS: Environmental Impact Statements

GEBCO: The General Bathymetric Chart of the Oceans operated by the International Hydrographic Organization (IHO) and Intergovernmental Oceanographic Commission (IOC) of UNESCO.

HYCOM: The U.S. Navy HYbrid Coordinate Ocean Model used for currents

MAH: Monocyclic aromatic hydrocarbons (monoaromatic), with only one six carbon ring

MICOM: Miami Isopycnic-Coordinate Ocean Model

NCODA: U.S. Navy Coupled Ocean Data Assimilation

NOAA: U.S. National Oceanic and Atmospheric Administration

NRC: U.S. National Research Council

NRDA: The U.S. Natural Resource Damage Assessment

NRDAM/CME: Natural Resource Damage Assessment Model for Coastal and Marine Environments

PAH: Polycyclic aromatic hydrocarbons (polyaromatic), with two or more six carbon rings

PPB: Part per billion, as referring to concentration. Roughly equivalent to µg/L.

PPM: Part per million, as referring to concentration

SIMAP: Release Impact Model Application Package, a 3D trajectory and fate model developed by RPS

THC: Total hydrocarbon concentrations

UNESCO: United Nations Educational, Scientific, and Cultural Organization

WOA: World Ocean Atlas, a database from NODC NOAA containing observational data of physical and chemical parameters of seawater from many thousands of cruises.

1 Introduction

RPS (previously Applied Science Associates, Inc.) conducted trajectory and fate modelling in support of an Environmental Impact Statement (EIS) for the Nexen Energy ULC Flemish Pass Exploration Drilling Project (2018-2028) (the Project) proposed in the region of the Flemish Pass offshore Newfoundland. The Project Area includes the Exploration Licenses EL 1144 and EL 1150, with the western edge approximately 400 km offshore, buffered by 20 km on all sides to accommodate the location and extent of ancillary activities that may be carried out in support of such drilling activities. The Project Area includes portions of the Flemish Cap and Flemish Pass. Stochastic modelling was performed at representative sites that were located approximately 420-460 km east of the Newfoundland Coast, where exploratory drilling is anticipated in waters that range in depth from 330 m to 1,200 m. Major currents, including the Labrador Current and the Gulf Stream, influence the circulation and biological productivity in this region.

This modelling was conducted to evaluate hypothetical unmitigated release events associated with exploration drilling, including large scale deep-water blowouts of crude oil (Bay du Nord) from the wellhead at the seafloor, smaller scale "batch spills," and a larger scale vessel collision incident releasing marine diesel at the surface. Three-dimensional (3D) oil spill trajectory and fate modelling and analyses were performed to support evaluation of the potential movement and behavior of oil following hypothetical releases within the Project Area and their potential to affect regions of the northwest Atlantic Ocean offshore Newfoundland. RPS's nearfield OILMAPDeep blowout model and the far-field Spill Impact Model Application Package (SIMAP) oil trajectory and fate models were used. This report provides a description of the Project Area and modelled scenarios, an overview of the modelling approach, details about the model input data used, and a presentation and discussion of the modelled results.

2 Background and Scenarios

2.1 Project Area

Newfoundland is comprised of a series of islands off the east coast of Canada, and along with Labrador forms the easternmost Canadian province. The relatively shallow waters of the continental shelf extend eastward into the northwest Atlantic Ocean up to 500 km off the Newfoundland coast. The Nexen Energy ULC Project Area (57 – 42°N, 70.6 – 27.5°W) contains the Flemish Cap and Flemish Pass (Figure 2-1). This area is known to contain substantial petroleum resources. The Hibernia, White Rose, and Terra Nova oil fields sit atop this biologically productive region. Bathymetry in the area ranges from less than

100 m over the Grand Bank to greater than 4,000 m deep in the Labrador Basin. The model domain extends as far west as 72° W and east to 28°W, encompassing Canadian, U.S., and International waters. This modelled extent is much larger than the Project Area, as hypothetical releases of oil will be tracked for extended periods of time (60 days).

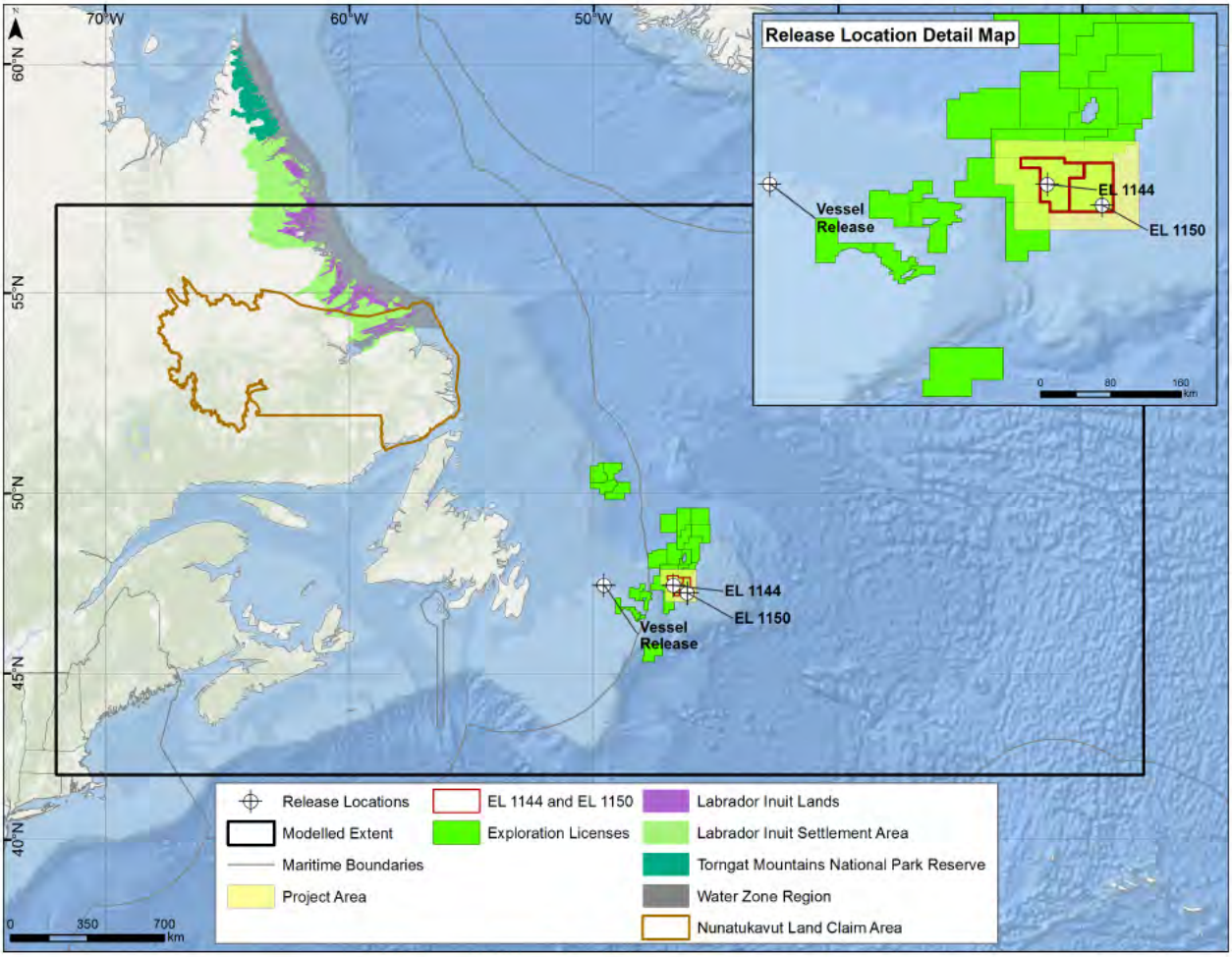

Figure 2-1. Project Area, including the two hypothetical release locations for the subsurface blowouts (EL 1144 and EL 1150 example well sites) and the hypothetical vessel release location. The black bounding box represents the modelling extent, while the smaller shaded boxes represent the Project Areas. The corresponding water depths (bathymetry) are depicted in shades of blue, whereby lighter shades represent shallow waters and darker shades represent deeper waters.

2.2 Modelling Approach

This modelling study employed a combined stochastic and deterministic approach to determine the potential trajectory and fate of hypothetical hydrocarbon releases from three sites east of Newfoundland including example well sites at the two Exploration Licenses (EL 1144 and EL 1150), and the Vessel Collision Location (VCL) between St. John's and the Project Area (Table 2-1). Stochastic modelling provides a probabilistic view of the likelihood that a given region might be exposed to released hydrocarbons over specified thresholds given the range of possible environmental conditions that may occur within and across multiple years. A deterministic analysis provides a view of the time history of the specific movement and behavior of released product from a given (e.g., representative) individual release. Together, these methods provide a more complete view of both the likelihood and degree of potential exposure.

For this report, stochastic information is presented for predicted surface oil thickness, shoreline oil mass, and subsurface contamination for the full year (i.e., annual), and for different seasons with variable ice-cover conditions (i.e., summer/ice-free and winter/ice-covered). Individual representative deterministic trajectories that characterize single release scenarios are also presented. Stochastic analyses of hypothetical blowouts were modelled at two sites using the physical-chemical properties of the specific oil type that may be released and 5 years of variable environmental data, which are discussed in Section 3. At each location, a total of 119 individual oil spill trajectories were modelled throughout the year (59 winter and 60 summer). The duration of each modelled blowout simulation was 60 days to represent the anticipated time required to contain a release through the use of a "Capping Stack" and/or other containment equipment. In addition, surface "batch spills" of marine diesel were analyzed to evaluate potential discharges between surface vessels (100 or 1000 L) as well as a larger (750,000 L) release representing a supply vessel collision and complete loss of containment (fuel and cargo).

Table 2-1. Site and release information used for the stochastic and deterministic approaches.

Spill Location	Depth of Release	Release Duration	Model Duration	Number of Model Runs	Released Product	Release Type	Release Volume
EL 1144 Example Well	1,137 m	30 days	60 days	119	BdN	Subsurface Blowout	877,610 m^3 (5,520,000 bbl)
EL 1150 Example Well	378 m						211,294 m^3 (1,329,000 bbl)
EL 1144 Example Well	Surface	Instantaneous	30 days	2	Marine Diesel	Batch Spills	100 L & 1,000 L (0.63 bbl & 6.3 bbl)
VCL				1		Vessel Collision	750,000 L (4,717 bbl)

The Vessel Collision Location (VCL) represents the midpoint between St. John's, Newfoundland and the Project Area

2.2.1 Modelling Tools

Hypothetical release scenarios were simulated using the OILMAPDeep blowout model and the SIMAP, oil trajectory and fate model, both developed by RPS. OILMAPDeep was used to define the near-field dynamics of the subsurface blowout plume, which was then used to initialize the far-field modelling conducted in SIMAP. The dynamics of the near-field plume dynamics are modelled to predict the mass, location, and droplet size distribution of the subsurface plume of oil at the termination (i.e., trap) height of the buoyant oil and gas plume, when it becomes diluted enough with surrounding seawater to become neutrally buoyant, based upon the environmental conditions, the specific chemical and physical properties of the oil, and other release parameters. Typically, the near-field model is on the timescale of seconds and length scale of hundreds of meters, whereas the far-field model is on the scale of many hours/days and tens or even hundreds of kilometers.

OILMAPDeep Model

The OILMAPDeep model incorporates the basic dynamics of a subsurface oil and gas plume and the associated complexities of increased hydrostatic pressure at depths deeper than 200 m. It contains two sub-models, i.e., a plume model and a droplet size model. The plume model predicts the evolution of plume position, geometry, centerline velocity, and oil and gas concentrations until the plume either surfaces or reaches a terminal height (i.e., trap height), at which point the plume no longer rises by buoyant forces and the oil contained within the plume escapes to the surrounding water and rises based on the individual buoyancies of the droplets. The jet created by the blowout is modelled by considering

the momentum of the oil discharge, the density difference between the expanding gas bubbles in the plume and the receiving water, the entrainment of water into the plume, the mixing by turbulence within the plume, hydrate formation, and transport by local ambient currents. The droplet size model predicts the size and volume (mass) distribution of the oil droplets in the release at the trap height or at the water surface, which influences trajectory and fates processes such as oil rise velocity and dissolution.

For oil discharged during a deep-water blowout, the oil droplet size distribution has a profound effect on how oil is transported and behaves after the initial release as a buoyant plume. The size of the individual droplets dictates buoyancy, which controls the length of time that oil will remain within the water column before surfacing. Large oil droplets surface faster than small ones, thus large droplets more quickly generate a floating oil slick, which may be transported by winds and surface currents. Small droplets remain in the water column longer than large droplets and are subjected to subsurface advection-diffusion processes and are therefore transported for a longer period of time. As oil is transported by subsurface currents away from the release location, natural dispersion of the oil droplets quickly reduces concentrations within the water column. However, the lower rise velocities associated with smaller oil droplets correspond to longer residence times of oil suspended in the water column, which can increase the dissolution of soluble components and potentially result in larger volumes of water being affected. Details of the OILMAPDeep model background, theory, inputs, algorithms, and outputs can be found in Appendix A.

SIMAP Model

The SIMAP model originated from the oil fate sub-model within the Natural Resource Damage Assessment Models for Coastal and Marine Environments (NRDAM/CME). RPS developed the NRDAM/CME in the early 1990s for the U.S. Department of the Interior for use in "type A" Natural Resource Damage Assessment (NRDA) regulations under the Comprehensive Environmental Response, Compensation and Liability Act of 1980 (CERCLA). The most recent version of the type A models, the NRDAM/CME (Version 2.4, April 1996) was published as part of the CERCLA type A NRDA Final Rule (Federal Register, May 7, 1996, Vol. 61, No. 89, p. 20559-20614). The technical documentation for the NRDAM/CME is in French et al. (1996). While the NRDAM/CME was developed for simplified NRDAs of small releases in the U.S., SIMAP was further developed to evaluate fate and exposure of both real and hypothetical releases in marine, estuarine, and freshwater environments worldwide. Additions and modifications to SIMAP include increasing model resolution, allowing site-specific input data, incorporating spatially and temporally varying current data, evaluating subsurface releases and

movements of subsurface oil, tracking multiple chemical components of the oil, enabling stochastic modelling, and facilitating analysis of results.

The 3D physical fates model estimates the distribution of whole oil and oil components on the water surface, on shorelines, in the water column, and in sediments as both mass and concentration. Because oil contains many chemicals with varying physical and chemical properties, and the environment is spatially and temporally variable, the oil rapidly separates into different environmental compartments through multiple fates processes. Oil fate processes included in SIMAP are oil spreading (gravitational and by shearing), evaporation, transport, randomized dispersion, emulsification, entrainment (natural and facilitated by dispersant), dissolution of the soluble fraction of oil into the water column, volatilization of dissolved hydrocarbons from the surface water, adherence of oil droplets to suspended sediments, adsorption of soluble and sparingly-soluble aromatics to suspended sediments, sedimentation, and degradation. Oil trajectory and weathering endpoints include surface oil, emulsified oil (mousse), tar balls, suspended oil droplets, oil adhered to particulate matter, dissolved hydrocarbon compounds in the water column and pore water, and oil on and in bottom sediments and shoreline surfaces. Additional details of the SIMAP model background, theory, inputs, algorithms, and outputs of SIMAP may be found in Appendix A.

2.2.2 Stochastic Approach

A stochastic approach was employed to determine the footprint and probability of areas that are at increased risk of oil exposure based upon the variability of meteorological and hydrodynamic conditions that might prevail during and after a release. A stochastic approach is a statistical analysis of results generated from many different individual trajectories of the same release scenario, with each trajectory starting at a randomized time from a relatively long-term window. For this project, individual trajectory start dates were selected randomly every 14 days throughout the window of environmental data coverage to ensure that the data was adequately sampled. This stochastic approach allows for the same type of release to be analyzed under varying environmental conditions (e.g., summer vs. winter or one year to the next). The results provide the probable behavior of the potential releases.

In order to reproduce the natural variability of winds and currents, the model requires both spatially- and temporally-varying datasets. Historical observations and models of multiple-year wind and current records were used to perform the simulations within the coinciding time period. These datasets allow for reproduction of the natural variability of the wind and current speeds and directions. Optimally, the minimum time window for stochastic analysis is at least five years so that various weather patterns from year to year are represented. Using wind and current data from throughout this long time period, a sufficient number of model runs will adequately sample the variability in the time sequences of wind

and current speeds and directions in the region of interest, and will result in a prediction of the probable oil pathways for a release at the prescribed location.

Stochastic analyses provide two types of information: 1) the areas associated with probability of oil exposure at some time during or after a release, and 2) the shortest time required for oil to reach any point within the areas predicted to be exposed above a specified threshold. The left panel of Figure 2-2 depicts four individual trajectories predicted by SIMAP for a generic example scenario. Because these trajectories were started on different dates and times, they experienced varying environmental conditions, and thus traveled in different directions. To compute the stochastic results, tens to hundreds of individual trajectories like the four depicted here were overlain and the number of times that each given location throughout the modelled domain was intersected by the different trajectories was used to calculate the probability of oil exposure for each specific location. This process is illustrated by the stacked runs in the right panel of Figure 2-2. The predicted footprint is the cumulative oil-exposed area for all of the ten to hundreds of individual releases combined. The color-coding represents a statistical analysis of all the individual trajectories to predict the probability of oil at each point in space, based upon the environmental variability. The footprint of any single release of oil, be it modelled or real, would be much smaller than the cumulative footprint of all the runs used in the stochastic analysis. Similarly, the footprint of oil from any individual release at a single time step (snapshot in time) would be even smaller than the cumulative swept area depicted here.

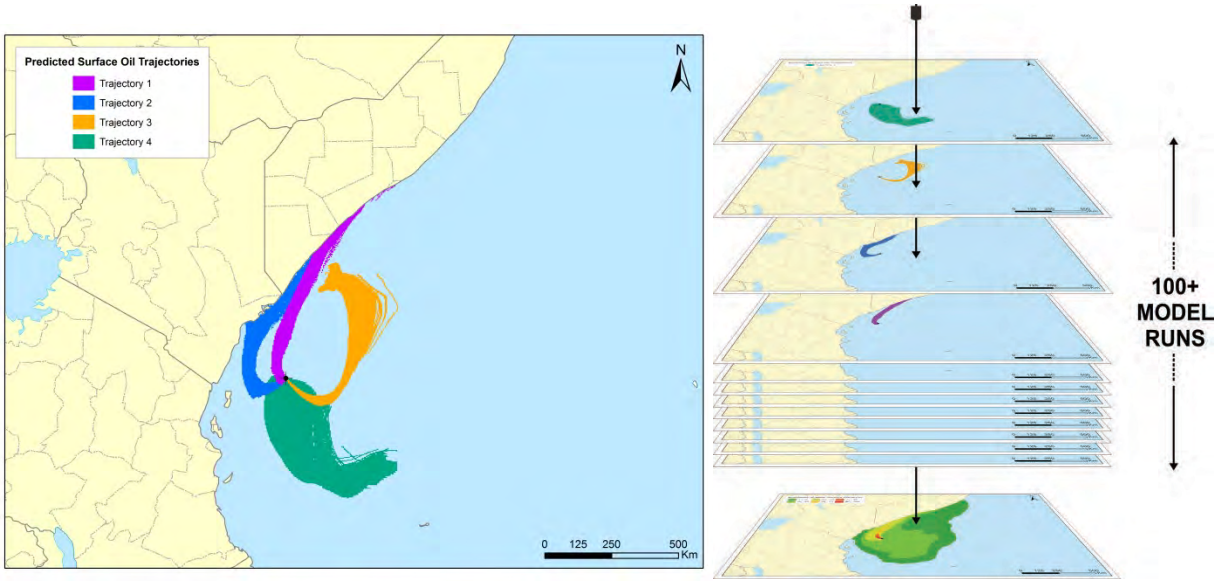

Figure 2-2. Examples of four individual release trajectories predicted by SIMAP for a generic release scenario simulated with different start dates and therefore environmental conditions. Tens to hundreds of individual trajectories are overlain (shown as the stacked runs on the right) and the frequency of contact with given locations is used to calculate the probability of threshold exceedance during a release.

The number of individual trajectories and the timeframe of a given stochastic analysis play roles in the spatial extent of the resulting stochastic footprints. More individual runs may incorporate greater environmental variability, which may result in larger footprints. As the number of trajectories modelled increases, the confidence and resolution of reported probabilities also increases. Annual footprints result in the largest footprint, encompassing all environmental variability throughout the years. Seasonal footprints may be smaller, encompassing only the environmental variability expected within the smaller time period (e.g., prevailing winds, seasonal patterns, etc.). It is important to note that a single trajectory encounters only a small portion of an overall stochastic probability footprint (e.g., an individual trajectory may be less than 10% of an annual stochastic footprint). Maps of probability and minimum time to oil exceeding identified thresholds are provided in Section 4.1.

2.2.3 Thresholds of Interest

In a stochastic analysis, multiple model runs (10's to 100's of releases) are overlaid upon one another to create a cumulative footprint of the potential trajectories. When combined with one another, the many individual deterministic footprints can be used to generate an area of probability that describes the potential areas that may be exposed to oil contamination from the entire suite of modelled conditions. To determine the probability or likelihood of potential exposure, specific thresholds for surface oil thickness, oil on shorelines and sediments, and in-water contamination were required (Table 2-2). Above these thresholds, previous studies have identified that there is the potential that negative effects may occur. Figures and further analyses in this study include the more conservative lower socioeconomic thresholds of concern calculated from stochastic results.

Floating surface oil is expressed as mass per unit area, averaged over a defined (grid cell) area. If the oil is evenly distributed in that area, it would be equivalent to a mean thickness, where 1 micron (µm) of thickness corresponds to a layer of oil that has a mass concentration of approximately 1 g/m^2. Surface oil thickness is typically associated with visual appearance by aerial observation for responders (NRC 1985; Bonn Agreement 2009, 2011; NOAA, 2016; Table 2-3). As an example, barely visible sheens may be observed above 0.04 µm and silver sheens correspond with surface oil thickness of approximately 0.3 µm. Crude and heavy fuel oils greater than 1 mm thick typically appear as black oil while light fuels and diesels that are greater than 1 mm thick may appear brown or reddish. Because of the differences between oils and their degree of weathering, floating oil will not always have the same appearance. As oil weathers, it may be observed in the form of scattered floating tar balls and tar mats where currents converge. Typically, oil slicks in the environment would be observed as a range of visual appearances including silver sheen, rainbow sheen, and metallic areas simultaneously, as a combination of thicknesses may be present (Figure 2-3). Thus, a model result presented as average oil mass per unit

area or "thickness" is actually a region with patches of oil of varying thickness, which when distributed evenly in the area of interest, would be on average a certain thickness.

Table 2-2. Thresholds used to define areas and volumes exposed above levels of concern.

Threshold Type	Cutoff Threshold	Rationale/Comments (Socio-economic, Response, Ecological)	Visual Appearance	References
Oil Floating on Water Surface	0.04 µm (equivalent to 0.04 g/m²)	**Socio-economic:** A conservative threshold used in several risk assessments to determine effects on socioeconomic resources (e.g., fishing may be prohibited when sheens are visible on the sea surface). Socio-economic resources and uses that could be affected by floating oil include commercial, recreational and subsistence fishing; aquaculture; recreational boating, port concerns such as shipping, recreation, transportation, and military uses; energy production (e.g., power plant intakes, wind farms, offshore oil and gas); water supply intakes; and aesthetics.	Fresh oil at this minimum thickness corresponds to a slick being barely visible or scattered sheen (colorless or silvery/grey), scattered tarballs, or widely scattered patches of thicker oil.	French McCay et al., 2011; French McCay et al., 2012; French McCay, 2016; Lewis, 2007, Bonn Agreement
	10 g/m² (equivalent to 10 g/m²)	**Ecological:** Mortality of birds on water has been observed at and above this threshold. Sublethal effects on marine mammals, sea turtles, and floating Sargassum communities are of concern.	Fresh oil at this thickness corresponds to a slick being a dark brown or metallic sheen.	French et al., 1996; French McCay, 2009 (based on review of Engelhardt, 1983, Clark, 1984, Geraci and St. Aubin 1988, and Jenssen 1994 on oil effects on aquatic birds and marine mammals); French McCay et al., 2011; French McCay et al., 2012; French McCay, 2016
Shoreline Oil	1.0 g/m²	**Socio-economic/Response:** A conservative threshold used in several risk assessments. This is a threshold for potential effects on socio-economic resource uses, as this amount of oil may trigger the need for shoreline cleanup on amenity beaches, and affect shoreline recreation and tourism. Socio-economic resources and uses that could be affected by shoreline oil include recreational beach and shore use, wildlife viewing, nearshore recreational boating, tribal lands and subsistence uses, public parks and protected areas, tourism, coastal dependent businesses, and aesthetics.	May appear as a coat, patches or scattered tar balls, stain	French-McCay et al., 2011; French McCay et al., 2012; French McCay, 2016
	100 g/m²	**Ecological:** This is a screening threshold for potential ecological effects on shoreline flora and fauna, based upon a synthesis of the literature showing that shoreline life has been affected by this degree of oiling. Sublethal effects on epifaunal intertidal invertebrates on hard substrates and on sediments have been observed where oiling exceeds this threshold. Assumed lethal effects threshold for birds on the shoreline.	May appear as black opaque oil.	French et al., 1996; French McCay, 2009; French McCay et al., 2011; French McCay et al., 2012; French McCay, 2016
In Water Concentration	1.0 ppb (µg/L) of dissolved PAHs; corresponds to ~100 ppb (µg/L) of whole oil (THC) in the water column (soluble PAHs are approximately 1% of the total mass of fresh oil)	Water column effects for both **ecological** and **socioeconomic** (e g., seafood) resources may occur at concentrations exceeding 1 ppb dissolved PAH or 100 ppb whole oil; this threshold is typically used as a screening threshold for potential effects on sensitive organisms.	N/A	Trudel et al., 1989; French-McCay 2004; French McCay 2002; French McCay et al., 2012

*Thresholds used in supporting stochastic results figures. For comparison, a bacterium is 1-10 µm in size, a strand of spider web silk is 3-8 µm, and paper is 70-80 µm thick. Oil averaging 1 g/m² is roughly equivalent to 1 µm.

Table 2-3. Oil appearances based on NOAA (2016), Bonn (2009, 2011), and Lewis (2007).

Code	Description	Layer-Thickness		Concentration		Generalized Thickness Used in Modelling Results*
		microns (µm)	Inches (in.)	m^3 per km^2	bbl/acre	microns (µm)
S	Silver Sheen	0.04 - 0.30	1.6×10^{-6} - 1.2×10^{-5}	0.04 - 0.30	1×10^{-3} - 7.8×10^{-3}	0.01
R	Rainbow Sheen	0.30 - 5.0	1.2×10^{-5} - 2.0×10^{-4}	0.3 - 5.0	7.8×10^{-3} - 1.28×10^{-1}	0.1
M	Metallic Sheen	5.0 - 50	2.0×10^{-4} - 2.0×10^{-3}	5.0 - 50	1.28×10^{-1} - 1.28	1-10
T	Transitional Dark (or true) Color	50 - 200	2.0×10^{-3} - 8×10^{-3}	50 - 200	1.28 - 5.1	100
D	Dark (or true) Color	> 200	$> 8 \times 10^{-3}$	> 200	> 5.1	>100
E	Emulsified	Thickness range is very similar to that of dark oil.				

Chart from Bonn Agreement Oil Appearance Code (BAOAC) May 2, 2006, modified by A. Allen

*Visual appearances and corresponding thicknesses of surface oil vary by oil type and environmental condition. Therefore, generalized thicknesses are used the portrayal of modelling results

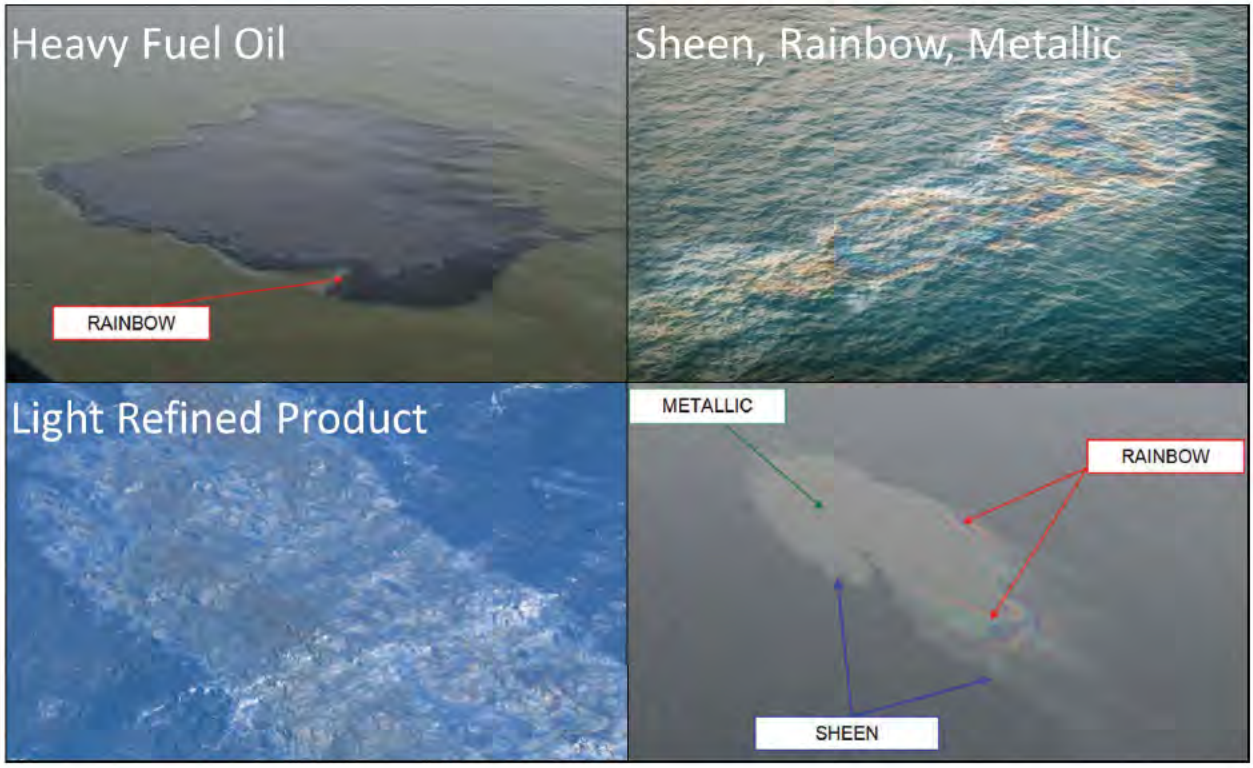

Figure 2-3. Aerial surveillance images of released oil in the environment as examples of different visual appearances based on surface oil thickness and product type (images from Bonn Agreement, 2011).

2.2.4 Deterministic Approach

Individual trajectories of interest were identified and selected from the stochastic ensemble of results for the deterministic analysis. The deterministic trajectory and fate simulations provided an estimate of the oil's fate and transport through the environment as well as its physical and chemical behavior for a specific set of environmental conditions. While the stochastic analysis provides insight into the probable behavior of oil spills given historic wind and current data for the Project Area, the deterministic analysis provides individual trajectory, oil weathering information, expected concentrations and thicknesses of oil contamination, mass balance, and other information related to a single release at a given location and time.

Each single run within a stochastic analysis represents a specific set of wind and current conditions for the modelled time period. When analyzed together, tens to hundreds of stochastic model runs provide a range of expected exposures. The exposures between cases may differ greatly, as the trajectory of each individual modelled release is unique. Therefore, the movement and behavior, as well as the resulting area of surface oil, mass of oil along the shoreline, and mass of oil within the water column, will be different for each modelled simulation. The 95th percentile "worst case" exposures for surface, and in-water contamination and 99th percentile for shoreline, were identified for each release location based upon the area, mass, and length of oil that was predicted in each environmental compartment of interest (i.e., water surface area, shoreline length, or mass in the water column). In addition, deterministic analyses of "batch spills" were modelled as surface releases at one site (the EL 1144 example well site) for small (100 L) and large (1,000 L) release volumes to evaluate any potential discharges during bunkering operations (i.e., transfer from a vessel) between surface vessels and MODU. A 750,000 L release was also modelled at the VCL to represent a vessel collision and complete loss of cargo and fuel from a supply vessel. Each "batch spill" scenario was conservatively chosen to occur during the calmest wind-speed period during the summer/ice-free conditions, as they would result in the largest amount of oil on the surface. Each simulation has its own trajectory, mass balance, surface oil thickness, in-water concentration of dissolved hydrocarbons, etc. reported individually.

The results of the deterministic simulations provide a time history of the fate and weathering of oil over the duration of the release (mass balance), expressed as the percentage of released oil on the water surface, on the shoreline, evaporated, entrained in the water column, and degraded. In addition, cumulative footprints of the individual trajectories over the course of the entire modelled duration will depict the cumulative path of floating surface oil, mass of shoreline oil, and the maximum concentration of dissolved hydrocarbons in the water column at any instant in time. The results are shown in figures presented in Section 4.2.

2.3 Model Scenarios

Two release locations were identified within the Project Area for modelling subsurface blowouts (Figure 2-1). One example well site was selected in each license, reflecting the range of potential wells that are planned to be drilled (water depth, total depth, reservoir properties, etc.). One hypothetical location represents a deeper Jurassic well in a deeper water depth in EL 1144 while the other represents a shallower Cretaceous well in a shallower water depth in EL 1150. Subsurface blowouts near the seafloor were modelled separately with OILMAPDeep and SIMAP at each location in a stochastic analysis that included 119 individual model runs per location. This analysis investigated the influence of environmental variability, throughout the year over multiple years, on trajectory and fate (Table 2-4). The estimated volumes of hydrocarbons released in the subsurface blowout scenarios represent the best technical estimate of potential wells that may be drilled during the license period. In essence, these blowout rates represent a credible "worst case" release volume given realistic inputs and drilling scenarios.

Table 2-4. Hypothetical subsurface release locations and stochastic scenario information.

Scenario Parameter	Release Locations of Unmitigated Subsurface Blowout Scenarios	
	EL 1144 Example Well	EL 1150 Example Well
Latitude	47°31'1.2194" N	47° 18' 54.757" N
Longitude	46°43'9.1987" W	46° 9' 40.394" W
Water Depth of Release	1,137 m	378 m
Product	Bay du Nord	
Release Duration	30 d	30 d
Gas to Oil Ratio	500 scf/bbl	
Pipe Diameter	12.35"	12.35"
Oil Discharge Temperature	96.3 °C	63.6 °C
Release Rate	184,000 bbl/d	44,291 bbl/d
Total Released Volume	5,520,000 bbl	1,329,000 bbl
Model Duration	60 d	60 d
Number of Stochastic Runs	119 annual (59 winter & 60 summer) for each site	

Results from the stochastic analyses were then used to inform an analysis of seasonal affects (i.e. wind and current speed and direction and ice cover) and deterministic analyses (i.e. representative individual trajectories), which identify credible "worst case" periods of time that result in the potential for larger predicted effects to the water surface, water column, and shorelines, separately. Results from the stochastic analyses were broken into two seasons depending on the majority of modelled days falling in ice free conditions (summer) from May – October or periods with ice-cover (winter) from November – April. This allowed for comparisons between probability and minimum time footprints based upon seasonal factors. In addition, analysis of representative deterministic scenarios were conducted for individual trajectories that were identified as the 95th (or 99th) percentile for surface oil exposure, contact with shoreline, and water column contamination from blowouts near the seafloor modelled in the stochastic analysis (Table 2-5).

In addition to the deterministic analyses of credible "worst case" effects to the water surface, shoreline, and water column, several instantaneous surface releases of marine diesel were modelled. This include "batch spills" representing the potential discharges during bunkering operations and a vessel collision and complete loss of cargo and fuel from a supply vessel (Table 2-5).

Table 2-5. Selected representative deterministic scenarios.

Scenario Parameter	Release Parameters for Representative Deterministic Scenarios								
	95th Percentile – EL 1144 Example Well			95th percentile – EL 1150 Example Well			Marine Diesel Releases		
Representative Scenario	Surface Oil Exposure Area	Water Column Oil Mass	Shoreline Contact Length*	Surface Oil Exposure Area	Water Column Oil Mass	Shoreline Contact Length	Small Volume	Large Volume	Full Tank Release
Release Site	EL 1144 Example Well			EL 1150 Example Well			EL 1144 Example Well		VCL
Release Type	Subsurface Blowout						Bunkering		Supply Vessel Collision
Depth of Release	1,137 m			378 m			Surface		
Released Product	BdN			BdN			Marine Diesel		
Release Rate	184,000 bbl/day			44,291 bbl/day			n/a		
Release Duration / Model Duration	30d / 60d			30d / 60d			Instantaneous/ 30d		
Total Release Volume	5,520,000 bbl			1,328,730 bbl			100 L	1,000 L	750,000 L
Modelled Start Date and Season	06/13/2006 Summer	03/22/2008 Winter	10/2/2008 Summer	04/20/2007 Summer	12/03/2006 Winter	No Shore Contact	6/15/2009 summer (calmest site-specific period identified between 2006-2010)		6/14/2009 summer (calmest site-specific period identified between 2006-2010)

*The 99th percentile shoreline contact length case was identified for analysis as the 95th percentile case resulted in no shoreline oiling.

2.4 Model Uncertainty and Validation

The SIMAP model has been developed over several decades to include past and recent information from laboratory based experiments and real-world releases to simulate the trajectory and fate of discharged oil. However, there are limits to the complexity of processes that can be modelled, as well as gaps in knowledge regarding the affected environment. Assumptions based on available scientific information and professional judgment were made in the development of the model, which represent a best assessment of the processes and potential exposures that could result from oil releases.

The major sources of uncertainty in the oil fate model is:

- Oil contains thousands of chemicals with differing physical and chemical properties that determine their fate in the environment. The model must, out of necessity, treat the oil as a mixture of a limited number of components, grouping chemicals by physical and chemical properties.
- The fates model contains a series of algorithms that are simplifications of complex physical-chemical processes. These processes are understood to varying degrees.
- The model treats each release as an isolated, singular event and does not account for any potential cumulative exposure from other sources of contamination.
- Several physical parameters including but not limited to hydrodynamics, water depth, total suspended solids concentration, and wind speed were not sampled extensively throughout the entire modelled domain. However, the data that did exist was sufficient for this type of modelling. When data was lacking, professional judgment and previous experience was used to refine the model inputs.

In the unlikely event of an actual release of oil, the trajectory, fate, and potential biological exposure will be strongly determined by the specific environmental conditions, the precise locations, and a myriad of details related to the event and specific timeframe of the release. Modelled results are a function of the scenarios simulated and the accuracy of the input data used. The goal of this study was not to forecast every detail that could potentially occur, but to describe a range of possible consequences and exposures of oil releases under various representative scenarios.

3 Model Input Data

3.1 Oil Characterization

Two hydrocarbon products and two release sites were modelled for this study including:

1. Bay du Nord (BdN) crude oil at both sites, and
2. Marine diesel in the surface batch spill and the vessel collision deterministic scenarios.

The physical and chemical data used to characterize these oils was provided by Nexen Energy ULC (BdN oil), with additional assays and measurements by S.L. Ross Environmental Research Ltd. (2016) and Petroforma (2013).

BdN is a light crude oil with low viscosity and a high aromatic content (Table 3-1 & Table 3-2). The marine diesel modelled is a standard diesel that also has a low viscosity and high content of soluble hydrocarbons. The low viscosity and high soluble content of these oil products provide conservative approximations of anticipated concentrations in the water following a release, as a relatively large proportion of constituents have the potential to dissolve into the water column, when compared to oils with lower soluble content. These oils would likely behave similarly in the event of a release, with Marine diesel being least persistent of the two.

The "pseudo-component" approach was used to simplify the tracking of thousands of chemicals comprising oil for modelling (Payne et al., 1984; 1987; French et al., 1996; Jones, 1997; Lehr et al., 2000). Chemicals in the oil mixture were grouped by physical-chemical properties, and the resulting component category behaved as if it were a single chemical with characteristics typical of the chemical group. In this component breakdown, aromatic (AR) groups were treated as both soluble (i.e., dissolve into the water column) and volatile (i.e., evaporate to the atmosphere), while the aliphatic (AL) groups were only volatile. The total hydrocarbon concentration (THC) within the boiling range of volatile components was the sum of all AR and AL components. The remainder of the oil was considered to be residual oil, which did not dissolve or volatilize but will degrade over time.

Table 3-1. Physical properties for the two oil products used in modelling.

Physical Property	BdN Crude Oil	Marine Diesel
Density (g/cm^3)	0.853441 @16°C 0.863 @0°C	0.83100 @25°C 0.83089 @16°C
Viscosity (cP)	5.48 @20°C 9.45 @0°C	2.76 @25°C 2.76 @15°C
API Gravity	34.07	38.8
Pour Point (°C)	-9	-50
Interface Tension (dyne/cm)	15.5	27.5
Emulsion Maximum Water Content (%)	72	0

Table 3-2. Fraction of the whole oil comprised of different distillation cuts for the two oil products. Note that the total hydrocarbon concentration (THC) is the sum of the aromatic (AR) and aliphatic (AL) groups. Numbers of carbons in the included compounds are listed.

Distillation Cut[1]	Boiling Point (°C)	Description	BdN Crude Oil	Marine Diesel
AR1	< 180	highly volatile and soluble monoaromatic hydrocarbons (BTEX[2] and MAHs C6-C9)	0.023739	0.019333
AR2	180 – 264	semi-volatile and soluble 2-ring aromatics (MAHs and PAHs C10-C12)	0.004166	0.011410
AR3	265 – 380	low volatility and solubility 3-ring aromatics (PAHs C13-C18)	0.066998	0.015605
AL1	< 180	highly volatile aliphatics (C4-C8)	0.206261	0.144667
AL2	180 – 280	semi-volatile aliphatics (C9-C16)	0.160834	0.478690
AL3	280 – 380	low volatility aliphatics (C17-C23)	0.168002	0.303295
THC1	< 180	total hydrocarbon fraction 1 (sum of AR1 and AL1)	0.230000	0.164000
THC2	180 – 280	total hydrocarbon fraction 2 (sum of AR2 and AL2)	0.165000	0.490100
THC3	280 – 380	total hydrocarbon fraction 3 (sum of AR3 and AL3)	0.235000	0.318900
Residuals	> 380	aromatics ≥ 4 rings and aliphatics > C20 that are neither volatile nor soluble	0.37000	0.02700

[1]Note that the terms "aromatic" and "aliphatic" are used in a modelling context. "Aromatic" refers to all soluble and volatile hydrocarbons and may include actual aliphatic compounds in the chemical sense that are soluble. In the modelling context, "aliphatic" refers to insoluble and volatile hydrocarbons.
[2]BTEX (benzene, toluene, ethylbenzene, xylene), MAHs (monocylic aromatic hydrocarbons), and PAHs (polycyclic aromatic hydrocarbons) are the more soluble, bioavailable, and potentially toxic components in oil.

3.2 Geographic and Habitat Data

For geographical reference, SIMAP uses rectilinear grids to designate the location of the shoreline, the water depth (bathymetry), and the shore or habitat type. The grids were generated from a digital shoreline using ESRI geoprocessing and Spatial Analyst Extension tools and the cells were coded for depth and habitat type. Geographical data were obtained from multiple international sources to provide the geographic and environmental data required for modelling (Table 3-3). Habitat data were used to define the bottom type and vegetation found in subtidal areas, areas of extensive mud flats and wetlands, and the shoreline type (e.g., sandy beach, rocky shoreline, etc.).

Table 3-3. Sources for habitat, shoreline, and bathymetry data.

Data Type	Data Source	Geographic Location	Reference
Habitat/Shoreline	Environment and Climate Change Canada	Canada	Therrien, A. 2017
	National Oceanic and Atmospheric Administration Environmental Sensitivity Index	United States (except Maine)	NOAA 2016
	Maine Environmental Vulnerability Index	United States - Maine	MDEP 2016
Bathymetry	General Bathymetric Chart of the Oceans Digital Atlas	Global	GEBCO 2003

The model used these grids to identify the location of the shoreline and amount of oil that may adhere once contact of the oil with the shoreline was made (Figure 3-1). Retention of oil on a shoreline depends on the shoreline type, physical and chemical properties (e.g., viscosity) of the oil, tidal amplitude in estuarine areas, and wave energy. The resolution of the habitat grid was approximately 1.8 km North-South by 2.5 km East-West (0.02225° on each side). Bathymetry data define the water depths within the modelled extent. The General Bathymetric Chart of the Oceans (GEBCO) one arc-minute interval grid was used, but was resampled into a grid with the same resolution as the habitat grid (Figure 3-1).

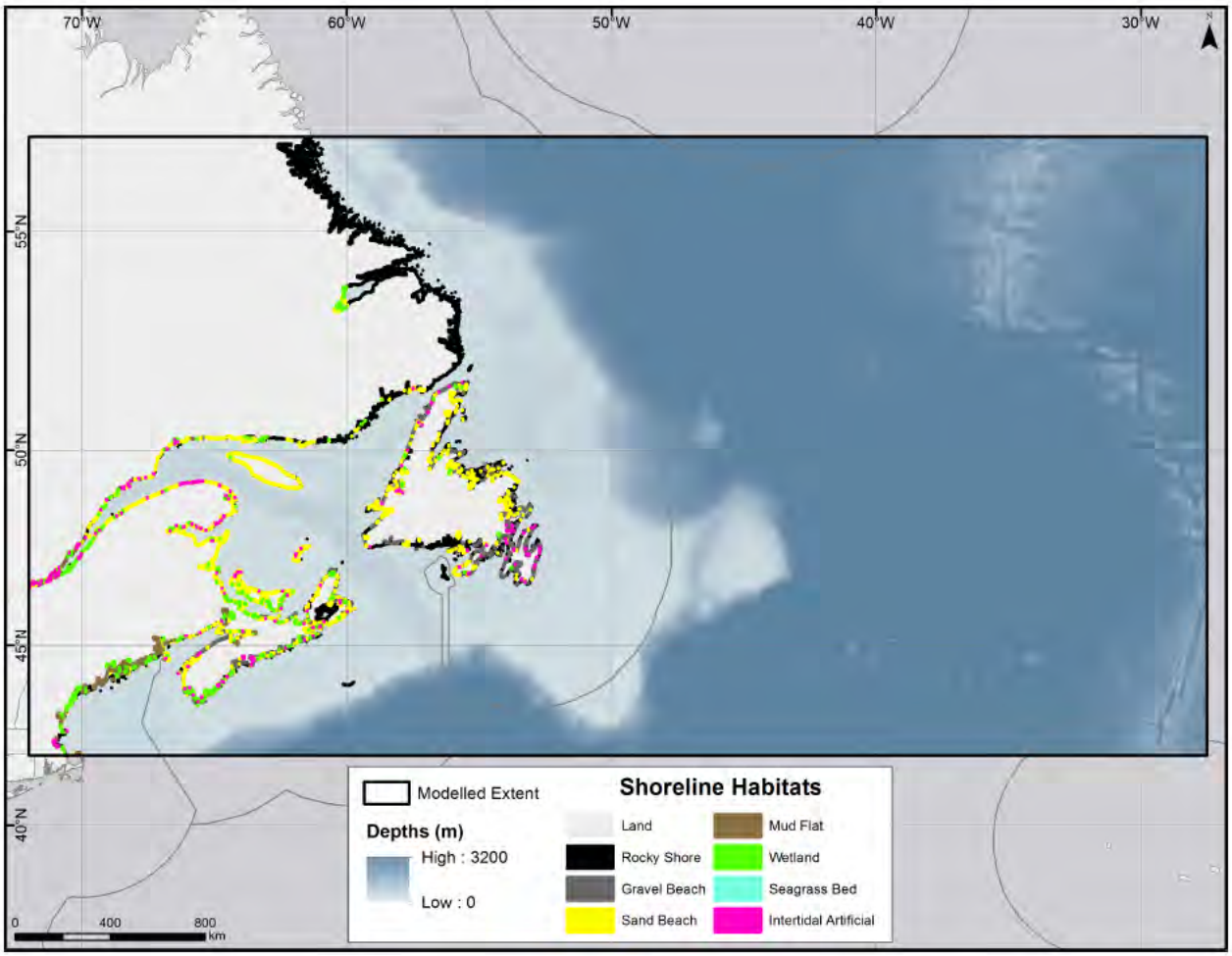

Figure 3-1. Shoreline habitat data and depth throughout the modelled domain. The black box represents the modelled extent.

3.3 Ice Cover

Sea ice is formed in the autumn in the Arctic and sub-Arctic regions of the world. The growth rate of sea ice depends on surface temperature and the heat flux in the underlying water. The formation and development of sea ice follows a progression of stages. The exact timing of these stages at any location is not the same from year to year because of subtle differences in climatic conditions. In the Northern Hemisphere during September and October, the air temperature lowers sufficiently to form a thin sheet of ice on the sea surface. The freezing temperature for average ocean salt water with a salinity of 35 ppt is about -2°C (NOAA 2014).

The movement and behavior of released oil is greatly affected by the presence of ice (Figure 3-2). Oil trapped in or under sea ice will weather more slowly than oil released in open water. Algorithms in SIMAP for modelling the movement and behavior of oil in the presence of sea ice are based on the percent of ice coverage. From 0 to ~30% coverage, the ice has no effect on the advection or weathering of surface floating oil. From approximately 30 to 80% ice coverage, oil advection is forced to the right of ice motion in the northern hemisphere, surface oil thickness generally increases due to ice-restricted spreading, and evaporation and entrainment are both reduced by damping/shielding the water surface from wind and waves. Above 80% ice coverage, surface oil moves with the ice and evaporation and entrainment cease.

The ice thickness can vary greatly based upon prevailing weather conditions. If oil is released under ice, water column exposures can be greater, due to the "capping" effect of the ice. Ice cover limits or prevents evaporative losses and could result in substantially greater dissolution of hydrocarbons into the water column.

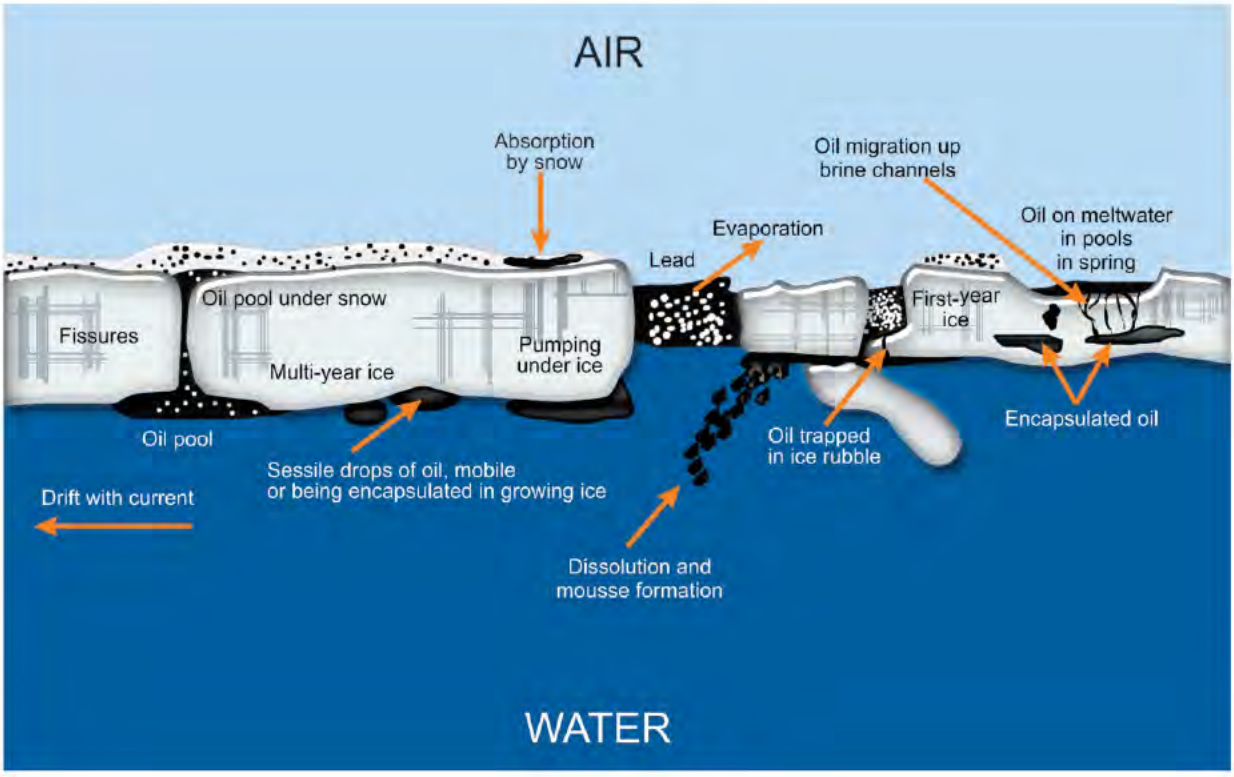

Figure 3-2. Oil and ice interactions at the water surface.

Ice data used as modelling inputs were obtained from the Canadian Ice Service (CIS; ECCC 2017) in weekly files spanning 2006 to 2010. These data were in the form of polygon data, with information on total ice concentration and stage of development. For each ice polygon, concentration codes were converted to concentration percentages. Average ice thickness was calculated based on the proportional concentration of the various stages of ice present for each week of the season over five years. The CIS data provides a range of thicknesses for each ice category and stage of development. In most cases, the mid-point of those ranges was used in the calculation of average ice thickness. If the stage was not identified, but there were concentrations provided, then sea ice stage was assumed to be first year medium ice (Table 3-4). The ice data was gridded at a resolution matching the habitat grid (0.0225°). A representative map depicting percentage of ice cover and thickness of ice for the first week of February 2010 is presented (Figure 3-3).

Table 3-4. Sea ice thickness used in the modelling characterized by CIS stage of development.

CIS Ice Category or Sea Ice Stage	Concentration	CIS Thickness Range (cm)	Model Applied Thickness (cm)
Ice Free	0%	n/a	n/a
Open Water	30%	n/a	50
Landfast Ice	100%	n/a	assumed full water depth
First year thick ice	Total concentration converted from tenths to percent ice cover	> 120	120
First year medium ice*		70 – 120	95
First year thin ice		30 – 70	50
Young ice		10 – 30	20
Grey white ice		15 – 30	22.5
Grey ice		10 – 15	12.5
New ice		< 10	5
Icebergs		unknown	100

* Default sea ice stage assumed when none was identified in the data.

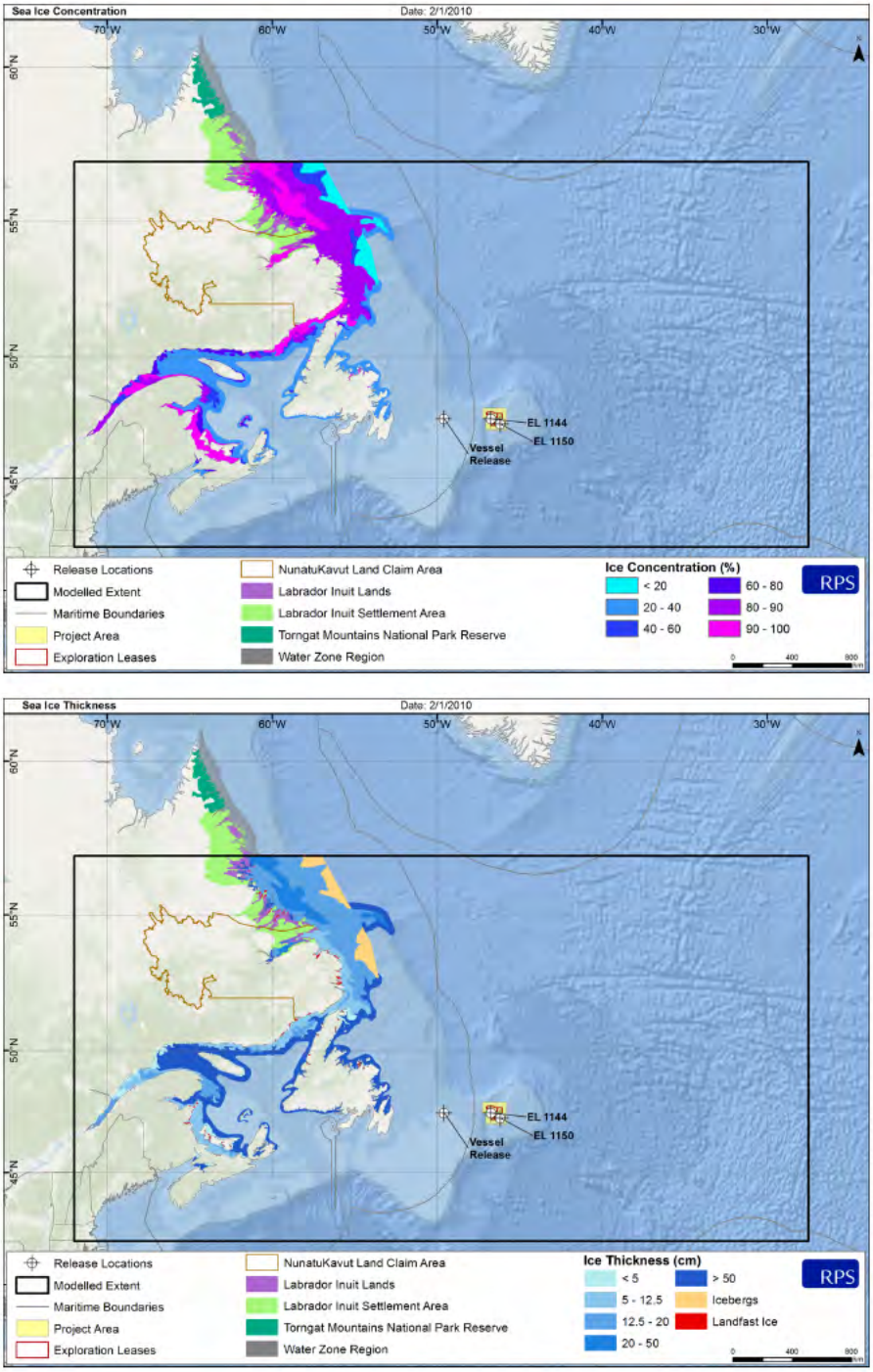

Figure 3-3. Representative percentage ice cover (top) and corresponding thickness (bottom) for the first week of February 2010.

3.4 Wind Data

A multiyear dataset of wind speed and direction was used in the SIMAP oil spill model to capture the variability that occurs on time scales that range from hours to years. Oil spill trajectories simulated using long-term wind datasets are representative of possible wind conditions at the site, assuming the temporal variability is on the timescale of changes in speed and direction. Because winds can change on time scales of minutes to hours, it is best to acquire data at the highest temporal resolution possible (typically every six hours for large global models, or at the very least daily averages). Oil released over extended periods of time has the potential to travel long distances by wind transport. To effectively model this, the wind speed and direction data must encompass a large geographic area in order to capture the spatial extent and any spatial variability in potential transport that may occur. Winds may physically transport oil on the water surface, thus wind speed and direction at the water surface may be the driving force between a simulation with limited versus extensive transport. The SIMAP model use time-varying wind speeds and directions for the period over which the release was simulated.

Wind data for this study were obtained from the National Centers for Environmental Prediction Climate Forecast System Reanalysis (CFSR) product for 2006 through 2010. The CFSR was designed and executed as a global, high-resolution, coupled atmosphere-ocean-land surface-sea ice system to provide the best estimate of the state of these coupled domains (Saha et al., 2010). The CFSR includes coupling of atmosphere and ocean, as well as assimilation of satellite radiances. The CFSR global atmospheric resolution is ~38 km, with 64 vertical levels extending from the surface to 0.26 hPa. CFSR winds were also used as one of the main driving forces in the hydrodynamic dataset used for modelling (see Section 3.5). The CFSR time series acquired for this study was available at 0.5-degree horizontal resolution at 6-hourly intervals.

Averaged annual wind data at the EL 1144 and EL 1150 example well sites were most frequently from the west-southwest direction (Figure 3-4). Monthly average wind speeds varied between 7 and 12 m/s throughout the year, with highest speeds occurring during winter months (November – March) and lowest speeds in July (Figure 3-6). These winds would be expected to transport oil generally away from nearby shorelines further into the open ocean.

Winds over the Grand Banks and Flemish Pass are predominantly from the southwest and west throughout the year. Winter season winds are most frequently from the west and northwest with higher velocity than summer season winds, which typically come from the southwest (Figure 3-4 through Figure 3-6). Spring and fall months are more dynamic transitional periods between the more consistent summer and winter wind regimes. Low pressure systems, tropical, and extra-tropical storms pass

through the Grand Banks on a regular basis generating substantial wind speeds for short periods of time. Significant wave heights are typically highest from November – February, in regions with no ice (C-NLOPB, 2014).

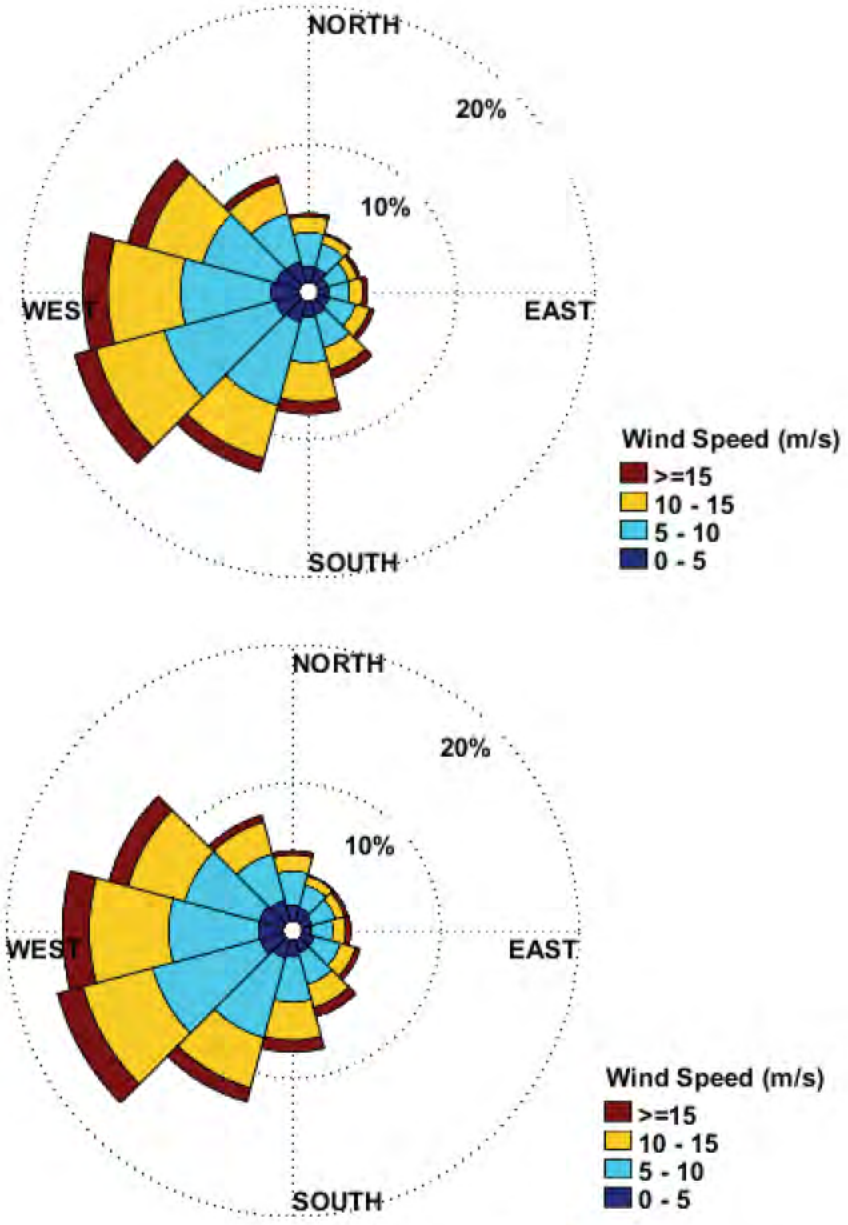

Figure 3-4. Annual CFSR wind rose near the EL 1144 (top) and EL 1150 (bottom) example well sites. Wind speeds are presented in m/s, using meteorological convention (i.e., direction wind is coming from).

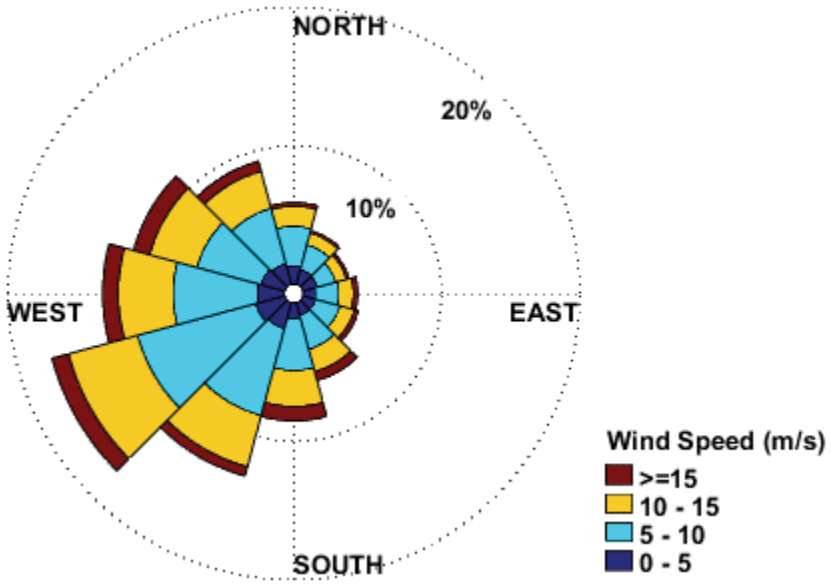

Figure 3-5. Annual CFSR wind rose near the supply route release location (VCL) for the vessel collision batch spill. Wind speeds are presented in m/s, using meteorological convention (i.e., direction wind is coming from).

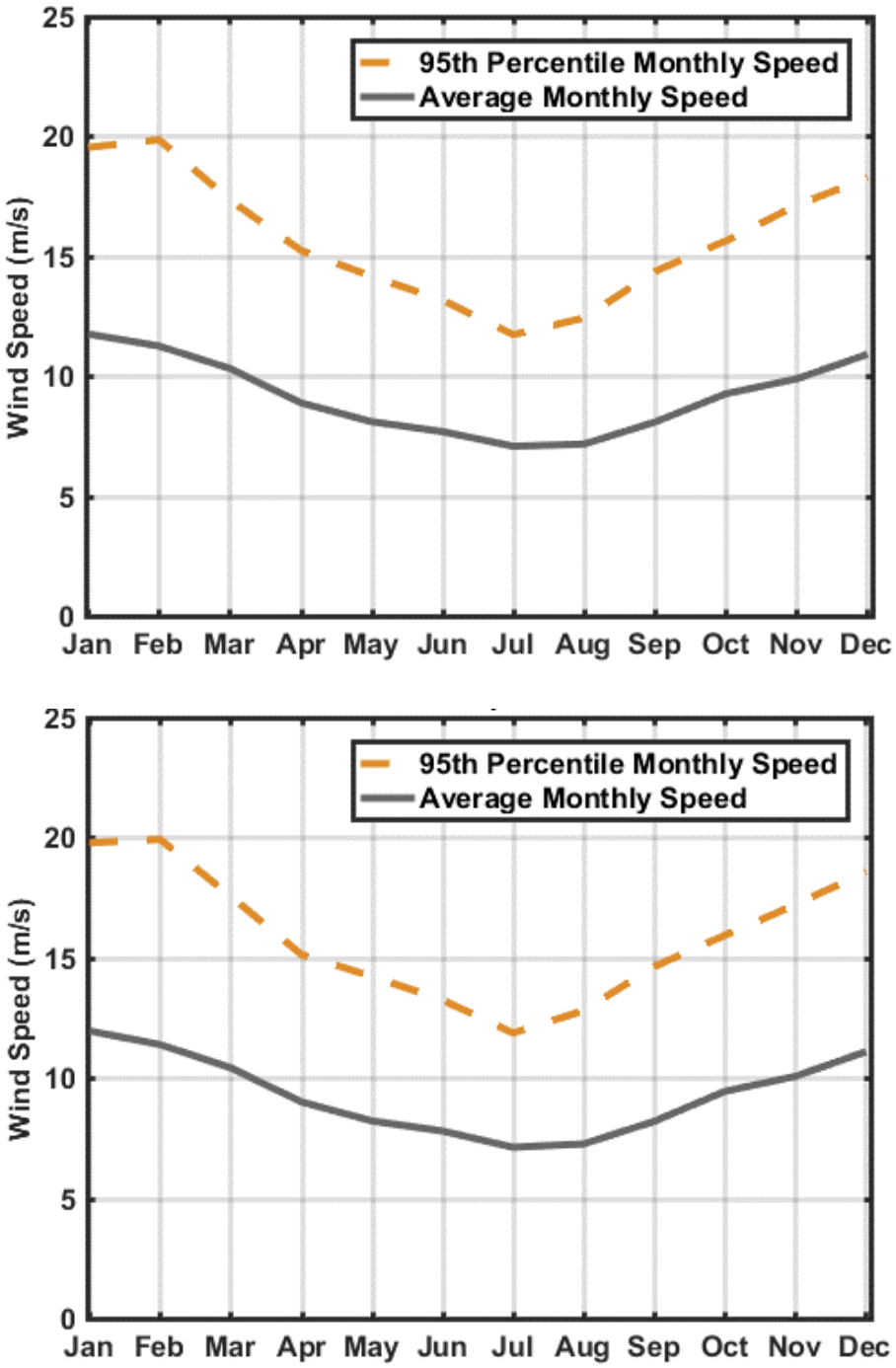

Figure 3-6. Average and 95th percentile monthly wind speeds near the EL 1144 (top) and EL 1150 (bottom) example well sites.

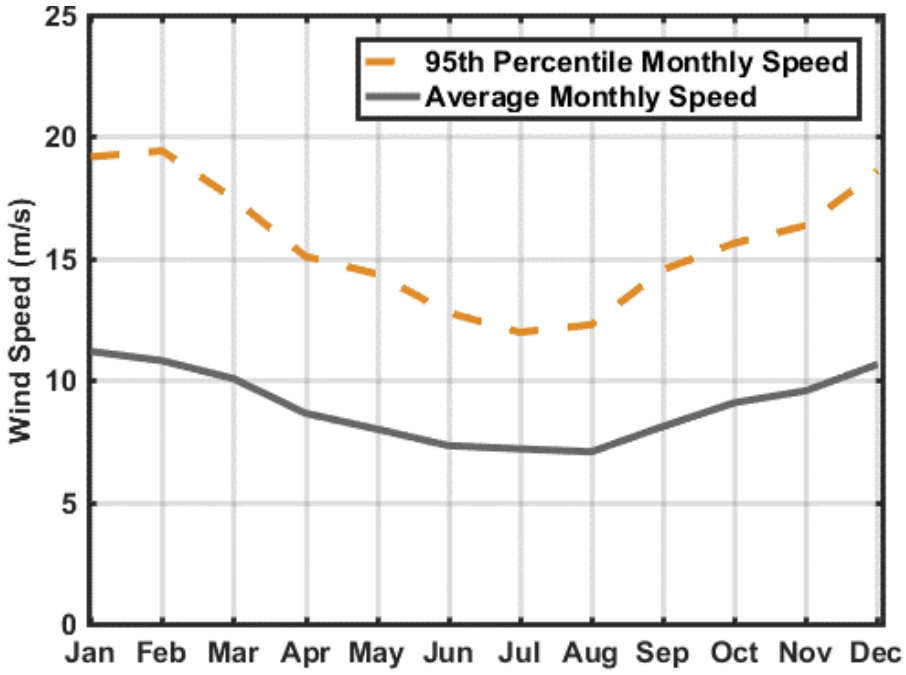

Figure 3-7. Average and 95th percentile monthly wind speeds near the supply route release location for the VCL batch spill.

3.5 Currents

The Labrador Current dominates the large-scale ocean circulation in the Newfoundland region originating in the Arctic Ocean and flowing south along the coasts of Labrador and Newfoundland (Figure 3-8). This southerly current intensifies as waters funnel through the offshore branch, which follows the Flemish Pass between the Grand Banks and Flemish Cap. To a lesser extent, a portion of the Labrador Current flows through an inshore branch, which follows the Avalon Channel between Newfoundland and the Grand Banks. Over parts of the Grand Banks, currents can be generally weak and flow southward (Statoil, 2016). Maximum current speeds in the upper 200 m of the water column range from 0.3 – 2.0 m/s (C-NLOPB, 2014). The strong southerly current dominates the yearly average flow and winds may only account for approximately 10% of current variability in this region (Petrie and Isenor, 1985). South of the Flemish Pass, the Labrador Current mixes with the North Atlantic current. The boundary where these two currents converge produces extremely energetic and variable frontal systems and eddies on smaller scales, on the order of kilometers (Volkov, 2005). Due to these eddies, local transport may advect parcels of water in nearly any direction. Satellite and drifter studies of current dynamics demonstrate this complexity; however, drifting parcels generally move to the south

and east (Han and Tang, 1999; Petrie, 1983; Petrie and Anderson, 1983; Richardson, 1983) where they intersect with the North Atlantic current.

Currents for the North Atlantic region were acquired from the HYCOM (HYbrid Coordinate Ocean Model) circulation model. HYCOM is a primitive-equation ocean general circulation model that evolved from the Miami Isopycnic-Coordinate Ocean Model (MICOM) (Halliwell, 2002; Halliwell et al., 1998, 2000; Bleck, 2002). MICOM has become one of the premier ocean circulation models, having been subjected to validation studies (Chassignet et al., 1996; Roberts et al., 1996; Marsh et al., 1996) and used in numerous ocean climate studies (New and Bleck, 1995; New et al., 1995; Hu, 1996; Halliwell, 1997, 1998; Bleck, 1998). The HYCOM global ocean system is a 3D dynamic model that is run each day, providing a 5-day hindcast and 5-day forecast of oceanic currents that works effectively in both deep and shallow waters. Hindcast data are used to validate the accuracy of each run to determine if modelled forcings produce results that match observational data. HYCOM uses Mercator projections between 78°S and 47°N and a bipolar patch for regions north of 47°N to avoid computational problems associated with the convergence of the meridians at the pole. The 1/12° equatorial resolution provides gridded ocean data with an average spacing of ~7 km between each point. Several studies have demonstrated that at least 1/10° horizontal resolution is required to resolve boundary currents and mesoscale variability in a realistic manner (Hurlburt and Hogan, 2000; Smith and Maltrud, 2000; Chassignet and Garaffo, 2001).

Data is assimilated through the Navy Coupled Ocean Data Assimilation (NCODA) system (Cummings, 2005). The NCODA system employs a Multi-Variate Optimal Interpolation scheme, which uses model forecasts as a first guess and then refines estimates from available satellite and in-situ temperature and salinity data that are applied through the water column using a downward projection of surface information (Cooper and Haines 1996). Bathymetry is derived from the U.S. Naval Research Laboratory BDB2 dataset. Surface forcing is derived from the Navy Operational Global Atmospheric Prediction System, which includes wind stress, wind speed, heat flux (using bulk formula), and precipitation.

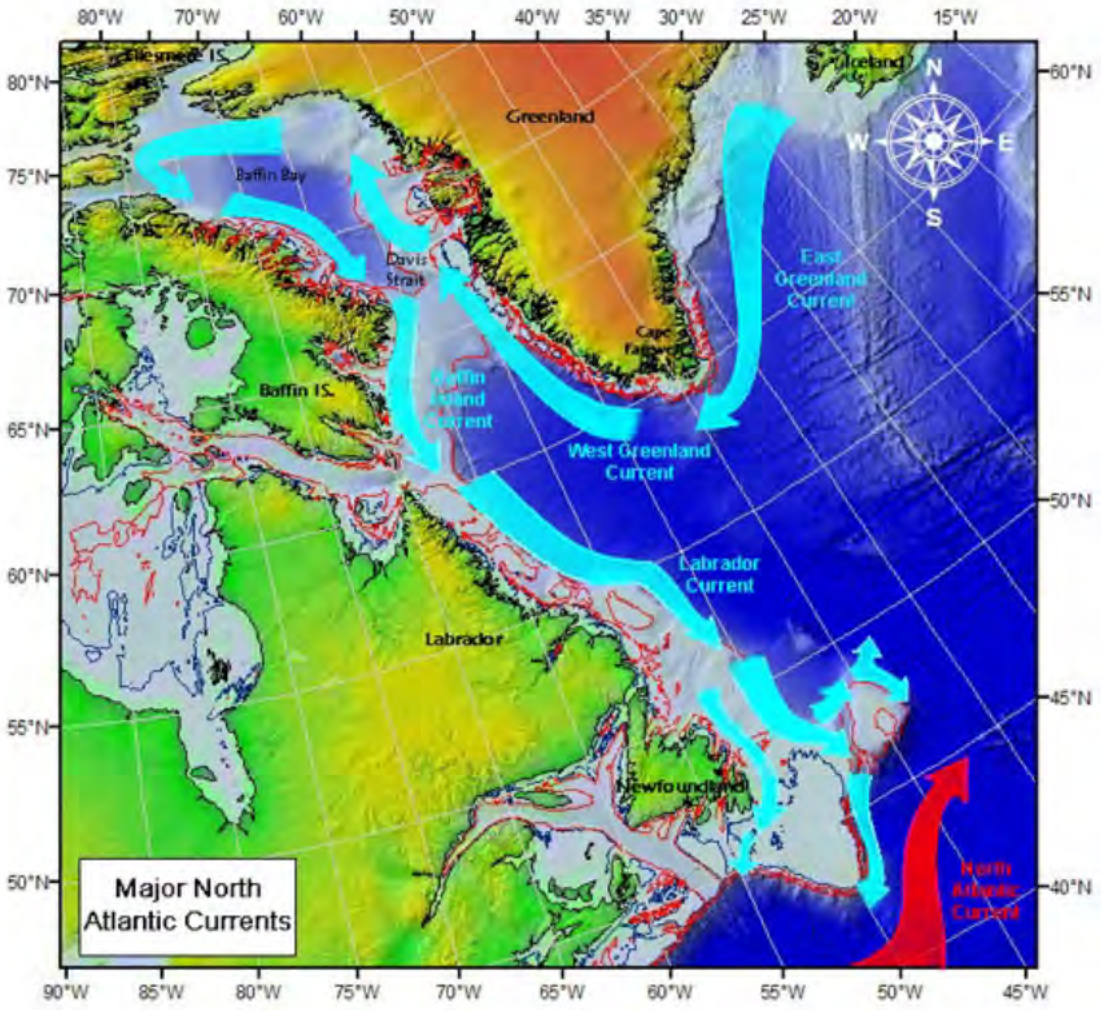

Figure 3-8. Large scale ocean currents in the Newfoundland region (USCG 2009).

For this study, daily current data were obtained for the period January 2006 through December 2010 for the North Atlantic region (Halliwell, 2002; HYCOM 2016). Because the data spanned 5 years, the variability in winds and currents would sample daily, weekly, seasonal, and inter-annual variability, which included calm periods, seasonal storms, and the full range of environmental forcing over the entire time period. While this subset of data is not the most recent five years of data, current and wind speed, direction, and variability in the study area are quite similar to those from 5-10 years ago and the data used in this study would be representative of environmental conditions present today. Similarly, while there may be questions regarding general circulation during specific time periods, it is important to note that trajectories are influenced by day to day currents, as opposed to averages. Additionally, a stochastic assessment samples the variability of speed and direction over the time period, as opposed to

just a single set of conditions. Surface forcing was derived from 1-hourly CFSR wind data with a horizontal resolution of 0.3125° and induced wind stress, wind speed, heat flux, and precipitation with bathymetry derived from the GEBCO dataset (HYCOM 2016). Average surface current speeds (Figure 3-9) and direction offshore Newfoundland (Figure 3-10) in the area from 2006 – 2010 depict larger scale features such as the Labrador current, North Atlantic Current, as well as bathymetric steering of currents around the Grand Banks and Flemish Cap. While these figures depict an average current speed and direction for visual purposes, oil transport was defined by the daily currents throughout each modelled simulation.

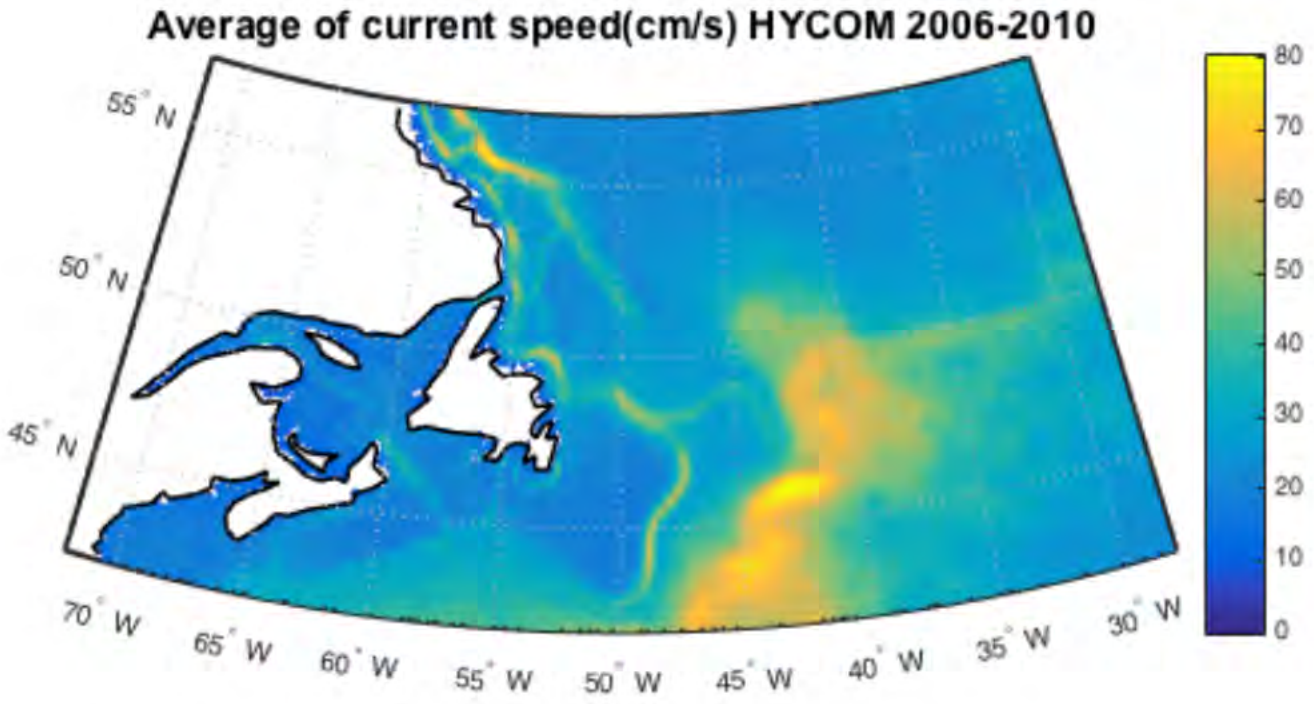

Figure 3-9. Average HYCOM surface current speeds (cm/s) off the coast of Newfoundland from 2006 – 2010.

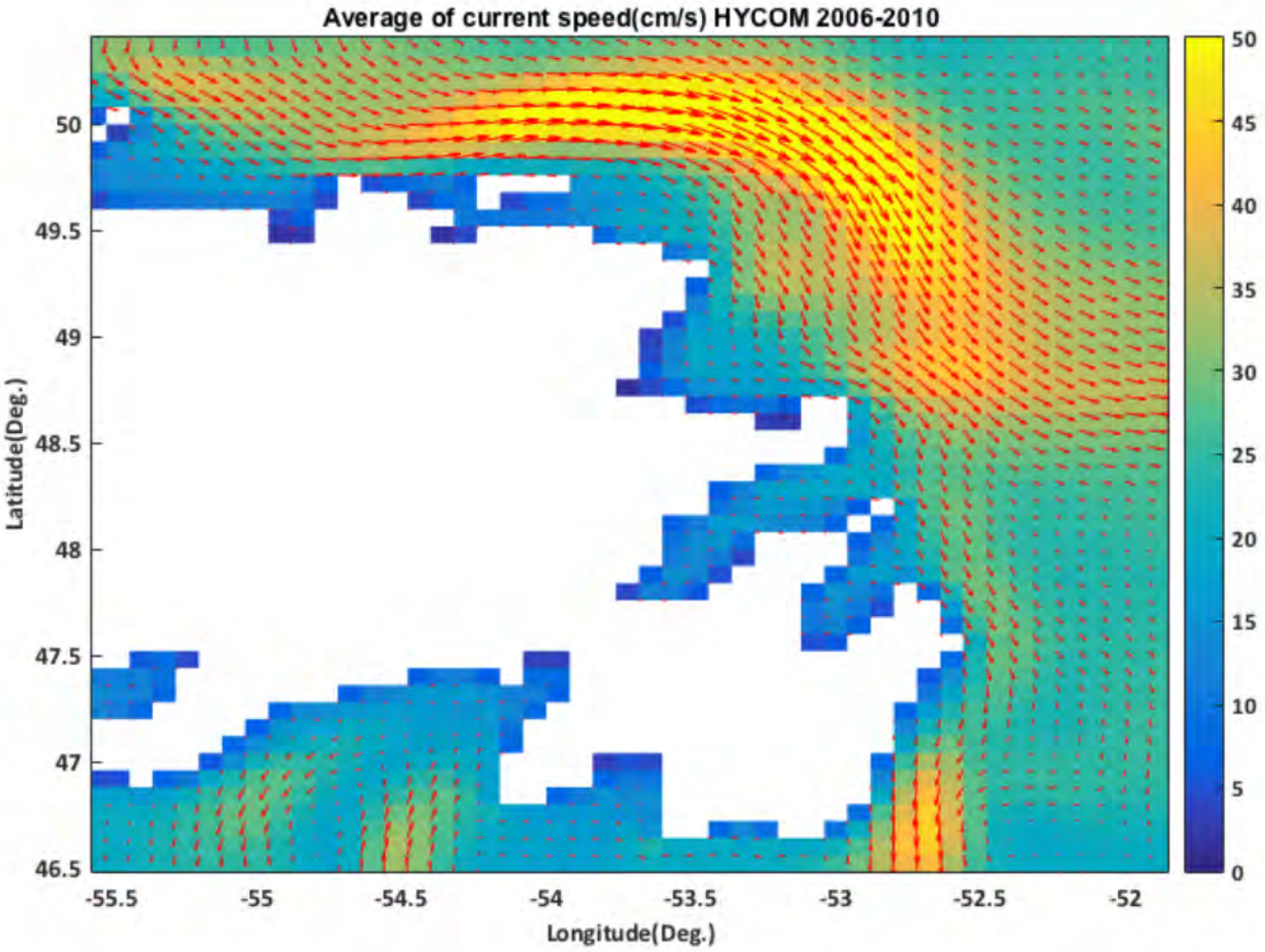

Figure 3-10. Averaged surface current speed (cm/s) in color, and direction presented as red vectors offshore Newfoundland from HYCOM (2006 – 2010).

3.6 Water Temperature & Salinity

Temperature and salinity values throughout the water column influence a number of oil transport and fate calculations. Temperature and salinity data have been obtained from the World Ocean Atlas (WOA) 2013 high-resolution dataset, Version 2, which is compiled and maintained by the U.S. National Oceanographic Data Center (Levitus et al., 2014). The WOA originated from the Climatological Atlas of the World Ocean (Levitus, 1982) and was updated with new data records in 1994, 1998, 2001 (Conkright et al., 2002), and 2013. These data records consist of observations obtained from various global data management projects. The dataset includes up to 57 depth bins from the sea surface to the seabed and

include averaged yearly, seasonally, and monthly data over a global grid with a 1/4° horizontal resolution.

3.7 Blowout Model Scenarios and Results

The nearfield model OILMAPDeep was used to predict the initial droplet size distribution associated with subsurface blowouts of BdN crude oil at two different release locations. Oil and gas were introduced to the water column near the seafloor to simulate an uncontrolled release from the wellhead frequently referred to as a blowout. The release depth ranged from about 378 m to 1,137 m between the two identified release locations. The droplet size model was used to predict the distribution of oil volume (mass) within different size ranges (measured by diameter) in response to the turbulence of the release, the gas content, the water depth, and the properties of the oil. The droplet model predicted the initial droplet size distributions for each scenario as well as the depth or "trap height" in the water column where the droplets would be released to the water column and rise according to their individual buoyancies. These values were then used to generate input files defining the size, mass, and depth of oil droplets entering the water column for use within the SIMAP far-field model.

Initial droplet sizes are primarily a function of the energy of the release, the chemical and physical parameters of the released oil, the gas to oil ratio (GOR), dispersant application, and several other factors. As an example, if the energy of a release or the amount of dispersant added were to increase, or if the viscosity of the released oil were lower, the resulting droplet sizes would be smaller. In the scenarios simulated for this study, the oil was assumed not to be treated with dispersant. The energy of the release is a function of the volumetric flow rate and discharge orifice size, with higher energy releases occurring as greater volumes pass through smaller openings more quickly.

Two subsurface blowout release events were evaluated as part of this study:

(1) EL 1144 Example Well Site – 30-day release of BdN, through a 31.37 cm (12.35-inch) orifice at a depth of 1,137 m and rate of 29,254 m^3/d (184,000 bbl/d)
(2) EL 1150 Example Well Site– 30-day release of BdN, through a 31.37 cm (12.35-inch) orifice at a depth of 378 m and rate of 7,042 m^3/d (44,291 bbl/d)

The predicted droplet size distribution was represented by seven discrete size bins for each modelled release scenario at the EL 1144 and EL 1150 example well sites (Table 3- 1). The non-uniform spacing between the droplet size bins is the result of the non-linear functionality of droplet size distribution. Each of the seven bins were determined such that an equal proportion of the released oil by mass (14.29%) was within each bin. Differences in release volume, duration, and depth of release resulted in different droplet size distributions for each of the two modelled releases.

Oil droplets rise through the water column at rates based on drag, calculated using their diameter (treated as a sphere) and the buoyancy, the density difference between the oil and the water, which varies with changing temperature and salinity by depth (Figure 3-11). Rise times for oil to reach the surface varied between minutes to many hours, depending on droplet size and depth of release. Rise time estimates are approximated, based on the initial droplet size, initial droplet density, and bottom water density; neglecting dispersion, dissolution, and degradation (which were tracked within the oil spill model and modified the rise rates). The longest rise times were associated with the smallest droplets and deepest release depths, with some rise times exceeding a day.

Table 3- 1. Summary of droplet size distribution results for each of four modelled subsurface blowout release events.

Median Droplet Size (d50) in Each of Seven Equal-Mass Bins, by Diameter (µm)	
EL 1144 Example Well BdN Crude Oil (156,000 bbl/d, 30-day release)	**EL 1150 Example Well BdN Crude Oil (26,200 bbl/d, 30-day release)**
221	485
505	1109
629	1380
758	1,662
914	2,004
1,144	2,510
2,012	4,413

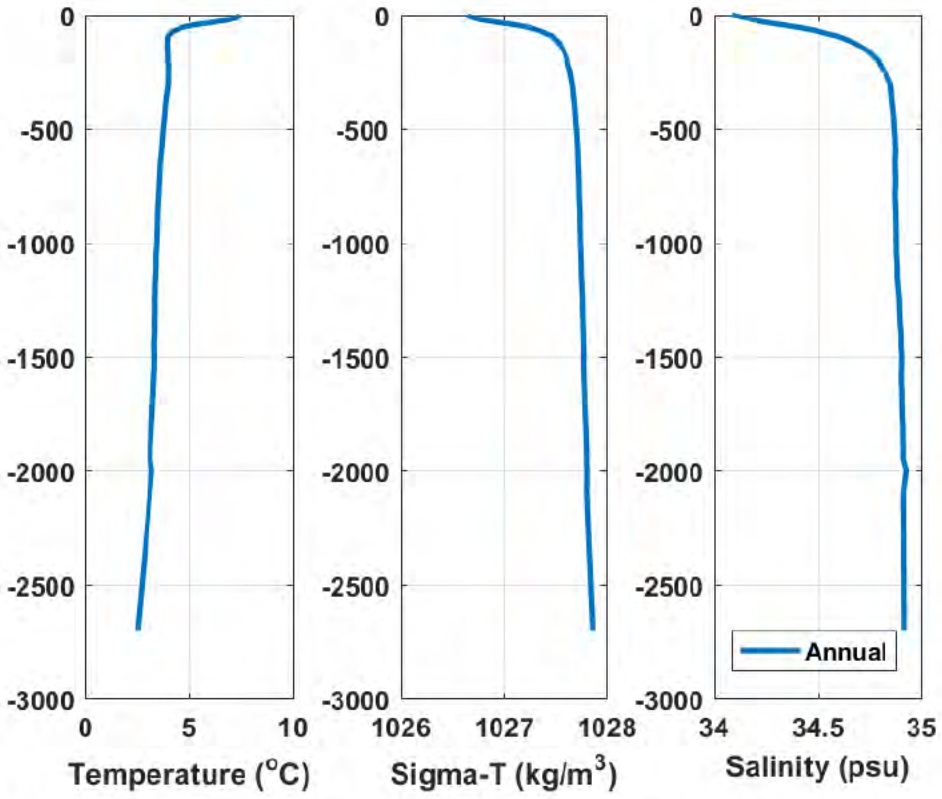

Figure 3-11. Water column profiles of temperature (left), salinity (right), and corresponding density (middle) in the vicinity of the release sites, represented as sigma-t. The density profile was generated based on the temperature and salinity profile using equations of state as published by UNESCO, 1981 (EOS – 80).

4 Model Results

4.1 Stochastic Analysis Results

Stochastic analyses characterize results from many tens to hundreds of individual modelled releases. This study included modelling 119 individual releases for 60 days over the course of 5 years of environmental data at the EL 1144 and EL 1150 example well sites to capture the natural variability in the environment.

Because ice cover can affect the trajectory and fate of oil, individual model runs were separated into two groups based upon the specific time periods modelled that included ice cover or ice-free conditions. Statistics for all 119 releases within a stochastic scenario are referred to as "annual," as they include all releases in any month over the course of the entire five years. Ice cover in the region is present in

specific regions from November through April, while May through October is mostly ice-free. Modelled releases that have the majority of their simulated days (≥30 of the 60-day modelled duration) experiencing mostly ice-free periods are referred to as "summer" analyses (60 modelled releases), while those that have a majority of days experiencing periods with ice cover are referred to as "winter" analyses (59 modelled releases). Ice cover very rarely extended far enough offshore to reach within kilometers of the release locations, and when it did, < 10% ice cover was predicted. However, ice was present along most of the coastline in winter months, with February typically having the largest expanses of 90-100% ice cover.

The figures presented in the stochastic modelling results section illustrate the possible spatial extent of surface floating oil, water column concentrations of dissolved hydrocarbons, and shoreline contact including both the probabilities and associated minimum times to threshold exceedance (Table 4-1) for the hypothetical release scenarios. The probability maps define the area of potential exposure and the associated probability with which sea surface oil, shoreline oil, or water column contamination are expected to exceed the specified thresholds at any point of time throughout the 60-day modelled duration. The colored contours in the stochastic maps signify the boundary for given percentiles of areas that may experience oil at or above the specified threshold for each release scenario. Darker color contours denote areas that are more likely to exceed the specified threshold while lighter color contours are less likely. Note that the lightest minty green line represents areas where oil may exceed the specified threshold in only 1% of release simulations. In other words, the likelihood that any oil exceeding the identified threshold would leave the area bounded by the minty green line is <1%. The area between this contour and the next (10%) has between a 1-10% probability of exceeding the threshold, given a release of the modelled scenario has occurred.

The probabilities of oil exposure were calculated from a statistical analysis of the ensemble of individual trajectories modelled for each release scenario. The fundamental assumption for this modelling was that an unmitigated release did occur. Therefore, probability contours should be interpreted as "In the unlikely event of a release, the probability that any one specific area may experience contamination above the specified threshold is X%". Stochastic figures do not imply that the entire contoured area would be covered with oil in the event of a single release, nor do they provide any information on the quantity of oil in a given area. Additionally, these figures do not provide the likelihood of a blowout occurring in any given year. Rather, these stochastic figures denote the probability of oil exceeding identified thresholds at any modelled time step (over 60 days), for each point within the modelled domain, assuming a release were to occur at some point in time.

In addition, stochastic maps depicting water column contamination by dissolved hydrocarbon concentrations do not specify the depth at which the threshold exceedance occurs. The maps depict the

vertical maximum at any time during or after the release. Thus, images do not imply that the entire water column (i.e., from surface to bottom) will experience a concentration above the threshold, but rather a concentration may be exceeded at a specific depth (typically within the surface few meters) in the mapped location.

The minimum time footprints correspond with the associated probability of oil exposure map. Each figure illustrates the shortest amount of time required (from the initial release) for each point within the footprint to exceed the defined threshold. The time reported is the minimum value for each point considering the entire ensemble of trajectories. Together, probability and minimum time figures can be interpreted together to read: "There is X% probability that oil is predicted to exceed the identified threshold at a specific location, and this exceedance could occur in as little as Y days".

The Exclusive Economic Zone for Canada and the U.S., as well as the international border, are depicted on each map to provide context for the spatial extent and potentially affected territorial waters from any potential release (VLIZ, 2014).

All figures depict data where probability of a region exceeding the threshold is > 1%. When comparing annual to seasonal results, the predicted percent exceedance depends on the total number of releases investigated in each subset of releases. Therefore, while only one scenario might be required to exceed the 1% threshold for visualization in seasonal results (60 or 59 modelled simulations), two scenarios would be required to exceed the same threshold in the annual analysis (119 modelled simulations), due to a greater number of modelled releases in the annual set of runs being analyzed. Figures depicting stochastic results are provided for surface oil thickness >0.04 µm, dissolved hydrocarbon contamination > 1 µg/L, and shoreline contact > 1 g/m^2 for annual, summer, and winter scenarios for the EL 1144 and EL 1150 example well sites (Figure 4-1 through Figure 4-18).

Appendix B has been provided to include higher resolution results figures to those found in this Technical Report. Each figure is provided as a full page with no modifications or additions.

4.1.1 EL 1144 Example Well Release Site

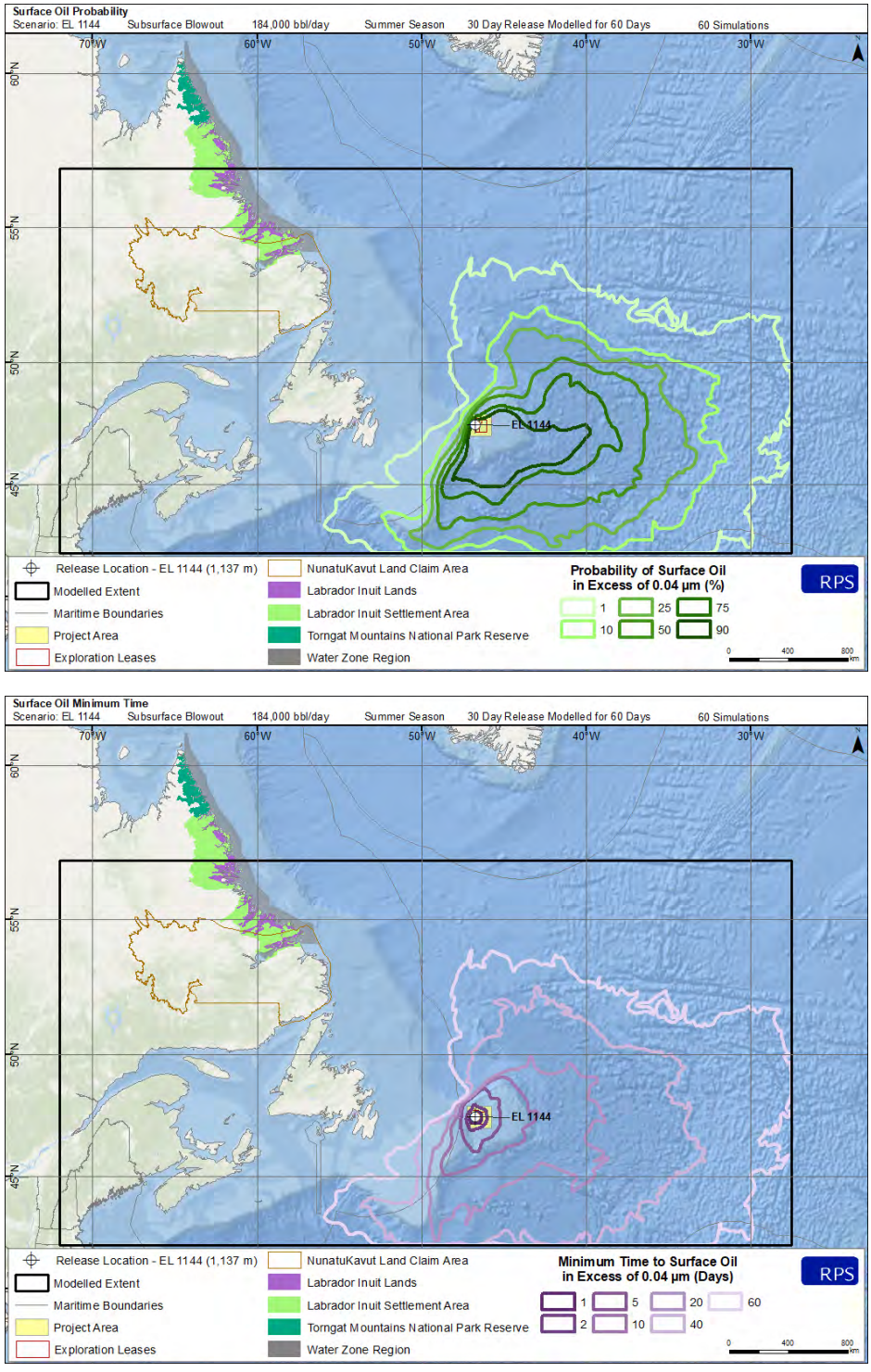

Figure 4-1. Summer probability of surface oil thickness > 0.04 µm (top) and minimum time to threshold exceedance (bottom) resulting from a 30-day subsurface blowout at EL 1144 example well site.

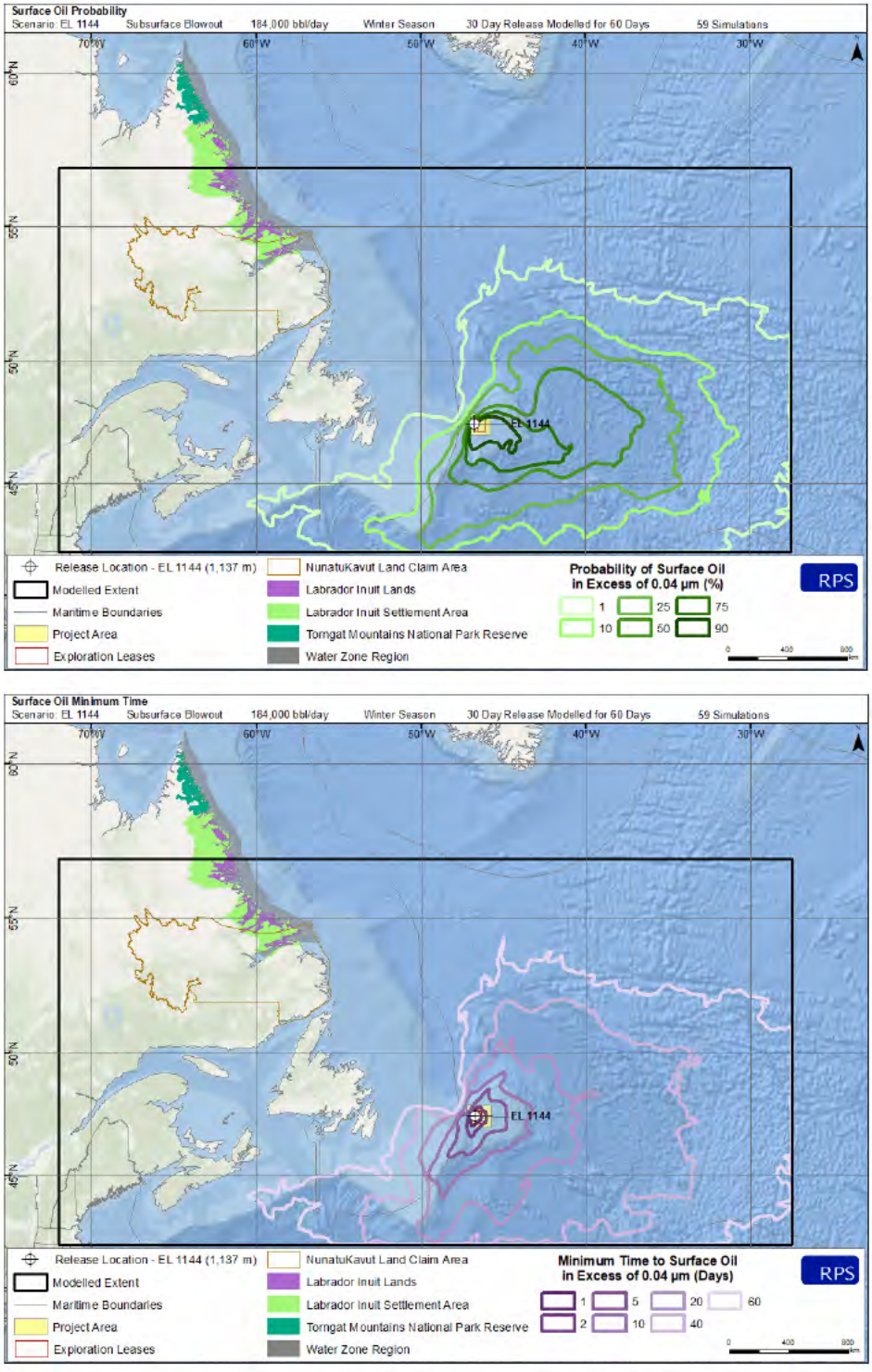

Figure 4-2. Winter probability of surface oil thickness > 0.04 µm (top) and minimum time to threshold exceedance (bottom) resulting from a 30-day subsurface blowout at EL 1144 example well site.

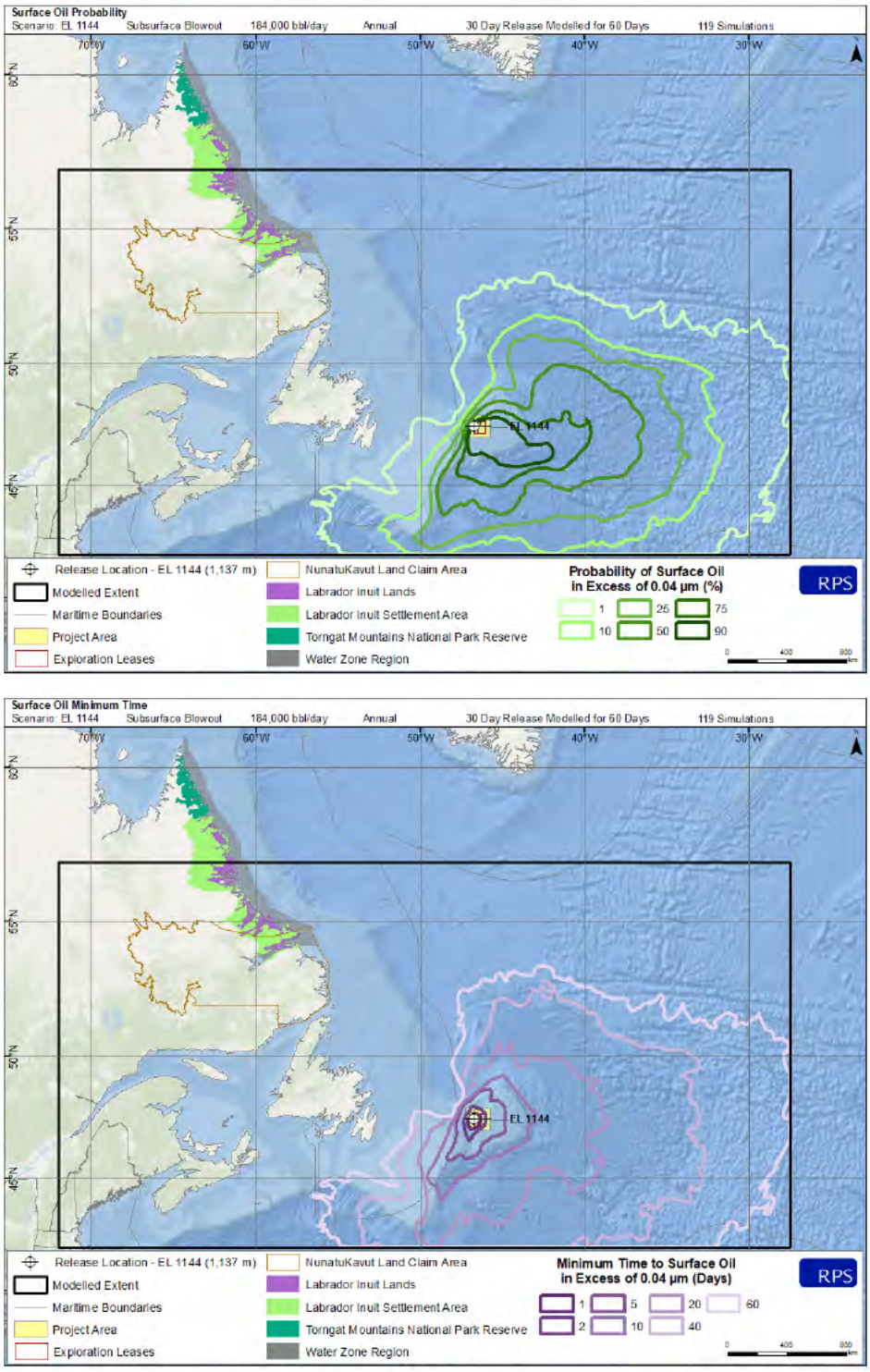

Figure 4-3. Annual probability of surface oil thickness > 0.04 µm (top) and minimum time to threshold exceedance (bottom) resulting from a 30-day subsurface blowout at EL 1144 example well site.

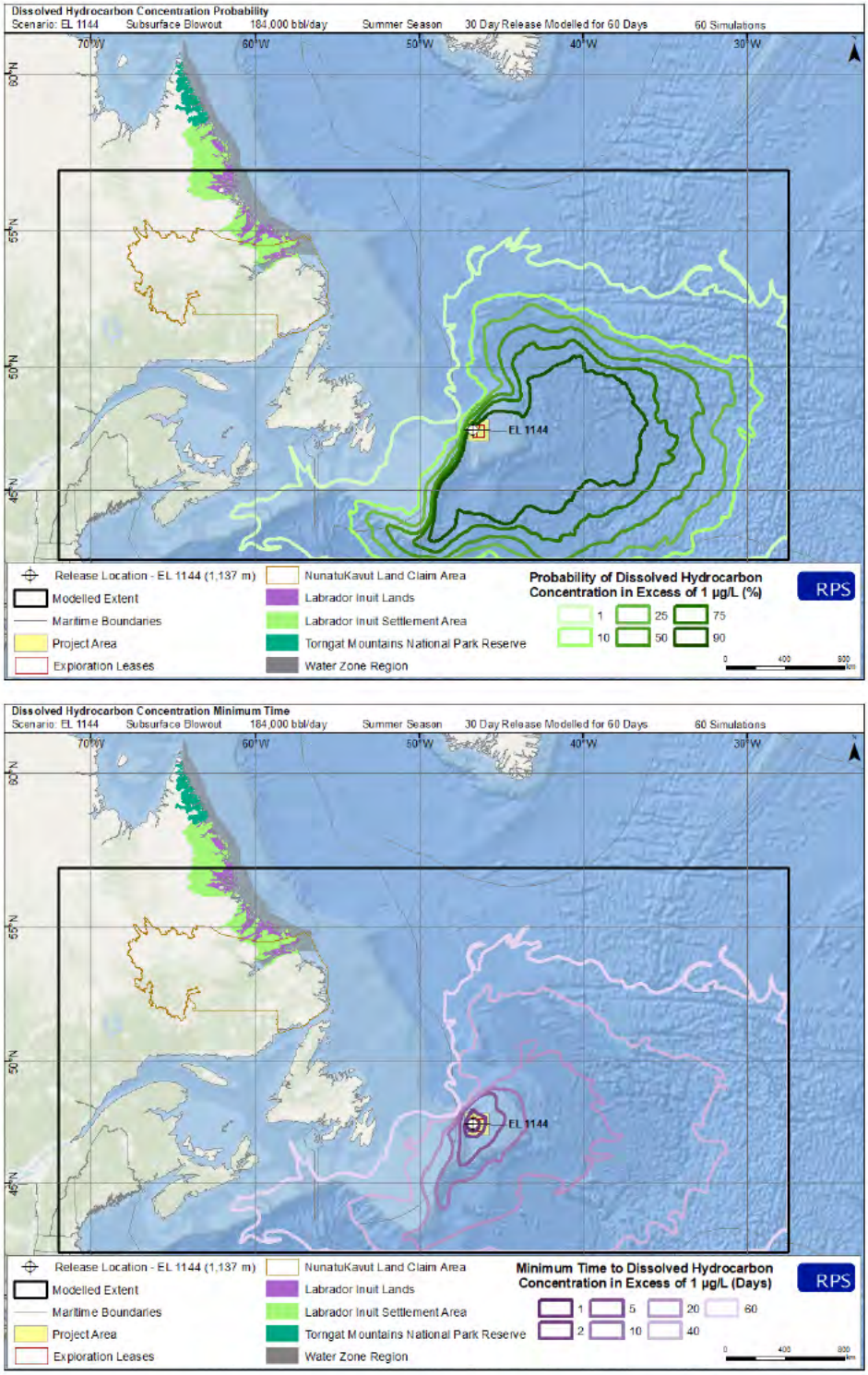

Figure 4-4. Summer probability of dissolved hydrocarbon concentrations > 1 µg/L at some depth in the water column (top) and minimum time to threshold exceedance (bottom) resulting from a 30-day subsurface blowout at EL 1144 example well site.

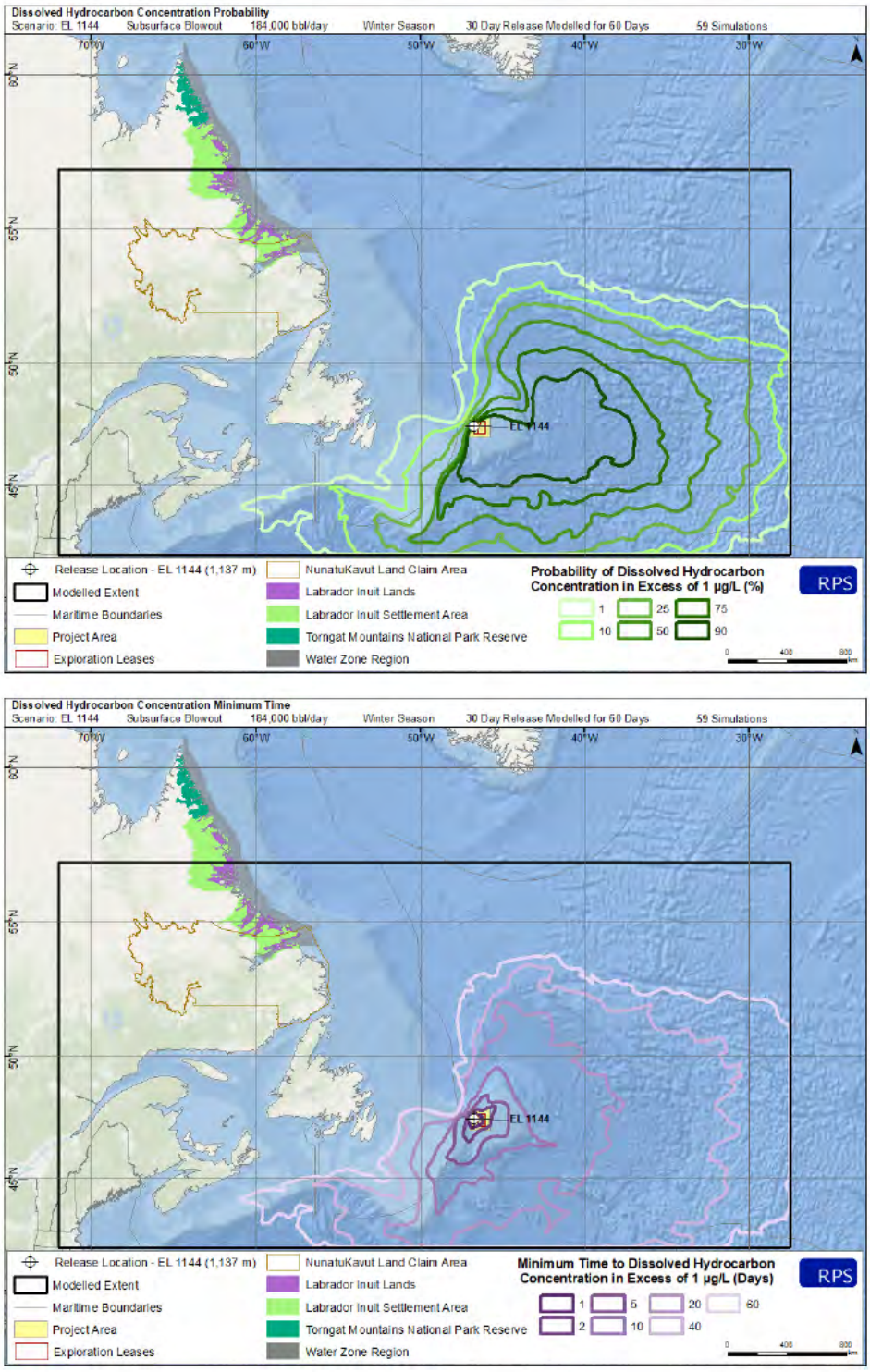

Figure 4-5. Winter probability of dissolved hydrocarbon concentrations > 1 µg/L at some depth in the water column (top) and minimum time to threshold exceedance (bottom) resulting from a 30-day subsurface blowout at EL 1144 example well site.

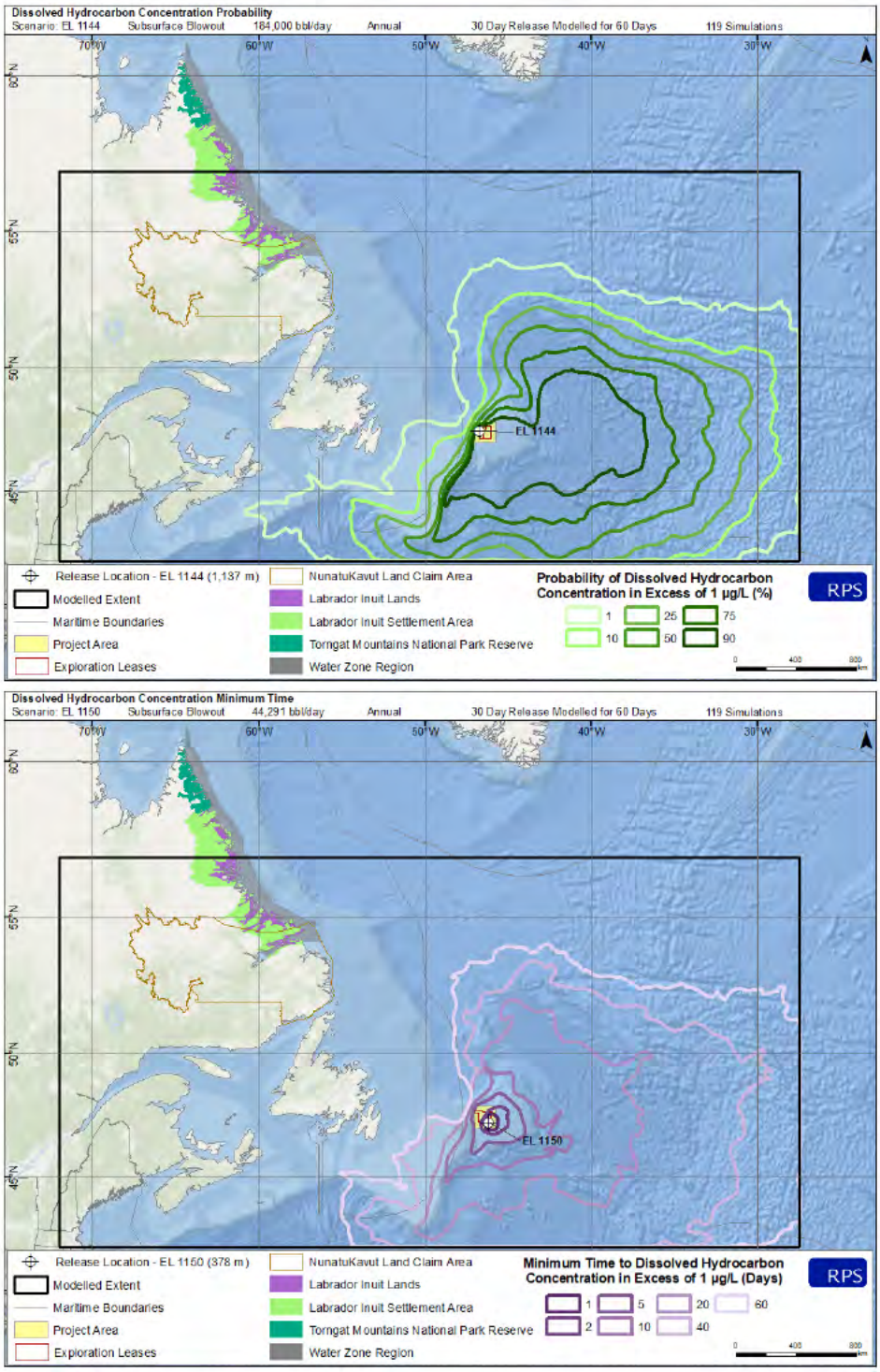

Figure 4-6. Annual probability of dissolved hydrocarbon concentrations > 1 µg/L at some depth in the water column (top) and minimum time to threshold exceedance (bottom) resulting from a 30-day subsurface blowout at EL 1144 example well site.

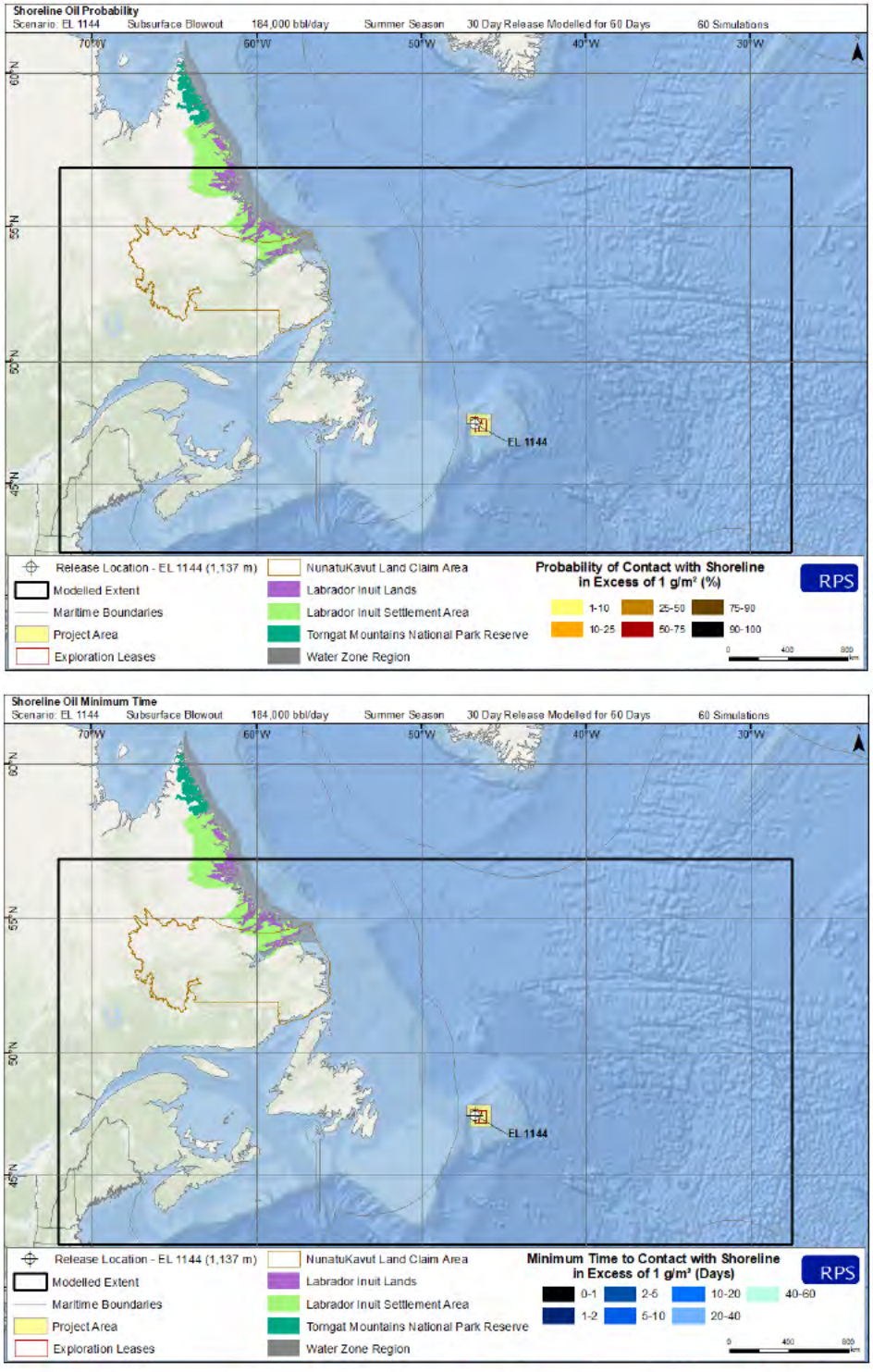

Figure 4-7. Summer probability of shoreline contact > 1 g/m² (top) and minimum time to threshold exceedance (bottom) resulting from a 30-day subsurface blowout at EL 1144 example well site. No shoreline contact was predicted for this scenario example well site.

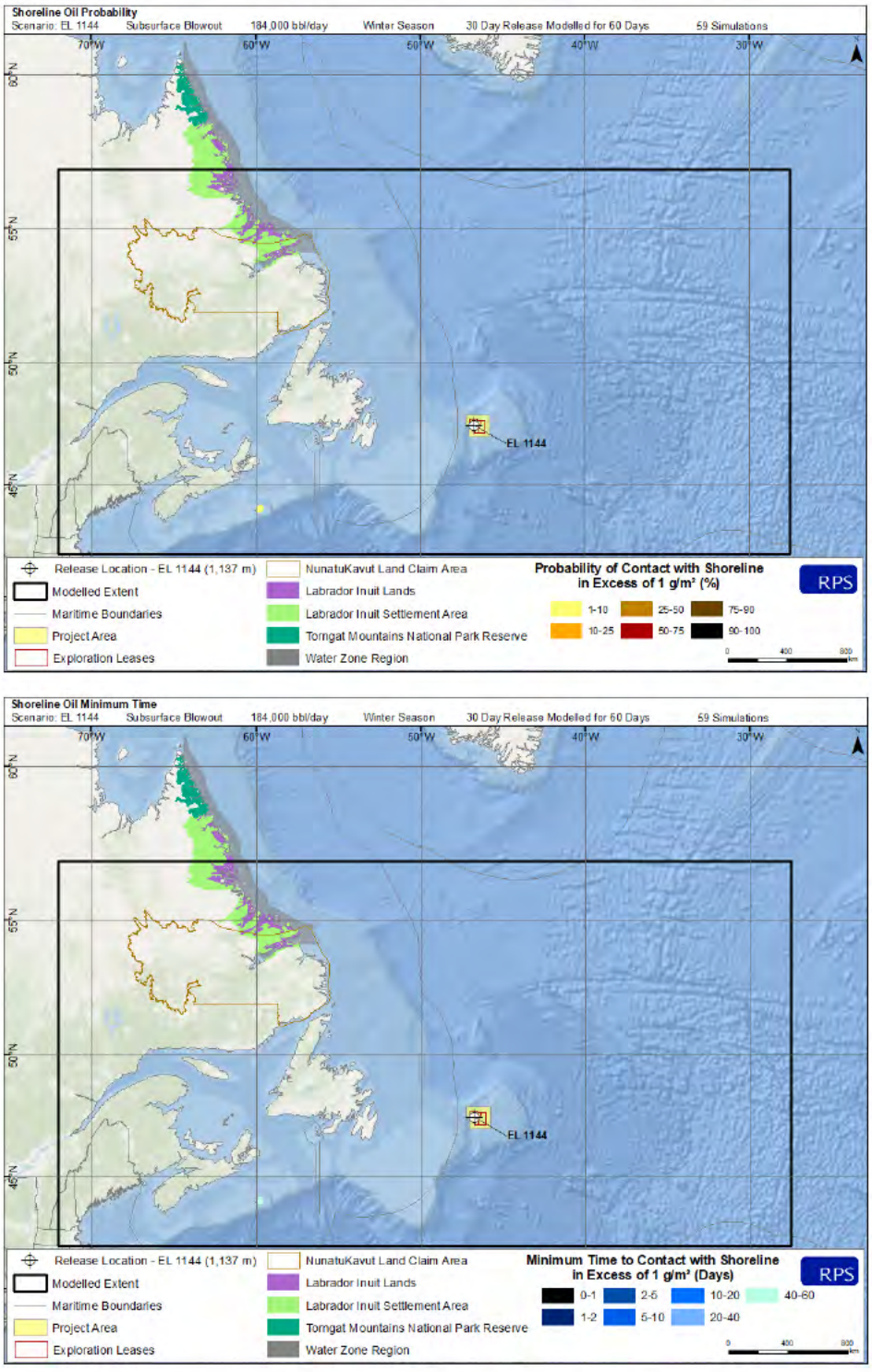

Figure 4-8. Winter probability of shoreline contact > 1 g/m^2 (top) and minimum time to threshold exceedance (bottom) resulting from a 30-day subsurface blowout at EL 1144 example well site.

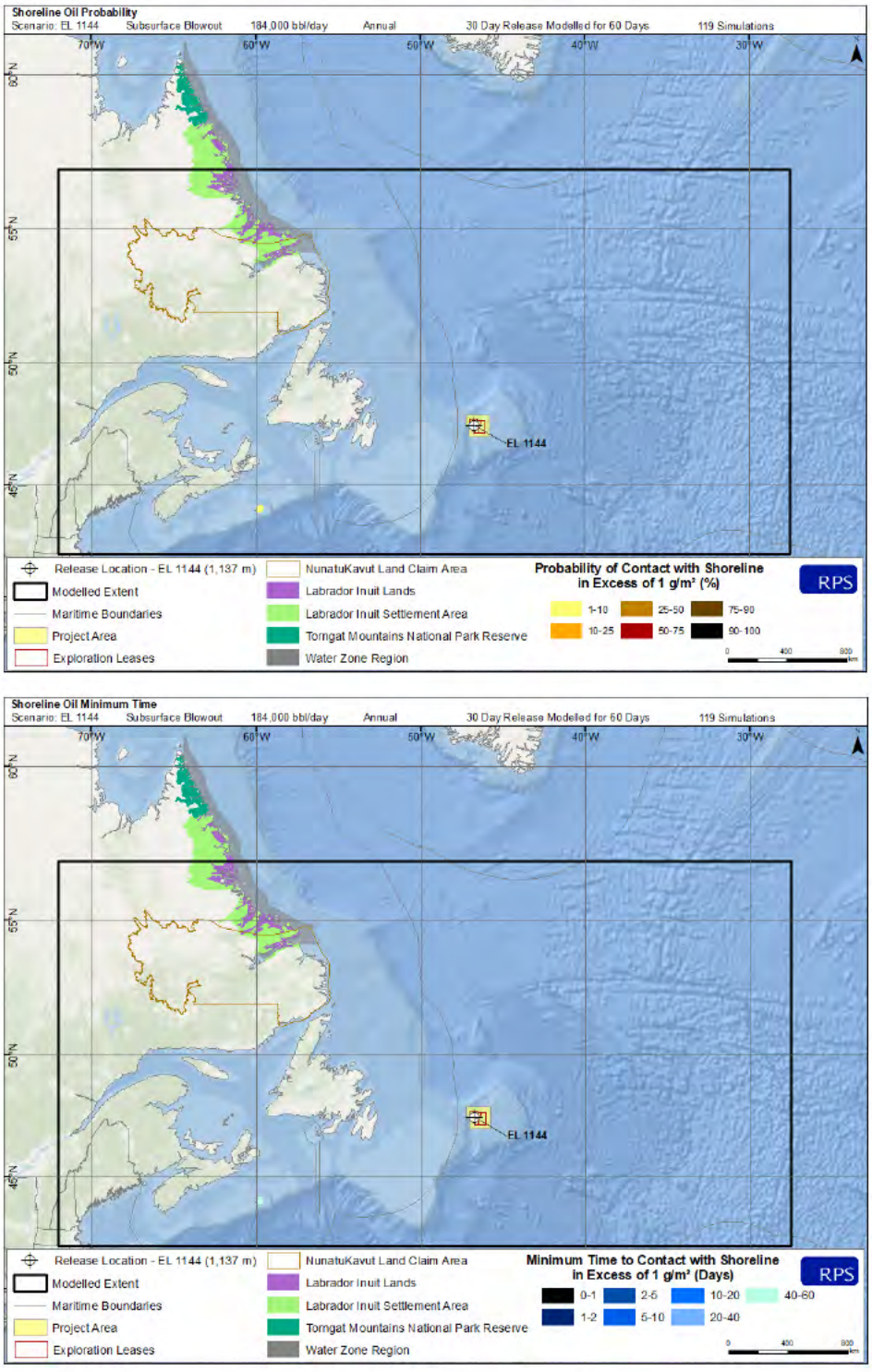

Figure 4-9. Annual probability of shoreline contact > 1 g/m^2 (top) and minimum time to threshold exceedance (bottom) resulting from a 30-day subsurface blowout at EL 1144 example well site.

4.1.2 EL 1150 Example Well Release Site

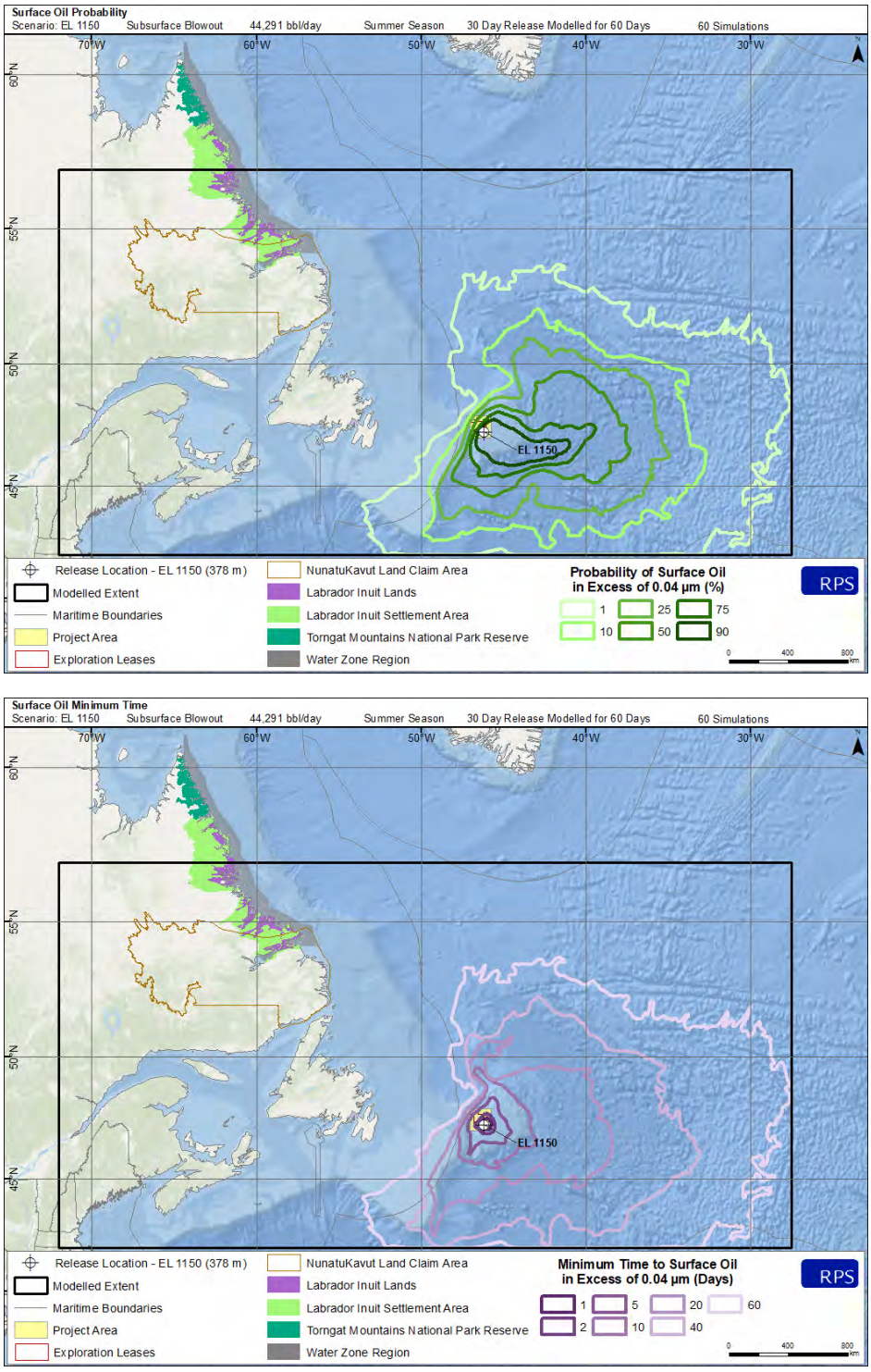

Figure 4-10. Summer probability of surface oil thickness > 0.04 µm (top) and minimum time to threshold exceedance (bottom) resulting from a 30-day subsurface blowout at EL 1150 example well site.

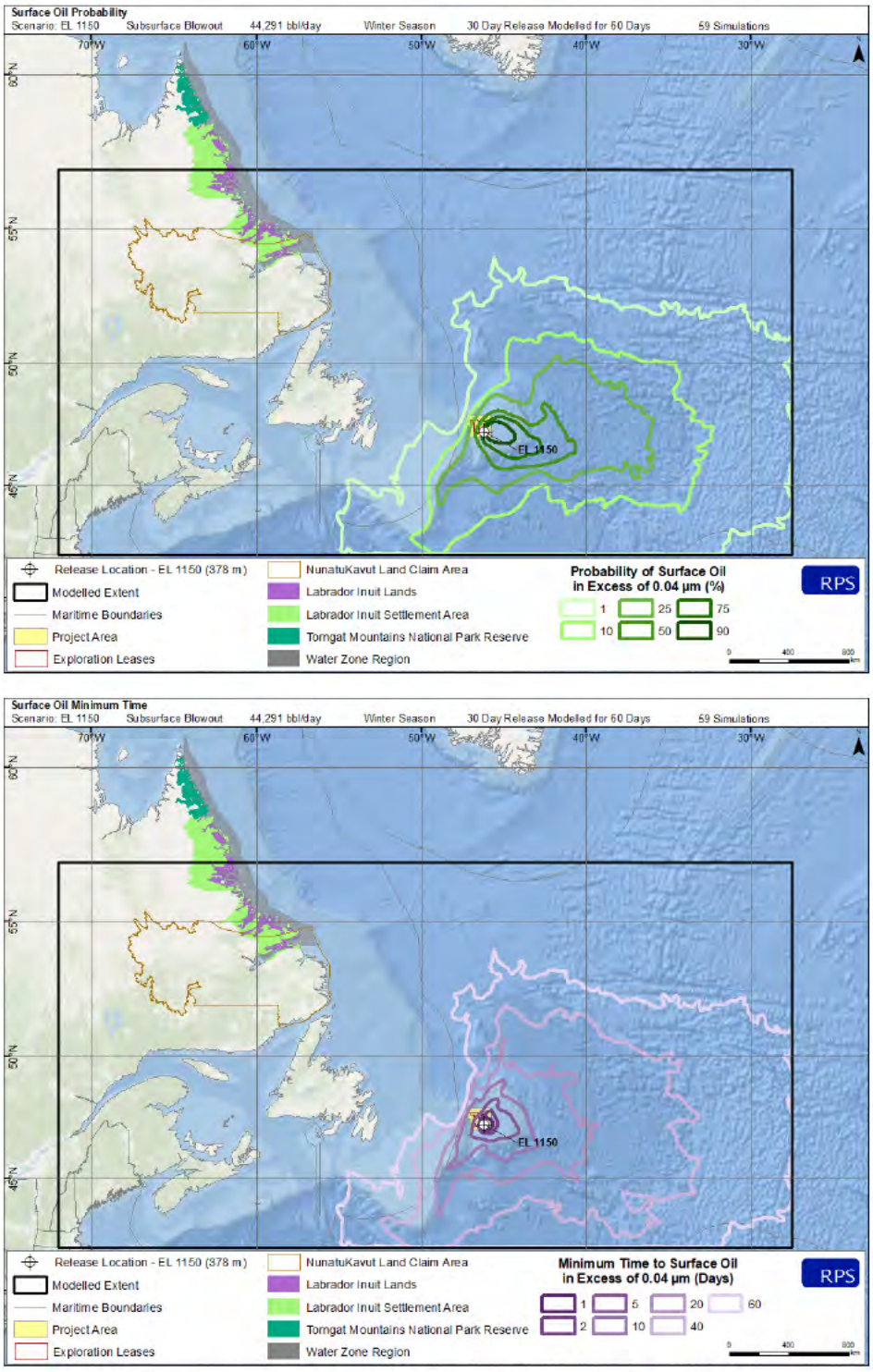

Figure 4-11. Winter probability of surface oil thickness > 0.04 µm (top) and minimum time to threshold exceedance (bottom) resulting from a 30-day subsurface blowout at EL 1150 example well site.

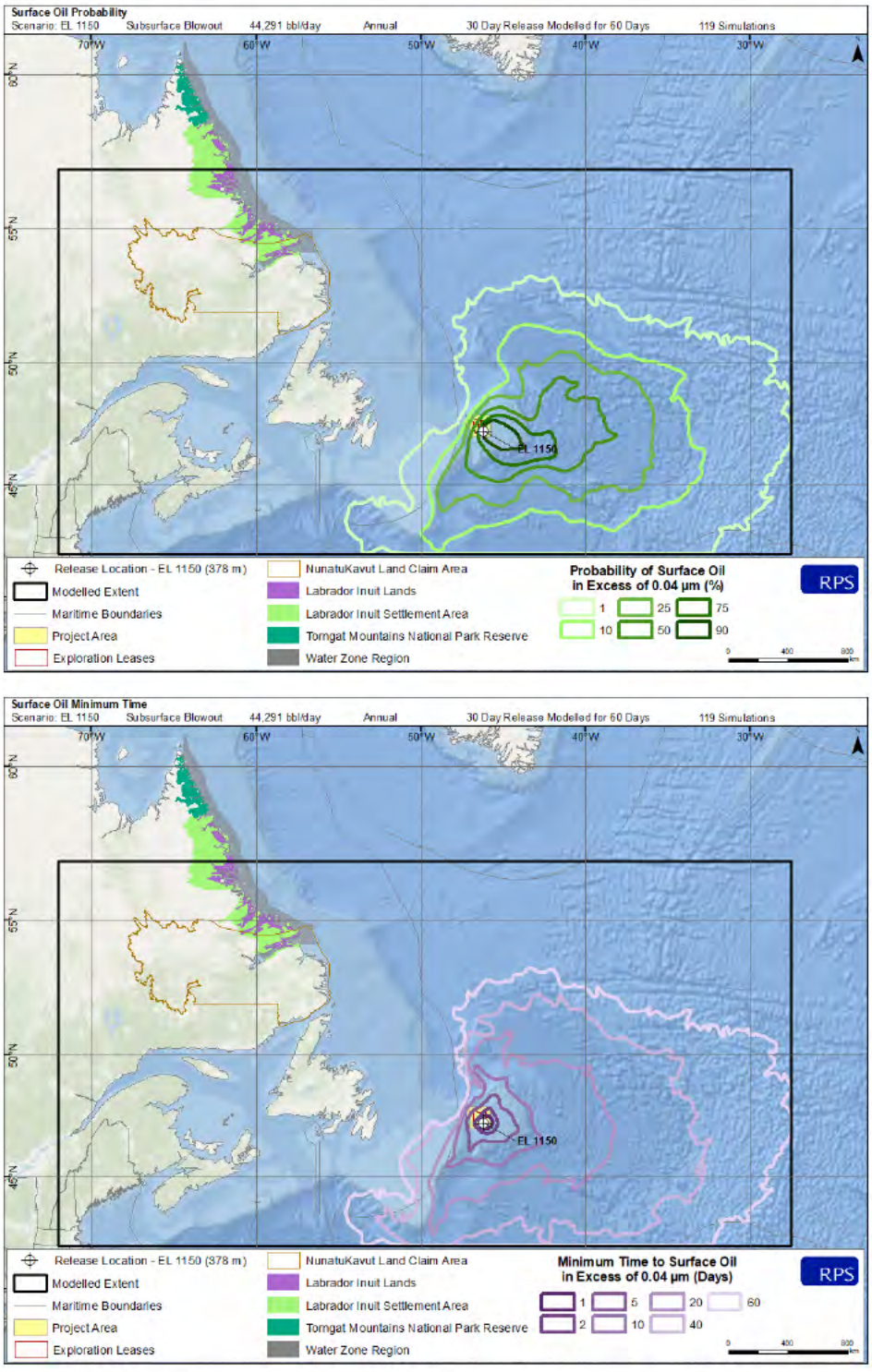

Figure 4-12. Annual probability of surface oil thickness > 0.04 µm (top) and minimum time to threshold exceedance (bottom) resulting from a 30-day subsurface blowout at EL 1150 example well site.

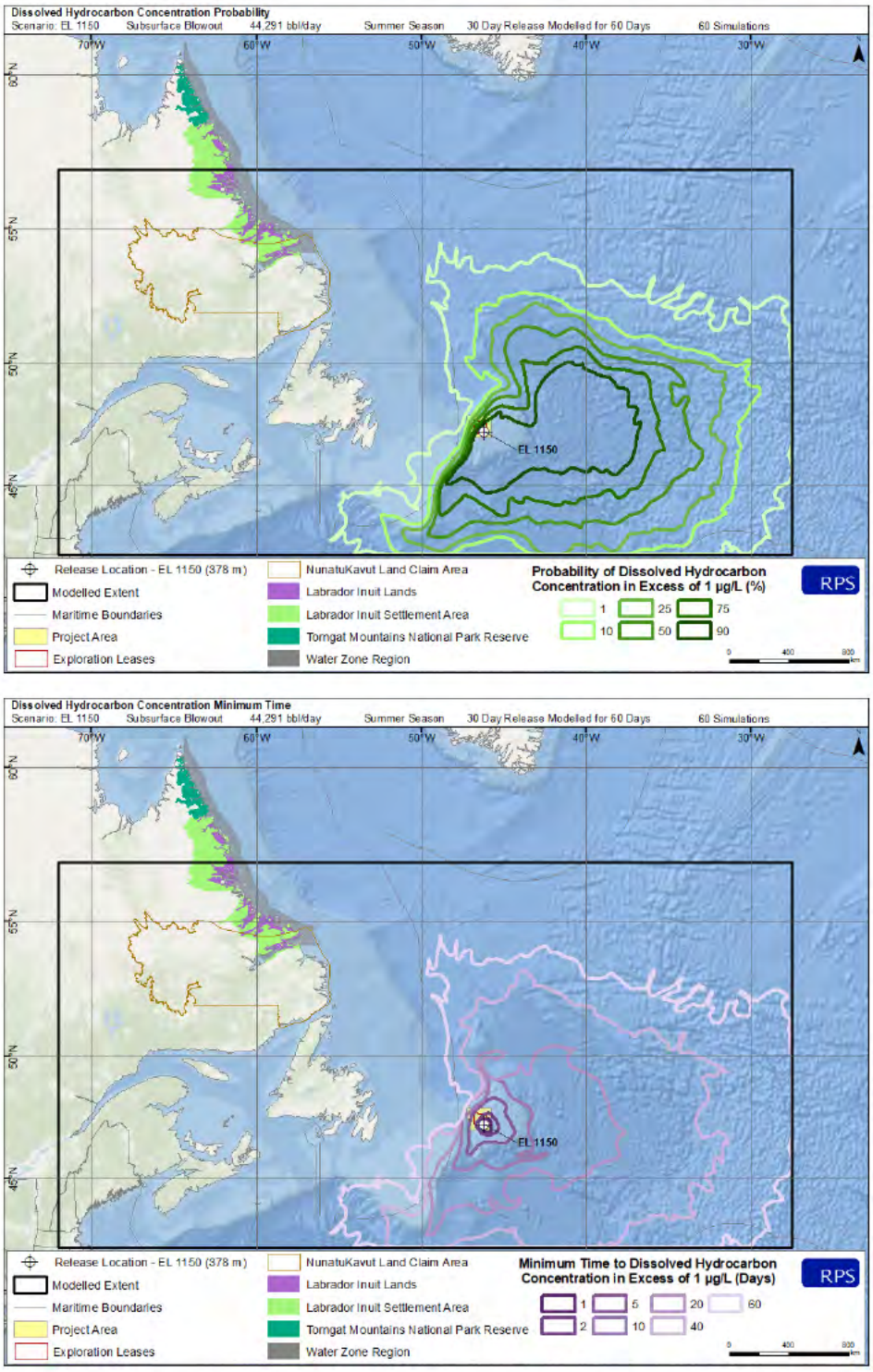

Figure 4-13. Summer probability of dissolved hydrocarbon concentrations > 1 µg/L at some depth in the water column (top) and minimum time to threshold exceedance (bottom) resulting from a 30-day subsurface blowout at EL 1150 example well site.

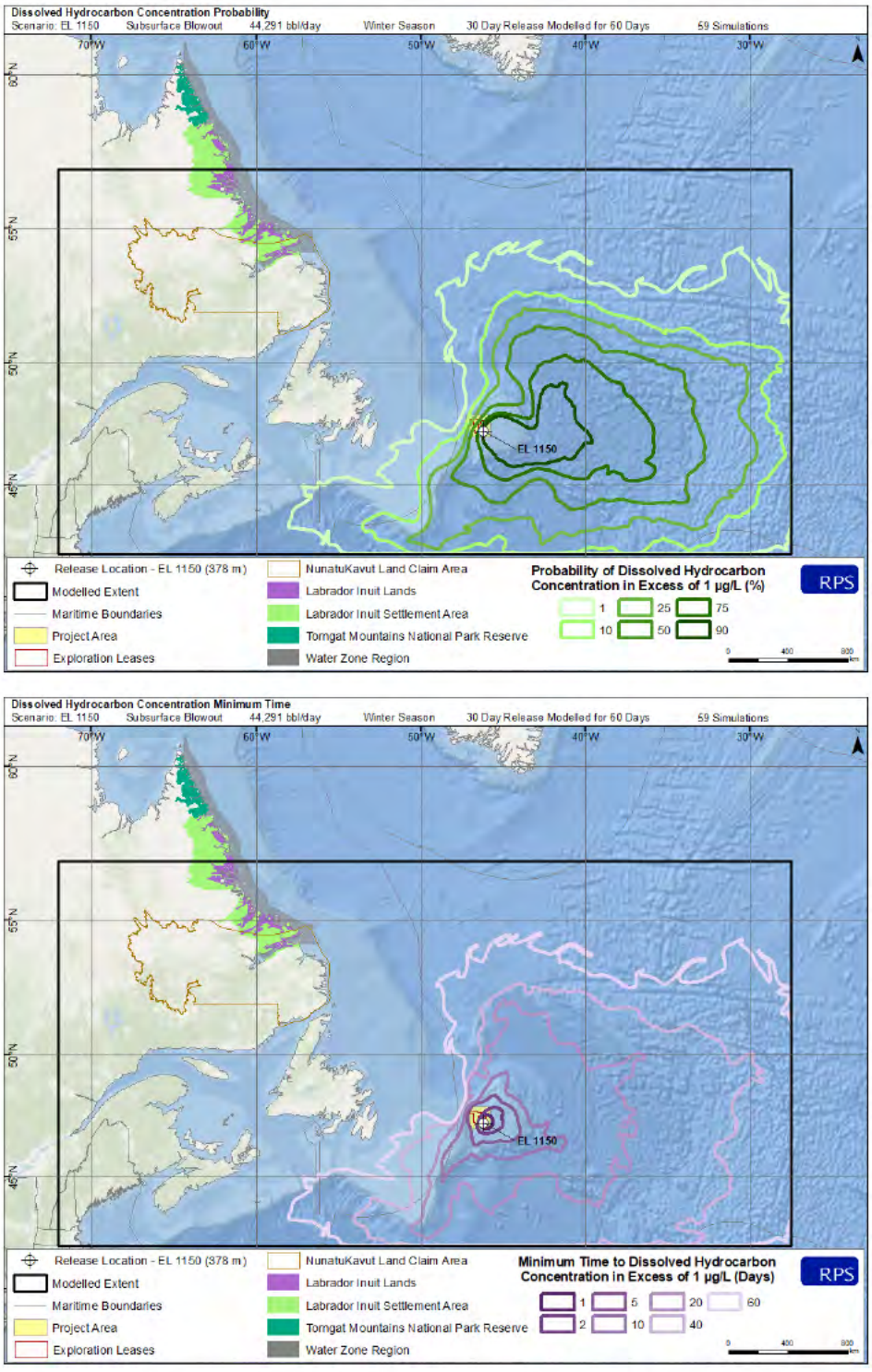

Figure 4-14. Winter probability of dissolved hydrocarbon concentrations > 1 µg/L at some depth in the water column (top) and minimum time to threshold exceedance (bottom) resulting from a 30-day subsurface blowout at EL 1150 example well site.

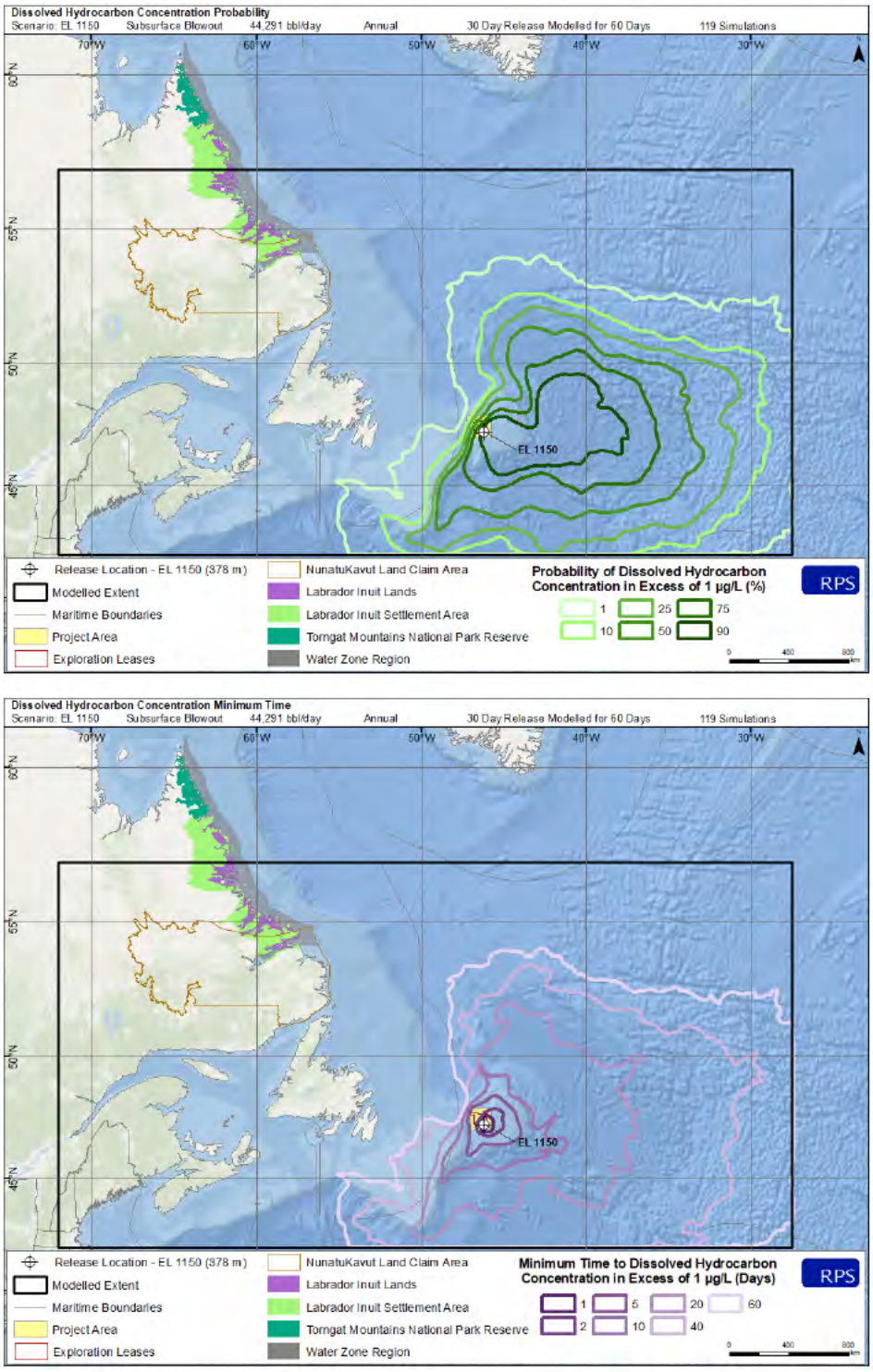

Figure 4-15. Annual probability of dissolved hydrocarbon concentrations > 1 µg/L at some depth in the water column (top) and minimum time to threshold exceedance (bottom) resulting from a 30-day subsurface blowout at EL 1150 example well site.

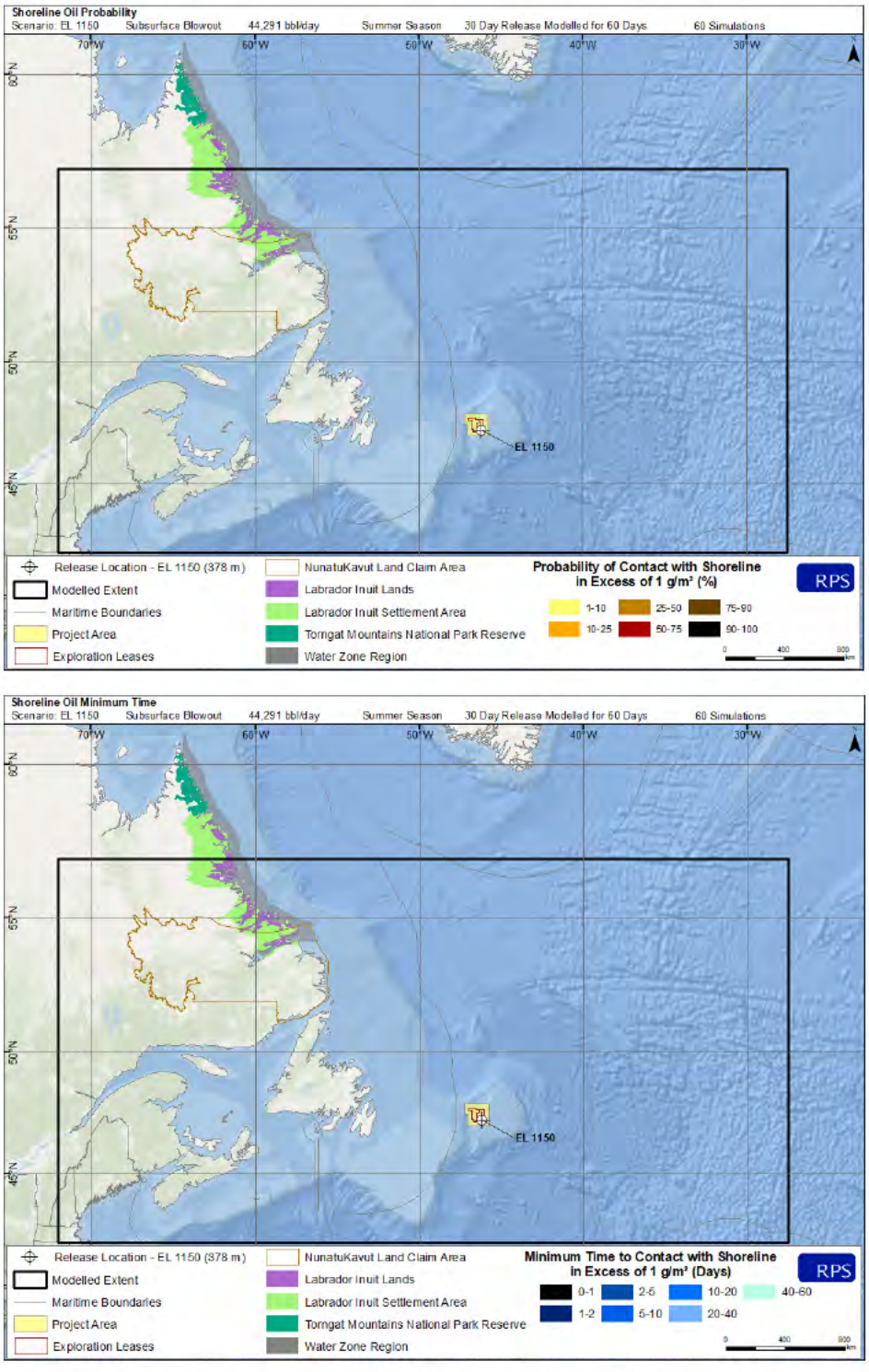

Figure 4-16. Summer probability of shoreline contact > 1 g/m² (top) and minimum time to threshold exceedance (bottom) resulting from a 30-day subsurface blowout at EL 1150 example well site. No shoreline contact was predicted for this scenario.

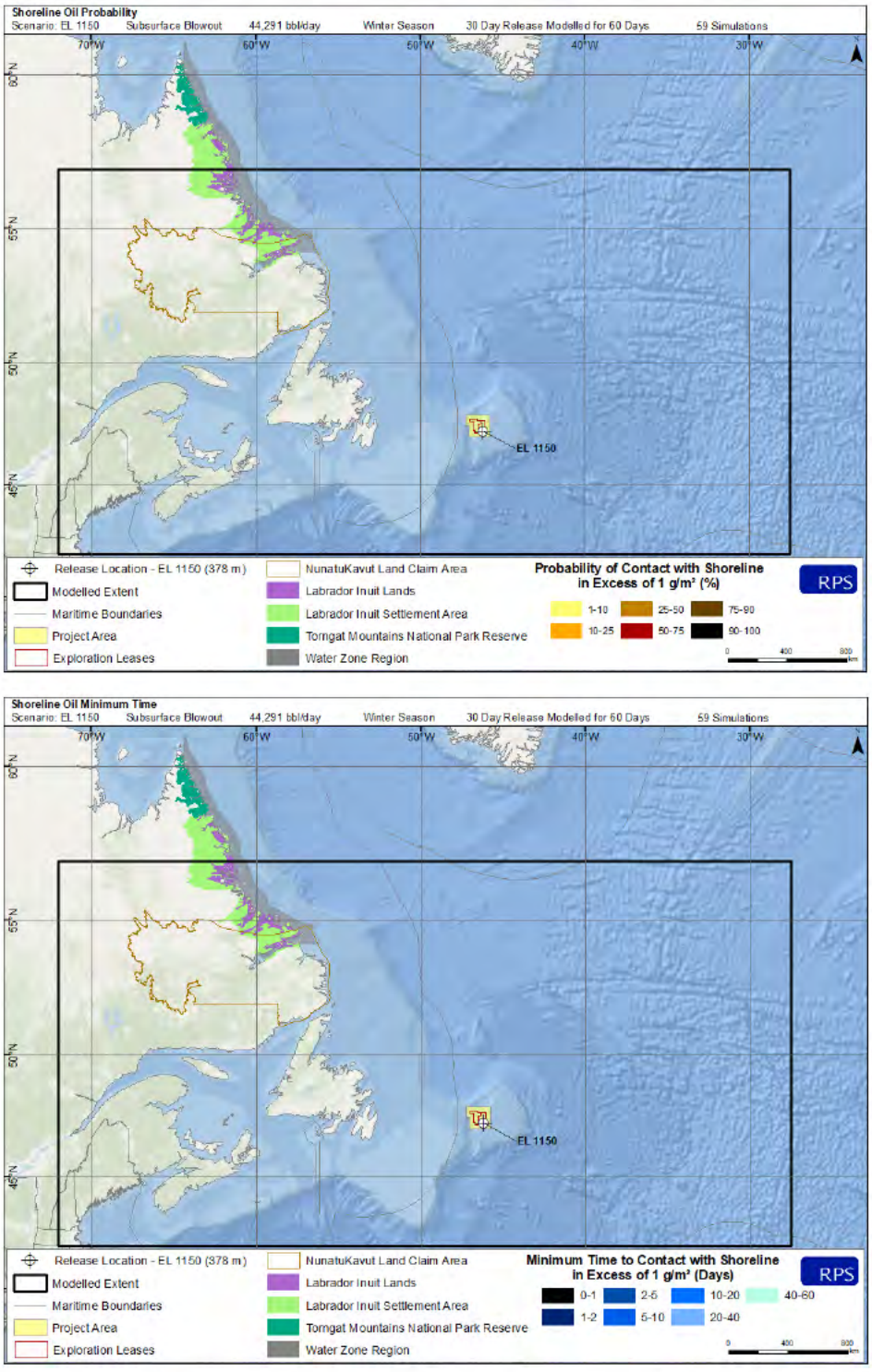

Figure 4-17. Winter probability of shoreline contact > 1 g/m² (top) and minimum time to threshold exceedance (bottom) resulting from a 30-day subsurface blowout at EL 1150 example well site. No shoreline contact was predicted for this scenario.

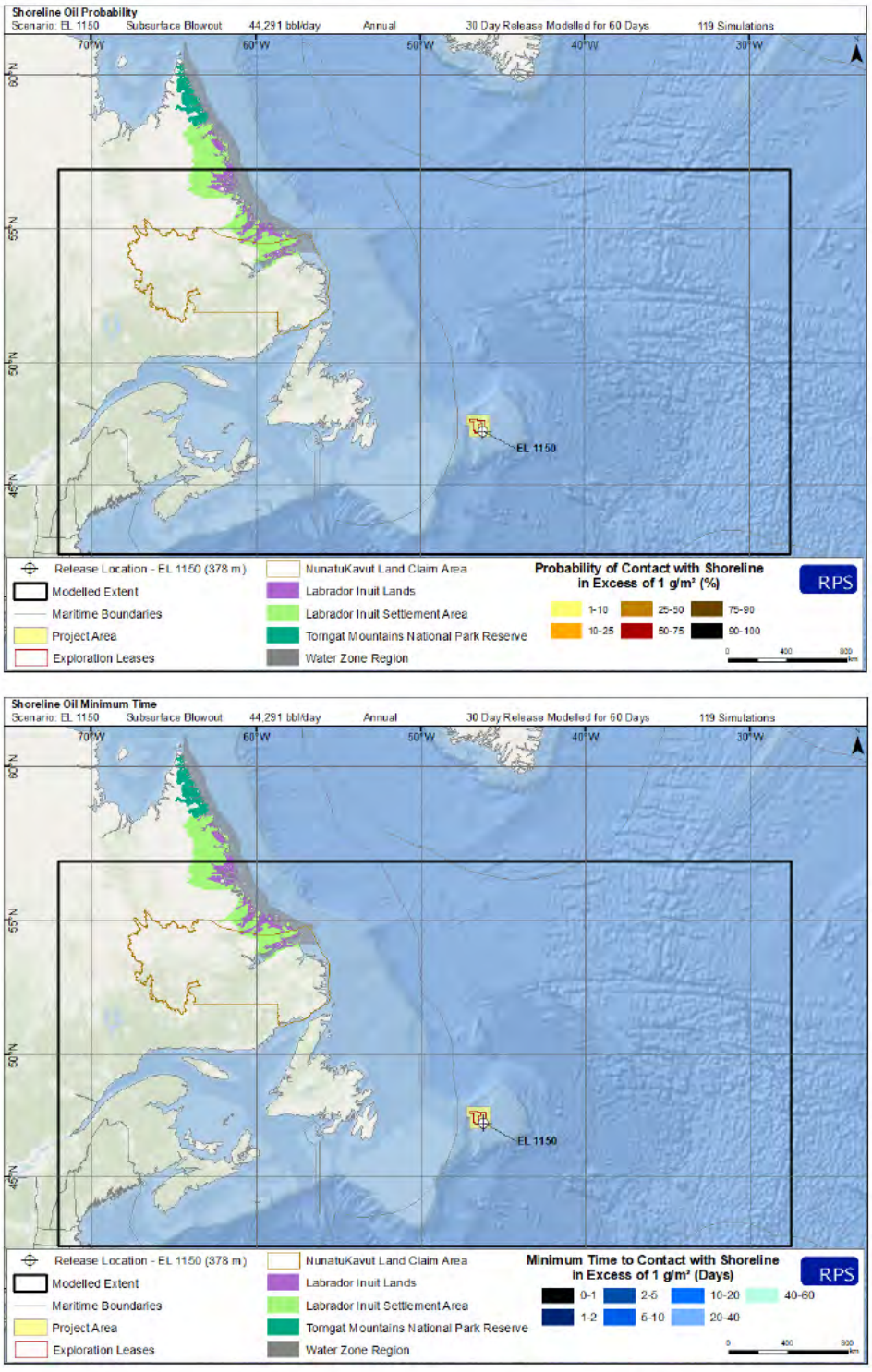

Figure 4-18. Annual probability of shoreline contact > 1 g/m^2 (top) and minimum time to threshold exceedance (bottom) resulting from a 30-day subsurface blowout at EL 1150 example well site. No shoreline contact was predicted for this scenario.

4.1.3 Summary of Stochastic Results

A total of 119 individual model runs were conducted for the statistical analysis for each modelled release at the EL 1144 and EL 1150 hypothetical example well release sites, representing subsurface blowouts (30-day) in waters offshore of Newfoundland. Two 30-day releases were modelled at the EL 1144 (1,137 m) and EL 1150 (378 m) example well sites to represent the amount of time required to respond and secure the source of a spill were modelled for a total of 60 days.

Summaries of the stochastic analyses of potential surface oil exposure and water column contamination by dissolved hydrocarbons depict areas with the highest potential likelihood (>90%) to exceed thresholds primarily to the east and south of the release sites. Much lower probabilities of threshold exceedance are predicted to the north and east (generally <25%) (Figure 4-1 through Figure 4-15). Releases were predicted to have potential effects on Canadian and International waters. In many cases, oil contamination above the identified threshold was predicted to extend beyond the extent of the model domain to the east and south. In these scenarios, the environmental forcing mechanisms (i.e., wind and currents) and long timeframe modelled (60 days) allowed for the transport of highly weathered oil (>50 days old) outside of the model domain.

The hypothetical 30-day release at the EL 1144 example well site (see figures in Section 4.1.1) was predicted to lead to a larger stochastic surface oil probability footprint, where oil may exceed the 0.04 µm thickness threshold in >1% of releases, when compared to the release at the EL 1150 example well site (Table 4-1) due to the larger release volume (5,520,000 bbl at the EL 1144 example well site vs. 1,329,000 bbl at the EL 1150 example well site). The > 90% probability footprints threshold exceedances were predicted to extend to the south and east of EL 1144 approximately 300-600 km for surface oil and 800-1,200 km for in water contamination (Figure 4-1 through Figure 4-6). For the EL 1150 example well site, the surface oil extents were closer to 200-400 km and in water contamination closer to 400-800 km (Figure 4-10 through Figure 4-15). Predicted threshold exceedance footprints were typically similar in size for each release location between seasons, however the surface oil exceedance was larger in the summer, due to calmer winds resulting in less entrainment and therefore more surface oil (Table 4-1). The larger release volume at the EL 1144 example well site resulted in larger surface oil and in water contamination predictions, then EL 1150. EL 1144 is located closer to shore than the EL 1150 example well site and was therefore predicted to result in a small probability (<3%) of shoreline oil contamination at Sable Island within 60 days (Figure 4-8 and Figure 4-9). Releases at the EL 1150 example well site were not predicted to make contact with the shore (Figure 4-16 through Figure 4-18.

General findings were very similar for the EL 1144 example well site, when compared to the EL 1150 example well site, especially for the lowest probability contours. However, the hypothetical releases at

the EL 1144 example well site were deeper, farther offshore, and had a release volume that was over 4 time larger than those at EL 1150, resulting in much larger predicted areas for the 10% and 90% likelihood of threshold exceedance (Table 2-1).

As stated previously, stochastic figures do not imply that the entire contoured area would be covered with oil in the event of a single release, nor do they provide any information on the quantity of oil in each area. The large threshold exceedance footprints in annual results are not the expected exposure from any single release of oil, but rather areas where there is >1% probability that exposure above the threshold could occur, based on the combination of either 119 (annual), 60 (summer), or 59 (winter) individual releases analyzed together.

The oil that was predicted to make contact with shorelines would be expected to be highly weathered, as minimum time estimates for first shoreline oil exposure ranged from approximately 52-53 days (Table 4-2). The oil that did make its way to shore would likely be patchy and discontinuous. Oil from the subsurface releases was transported by subsurface currents, which had a higher potential to transport subsurface oil to the west and southwest prior to surfacing than did surface currents.

Table 4-1. Summary of areas of with potential threshold exceedance (km²) for surface, water column, and shoreline oil at each site (EL 1144 and EL 1150 example well sites). Areas are displayed by season (annual, winter, summer) and by the size of the regions within the modelled domain that had >1%, 10%, or 90% likelihood of exposure to oil.

Stochastic Scenario Parameters				Areas Exceeding Threshold (km²)		
Component and Threshold	Scenario	Example Well Site	Probability Contour or Bin*	Annual Results	Winter (ice cover)	Summer (ice-free)
Surface Oil > 0.04 µm, on average	30-day release	EL 1144 (184,000 bpd)	1%	1,942,000	2,102,000	1,927,000
			10%	1,140,000	1,115,000	1,145,000
			90%	56,100	24,750	128,300
		EL 1150 (44,291 bpd)	1%	1,783,000	1,945,000	1,776,000
			10%	849,200	789,900	899,300
			90%	16,750	10,180	51,470
Water Column Dissolved Hydrocarbons > 1 µg/L at some depth within the water column	30-day release	EL 1144 (184,000 bpd)	1%	223,600	215,100	2,346,000
			10%	162,000	171,900	1,513,000
			90%	32,950	26,810	456,000
		EL 1150 (44,291 bpd)	1%	210,100	225,000	203,500
			10%	146,000	155,800	136,200
			90%	18,550	10,610	28,790
Shoreline Oil > 1 g/m², on average	30-day release	EL 1144 (184,000 bpd)	1 - 5%	9	18	-
			5 - 15%	-	-	-
			15 - 35%	-	-	-
		EL 1150 (44,291 bpd)	1 - 5%	-	-	-
			5 - 15%	-	-	-
			15 - 35%	-	-	-

*Bins are based on stochastic probabilities; for example, 56,100 km² of the ocean surface is predicted to exceed the 0.04 µm surface oil threshold in 90% of the 119 modelled simulations over the entire modelled duration.

Table 4-2. Shoreline contamination probabilities and minimum time for oil exposure exceeding 1 g/m^2.

Scenario	Example Well Release Site	Scenario Timeframe	Average Probability of Shoreline Oil Contamination (%)	Maximum Probability of Shoreline Oil Contamination (%)	Minimum Time to Shore (days)	Maximum Time to Shore (days)
30-day release	EL 1144 (184,000 bpd)	Annual	2	2	52	54
		Winter	2.5	3	53	54
		Summer	-	-	-	-
	EL 1150 (44,291 bpd)	Annual	-	-	-	-
		Winter	-	-	-	-
		Summer	-	-	-	-

4.2 Deterministic Analysis Results

Five individual trajectories of interest were selected from the stochastic ensemble of results for the deterministic analysis (see Table 2-5 in Section 2.3). The deterministic trajectory and fate simulations provided an estimate of the oil's transport through the environment as well as its physical and chemical behavior for a specific set of environmental conditions. The 95th percentile results for surface oil exposure and water column dissolved hydrocarbon concentrations were identified from the stochastic model scenarios for each site. For the EL 1144 example well site, the 99th percentile shoreline results were used in the deterministic analysis, as the 95th percentile release did not result in any shoreline oiling. A representative shoreline case for the EL 1150 example well site was not selected, as no oil was predicted to make contact with shorelines within 60 days. In addition to the five deterministic spill scenarios of subsurface releases, two cases representing 100 L and 1,000 L batch releases of marine diesel from surface vessels were modelled at the EL 1144 example well site and one additional case representing a vessel collision was modelled at the VCL.

The following sections contain figures corresponding to each identified representative case and tables summarizing the areas exceeding specified thresholds. During modelling, components of oil were tracked as floating surface oil, entrained droplets of oil, dissolved hydrocarbon constituents, and stranded shoreline oil. The figures provided display the cumulative footprint of all oil experienced by a region over the entire 60-day duration of modelling. Therefore, the footprints are much larger than the amount of oil predicted to be present in a region at any given point in time. This concept is illustrated in Figure 4-19, which portrays average surface oil thickness in each grid cell at five specific time steps (days 1, 5, 15, 30, and 60) during the 95th percentile surface oil thickness case, and in Figure 4-20, which portrays the cumulative maximum footprint (over 60 days) of average surface oil thickness experienced

at any of the modelled individual time steps. The remaining figures in this report display the cumulative footprints of oil exposure over the entire model duration.

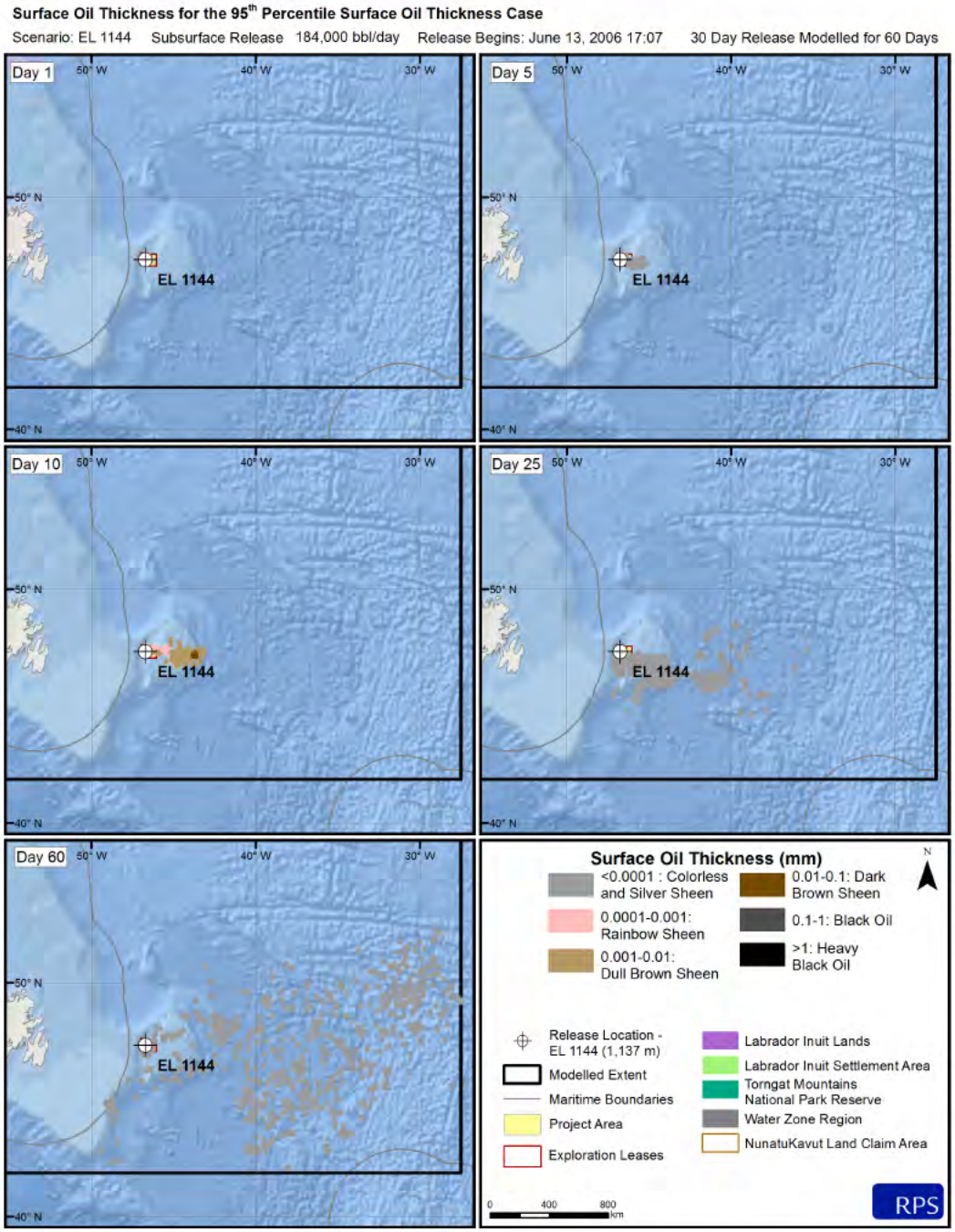

Figure 4-19. Average surface oil thickness for the 95th percentile surface oil exposure case of a 30-day blowout at the EL 1144 example well site at days 1, 5, 15, 30, and 60 to illustrate the variation in size of the surface oil footprint over the course of the model duration.

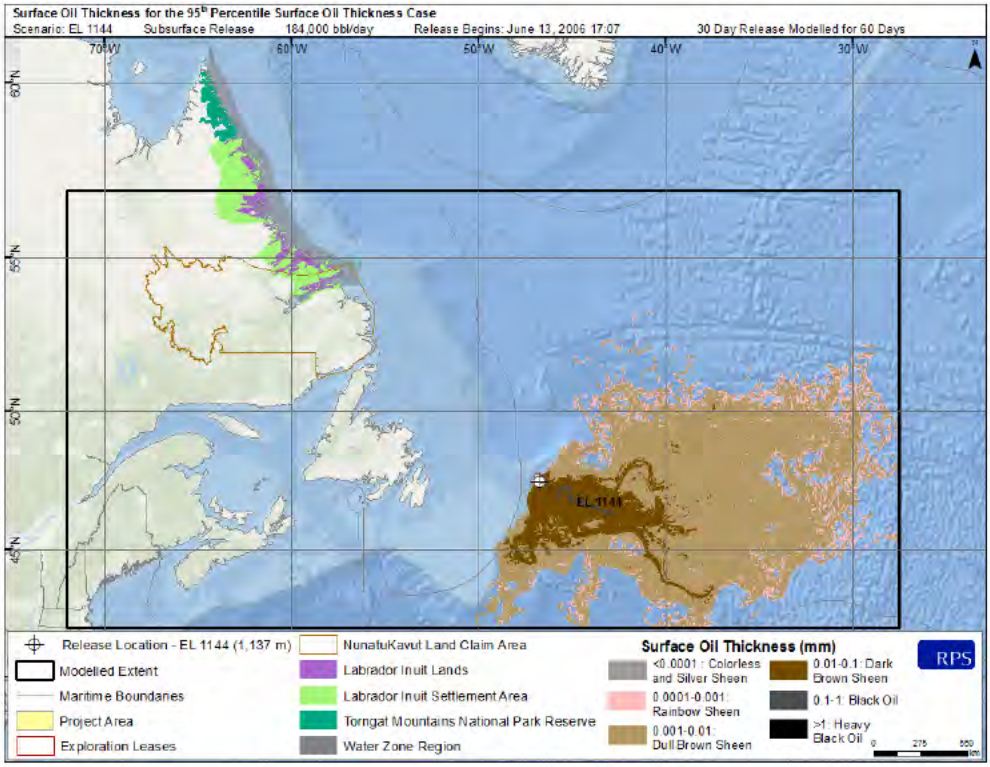

Figure 4-20. Average surface oil thickness for the 95th percentile surface oil exposure case of a 30-day blowout at the EL 1144 example well site to illustrate the much larger size of the cumulative surface oil footprint over the entire model duration, compared to the size of the surface oil footprint on any one day or time step.

The types of figures that were used to summarize modelling results are provided, along with brief descriptions of the information that they portray.

1. **Mass Balance Plots**: Illustrate the predicted weathering and fate of oil for a specific run over the entire model duration as a fraction of the oil released up to that point. Components of the oil tracked over time include the amount of oil on the sea surface, the total entrained hydrocarbons in the water column, amount of oil in contact with the shore, oil evaporated into the atmosphere, and that which has degraded (accounts for both photo-oxidation and biodegradation).
2. **Surface Oil Thickness Maps:** Depict the predicted footprint of maximum floating surface oil and the associated oil thicknesses (mm) over all modelled time steps for an individual release simulation.
3. **Water Column Dissolved Hydrocarbon Concentration Maps**: Depict the predicted footprint of the vertical maximum water column concentration of dissolved hydrocarbons over all modelled time steps for an individual release simulation. Dissolved hydrocarbons are the constituents of the oil with the greatest potential to affect water column biota. Only

concentrations above 1 µg/L for the representative cases are displayed (see Table 2-2). For the marine diesel "batch spills", the volumes released were insufficient to produce dissolved hydrocarbon footprints at the gridded resolution used (the dissolved hydrocarbons comprise roughly 1% of total hydrocarbons released). Therefore, total hydrocarbon concentrations in the water column are displayed instead of the dissolved hydrocarbons.

4. **Water Column Total Hydrocarbon Concentration Maps:** Depict the predicted footprint of the vertical maximum water column concentration of total hydrocarbons over all modelled time steps for an individual release simulation. Only concentrations above 1 µg/L for the representative cases are displayed (Table 2-2).
5. **Shoreline and Sediment Total Hydrocarbon Concentration Maps:** Depict the predicted total mass of oil (per unit area as g/m^2) deposited onto the shoreline and on sediments.

4.2.1 Surface Oil Exposure Cases

Results for the identified 95th percentile scenarios for floating surface oil exposure > 0.04 µm for the 30-day releases at the EL 1144 and EL 1150 example well sites are provided. Note that the modelled release dates for the representative scenarios at each site differed (Table 2-5). The 30-day release at the EL 1144 example well site was modelled for 60 days spanning mid-June through mid-August 2006, while at the EL 1150 example well site it spanned mid-April through mid-June 2007 (Table 2-5). For both sites, the released oil was predicted to rise rapidly to the surface where it spread, being transported by surface winds and currents forming patchy and discontinuous surface slicks (Figure 4-22). In both scenarios, surface oil was predicted to be thickest within several kilometers of the spill sites, with a visual appearance of heavy black oil and black oil. However, the light and low viscosity BdN was predicted to spread quickly to brown sheens and then dull brown sheens. Thicker oil was predicted over broader areas for the larger blowouts at the EL 1144 example well site, when compared to the EL 1150 example well site. The majority of both footprints were predicted to have a maximum thickness closer in appearance to a dull brown sheen. These surface oil footprints formed some of the largest predicted cumulative footprints over the 60-day simulations. The majority of the cumulative maximum surface expression was predicted to appear as a discontinuous dull brown sheen, with rainbow sheen possible on the outermost edges.

The combined effects of a subsurface release and the entrainment of surface oil into the water column by high winds, which induced surface breaking waves, was predicted to result in concentrations of dissolved and total hydrocarbons in the water column that exceed the identified thresholds (Figure 4-23 and Figure 4-24). Due to the larger release volume, the 30-day releases at the EL 1144 example well site were predicted to result in larger footprints of dissolved hydrocarbons and total hydrocarbon concentrations (THC), when compared to the EL 1150 example well site. Neither of the representative surface oil cases were predicted to result in oil contacting shorelines (Figure 4-25).

At the end of the 60-day surface oil exposure simulations at the EL 1144 and EL 1150 example well sites, <6% of the released volume was predicted to remain floating on the water surface, 41-42% evaporated into the atmosphere, 20-25% remained entrained in the water column, <0.02% adhered to suspended sediment, 0% contacted the shore, 32% degraded, and up to 2% was transported outside the modelled domain (Figure 4-21 and Table 4-3).

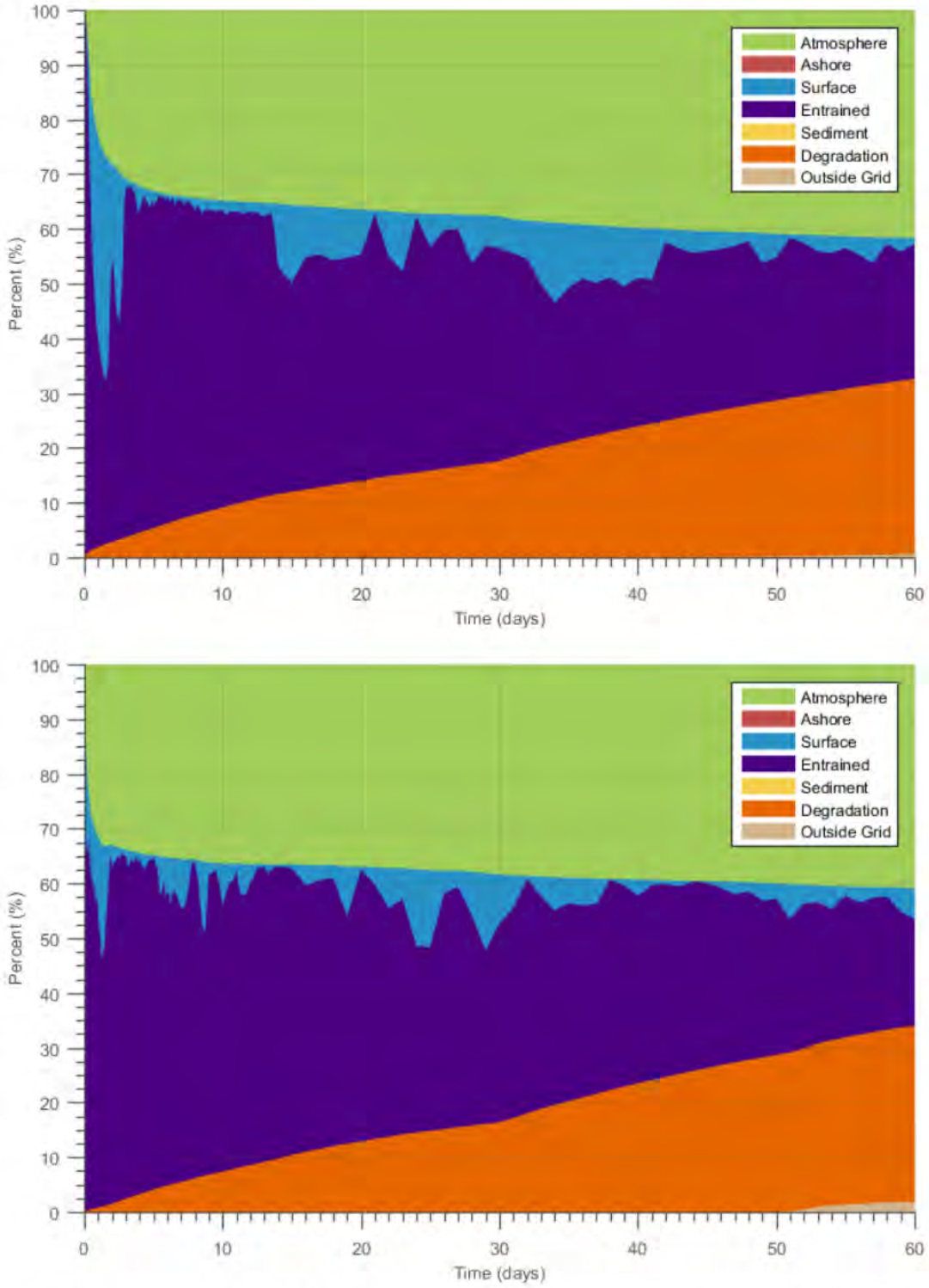

Figure 4-21. Mass balance plots of the 95th percentile surface oil thickness cases resulting from a 30-day blowout at the EL 1144 (top) and the EL 1150 (bottom) example well sites.

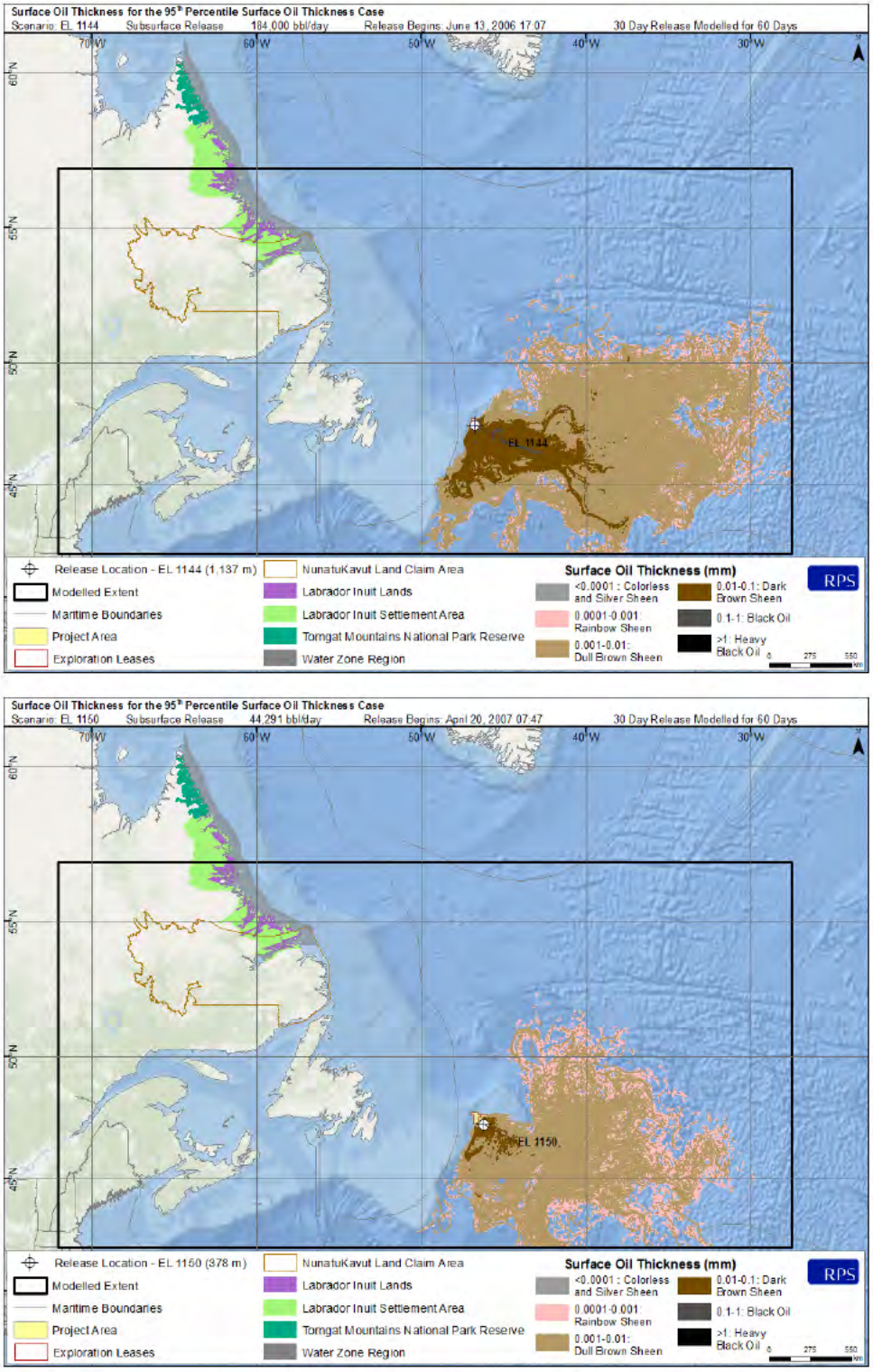

Figure 4-22. Representative scenario for 95th percentile average surface oil thickness resulting from a 30-day subsurface blowout at the EL 1144 (top) and the EL 1150 (bottom) example well sites.

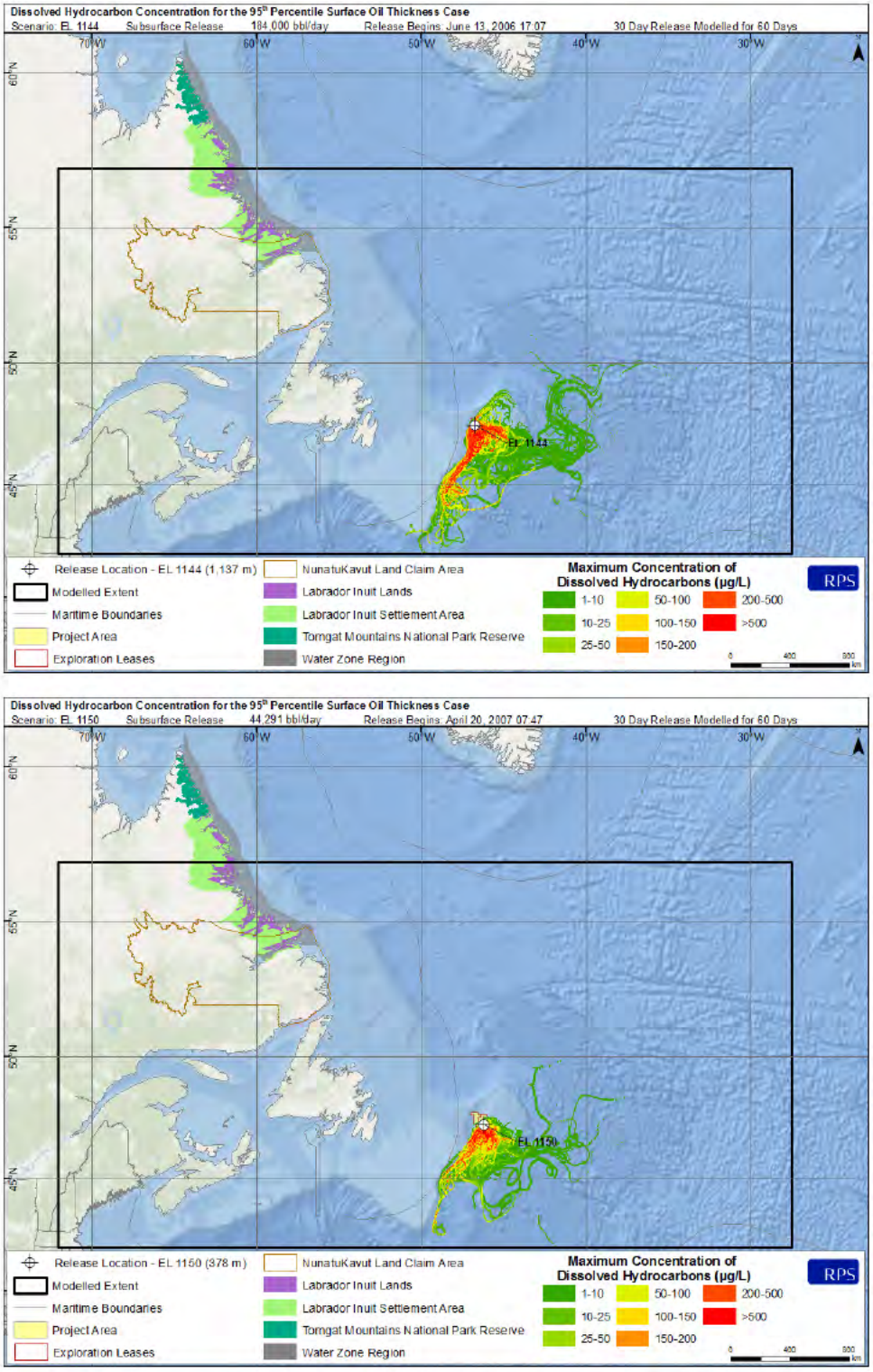

Figure 4-23. Maximum dissolved hydrocarbon concentration at any depth in the water column for the 95th percentile surface oil thickness case resulting from a 30-day subsurface blowout at the EL 1144 (top) and EL 1150 (bottom) example well sites.

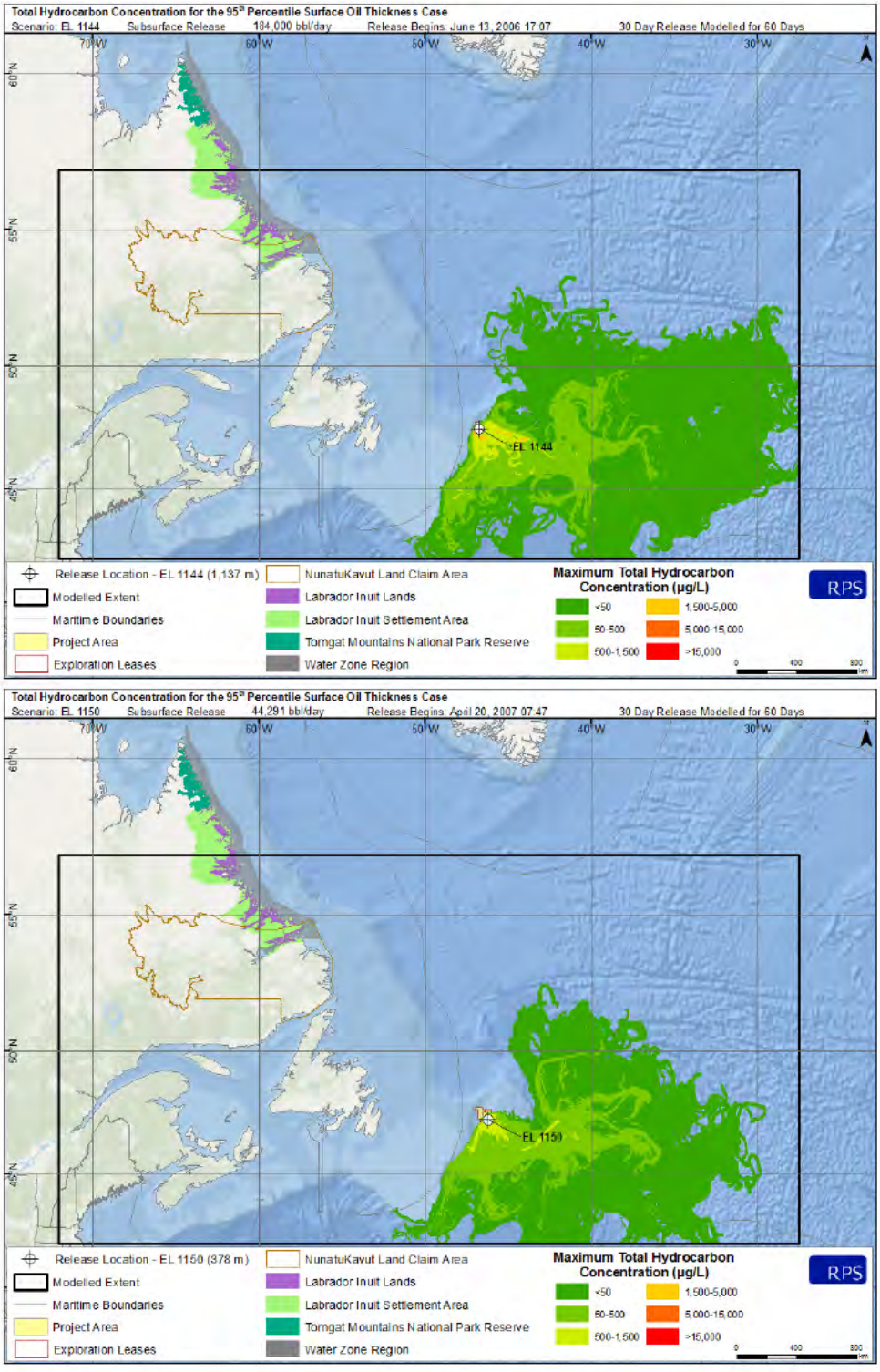

Figure 4-24. Maximum total hydrocarbon concentration (THC) at any depth in the water column for the 95th percentile surface oil thickness case resulting from a 30-day subsurface blowout at the EL 1144 (top) and EL 1150 (bottom) example well sites.

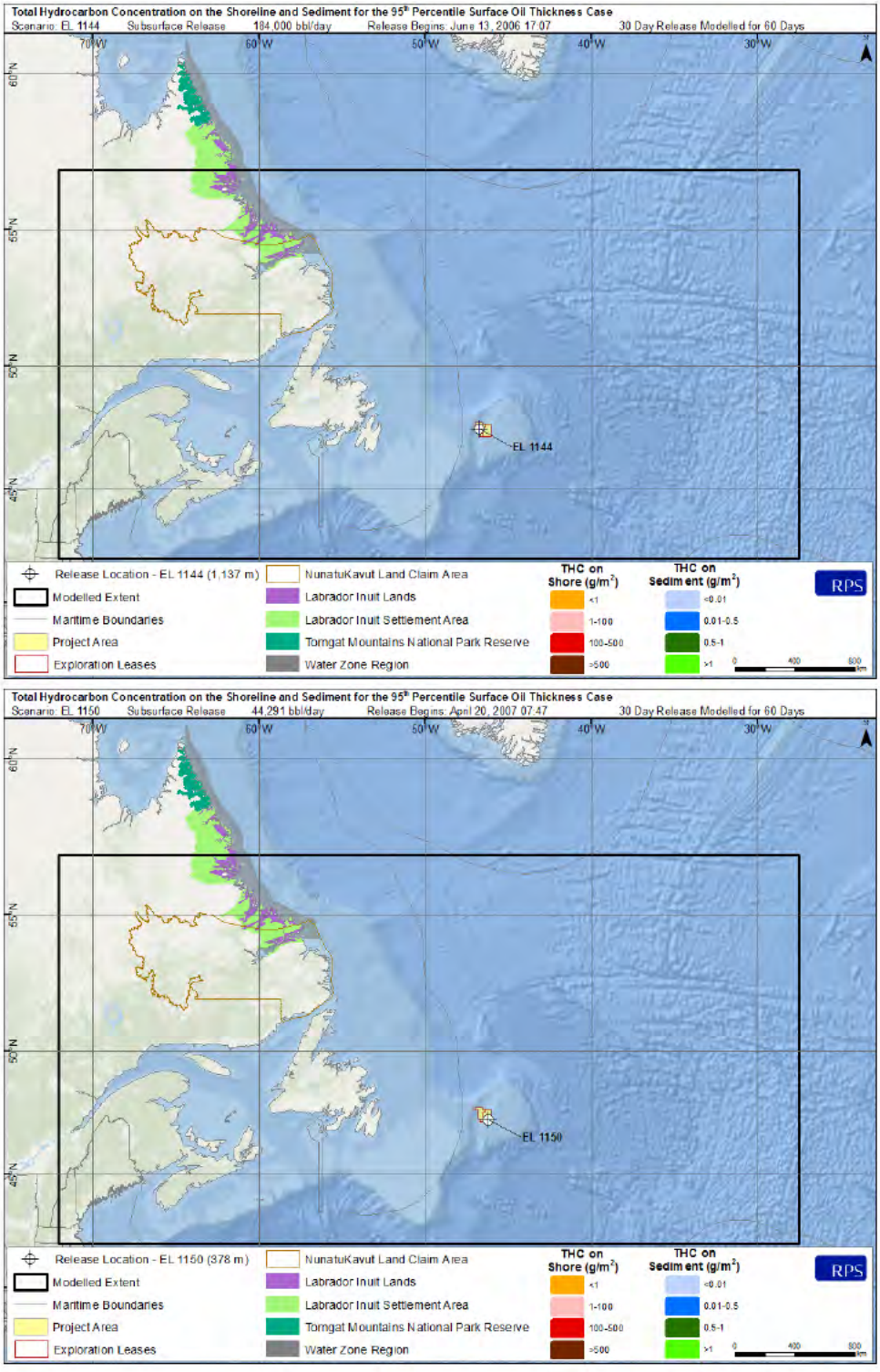

Figure 4-25. Total hydrocarbon concentration (THC) on the shore and sediment for the 95th percentile surface oil thickness case resulting from a 30-day subsurface blowout at the EL 1144 (top) and EL 1150 (bottom) example well sites. No shoreline contact was predicted for this scenario.

4.2.2 Water Column Exposure Cases

Results for the identified 95th percentile water column exposure cases for the 30-day releases at the EL 1144 and EL 1150 example well sites are provided below. Note that the modelled release dates for the representative scenarios at each site differed. Each of the trajectories in the stochastic analysis represented a different start date and associated environmental conditions (e.g. wind and current speed and direction), which resulted in different outcomes. The representative scenarios identified for deterministic analysis were aimed at identifying the 95th percentile worst cases. The 30-day release modelled for 60 days at the EL 1144 example well site spanned late-March through late-May 2008, while at the EL 1150 example well site it spanned early-December 2006 through early-February 2007 (Table 2-5). To reiterate, the combined effects of a subsurface release and the entrainment of surface oil (Figure 4-27) from wind-induced surface breaking waves into the water column was predicted to result in both dissolved and total hydrocarbon concentrations in the water column that exceeded the identified thresholds (Figure 4-28 and Figure 4-29).

Concentrations of dissolved and total hydrocarbons were predicted to be highest around the modelled release sites, dissipating as the oil was transported away where it continued to evaporate to the atmosphere and degrade, as well as dissolve, and disperse/dilute within the water column. As total hydrocarbons represent the sum of the dissolved phase (i.e., soluble fraction making up approximately 1% of the whole oil) and the particulate phase (i.e., whole oil droplets) within the water column, THC was predicted to have a larger footprint and a higher concentration than the dissolved phase. The EL 1144 example well site was predicted to have higher concentrations and a larger cumulative footprint, compared to that of the EL 1150 example well site, due to the release volume being over four times larger for the EL 1144 example well site. Due to the winds and currents in the area at the modelled times, concentration exceedances were predicted to the east and south of the release locations (Figure 4-28 and Figure 4-29). While the highest concentrations of THC were predicted near the release site at the trap height (see Section 3.7), the majority of the predicted THC concentrations more than a few km from the wellhead were predicted within a few tens of meters of the surface. This was due to the majority of the predicted THC being the result of entrained oil from wind-induced surface breaking waves.

There was no shoreline contact predicted from oil released for the 95th percentile water column contamination case at the EL 1144 or at the EL 1150 example well sites (Figure 4-30).

At the end of the 60-day water column exposure simulations at the EL 1144 and EL 1150 example well sites, <2% of the released volume was predicted to remain floating on the water surface, 40-41% evaporated into the atmosphere, 27% remained entrained in the water column, <0.02% adhered to

suspended sediment, 0% contacted the shore, 32% degraded, and <1% was transported outside the modelled domain (Figure 4-26 and Table 4-3).

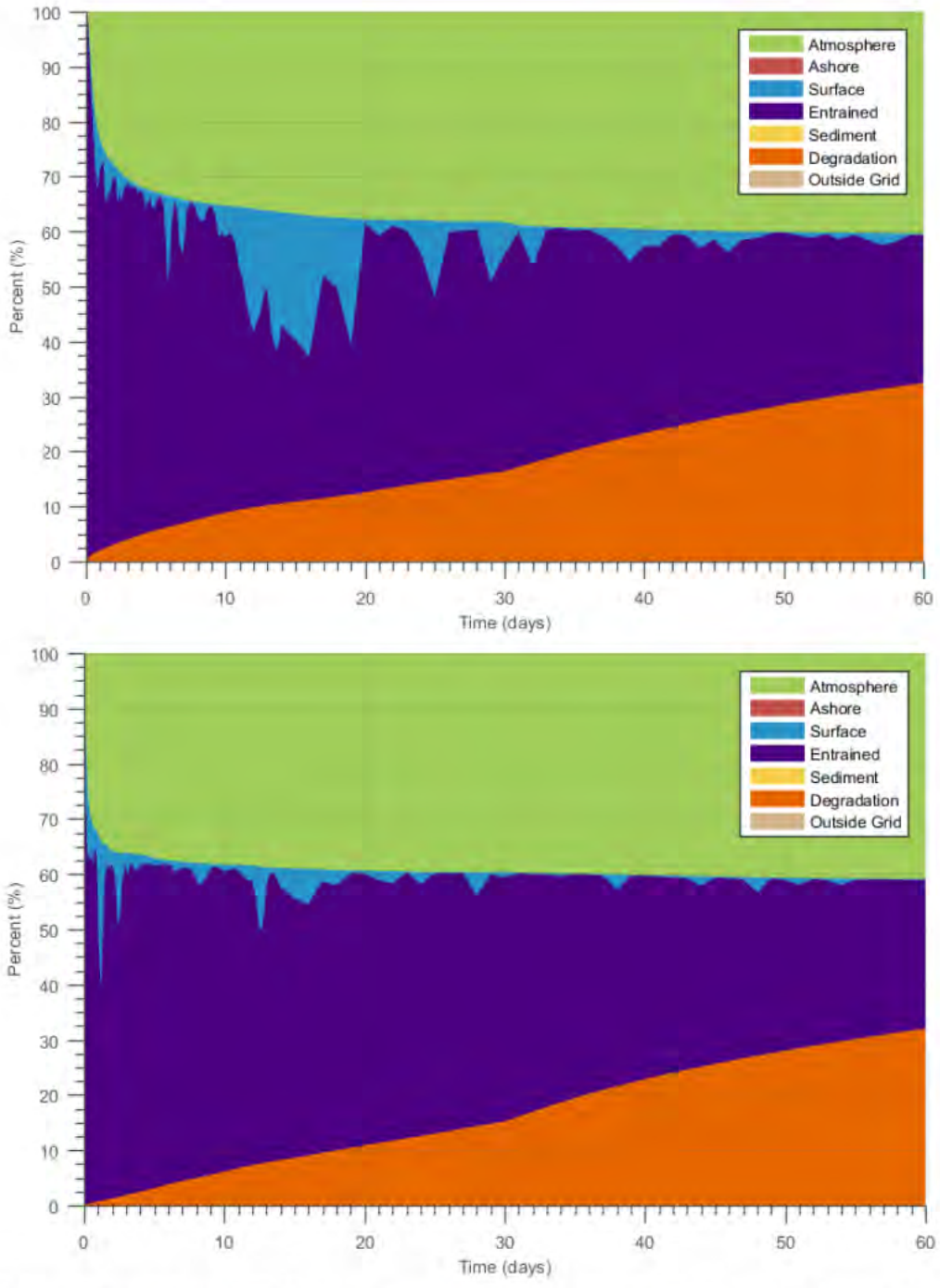

Figure 4-26. Mass balance plots of the 95th percentile water column contamination cases resulting from a 30-day blowout at the EL 1144 (top) and the EL 1150 (bottom) example well sites.

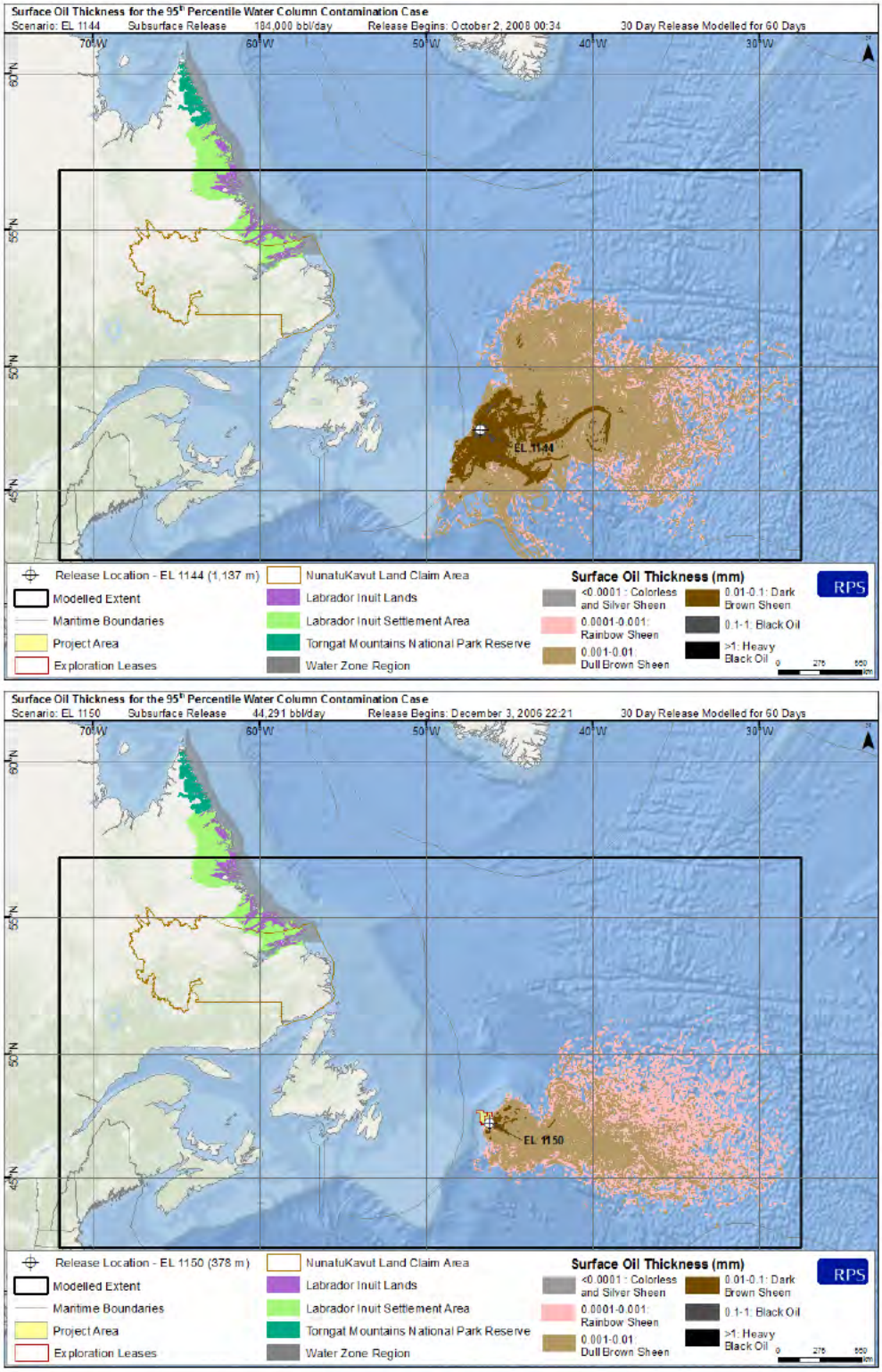

Figure 4-27. Surface oil thickness for the 95th percentile water column contamination case resulting from a 30-day subsurface blowout at the EL 1144 (top) and EL 1150 (bottom) example well sites.

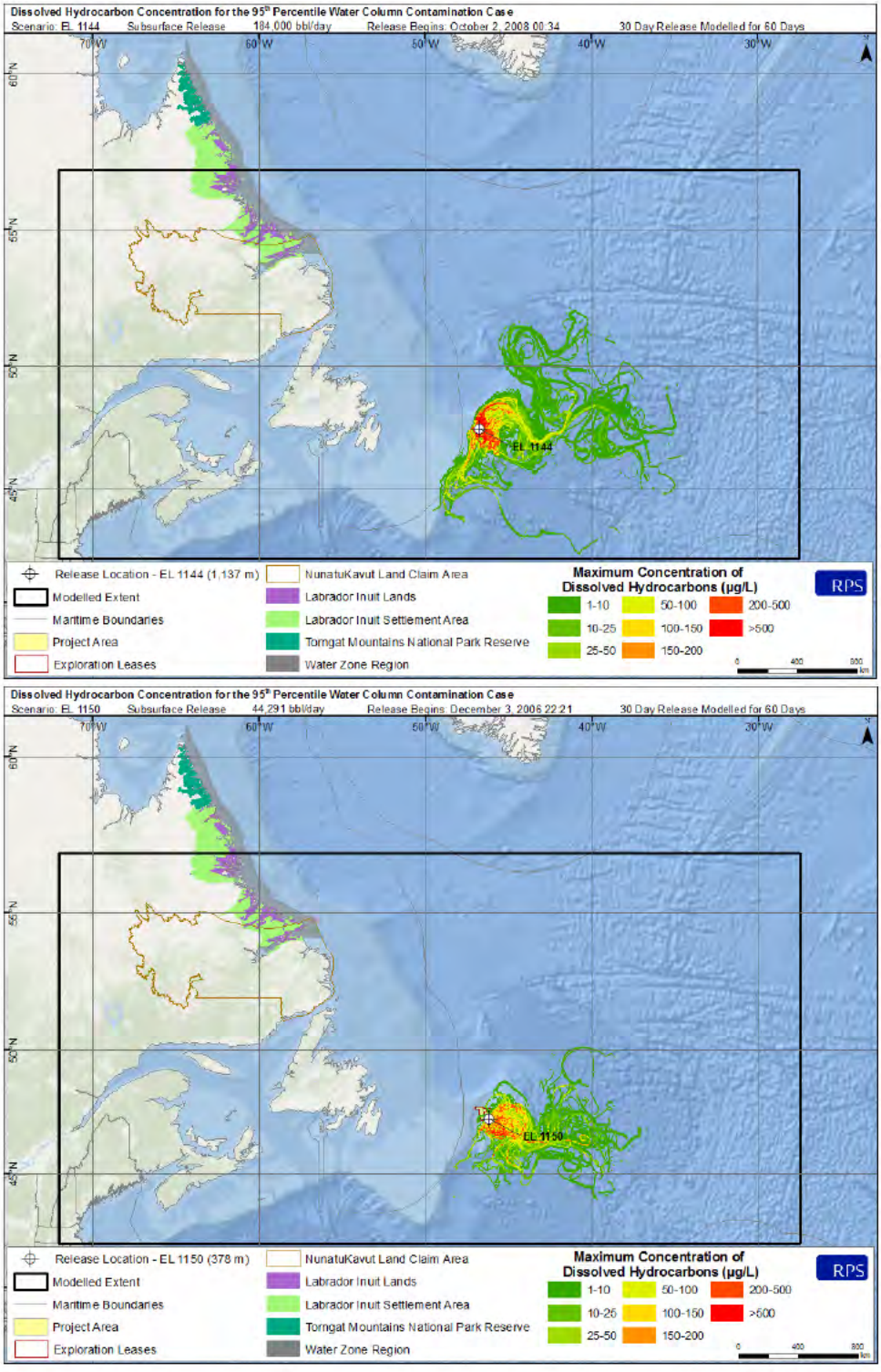

Figure 4-28. Maximum dissolved hydrocarbons at any depth in the water column for the 95th percentile water column contamination case resulting from a 30-day subsurface blowout at the EL 1144 (top) and EL 1150 (bottom) example well sites.

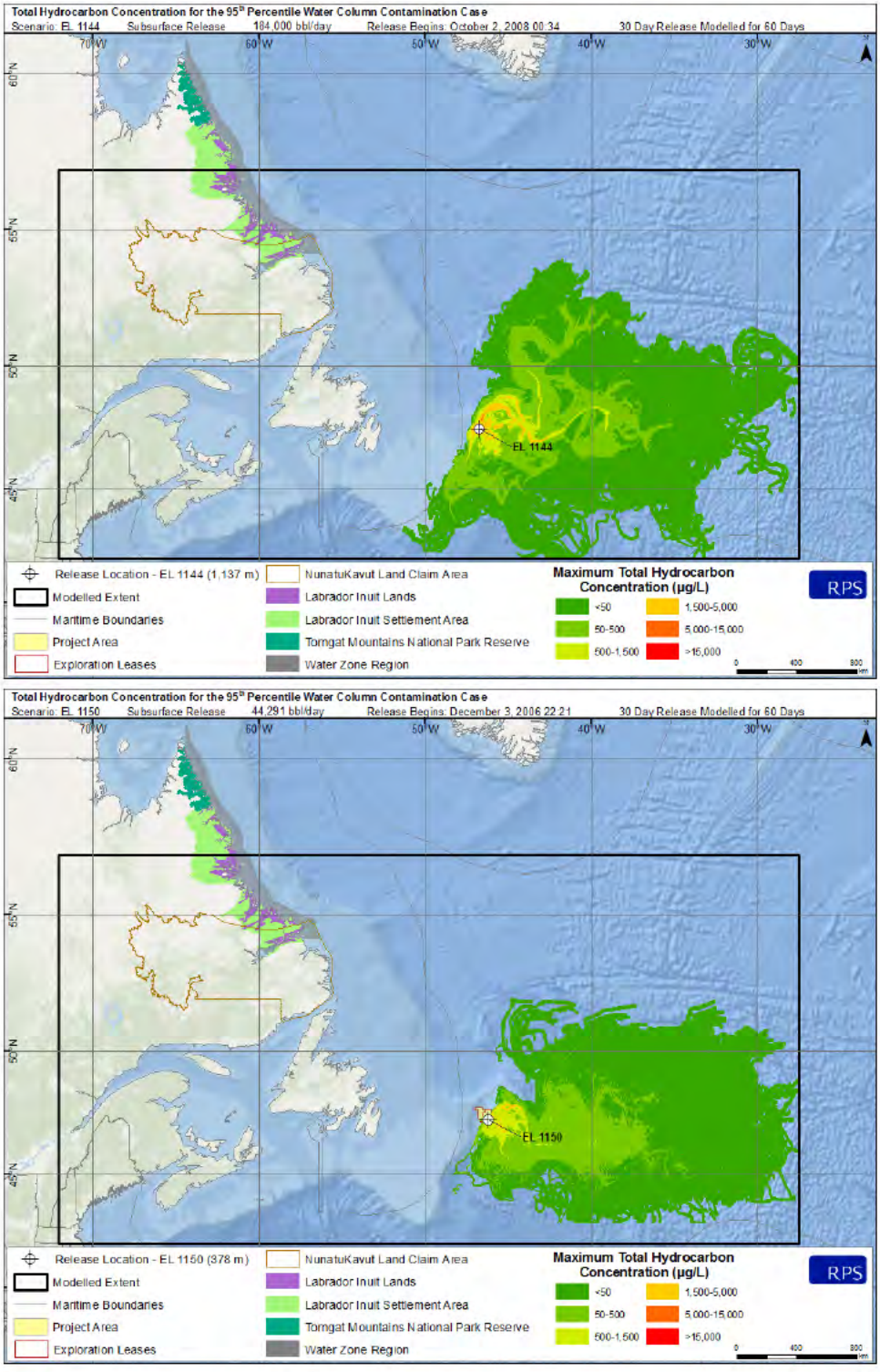

Figure 4-29. Maximum total hydrocarbon concentration (THC) at any depth in the water column for the 95th percentile water column contamination case resulting from a 30-day subsurface blowout at the EL 1144 (top) and EL 1150 (bottom) example well sites.

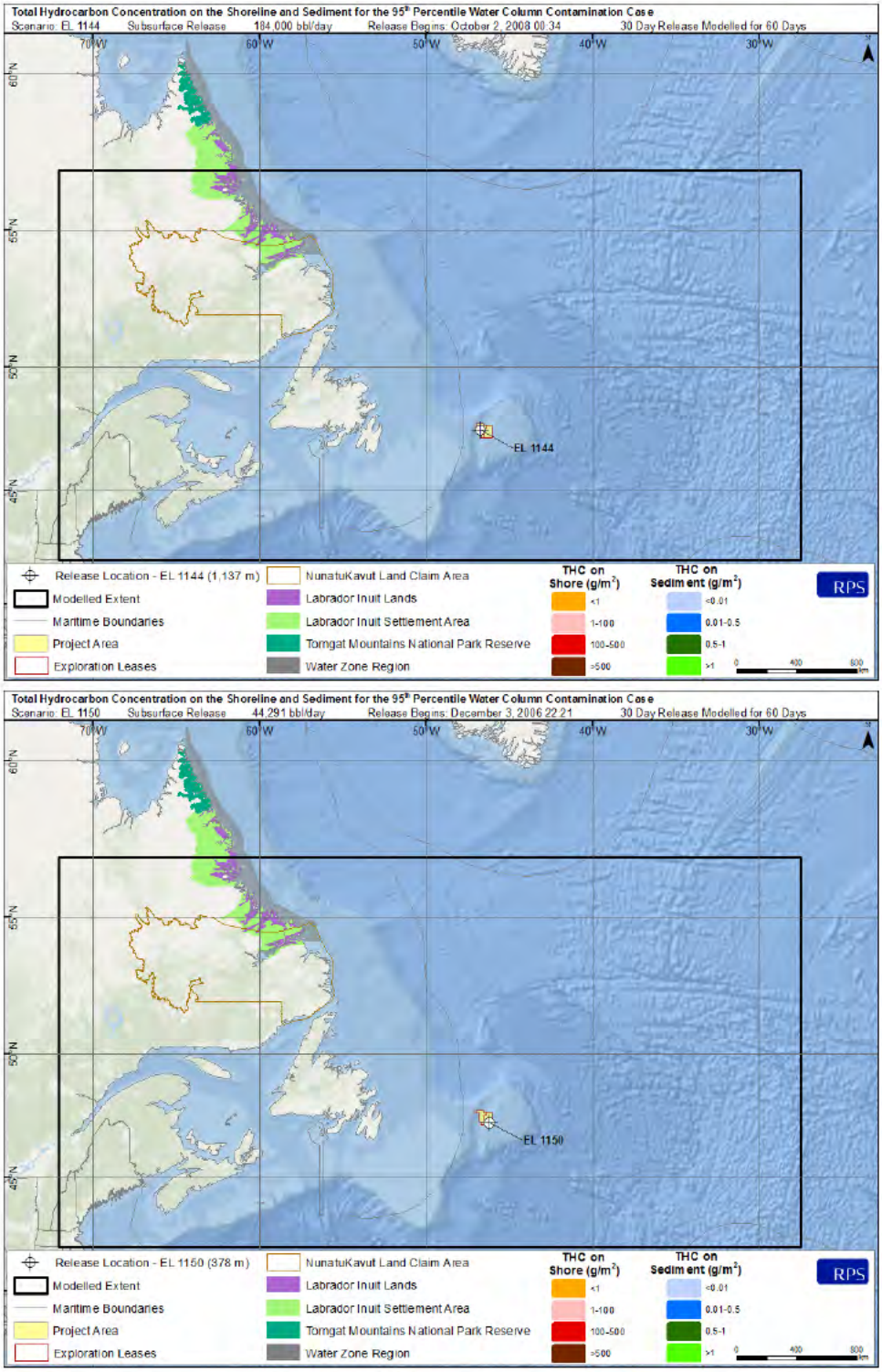

Figure 4-30. Total hydrocarbon concentration (THC) on the shore and sediment for the 95th percentile water column contamination case resulting from a 30-day subsurface blowout at the EL 1144 (top) and EL 1150 (bottom) example well sites.

4.2.3 Shoreline Exposure Cases

Results for the identified 99th percentile shoreline exposure cases for the releases at the EL 1144 example well site are provided below. Note that oil from the subsurface spill at the EL 1150 example well site was not predicted to make contact with the shoreline and thus, a representative shoreline exposure case was not identified. The 30-day release at the EL 1144 example well site that was modelled for 60 days spanned early-October through early-December 2007 (Table 2-5). The predicted contact with shore occurred on Sable Island (Figure 4-35). However, only a very small portion of the released oil is predicted to move in this direction. In the case of the 99th percentile shoreline exposure cases at the EL 1144 example well site, only a very small portion of the release (<0.01%) was predicted to make contact with the shoreline. The oil that was predicted to make contact with shorelines is expected to be highly weathered, patchy, and discontinuous, as the estimated time for first shoreline oil contact was greater than 50 days.

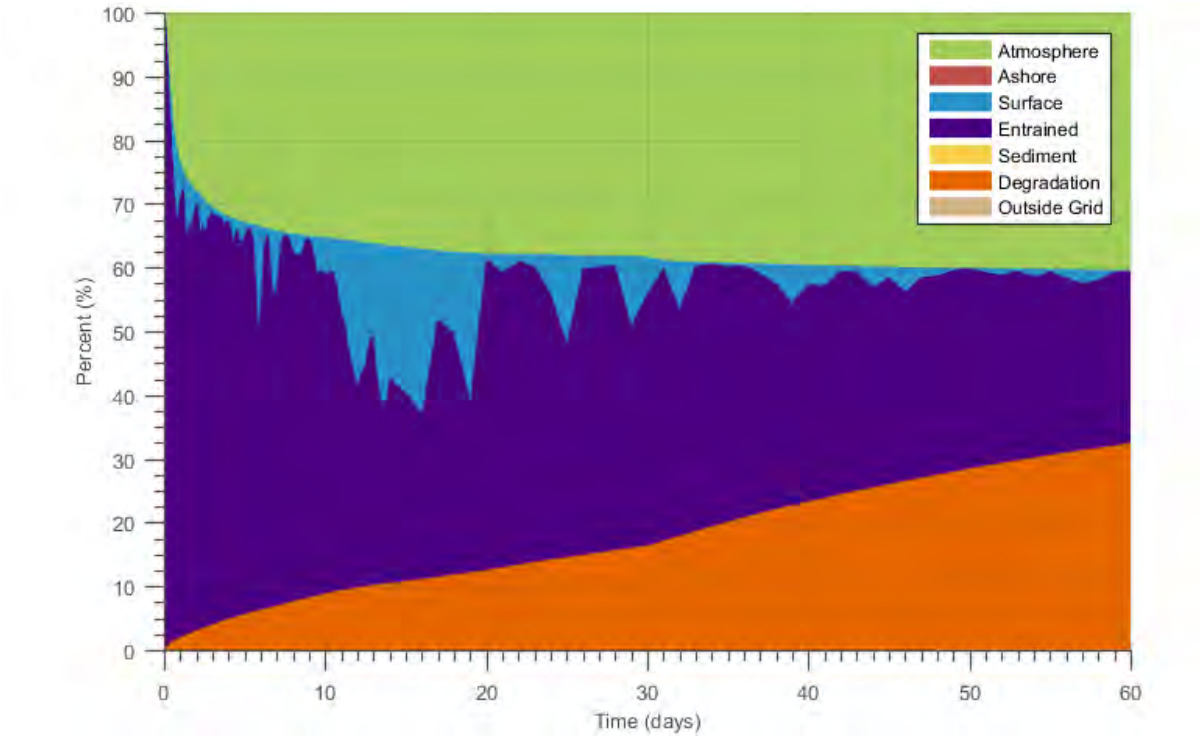

Figure 4-31. Mass balance plots of the 99th percentile shoreline contact case resulting from a 30-day blowout at the EL 1144 example well site.

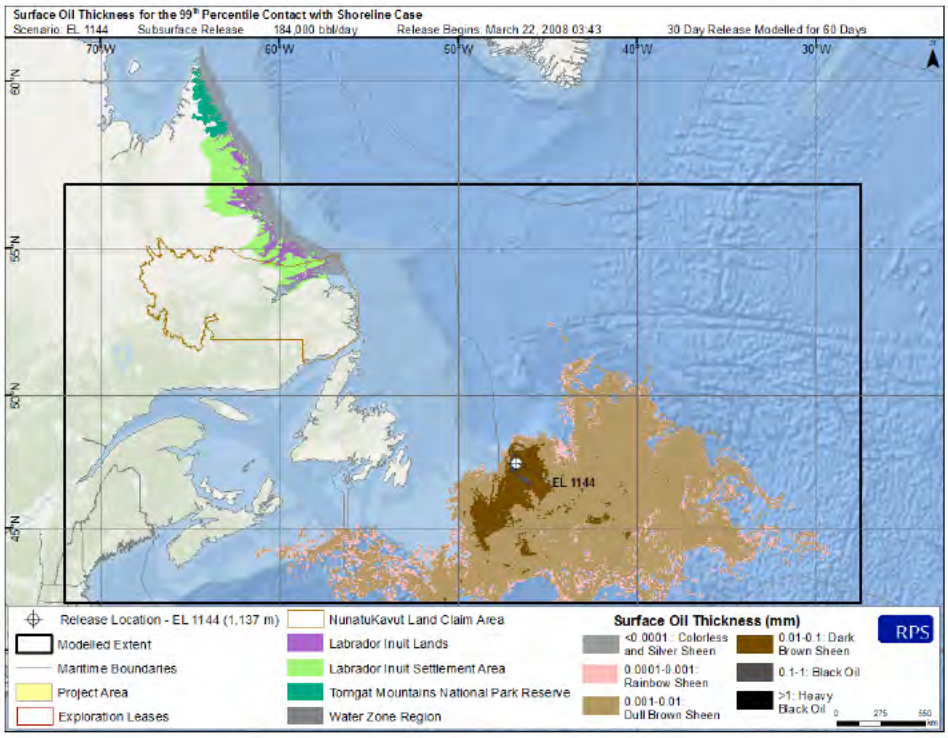

Figure 4-32. Surface oil thickness for the 99th percentile contact with shoreline case resulting from a 30-day subsurface blowout at the EL 1144 example well site.

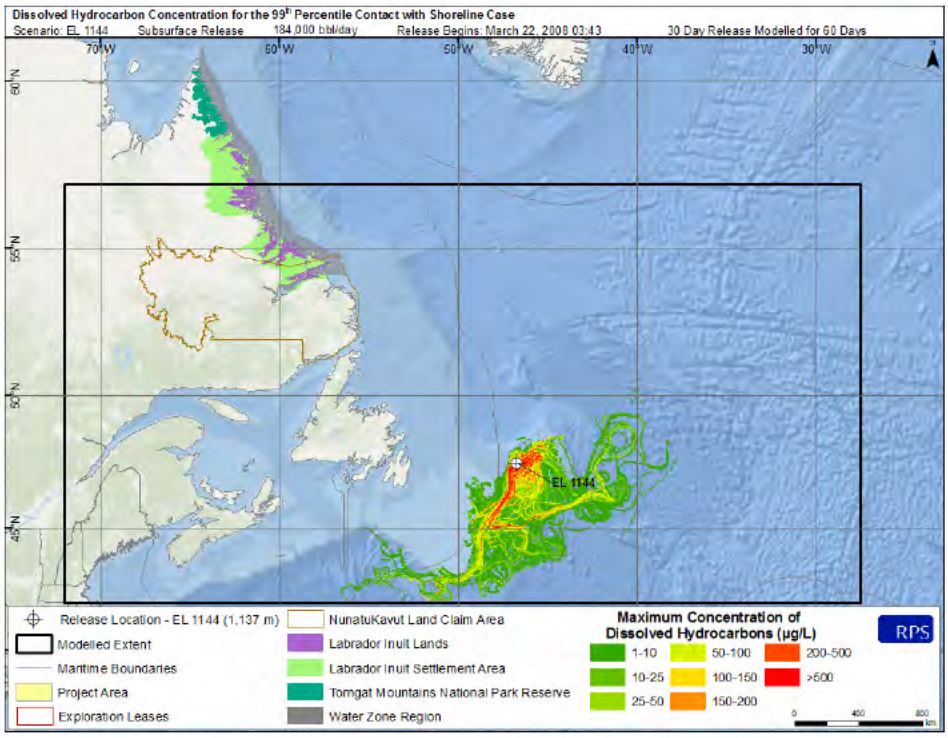

Figure 4-33. Maximum dissolved hydrocarbons at any depth in the water column for the 99th percentile contact with shoreline case resulting from a 30-day subsurface blowout at the EL 114 example well site.

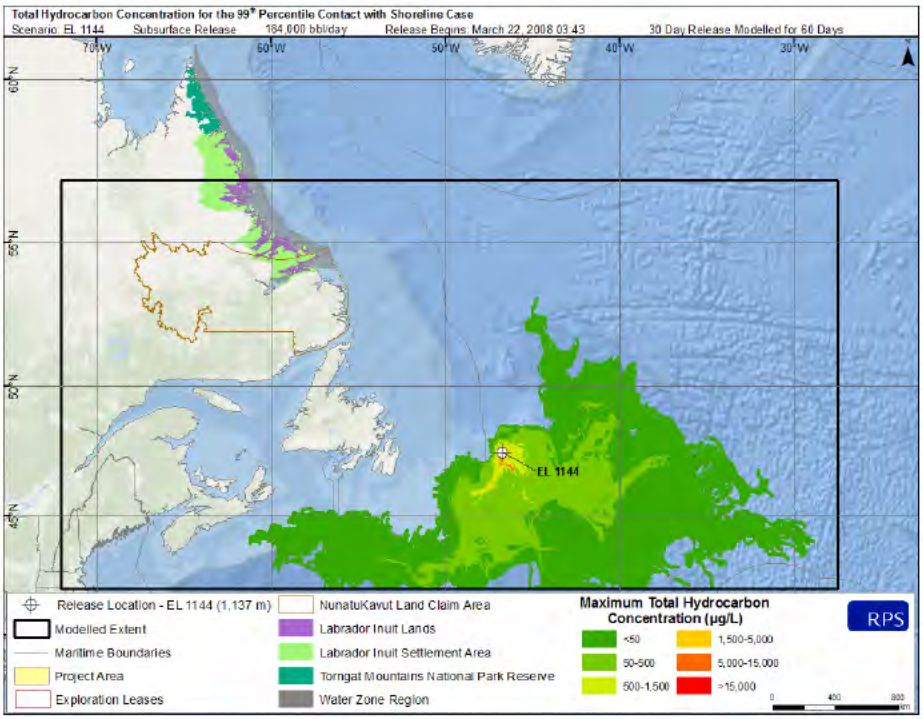

Figure 4-34. Maximum total hydrocarbon concentration (THC) at any depth in the water column for the 99th percentile contact with shoreline case resulting from a 30-day subsurface blowout at the EL 1144 example well site.

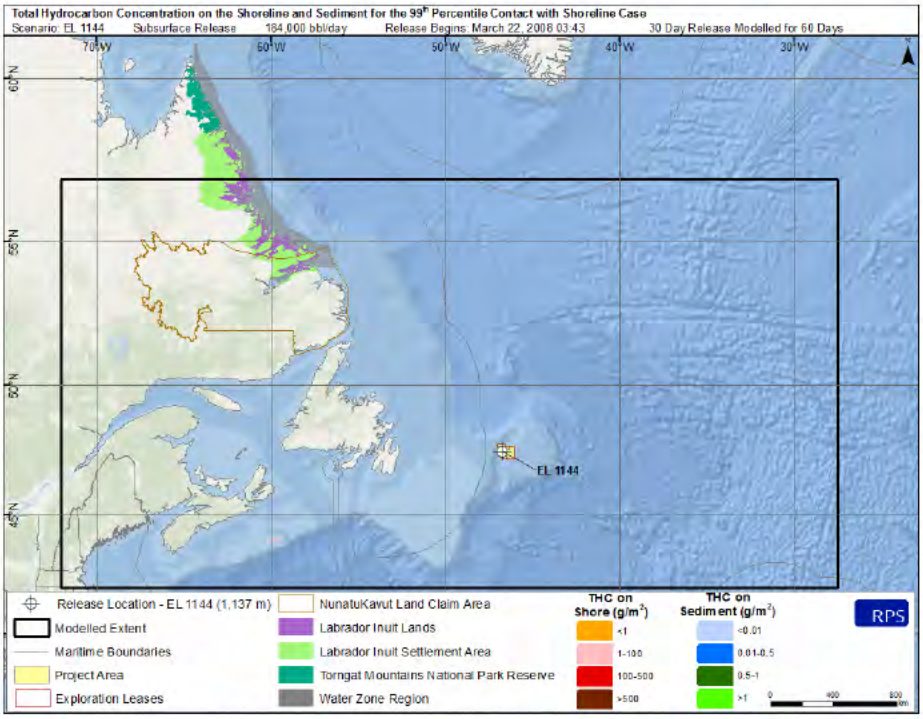

Figure 4-35. Total hydrocarbon concentration (THC) on the shore and sediment for the 99th percentile contact with shoreline case resulting from a 30-day subsurface blowout at the EL 1144 example well site. Only limited shoreline contact was predicted for this scenario at Sable Island.

4.2.4 Marine Diesel Releases

Results for the representative marine diesel "batch spill" scenarios (100 L and 1000 L) at the EL 1144 example well site and the vessel collision (750,000 L) scenario at VCL are presented in the following section. The "batch spill" releases were modelled to be representative of releases that could occur during bunkering operations (i.e., transfer from a vessel). The vessel collision was modelled to be representative of a release that could occur should a supply vessel collide with another vessel with a complete loss of containment for both fuel and cargo. The scenarios were selected to occur during the calmest wind-speed period during the summer/ice-free conditions, which would conservatively result in the largest amount of oil on the water surface. The selected dates were June 15, 2009 at EL 1144 and June 14, 2009 at VCL.

Due to the small release volumes for the "batch spills" and the size of the concentration gridding (1 km by 1 km), the predicted concentrations of dissolved hydrocarbons were not sufficient to produce reportable concentrations and figures have therefore not been presented below. Furthermore, the predicted concentrations for total hydrocarbons were minimal, when compared to the blowout footprints, and located within the immediate vicinity of the spill site (Figure 4-38). For the 100 L release, this was generally limited to a few hundred meters, while for the 1,000 L release was closer to 5 km. For the vessel collision release, total hydrocarbon concentrations exceeding the 1 µg/L threshold were predicted over 300 km to the south and east of the release location (Figure 4-42). The predicted THC concentrations were within the surface mixed layer (tens of meters), as they were the result of dissolution from the surface slick and entrainment of oil from wind-induced surface breaking waves.

For the smaller "batch spills", the predicted average surface oil thickness > 0.04 µm was extremely patchy for the 100 L and 1,000 L releases (Figure 4-37). Maximum surface oil as thickness corresponding to a colorless or silver sheen were predicted. For the larger vessel collision release, surface oil as thick as a rainbow sheen was predicted for the first 50 km to the southwest, with silver sheen possible for over 300 km (Figure 4-41).

Neither of the "batch spills" nor the vessel collision release were predicted to result in any oil contacting shorelines (Figure 4-39 and Figure 4-43).

At the end of the 30-day simulations for all three marine diesel spills, <0.1% of the released volume was predicted to remain floating on the water surface, 63-76% evaporated into the atmosphere, 8-14% remained entrained in the water column, ≤0.01% adhered to suspended sediment, 0% contacted the shore, 16-45% degraded (Figure 4-36 and Figure 4-40).

4.2.4.1 Batch Spills at EL 1144

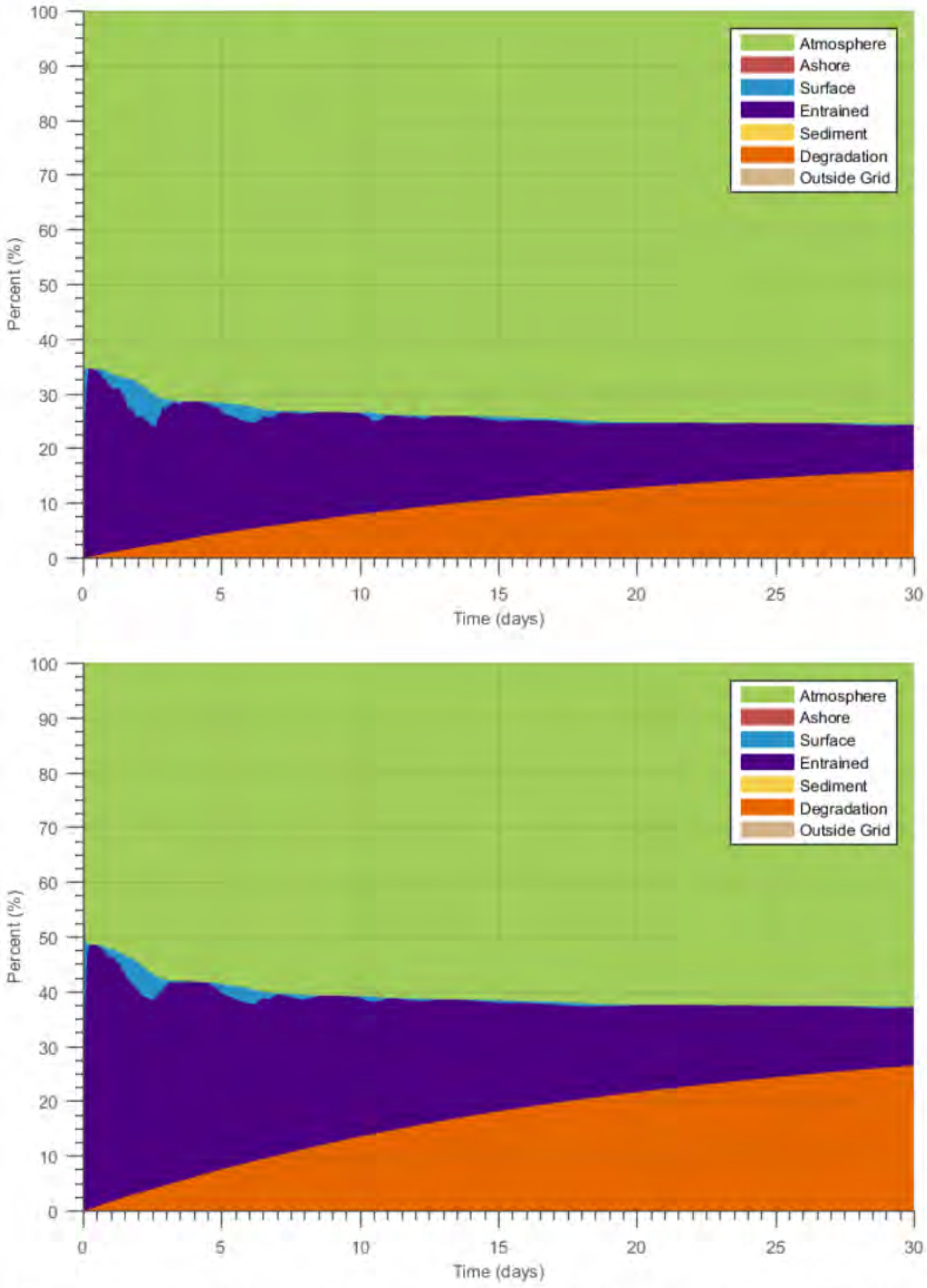

Figure 4-36. Mass balance plots of the EL 1144 example well site release of marine diesel from batch spills of 100 L (top) and 1,000 L (bottom).

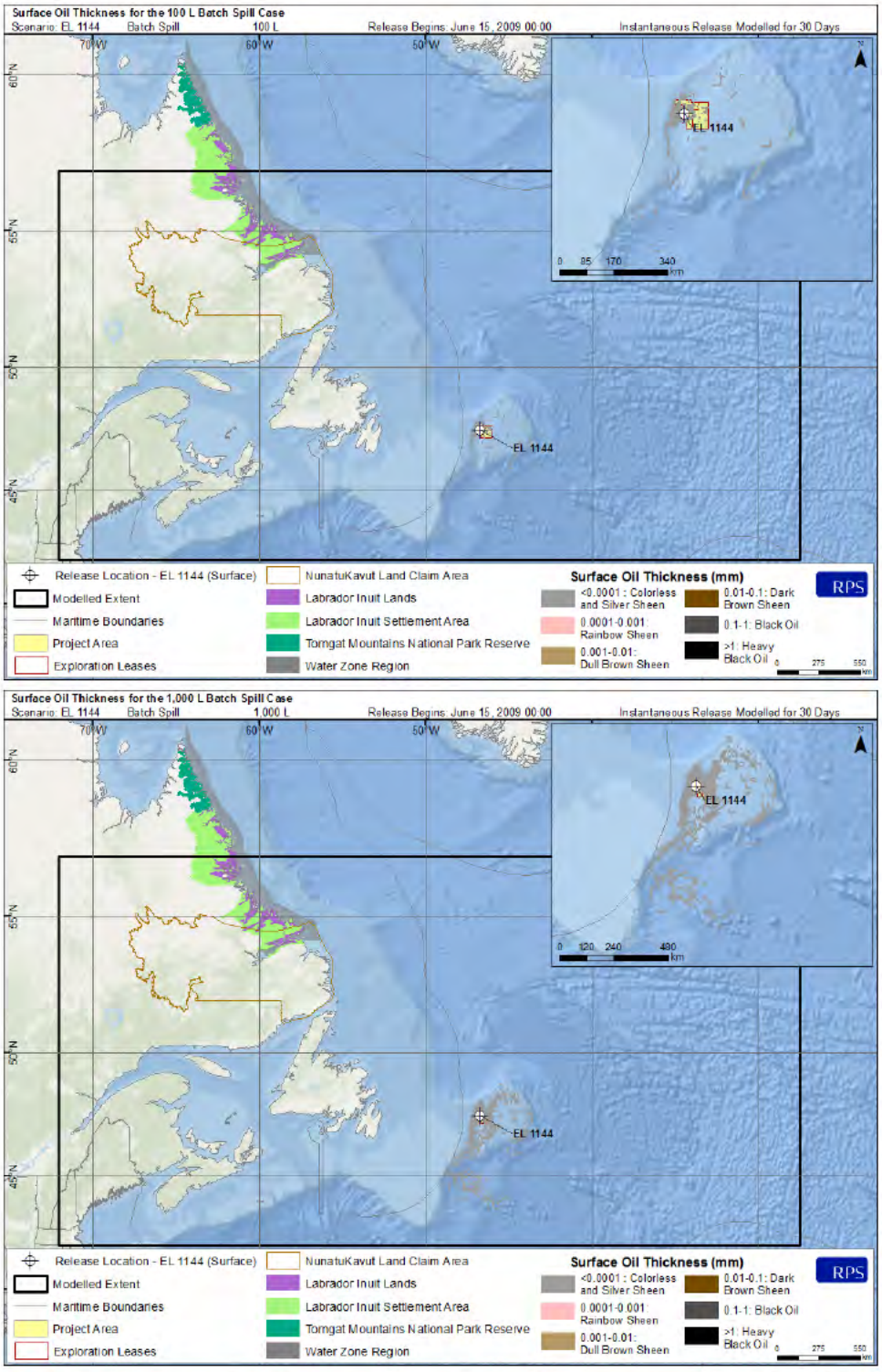

Figure 4-37. Surface oil thickness resulting from the EL 1144 example well site release of marine diesel from batch spills of 100 L (top) and 1,000 L (bottom).

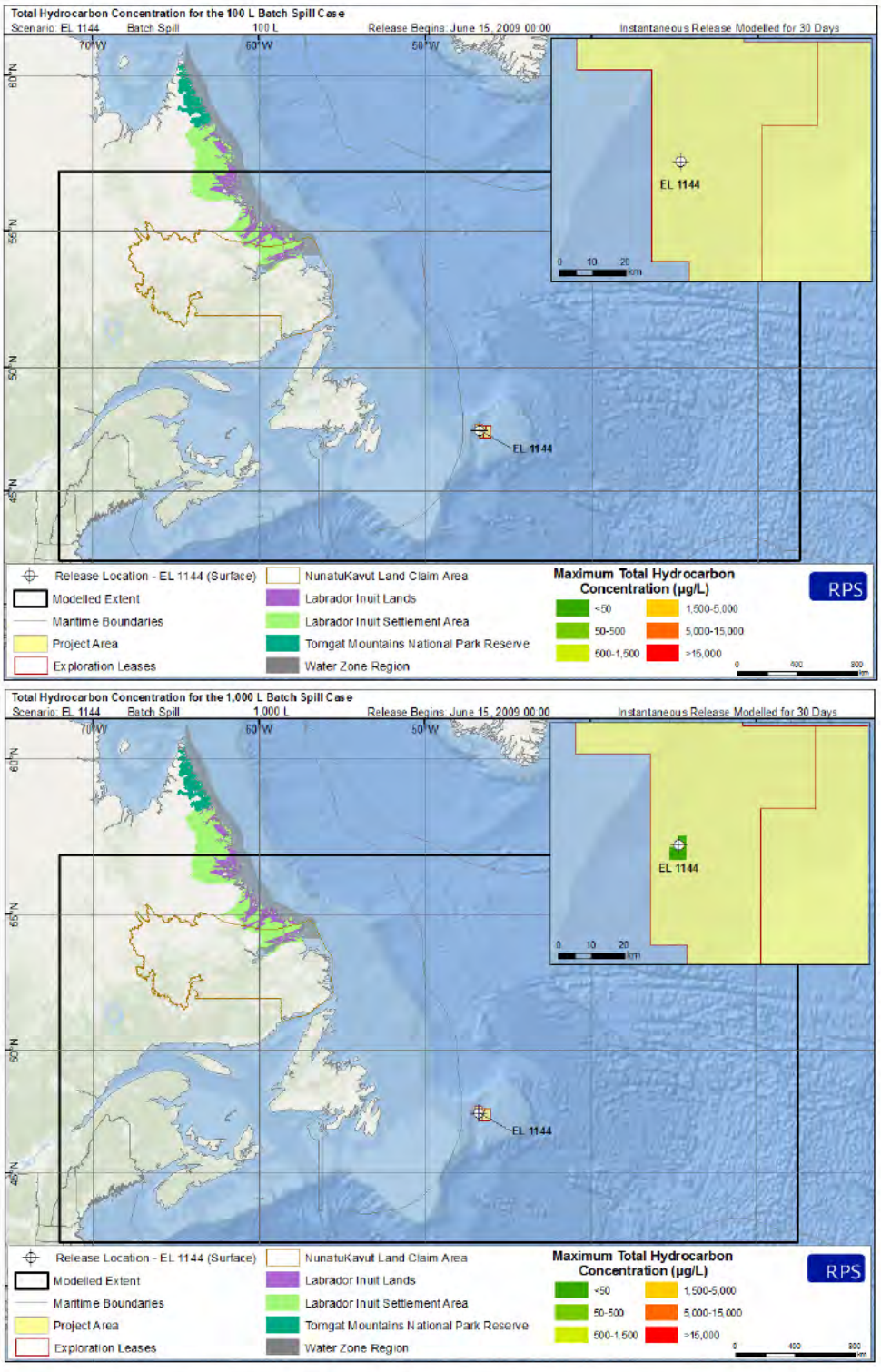

Figure 4-38. Maximum total hydrocarbon concentration (THC) at any depth in the water column resulting from the EL 1144 example well site release of marine diesel from batch spills of 100 L (top) and 1,000 L (bottom). Due to the small volume of the 100 L release and the concentration gridding, concentrations of THC were not sufficient to produce results.

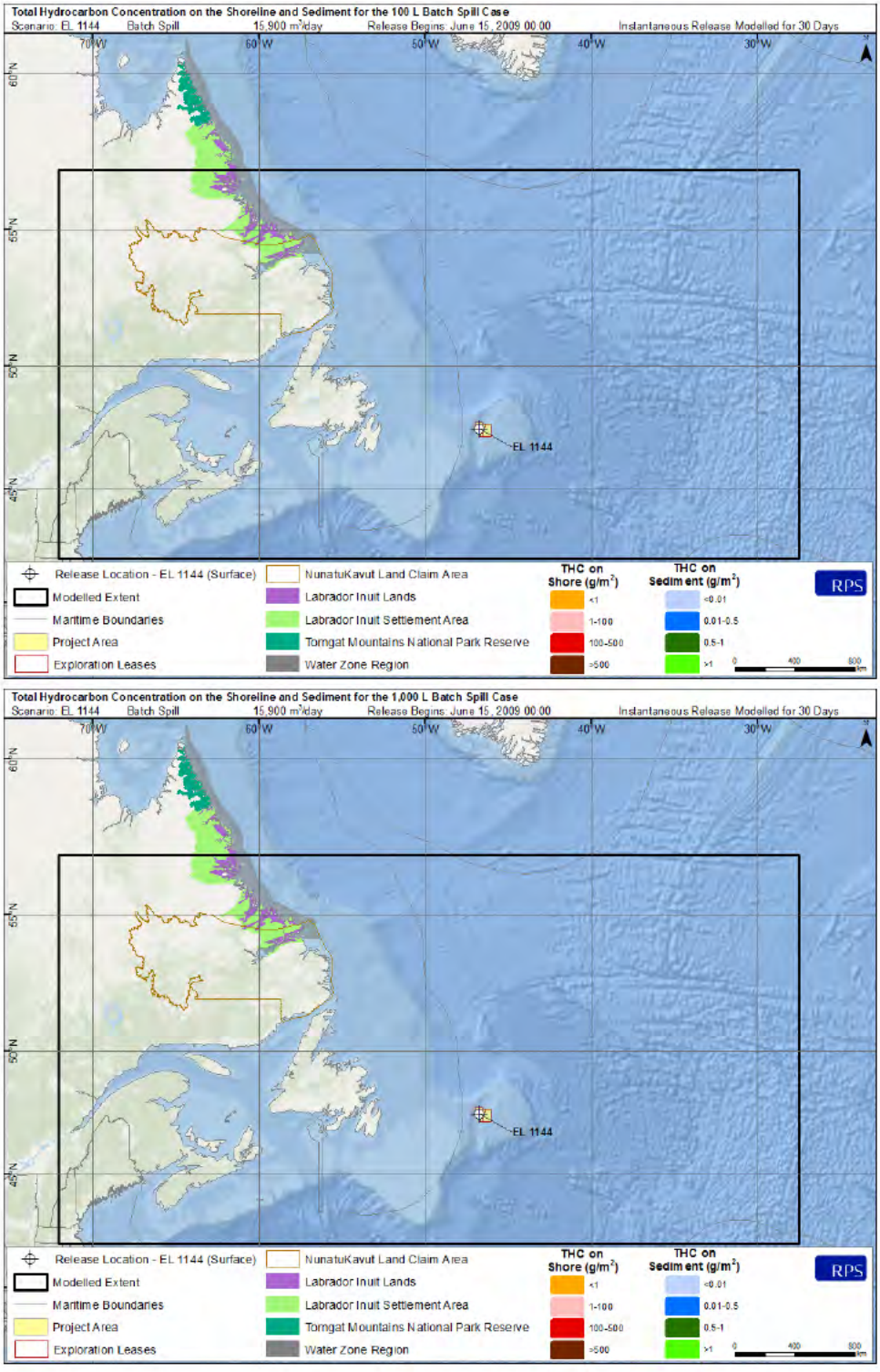

Figure 4-39. Total hydrocarbon concentration (THC) on the shore and sediment resulting from the EL 1144 example well site release of marine diesel from batch spills of 100 L (top) and 1,000 L (bottom). No shore or sediment contamination was predicted.

4.2.4.2 Supply Vessel Collision

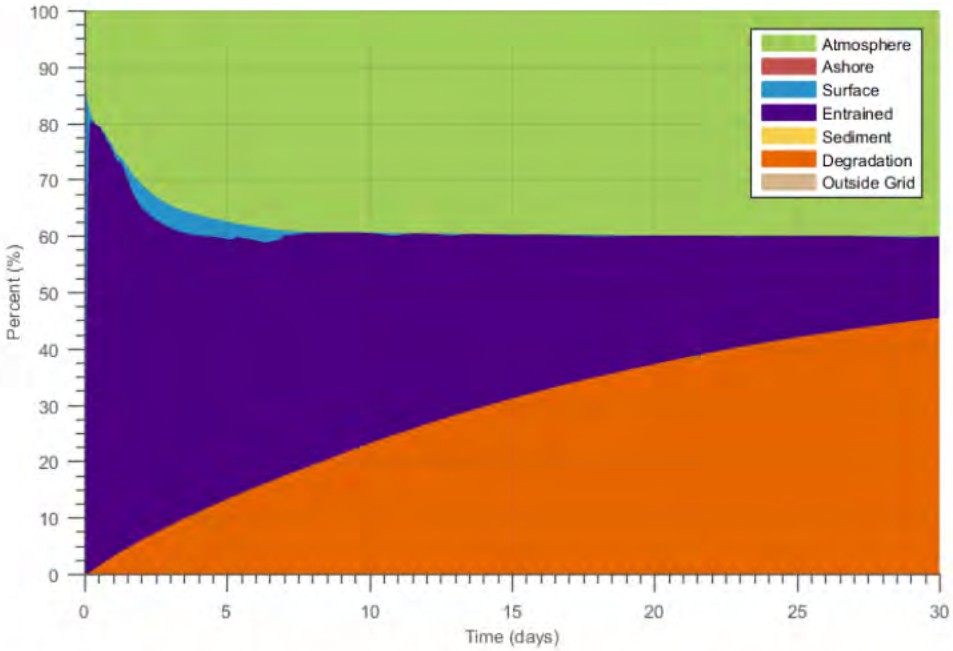

Figure 4-40. Mass balance plots of the VCL release site of marine diesel from the vessel collision release of 750,000 L.

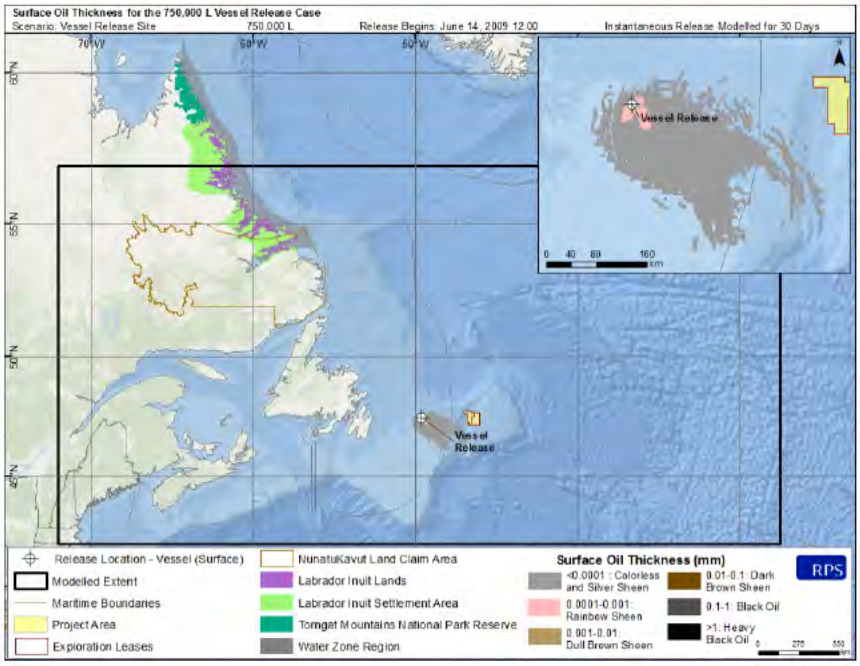

Figure 4-41. Surface oil thickness resulting from the VCL release of marine diesel from the vessel collision release of 750,000 L.

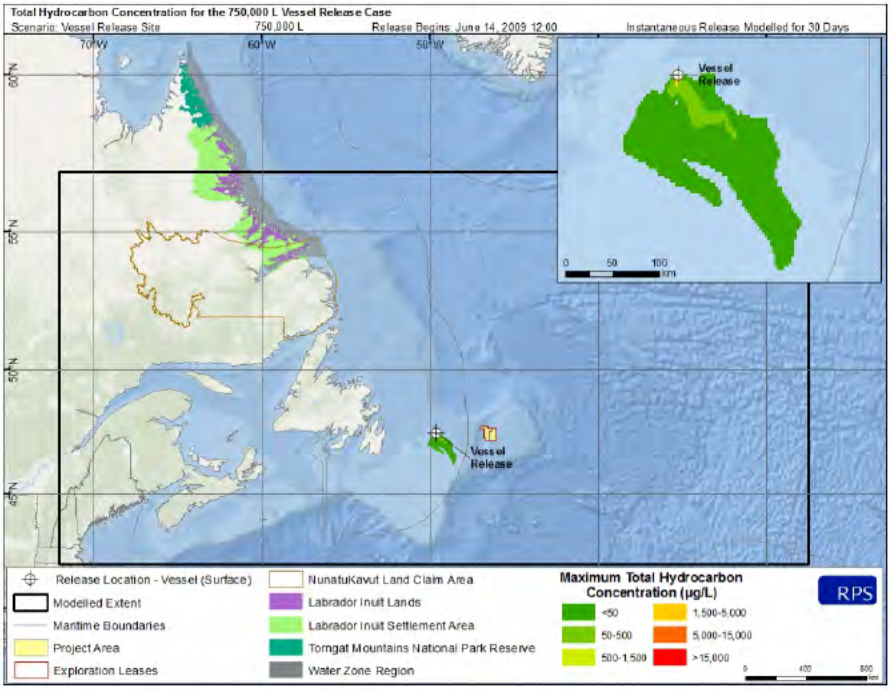

Figure 4-42. Maximum total hydrocarbon concentration (THC) at any depth in the water column resulting from the VCL release of marine diesel from the vessel collision release of 750,000 L.

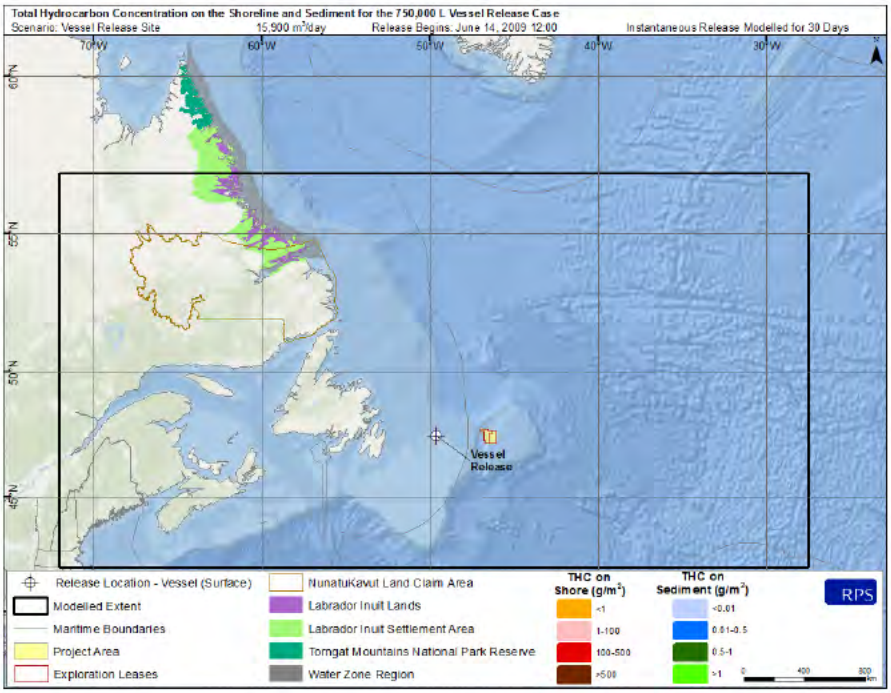

Figure 4-43: Total hydrocarbon concentration (THC) on the shore and sediment resulting from the VCL release of marine diesel from the vessel collision release of 750,000 L. No shore or sediment contamination was predicted.

4.2.5 Summary of Deterministic Results

The 95th percentile cases represent realistic "worst case" scenarios that may occur following the unmitigated blowouts that were modelled. The site-specific (in space and time) environmental conditions in each identified case resulted in maximizing the potential exposure to either surface oil, in water contamination, and shoreline oil in each of the identified cases. Note that all scenarios were assumed to be completely unmitigated, which is an unlikely situation, as response efforts would likely be implemented immediately, provided it is safe to do so, following a release.

For surface oil, both the 95th percentile release cases at the EL 1144 and EL 1150 example well sites occurred during the summer season (defined as ice-free for more than half the days of the model run) where wind speeds were sufficiently low to prevent entrainment and allow for more extensive surface slicks. The 99th percentile shoreline oiling case was identified in the late summer, where weather patterns were sufficient to transport oil to the south and west, where a small fraction of oil (<0.01%) was transported to the shores of Sable Island. For the 95th percentile water column contamination cases, scenarios were always during winter months, where high wind speeds were sufficient to generate surface breaking waves with entrained surface oil and resulted in the largest amounts of oil in the water column. For the representative "batch spills" and vessel collision, low wind speed periods were identified for each of the three scenarios which occurred during the summer.

The depth of release and the total release volume impacted results for the subsurface blowouts. The EL 1150 example well was the shallower water depth of the two sites (378 m), which contributed to faster surfacing of subsurface oil. However, even though the release at the EL 1144 example well site was much deeper water depth (1,137 m), the much larger release volume (over 4 times that of the EL 1150 example well site) was predicted to result in thicker surface area over broader areas. There were some limited areas with the potential for black oil (0.1 – 1 mm) at distances greater than 10 km from the release point and a greater areal extent of dark brown sheens (0.01-0.1 mm). For releases at EL 1150, surface thicknesses were predicted to be closer to dark brown sheens away from the release point over a smaller area due to the smaller release volume (Figure 4-22).

For all representative deterministic scenarios, the majority of the surface oil (94-99%) was predicted to either entrain, evaporate, or degrade by the end of the simulation, with <1-6% predicted to remain on the surface after 60 days (Table 4-3). For the marine diesel releases, <0.01% of marine diesel was predicted to remain on the surface after 30 days. This high volatility and solubility of the BdN and marine diesel facilitated the large amount of predicted evaporation to the atmosphere (35-42% for BdN and 40-76% for diesel) and dissolution into and degradation within the water column (32-38% for BdN and 16-45% for diesel). Predicted entrained oil in the water column ranged between 20% and 27% for

the blowouts of BdN and 8-14% for the marine diesel releases after 30 and 60 days, respectively. Shoreline oiling was not predicted for approximately 97% of the modelled blowout simulations. As predicted in the 99th percentile shoreline contact case, less than 0.01% of the released oil reached the shores of Sable Island after more than 50 days. In each case, oil on the sediments was predicted to be extremely limited, with less than 0.02% of the release making its way to the bottom. In many simulations, some portion of the released oil mass was predicted to travel outside of the model domain, in some cases up to 2%.

The maximum subsurface water volume exposed to THC concentrations above 1 µg/L for the two 95th percentile water column cases are comparable to one another, with 58,842 km^3 predicted for EL 1144 and 54,943 km^3 predicted for the EL 1150 example well site. This volume is comparable to the predicted areal footprints of contamination for surface oil down to mixed layer depths (tens of meters). For the 95th percentile water column contamination cases at the EL 1144 example well site, the region that may experience concentrations >200 µg/L for dissolved hydrocarbons at any point over the 60-day simulation was predicted primarily within 200 km to the south east and north of the release site. At the EL 1150 example well site, dissolved hydrocarbon concentrations >200 µg/L were found to the southeast of the release within approximately 150 km. Entrained oil concentrations in surface waters were predicted to vary considerably from day to day, as would be expected due to the dependence on variable wind induced surface breaking wave formation.

The 99th percentile shoreline exposure case was identified for the EL 1144 example well site rather than the 95th percentile, as no shoreline oiling was predicted for the 95th percentile case. For the EL 1150 example well site, there was no scenario that resulted in shoreline exposure within 60 days. The predicted shoreline oiling from the release at the EL 1144 example well site was predicted to occur on Sable Island (Figure 4-35). The area of shore where shoreline oil exceeded the 1 g/m^2 threshold was predicted to be approximately 13 km^2. However, shoreline oil was predicted to comprise an extremely small portion of the total mass of released oil (<0.01%) in this case.

For the "batch spill" releases of marine diesel, mass balance predictions portray the rapid entrainment of a large portion (30-45%) of surface oil within several hours of the release (Figure 4-36). After 24 hours, 52-66% was predicted to evaporate, with less than 3% remaining on the surface. Some of the entrained oil was predicted to resurface within a day or two, however by day 7 nearly all the surface oil was either evaporated, entrained, or degraded. For the vessel collision release, a large portion (approximately 80%) of the oil was predicted to entrain within the first two days. More quiescent conditions resulted in the resurfacing of approximately 5% of the released oil and rapid evaporation of approximately 40%. On day 8, another wind event resulted in the complete entrainment of the surface oil and mixing within the water column, which reduced the amount of evaporation and resulted in

degradation being a major fate pathway for this release, accounting for approximately 45% of the release volume. For all three batch spill cases, less than 0.01% of oil was predicted to remain on the surface by the end of the 30-day simulation, with a significant portion evaporated (40-76%), a portion in the water column (8-14%), and the rest degraded (16-45%). No shoreline oiling and negligible oil on the sediments was predicted.

For the small volume "batch spills" modelled at the EL 1144 example well site, patchy and discontinuous colorless and silver sheens <0.0001 mm (0.1 µm) predicted over limited distances (Figure 4-37 and Figure 4-41). The cumulative area of average surface oil thickness >0.04 µm was <1 km^2 for the 100 L release and approximately 8 km^2 for the 1,000 L release (Table 4-4). Total hydrocarbon concentrations were not predicted to exceed 1 µg/L for the 100 L release and the vertical maximum THC concentrations for the 1,000 L release were only predicted to reached 2 µg/L within about 5 km of the release site. Note that water column contamination for the marine batch release cases was reported as THC, as opposed to dissolved hydrocarbons reported for the other deterministic and stochastic scenarios, as release volumes were insufficient to create reportable concentrations.

The 750,000 L vessel collision was predicted to result in more extensive surface oil, when compared to the modelled "batch spills." The release would be predicted to result in patchy and discontinuous surface sheens, although the large release volume would likely result in a rainbow sheen for approximately 40 km before transitioning to the colorless and silver sheen that was predicted for the "batch spills." The predicted exposure area for surface oil from the vessel collision was 925 km^2 for the lower 0.04 µm socioeconomic threshold and 13 km^2 for the higher 10 µm ecological threshold.

Table 4-3. Summary of the mass balance information for all representative scenarios. All values represent a percentage of the total amount of released oil.

Summary of Mass Balance Information at the End of the Simulation (Percentage of Released Oil)									
Scenario Information			Surface (%)	Evaporated (%)	Water Column (%)	Sediment (%)	Ashore (%)	Degraded (%)	Outside Grid (%)
Example Well Site	Scenario	Product							
EL 1144	95th percentile surface oil exposure case	BdN	1.08	41.66	24.63	0.01	0.00	32.02	0.59
	95th percentile water column case		0.19	40.40	26.96	0.01	0.00	32.37	0.08
	99th percentile shoreline contact case		3.47	34.80	23.34	0.01	<0.01	37.64	0.73
EL 1150	95th percentile surface oil exposure case		5.58	40.91	19.52	0.01	0.00	32.17	1.82
	95th percentile water column case		0.13	40.89	26.95	0.02	0.00	31.98	0.02
	95th percentile shoreline contact case*		NA	NA	NA	NA	NA	NA	NA
EL 1144	100 L Batch Spill	Marine Diesel	<0.01	75.65	8.40	<0.01	0.00	15.95	0.00
	1,000 L Batch Spill		<0.01	62.84	10.71	<0.01	0.00	26.45	0.00
VCL	750,000 L Batch Spill		<0.01	40.11	14.45	0.01	0.00	45.43	0.00

*For EL 1150, there was no scenario that resulted in shoreline exposure within 60 days

Table 4-4. Representative deterministic cases and associated areas exceeding specified thresholds (km²) for 95th percentile surface and water column and 99th percentile shoreline contamination trajectories and marine diesel trajectories at the EL 1144 and EL 1150 example well sites and VCL.

Scenario Name	Example Well Site	Released Volume	Approximate Surface Area exceeding thickness thresholds (km²)		Approximate Shore area exceeding mass per unit area thresholds (km²)		Approximate Subsurface Volume exceeding THC threshold (km³)^
			Socioeconomic (0.04 µm)	Ecologic (10 µm)	Socioeconomic (1 g/m²)	Ecologic (100 g/m²)	Socioeconomic (1 µg/L)
95th percentile surface oil exposure case – 30 d	EL 1144	184,000 bbl/d	936,529	101,196	-	-	62,236
95th percentile water column case – 30 d			716,187	71,489	-	-	58,842
99th percentile shoreline contact case – 30 d			848,758	51,415	13	<1	22,751
95th percentile surface oil exposure case – 30 d	EL 1150	44,291 bbl/d	638,983	9,601	-	-	52,350
95th percentile water column case – 30 d			430,410	2,838	-	-	54,943
95th percentile shoreline contact case – 30 d*			NA	NA	NA	NA	NA
100 L marine diesel batch spill	EL 1144	100 L	<1	<1	-	-	<1
1,000 L marine diesel batch spill		1,000 L	8	<1	-	-	<1
750,000 L marine diesel batch spill	VCL	750,000 L	925	13	-	-	100

* For EL 1150, there was no scenario that resulted in shoreline exposure within 60 days

^ There is only 1 category threshold (socioeconomic) for THC – calculated by multiplying the area times the depth of the grid cell.

5 Discussion and Conclusions

For each of the modelled releases, oil on the surface was most likely to move to the east due to the prevailing westerly winds and surface currents within the region. Winds and currents in the Project Area are similar throughout the year, with most notable differences in wind intensity. The increased winds during wintertime conditions have the potential to enhance surface breaking waves and results in more complete entrainment of oil, which lowered the amount of oil that would remain on the surface for extended periods of time. In general, after 60 days, the majority of the oil was predicted to evaporate, entrain, and degrade, with very little oil remaining on the surface after 30 or 60 days, negligible sediment oiling, and extremely limited or non-existent shoreline oiling. Shoreline contact with oil was not predicted to be likely from any of the modelled releases. The maximum probability of shoreline oiling was 3% and only for wintertime releases from the EL 1144 example well site. The shoreline oiling that was predicted was localized to Sable Island.

The releases modelled in this study may be considered representative of other potential releases in the Project Area. The water depth of release of the EL 1144 and EL 1150 example well sites (1,137 and 378 m below sea level, respectively) are within the range of depths found throughout the Project Area.

The hypothetical releases modelled in this study are not intended to predict a specific future event, but rather to be used as a tool in environmental assessments and release contingency planning. The results presented in this document demonstrate that there are a range of potential trajectories and fates that could result if a release of crude oil or a batch spill of marine diesel were to occur, and those trajectories and fates vary based upon the environmental conditions occurring at the time. While each oil release is unique and therefore uncertainties exist, the results of this modelling study suggest that if oil were to be released in the Project Area, it has the highest likelihood of moving away from shore to the east.

6 References

Bleck, R., 1998: Ocean modeling in isopycnic coordinates. Chapter 18 in Ocean Modeling and Parameterization, E. P. Chassignet and J. Verron, Eds., NATO Science Series C: Mathematical and Physical Sciences, Vol. 516, Kluwer Academic Publishers, 4223-448.

Bleck, R. 2002. An oceanic general circulation model framed in hybrid isopycnic-cartesian coordinates. Ocean Modeling, 4, 55-88.

Bonn Agreement. 2009. Bonn Agreement Aerial Operations Handbook, 2009. London, UK. Available: http://www.bonnagreement.org/site/assets/files/1081/ba-aoh revision 2 april 2012-1.pdf, Accessed 4 June 2015.

Bonn Agreement, 2011. Bonn Agreement Oil Appearance Code Photo Atlas. Available: http://www.bonnagreement.org/site/assets/files/1081/photo_atlas_version_20112306-1.pdf. Accessed: April 2017.

Canada-Newfoundland and Labrador Offshore Petroleum Board (C-NLOPB). 2014. Eastern Newfoundland Strategic Environmental Assessment. Final Report. Prepared by AMEC Environment & Infrastructure, AMEC TF 1382502. Available: http://www.cnlopb.ca/pdfs/enlsea/ch1-3.pdf?lbisphpreq=1. Accessed: March 2017.

Chassignet, E. P., L. T. Smith, R. Bleck, and F. O. Bryan, 1996: A model comparison: numerical simulations of the North and Equatorial Atlantic oceanic circulation in depth and isopycnic coordinates. J. Phys. Oceanogr., 26, 1849-1867.

Chassignet, E.P., Z.D. Garraffo, 2001. Viscosity parameteriation and gulf stream separation. In: Hawaii U., Muller P., Henderson, D. (Eds.). String to Mixing in Stratified Ocean, Proceedings of Aha Huliko'a Hawaiian Winter Workshop, pp. 27-41.

Conkright, M.E., J.I. Antonov, O. Baranova, T.P. Boyer, H.E. Garcia, R. Gelfeld, D. Johnson, R.A. Locarnini, P.P. Murphy, T.D. O'Brien, I. Smolyar, and C. Stephens. 2002. World Ocean Database 2001, Volume 1: Introduction. Sydney Levitus (ed.). NOAA Atlas NESDIS 42, U.S. Government Printing Office, Washington, D.C., 167 pp.

Cooper, M. and K.A. Haines, 1996.Altimetric assimilation with water property conservation. Journal of Geophysical Research, vol. 24, pp. 1059-1077.

Cummings, J.A. 2005. Operational multivariate ocean data assimilation. Quarterly Journal of the Royal Meteorological Society. Part C, 133(613), 3583-3604.

Environment and Climate Change Canada (ECCC). 2017. Canadian Ice Service. Available: https://www.ec.gc.ca/glaces-ice/. Accessed: March 2017.

Environmental Science and Technology Center (ESTC), 2001. Release Technology Database, Oil Technology Database. Available: http://www.etc-cte.ec.gc.ca/databases/OilProperties/oil_prop_e.html. Accessed: 2016.

French, D., M. Reed, K. Jayko, S. Feng, H. Rines, S. Pavignano, T. Isaji, S. Puckett, A. Keller, F.W. French III, D. Gifford, J. McCue, G. Brown, E. MacDonald, J. Quirk, S. Natzke, R. Bishop, M. Welsh, M. Phillips, and B.S. Ingram, 1996. Final Report, The CERCLA Type A Natural Resource Damage Assessment Model for Coastal and Marine Environments (NRDAM/CME), Technical Documentation, Vol. I - V., Office of Environmental Policy and Compliance, U.S. Department of the Interior, Washington, DC, Contract No. 14-0001-91-C-11.

French McCay, D.P., 2002. Development and Application of an Oil Toxicity and Exposure Model, OilToxEx. Environmental Toxicology and Chemistry 21(10): 2080-2094.

French McCay, D.P., 2004. Oil release impact modelling: Development and validation. Environmental Toxicology and Chemistry 23(10): 2441-2456.

French McCay, D.P. and J.J. Rowe. 2004. Evaluation of Bird Impacts in Historical Oil Release Cases Using the SIMAP Oil Release Model. Proceedings of the Twenty-seventh Arctic and Marine Oilrelease Program (AMOP) Technical Seminar. Emergencies Science Division, Environment Canada, Ottawa, ON, Canada. pp. 421-452.

French McCay, D.P, 2009. State-of-the-Art and Research Needs for Oil Release Impact Assessment Modelling. In Proceedings of the 32nd AMOP Technical Seminar on Environmental Contamination and Response, Emergencies Science Division, Environment Canada, Ottawa, ON, Canada, pp. 601-653.

French McCay, D., Reich, D., Rowe, J., Schroeder, M., and E. Graham. 2011. Oil Spill Modeling Input to the Offshore Environmental Cost Model (OECM) for US-BOEMRE's Spill Risk and Cost Evaluations. In Proceedings of the 34th AMOP Technical Seminar on Environmental Contamination and Response, Emergencies Science Division, Environment Canada, Ottawa, ON, Canada.

French McCay, D., Reich, D., Michel, J., Etkin, D., Symons, L., Helton, D., and J. Wagner. 2012. Oil Spill Consequence Analyses of Potentially-Polluting Shipwrecks. In Proceedings of the 34th AMOP Technical Seminar on Environmental Contamination and Response, Emergencies Science Division, Environment Canada, Ottawa, ON, Canada.

French McCay, D., 2016. Potential Effects Thresholds for Oil Spill Risk Assessments. p. 285-303 In: Proceedings of the 39th AMOP Technical Seminar on Environmental Contamination and Response, Emergencies Science Division, Environment Canada, Ottawa, ON, Canada.

General Bathymetric Chart of the Oceans (GEBCO). 2003. Centenary Edition of the GEBCO Digital Atlas, published on behalf of the Intergovernmental Oceanographic Commission (IOC) and the

International Hydrographic Organization (IHO) as part of the General Bathymetric Chart of the Oceans; British Oceanographic Data Centre (BODC), Liverpool.

Halliwell, G. R., Jr., 1997.Simulation of decadal/interdecadal variability the North Atlantic driven by the anomalous wind field.Proceedings, Seventh Conference on Climate Variations, Long Beach, CA, 97-102.

Halliwell, G. R., Jr., 1998. Simulation of North Atlantic decadal/multi-decadal winter SST anomalies driven by basin-scale atmospheric circulation anomalies. Journal of Physical Oceanography, 28, 5-21.

Halliwell, G.R. 2002.HYCOM Overview. http://www.hycom.org. June 27, 2011.

Halliwell, G. R., Jr., R. Bleck, and E. Chassignet, 1998. Atlantic Ocean simulations performed using a new hybrid-coordinate ocean model. EOS, Fall 1998 AGU Meeting.

Halliwell, G .R, R. Bleck, E. P. Chassignet, and L.T. Smith, 2000: mixed layer model validation in Atlantic Ocean simulations using the Hybrid Coordinate Ocean Model (HYCOM). EOS, 80, OS304.

Han, G. and C.L. Tang. 1999. Velocity and transport of the Labrador Current determined from altimetric, hydrographic, and wind data. Journal of Geophysical Research: Oceans. Volume 104, Issue C8, 15 August, 1999. DOI: 10.1029/1999JC900145.

Hu, D., 1996: On the Sensitivity of Thermocline Depth and Meridional Heat Transport to Vertical Diffusivity in OGCMs. J. Physical Oceanography, 26, 1480-1494.

Hurlburt, H.E., Hogan, P.J., 2000. Impact of 1/8 to 1/64 resolution on Gulf stream model-data comparisons in basin-scale Atlantic Ocean models. Dynamics of Atmospheres and Oceans, No. 32, pp. 283-329.

HYCOM. 2016. HYCOM Data Server: HYbrid Coordinate Ocean Model; Center for Ocean-Atmospheric Prediction Studies (COAPS) Accessed: https://hycom.org/dataserver/

Intertek, 2016. Preliminary Laboratory Report for Statoil Petroleum AS. Analysis of water sample from L-76-z. Intertek West Lab AS, Tananger Norway. 23 February 2016.

Jones, R.K., 1997. A Simplified Pseudo-Component of Oil Evaporation Model. In Proceedings of the 20th Arctic and Marine Oil Spill Program (AMOP) Technical Seminar, Environment Canada, pp. 43-61.

Lehr, W.J., D. Wesley, D. Simecek-Beatty, R. Jones, G. Kachook, and J. Lankford, 2000. Algorithm and interface modifications of the NOAA oil spill behavior model. In Proceedings of the 23rd Arctic and Marine Oil Spill Program (AMOP) Technical Seminar, Vancouver, BC, Environmental Protection Service, Environment Canada, pp. 525-539.

Levitus, S. 1982. Climatological Atlas of the World Ocean, NOAA/ERL GFDL Professional Paper 13, Princeton, N.J., 173 pp. (NTISPB83-184093).

Levitus, S., T.P., Boyer, H.E. Garcia, R.A. Locarnini, M.M. Zweng, A.V. Mishonov, J.R. Reagan, J.I. Antonov, O.K. Baranova, M. Biddle, M. Hamilton, D.R. Johnson, C.R. Paver, and D. Seidov. 2014. World Ocean Atlas 2013 (NODC accession 0114815). National Oceanographic Data Center, NOAA.

Lewis, A. 2007. Current Status of the BAOAC; Bonn Agreement Oil Appearance Code. A report to the Netherlands North Sea Agency Directie Noordzee. Alan Lewis Oil Release Consultant, submitted January, 2007.

Maine Department of Environmental Protection (MDEP). 2016. Releases and Site Cleanup: Maine Environmental Vulnerability Index Maps. Available: http://www.maine.gov/dep/releases/emergreleaseresp/evi/. Accessed: March 2017.

Marsh, R., M. J. Roberts, R. A. Wood, and A. L. New, 1996: An intercomparison of a Bryan-Cox-type ocean model and an isopycnic ocean model, part II: the subtropical gyre and meridional heat transport. J. Phys. Oceanogr., 26, 1528-1551.

McAuliffe, C.D., 1987. Organism exposure to volatile/soluble hydrocarbons from crude oil releases –a field and laboratory comparison. Proceedings of the 1987 Oil Release Conference. Washington, D.C.: API. pp. 275-288.

National Oceanic and Atmospheric Administration (NOAA), 2014. Can the ocean freeze? Available: http://oceanservice.noaa.gov/facts/oceanfreeze.html. Accessed: April 2017.

National Oceanic and Atmospheric Administration (NOAA), 2016. Environmental Sensitivity Index (ESI). Accessed: https://response.restoration.noaa.gov/maps-and-spatial-data/download-esi-maps-and-gis-data.html

National Oceanic and Atmospheric Administration (NOAA). 2016. Open water oil identification job aid for aerial observation. U.S. Department of Commerce, Office of Response and Restoration [http://response.restoration.noaa.gov/oil-and-chemical-releases/oil-releases/resources/open-water-oil-identification-job-aid.html]

Maps. Available: http://response.restoration.noaa.gov/maps-and-spatial-data/environmental-sensitivity-index-esi-maps.html. Accessed: 2011 - 2012.

National Research Council (NRC), 1985. Oil in the Sea: Inputs, Fates and Effects. National Academy Press, Washington, D.C. 601p.

National Research Council (NRC), 2003. Oil in the Sea III: Inputs, Fates and Effects. National Academy Press, Washington, D.C. 280p.

New, A. and R. Bleck, 1995: An isopycnic model of the North Atlantic, Part II: interdecadal variability of the subtropical gyre. J. Phys. Oceanogr., 25, 2700-2714.

New, A., R. Bleck, Y. Jia, R. Marsh, M. Huddleston, and S. Barnard, 1995: An isopycnic model of the North Atlantic, Part I: model experiments. J. Phys. Oceanogr., 25, 2667-2699.

Payne, J.R., B.E. Kirstein, G.D. McNabb, Jr., J.L. Lambach, R. Redding R.E. Jordan, W. Hom, C. deOliveria, G.S. Smith, D.M. Baxter, and R. Gaegel, 1984. Multivariate analysis of petroleum weathering in the marine environment – sub Arctic. Environmental Assessment of the Alaskan Continental Shelf, OCEAP, Final Report of Principal Investigators, Vol. 21 and 22, Feb. 1984, 690p.

Payne, J.R., B.E. Kirstein, J.R. Clayton, Jr., C. Clary, R. Redding, G.D. McNabb, Jr., and G. Farmer, 1987. Integration of suspended particulate matter and oil transportation study. Final Report. Minerals Management Service, Environmental Studies Branch, Anchorage, AK. Contract No. 14 12-0001-30146, 216 p.

Petrie, B., 1983. Circulation of the Newfoundland Continental Shelf. Atmosphere-Ocean, vol. 21, no. 2, pp. 207-226.

Petrie, B. C. Anderson. 1983. Circulation on the Newfoundland continental shelf. Atmosphere-Ocean. Volume 21, 1983 - Issue 2. DOI: 10.1080/07055900.1983.9649165.

Petrie, B. A. Isenor, 1985. The Near-Surface Circulation and Exchange in the Newfoundland Grand Banks Region. Atmosphere-Ocean, vol. 23, no. 3, pp. 209-227.

Petroforma, 2013. Reservoir Fluid PVT Analyses for Statoil Canada. C30+ Composition, OBM Contamination Analysis, Constant Composition Expansion and Live Viscosity Study on Bay du Nord Flemish Pass, Zone Ti-2, MRSC 273.

Richardson, P.L. 1983. Eddy kinetic energy in the North Atlantic from surface drifters. Journal of Geophysical Research: Oceans. Volume 88, Issue C7, 20 May 1983, pp. 4355-4367. DOI: 10.1029/JC088iC07p04355.

Roberts, M. J., R. Marsh, A. L. New, and R. A. Wood, 1996: An intercomparison of a Bryan-Cox-type ocean model and an isopycnic ocean model, part I: the subpolar gyre and highlatitudeprocesses. J. Phys. Oceanogr., 26, 1495-1527.

RPS ASA, 2013. NRC categories and observations of oil releases.

Saha, S., et al. 2010. NCEP Climate Forecast System Reanalysis (CFSR) 6-hourly Products, January 1979 to December 2010. Research Data Archive at the National Center for Atmospheric Research, Computational and Information Systems Laboratory. http://dx.doi.org/10.5065/D69K487J.

S.L. Ross Environmental Research Ltd., 2011. Oil Release Fate and Behavior Modelling in Support of Corridor Resources Old Harry Prospect Drilling EA. Prepared for Corridor Resources Inc. 40 pp. + Appendix.

S.L. Ross Environmental Research Ltd., 2008. The Fate and Behavior of Hypothetical Oil Releases form the StatoilHydro 2008 Mizzen Drilling Program. Prepared for StatoilHydro Canada E&P. January 2008.

S.L. Ross Environmental Research Ltd., 2016. Release-related Properties of BdNL-76Z Ti-3 DST Dead Oil. 30 pp. + Appendices.

Smith, R.D. Maltrud, M.E., 2000. Numerical simulations of the North Atlantic Ocean at 1/10. Journal of physical Oceanography, no. 30, pp.1532-1561.

Statoil 2016. Response to Comments – 2016 Drilling EA Amendment. SC-CNO-0122-16. December 15, 2016.

Therrien, A., 2017. Shoreline Segmentation (SCAT Classification). Environment and Climate Change Canada

Trudel, B.K., R.C. Belore, B.J. Jessiman and S.L. Ross., 1989. A micro-computer based release impact assessment system for untreated and chemically dispersed oil releases in the U.S. Gulf of Mexico. 1989 International Oil Release Conference.

United States Coast Guard (USCG). 2009. How do the Labrador and Gulf Stream Currents Affect Icebergs. Labrador and Gulf Stream currents affect icebergs in the North Atlantic Ocean. USCG Navigation Center. U.S. Department of Homeland Security. Available: https://navcen.uscg.gov/?pageName=iipHowDoTheLabradorAndGulfStreamCurrentsAffectIcebergsInTheNorthAtlanticOcean. Accessed: March 2017.

UNESCO, 1981: The Practical Salinity Scale 1978 and the International Equation of State of Seawater 1980. UNESCO technical papers in marine science 36, 25 pp.

VLIZ (2014). Maritime Boundaries Geodatabase, version 8. Available online at http://www.marineregions.org/. Consulted on 2014-04-14.

Volkov, D.L., 2005. Interannual Variability of the Altimetry-Derived Eddy Field and Surface Circulation in the Extratropical North Atlantic Ocean in 1993-2001. Journal of Physical Oceanography, Vol. 35, pp. 405-426.

Wang, Z., P. Jokuty, M. Fingas, et al., 2001. Characterization of Federated Oil fractions used for the PTAC project to study the petroleum fraction-specific toxicity to soils. Proceedings of the 18th AMOP Conference, 2001. pp 79-98.

Trajectory Modelling in Support of the Nexen Energy ULC Flemish Pass Exploration Drilling Project (2018-2028)

Appendix A: SIMAP and OILMAPDeep Model Descriptions

Prepared for: Nexen Energy ULC

Project Number:
2017-657

Date Submitted:
1/26/2018

Version:
Final Appendix

Project Manager
Matthew Horn, Ph.D.

RPS
55 Village Square Dr.
South Kingstown, RI USA
02879-8248

Release	File Name	Date Submitted	Notes
Draft	Nexen - RPS Technical Report_20180126 _AppendixA.docx	1/26/2018	RPS final draft version of Appendix A following review by Wood plc and Nexen Energy ULC
Draft	Nexen - RPS Technical Report_20171222 _AppendixA.docx	12/22/2017	RPS Draft final version of Appendix A following senior technical review

Summary

This Appendix A is provided as a reference to RPS Technical Report: Trajectory Modelling in Support of the Nexen Energy ULC Flemish Pass Exploration Drilling Project (2018-2028). Appendix A provides a detailed description of the SIMAP model and the fates processes and algorithms that were used, as well as a description of the theory and implementation of the OIMAP Deep model.

Table of Contents

List of Figures

1 SIMAP Model Description

The analysis was performed using the model system developed by Applied Science Associates (ASA) called SIMAP (Spill Impact Model Analysis Package). SIMAP originated from the oil fates and biological effects submodels in the Natural Resource Damage Assessment Models for Coastal and Marine Environments (NRDAM/CME) and Great Lakes Environments (NRDAM/GLE), which ASA developed in the early 1990s for the U.S. Department of the Interior for use in "type A" Natural Resource Damage Assessment (NRDA) regulations under the Comprehensive Environmental Response, Compensation and Liability Act of 1980 (CERCLA). The most recent version of the type A models, the NRDAM/CME (Version 2.4, April 1996) was published as part of the CERCLA type A NRDA Final Rule (Federal Register, May 7, 1996, Vol. 61, No. 89, p. 20559-20614). The technical documentation for the NRDAM/CME is in French et al. (1996 a-c). This technical development involved several in-depth peer reviews, as described in the Final Rule.

While the NRDAM/CME and NRDAM/GLE were developed for simplified natural resource damage assessments of small spills in the United States, SIMAP is designed to evaluate fates and effects of both real and hypothetical spills in marine, estuarine and freshwater environments worldwide. Additions and modifications to prepare SIMAP were made to increase model resolution, allow modification and site-specificity of input data, allow incorporation of temporally varying current data, evaluate subsurface releases and movements of subsurface oil, track multiple chemical components of the oil, enable stochastic modelling, and facilitate analysis of results.

Below are brief descriptions of the fates and effects models presented in SIMAP. Detailed descriptions of the algorithms and assumptions in the model are in published papers (French McCay, 2002; 2003; 2004; 2009). The model has been validated with more than 20 case histories, including the *Exxon Valdez* and other large spills (French and Rines, 1997; French McCay, 2003; 2004; French McCay and Rowe, 2004) as well as test spills designed to verify the model (French et al., 1997).

1.1 Physical Fates Model

The three-dimensional physical fates model estimates distribution (as mass and concentrations) of whole oil and oil components on the water surface, on shorelines, in the water column, and in sediments. Oil fate processes included are oil spreading (gravitational and by shearing), evaporation, transport, randomized dispersion, emulsification, entrainment (natural and facilitated by dispersant), dissolution, volatilization of dissolved hydrocarbons from the surface water, adherence of oil droplets to suspended sediments, adsorption of soluble and sparingly-soluble aromatics to suspended sediments, sedimentation, and degradation.

Oil is a mixture of hydrocarbons of varying physical, chemical, and toxicological characteristics. In the model, oil is represented by component categories, and the fate of each component is tracked separately. The "pseudo-component" approach (Payne et al., 1984; 1987; French et al., 1996a; Jones, 1997; Lehr et al., 2000) is used, where chemicals in the oil mixture are grouped by physical-chemical

properties, and the resulting component category behaves as if it were a single chemical with characteristics typical of the chemical group.

The most toxic components of oil to aquatic organisms are low molecular weight aromatic compounds (monoaromatic and polycyclic aromatic hydrocarbons, MAHs and PAHs), which are both volatile and soluble in water. Their acute toxic effects are caused by non-polar narcosis, where toxicity is related to the octanol-water partition coefficient (K_{ow}), a measure of hydrophobicity. The more hydrophobic the compound, the more toxic it is likely to be. However, as K_{ow} increases, the compound also becomes less soluble in water, and so there is less exposure to aquatic organisms. The toxicity of compounds having log(K_{ow}) values greater than about 5.6 is limited by their very low solubility in water, and consequent low bioavailability to aquatic biota (French McCay, 2002, Di Toro et al., 2000). Thus, the potential for acute effects is the result of a balance between bioavailability (exposure), toxicity once exposed, and duration of exposure. French McCay (2002) contains a full description of the oil toxicity model in SIMAP, and French McCay (2002) describes the implementation of the toxicity model in SIMAP.

Because of these considerations, the SIMAP fates model focuses on tracking the lower molecular weight aromatic components divided into chemical groups based on volatility, solubility, and hydrophobicity. In the model, the oil is treated as comprising eight components (defined in Table 1). Six of the components (i.e., all but the two non-volatile residual components representing non-volatile aromatics and aliphatics) evaporate at rates specific to the pseudo-component. Solubility is strongly correlated with volatility, and the solubility of aromatics is higher than aliphatics of the same volatility. The MAHs are the most soluble, the 2-ring PAHs are less soluble, and the 3-ring PAHs slightly soluble (Mackay et al., 1992). Both the solubility and toxicity of the non-aromatic hydrocarbons are much less than for the aromatics, and dissolution (and water concentrations) of non-aromatics is safely ignored. Thus, dissolved concentrations are calculated only for each of the three soluble aromatic pseudo-components.

Table 1. Definition of four distillation cuts and the eight pseudo-components in the model (Monoaromatic Hydrocarbons, MAHs; Benzene + Toluene + Ethylbenzene + Xylene, BTEX; Polycyclic Aromatic Hydrocarbons, PAHs).

Characteristic	Volatile and Highly Soluble	Semi-volatile and Soluble	Low Volatility and Slightly Soluble	Residual (non-volatile and very low solubility)
Distillation cut	1	2	3	4
Boiling Point (°C)	< 180	180 - 265	265 - 380	>380
Molecular Weight	50 - 125	125 - 168	152 - 215	> 215
Log(K_{ow})	2.1-3.7	3.7-4.4	3.9-5.6	>5.6
Aliphatic pseudo-components: Number of Carbons	volatile aliphatics: C4 – C10	semi-volatile aliphatics: C10 – C15	low-volatility aliphatics: C15 – C20	non-volatile aliphatics: > C20
Aromatic pseudo-component name: included compounds	MAHs: BTEX, MAHs to C3-benzenes	2 ring PAHs: C4-benzenes, naphthalene, C1-, C2-naphthalenes	3 ring PAHs: C3-, C4-naphthalenes, 3-4 ring PAHs with log(K_{ow}) < 5.6	≥4 ring aromatics: PAHs with log(K_{ow}) > 5.6 (very low solubility)

This number of components provides sufficient accuracy for the evaporation and dissolution calculations, particularly given the time frame (minutes) over which dissolution occurs from small droplets and the rapid resurfacing of large droplets (see discussion above). The alternative of treating oil as a single compound with empirically-derived rates (e.g., Mackay et al., 1980; Stiver and Mackay, 1984) does not provide sufficient accuracy for environmental effects analyses because the effects to water column organisms are caused by MAHs and PAHs, which have specific properties that differ from the other volatile and soluble compounds. The model has been validated both in predicting dissolved concentrations and resulting toxic effects, supporting the adequacy of the use of this number of pseudo-components (French McCay, 2003).

The lower molecular weight aromatics dissolve from the whole oil and are partitioned in the water column and sediments according to equilibrium partitioning theory (French et al., 1996a; French McCay, 2004). The residual fractions in the model are composed of non-volatile and insoluble compounds that remain in the "whole oil" that spreads, is transported on the water surface, strands on shorelines, and disperses into the water column as oil droplets or remains on the surface as tar balls. This is the fraction that composes black oil, mousse, and sheen.

1.2 Oil Fate Model Processes

The schematic in Figure 1 depicts oil fates processes simulated in open water conditions, while the schematic in Figure 2 depicts oil fates processes that are simulated at and near the shoreline. Because oil contains many chemicals with varying physical-chemical properties, and the environment is spatially and temporally variable, the oil rapidly separates into different phases or parts of the environment:

- Surface oil
- Emulsified oil (mousse) and tar balls
- Oil droplets suspended in the water column
- Oil adhering to suspended particulate matter in the water
- Dissolved lower molecular weight components (MAHs, PAHs, and other soluble components) in the water column
- Oil on and in the sediments
- Dissolved lower molecular weight components (MAHs, PAHs, and other soluble components) in the sediment pore water
- Oil on and in the shoreline sediments and surfaces

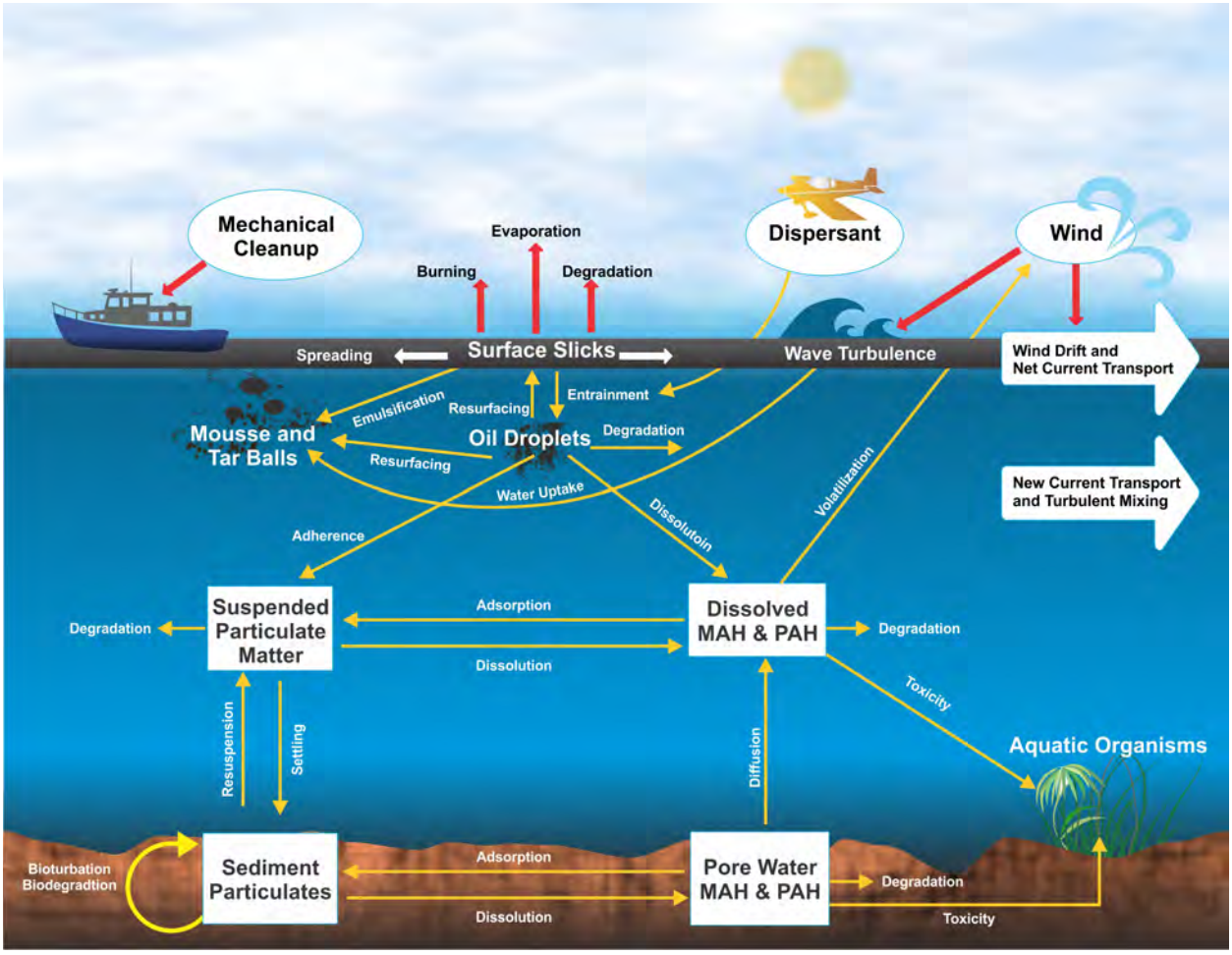

Figure 1. Simulated oil fates processes in open water.

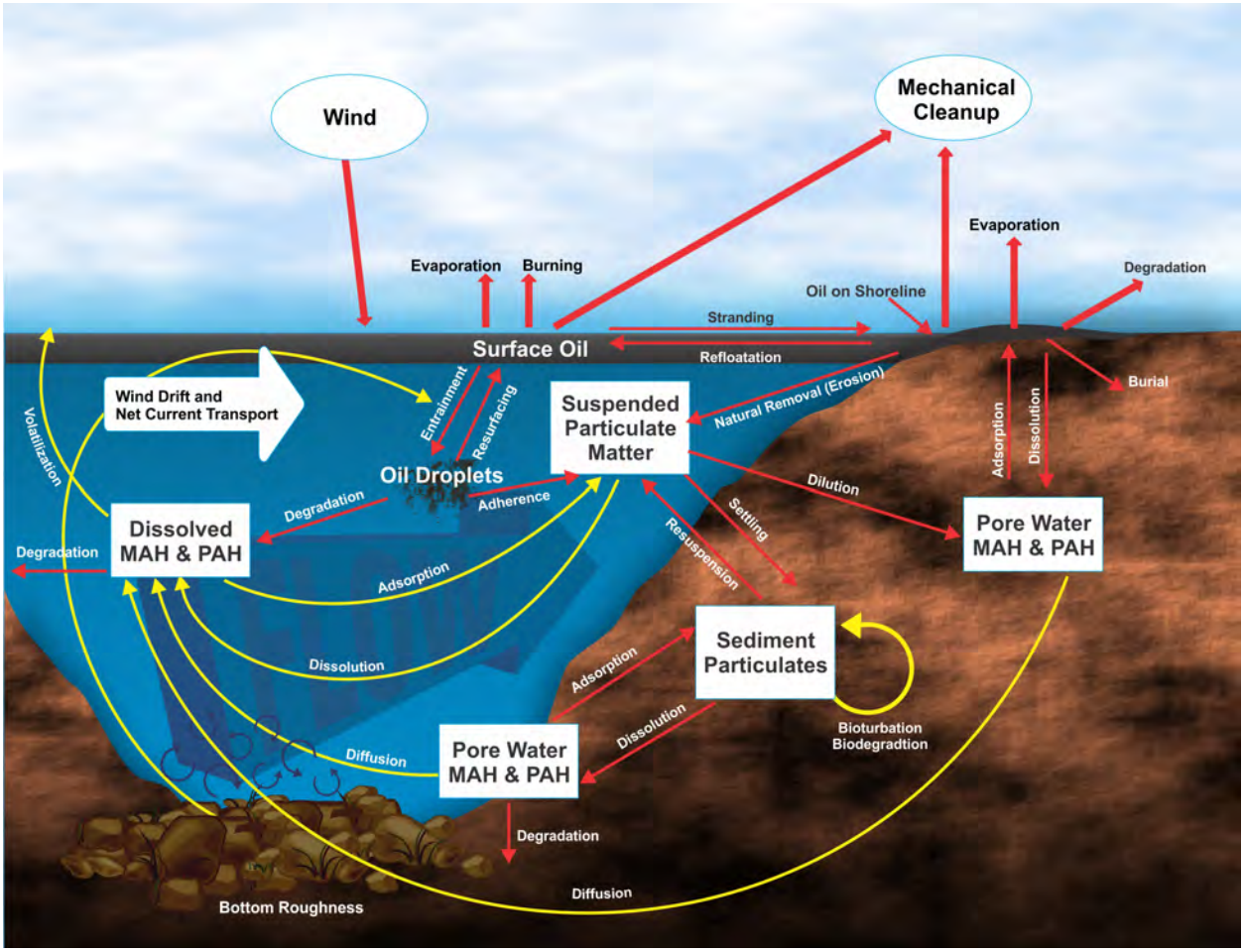

Figure 2. Simulated oil fates processes at the shoreline.

The schematics in Figure 1 and Figure 2 represent oil fates processes that are simulated in the model:

- Spreading is the thinning and broadening of surface slicks caused by gravitational forces and surface tension. This occurs rapidly after oil is spilled on the water surface. The rate of spreading is faster if oil viscosity is lower. Viscosity decreases as temperature increases. Viscosity increases as oil emulsifies.
- Transport is the process where oil is carried by currents.
- Turbulent dispersion: Typically there are also “sub-scale” currents (not included in the current data), better known as turbulence that move oil and mix it both in three dimensions. The process by which turbulence mixes and spreads oil components on the water surface and in the water is called turbulent dispersion.
- Evaporation is the process where volatile components of the oil diffuse from the oil and enter the gaseous phase (atmosphere). Evaporation from surface and shoreline oil increases as the oil

surface area, temperature, and wind speed increase. As lighter components evaporate off, the remaining "weathered" oil becomes more viscous.

- Emulsification is the process where water is mixed into the oil, such that the oil makes a matrix with embedded water droplets. The resulting mixture is commonly called mousse. It is technically referred to as a water-in-oil emulsion. The rate of emulsification increases with increasing wind speed and turbulence on the surface of the water. Viscosity increases as oil emulsifies.
- Entrainment is the process where waves break over surface oil and carry it as droplets into the water column. At higher wind speeds, or where currents and bottom roughness induce turbulence, wave heights may reach a threshold where they break. In open waters, waves break beginning at about 12 knots of wind speed and wave breaking increases as wind speed becomes higher. Thus, entrainment becomes increasingly important (higher rate of mass transfer to the water) the higher the wind speed. As turbulence from whatever source increases, the oil droplet sizes become smaller. Application of chemical dispersant increases the entrainment rate of oil and decreases droplet size at a given level of turbulence. Entrainment rate is slower, and droplet size is larger, as oil viscosity increases (by emulsification and evaporation loss of lighter volatile components). The droplet size determines how fast and whether the oil resurfaces.
- Resurfacing of entrained oil rapidly occurs for larger oil droplets. Smaller droplets resurface when the wave turbulence decreases. The smallest droplets do not resurface, as typical turbulence levels in the water keep them in suspension indefinitely. Local winds at the water surface can also prevent oil from surfacing. Resurfaced oil typically forms sheens. In open water where currents are relatively slow, surface slicks are usually blown down wind faster than the underlying water, resurfacing droplets come up behind the leading edge of the oil, effectively spreading the slicks in the down-wind direction.
- Dissolution is the process where water-soluble components diffuse out of the oil into the water. Dissolution rate increases the higher the surface area of the oil relative to its volume. As the surface area to volume ratio is higher for smaller spherical droplets, the smaller the droplets the higher the dissolution rate. The higher the wave turbulence, the smaller the droplets of entrained oil. Dissolution from entrained small droplets is much faster than from surface slicks in the shape of flat plates. The soluble components are also volatile, and evaporation from surface slicks is faster than dissolution into the underlying water. Thus, the processes of evaporation and dissolution are competitive, with evaporation the dominant process for surface oil.
- Volatilization of dissolved components from the water to the atmosphere occurs as they are mixed and diffuse to the water surface boundary and enter the gas phase. Volatilization rate increase with increasing air and water temperature.
- Adsorption of dissolved components to particulate matter in the water occurs because the soluble components are only sparingly so. These compounds (MAHs and PAHs) preferentially adsorb to particulates when the latter are present. The higher the concentration of suspended

particulates, the more adsorption. Also, the higher the molecular weight of the compound, the less soluble, and the more the compound adsorbs to particulate matter.

- Adherence is the process where oil droplets combine with particles in the water. If the particles are suspended sediments, the combined oil/suspended sediment agglomerate is heavier than the oil itself and than the water. If turbulence subsides sufficiently, the oil-sediment agglomerates will settle.
- Sedimentation (settling) is the process where oil-sediment agglomerates and particles with adsorbed sparingly-soluble components (MAHs and PAHs) settle to the bottom sediments. Adherence and sedimentation can be an important pathway of oil in near shore areas when waves are strong and subsequently subside. Generally, oil-sediment agglomerates transfer more PAH to the bottom than sediments with PAHs that were adsorbed from the dissolved phase in the water column.
- Resuspension of settled oil-sediment particles and particles with adsorbed sparingly-soluble components (MAHs and PAHs) may occur if current speeds and turbulence exceed threshold values where cohesive forces can be overcome.
- Diffusion is the process where dissolved compounds move from higher to lower concentration areas by random motion of molecules and micro-scale turbulence. Dissolved components in bottom and shoreline sediments can diffuse out to the water where concentrations are relatively low. Bioturbation, groundwater discharge and hyporheic flow of water through stream-bed sediments can greatly increase the rate of diffusion from sediments (see below).
- Dilution occurs when water of lower concentration is mixed into water with higher concentration by turbulence, currents, or shoreline groundwater.
- Bioturbation is the process where animals in the sediments mix the surface sediment layer while burrowing, feeding, or passing water over their gills. In open-water soft-bottom environments, bioturbation effectively mixes the surface sediment layer about 10 cm thick (in non-polluted areas).
- Degradation is the process where oil components are changed either chemically or biologically (biodegradation) to another compound. It includes breakdown to simpler organic carbon compounds by bacteria and other organisms, photo-oxidation by solar energy, and other chemical reactions. Higher temperature and higher light intensity (particularly ultraviolet wavelengths) increase the rate of degradation.
- Floating oil may strand on shorelines and refloat as water levels rise, allowing the oil to move further down current (downstream).

For a spill on the water surface, the gravitational spreading occurs very rapidly (within hours) to a minimum thickness. Thus, the area exposed to evaporation is high relative to the oil volume. Evaporation proceeds faster than dissolution. Thus, most of the volatiles and semi-volatiles evaporate, with a smaller fraction dissolving into the water. Degradation (photo-oxidation and biodegradation) also occurs at a relatively slow rate compared to these processes.

Evaporation is more rapid as the wind speed increases. However, above about 12 knots (6 m/s) of wind speed and in open water, white caps begin to form and the breaking waves entrain oil as droplets into the water column. Higher wind speeds (and turbulence) increase entrainment and results in smaller droplet sizes. From Stoke's Law, larger droplets resurface faster and form surface slicks. Thus, a dynamic balance evolves between entrainment and resurfacing. As high-wind events occur, the entrainment rate increases. When the winds subside to less than 12 knots, the larger oil droplets resurface and remain floating. Similar dynamics occur in turbulent streams.

The smallest oil droplets remain entrained in the water column for an indefinite period. Larger oil droplets rise to the surface at varying rates. While the droplets are under water, dissolution of the light and soluble components occurs. Dissolution rate is a function of the surface area available. Thus, most dissolution occurs from droplets, as opposed to from surface slicks, since droplets have a higher surface area to volume ratio, and they are not in contact with the atmosphere (and so the soluble components do not preferentially evaporate as they do from surface oil).

If oil is released or driven underwater, it forms droplets of varying sizes. More turbulent conditions result in smaller droplet sizes. From Stoke's Law, larger droplets rise faster, and surface if the water is shallow. Resurfaced oil behaves as surface oil after gravitational spreading has occurred. The surface oil may be re-entrained. The smallest droplets in most cases remain in the water permanently. As a result of the higher surface area per volume of small droplets, the dissolution rate is much higher from subsurface oil than from floating oil on the water surface.

Because of these interactions, the majority of dissolved constituents (which are of concern because of potential effects on aquatic organisms) are from droplets entrained in the water. For a given spill volume and oil type/composition, with increasing turbulence either at the water surface and/or at the stream bed: there is an increasing amount of oil entrained; the oil is increasingly broken up into smaller droplets; there is more likelihood of the oil remaining entrained rather than resurfacing; and the dissolved concentrations will be higher. Entrainment and dissolved concentrations increase with (1) higher wind speed, (2) increased turbulence from other sources of turbulence (waves on a beach, rapids, and waterfalls in rivers, etc.), (3) subsurface releases (especially under higher pressure and turbulence), and (4) application of chemical dispersants. Chemical dispersants both increase the amount of oil entrained and decrease the oil droplet size. Thus, chemical dispersants increase the dissolution rate of soluble components.

These processes that increase the rate of supply of dissolved constituents are balanced by loss terms in the model: (1) transport (dilution), (2) volatilization from the dissolved phase to the atmosphere, (3) adsorption to suspended particulate material (SPM) and sedimentation, and (4) degradation (photo-oxidation or biologically mediated). Also, other processes slow the entrainment rate: (1) emulsification increases viscosity and slows or eliminates entrainment; (2) adsorption of oil droplets to SPM and settling removes oil from the water; (3) stranding on shorelines removes oil from the water; and (4) mechanical cleanup and burning removes mass from the water surface and shorelines. Thus, the model-

predicted concentrations are the resulting balance of all these processes and the best estimates based on our quantitative understanding of the individual processes.

The algorithms used to model these processes are described in French McCay (2004). Lagrangian elements (spillets) are used to simulate the movements of oil components in three dimensions over time. Surface floating oil, subsurface droplets, and dissolved components are tracked in separate spillets. Transport is the sum of advective velocities by currents input to the model, surface wind drift, vertical movement according to buoyancy, and randomized turbulent diffusive velocities in three dimensions. The vertical diffusion coefficient is computed as a function of wind speed in the surface wave-mixed layer. The horizontal and deeper water vertical diffusion coefficients are model inputs.

The oil (whole and as pseudo-components) separates into different phases or parts of the environment, i.e., surface slicks; emulsified oil (mousse) and tar balls; oil droplets suspended in the water column; dissolved lower molecular weight components (MAHs and PAHs) in the water column; oil droplets adhered and hydrocarbons adsorbed to suspended particulate matter in the water; hydrocarbons on and in the sediments; dissolved MAHs and PAHs in the sediment pore water; and hydrocarbons on and in the shoreline sediments and surfaces.

1.3 Oil Fates Algorithms

1.3.1 Transport

Lagrangian particles (spillets) are moved in three dimensions over time. For each model time step, the new vector position of the spillet centre is calculated from the old plus the vector sum of east-west, north-south, and vertical components of advective and diffusive velocities:

$$X_t = X_{t-1} + \Delta t \, (U_t + D_t + R_t + W_t)$$

where X_t is the vector position at time t, X_{t-1} is the vector position the previous time step, Δt is the time step, U_t is the sum of all the advective (current) velocity components in three dimensions at time t, D_t is the sum of the randomized diffusive velocities in three dimensions at time t, R_t is the rise or sinking velocity of whole oil droplets in the water column, and W_t is the surface wind transport ("wind drift"). The magnitudes of the components of D_t are scaled by horizontal and vertical diffusion coefficients (Okubo and Ozmidov, 1970; Okubo, 1971). The vertical diffusion coefficient is computed as a function of wind speed in the surface wave-mixed layer (which ranges from centimetre scales in rivers and near lee shorelines to potentially metres in large water bodies away from shore when wind speeds are high), based on Thorpe (1984). R_t is computed by Stokes law, where velocity is related to the difference in density between the particle and the water, and to the particle diameter. The algorithm developed by Youssef and Spaulding (1993) is used for wind transport in the surface wave-mixed layer (W_t, described below).

1.3.2 Shoreline Stranding

The fate of spilled oil that reaches the shoreline depends on characteristics of the oil, the type of shoreline, and the energy environment. The stranding algorithm is based on work by CSE/ASA/BAT (1986), Gundlach (1987), and Reed and Gundlach (1989) in developing the COZOIL model for the U.S. Minerals Management Service. In SIMAP, deposition occurs when an oil spillet intersects shore surface. Deposition ceases when the volume holding capacity for the shore surface is reached. Subsequent oil coming ashore is not allowed to remain on the shore surface. It is refloated by rising water, and carried away by currents and wind drift. The remaining shoreline oil is then removed exponentially with time. Data for holding capacity and removal rate are taken from CSE/ABA/BAT (1986) and Gundlach (1987), and are a function of oil viscosity and shore type. The algorithm and data are in French et al. (1996a).

1.3.3 Spreading

Spreading determines the areal extent of the surface oil, which in turn influences its rates of evaporation, dissolution, dispersion (entrainment) and photo-oxidation, all of which are functions of surface area. Spreading results from the balance among the forces of gravity, inertia, viscosity, and surface tension (which increases the diameter of each spillet); turbulent diffusion (which spreads the spillets apart); and entrainment followed by resurfacing, which can spatially separate the leading edge of the oil from resurfaced oil transported in a different direction by subsurface currents.

For many years Fay's (1971) three-regime spreading theory was widely used in oil spill models (ASCE, 1996). Mackay et al. (1980; 1982) modified Fay's approach and described the oil as thin and thick slicks. Their approach used an empirical formulation based on Fay's (1971) terminal spreading behaviour. They assumed the thick slick feeds the thin slick and that 80-90% of the total slick area is represented by the thin slick. In SIMAP, oil spillets on the water surface increase in diameter according to the spreading algorithm empirically-derived by Mackay et al. (1980; 1982). Sensitivity analyses of this algorithm led to the discovery that the solution was affected by the number of spillets used. Thus, a formulation was derived to normalize the solution under differing numbers of surface spillets (Kolluru et al., 1994). Spreading is stopped when an oil-specific terminal thickness is reached.

1.3.4 Evaporation

The rate of evaporation depends on surface area, thickness, vapour pressure and mass transport coefficient, which in turn are functions of the composition of the oil, wind speed and temperature (Fingas, 1996; 1997; 1998; 1999; Jones, 1997). As oil evaporates its composition changes, affecting its density and viscosity as well as subsequent evaporation. The most volatile hydrocarbons evaporate most rapidly, typically in less than a day and sometimes in under an hour (McAuliffe, 1989). As the oil continues to weather, and particularly if it forms a water-in-oil emulsion, evaporation will be significantly decreased.

The evaporation algorithm in SIMAP is based on accepted evaporation theory, which follows Raoult's Law that each component will evaporate with a rate proportional to the saturation vapour pressure and mole fraction present for that component. The pseudo-component approach (Payne et al., 1984; French et al., 1996a; Jones, 1997; Lehr et al., 2000) is used, such that each component evaporates according to its mean vapour pressure, solubility, and molecular weight (Table 2-3). The mass transfer coefficient is calculated using the methodology of Mackay and Matsugu (1973), as described in French et al. (1996a).

1.3.5 Entrainment

As oil on the water surface is exposed to wind and waves, or if oil moves into a turbulent area of a stream or river, it is entrained (or dispersed) into the water column. Entrainment is a physical process where globules of oil are transported from the water surface into the water column due to breaking waves or other turbulence. It has been observed that entrained oil is broken into droplets of varying sizes. Smaller droplets spread and diffuse in the water column, while larger ones rise back to the surface.

Entrainment by Breaking Surface Wave Action

In open waters, breaking waves created by the action of wind and waves on the water surface are the primary sources of energy for entrainment. Entrainment is strongly dependant on turbulence and is greater in areas of high wave energy (Delvigne and Sweeney, 1988).

Delvigne and Sweeney (1988), using laboratory and flume experimental observations, developed a relationship for entrainment rate and oil droplet size distribution as a function of turbulent energy level and oil viscosity. Entrained droplets in the water column rise according to Stokes law, where velocity is related to the difference in density between the particle and the water, and to the particle diameter. The data and relationships in Delvigne and Sweeney (1988) are used in SIMAP to calculate mass and particle size distribution of droplets entrained. Particle size decreases with higher turbulent energy level and lower oil viscosity. The natural dispersion particle sizes observed by Delvigne and Sweeney (1988) are confirmed by field observations by Lunel (1993a,b).

Use of chemical dispersants (not modelled in the scenarios examined here) decrease the median particle size, increasing the number of droplets in the <70 μm range (Daling et al., 1990; Lunel, 1993a,b). Particle size distributions for dispersed oil are available for several oils from these studies. When dispersant is applied, the model entrains surface oil, creating subsurface droplets in the appropriate size distribution for dispersant use. The median particle size for permanently dispersed droplets is set at 20 microns, the median size observed by Lunel (1993a,b). The fraction of oil permanently dispersed is set by the assumed dispersant efficiency. The IKU/SINTEF studies provide data on the viscosity range where oils may be dispersed chemically. Typically, dispersants are effective up to about 10,000 cp (Aamo et al., 1993; Daling and Brandvik, 1988; 1991; Daling et al., 1997). In the model, oil is dispersed up to 10,000 cp.

Entrained oil is well mixed in (i.e., mixed uniformly throughout) the wave-mixed zone. Vertical mixing is simulated by random placement of particles within the wave-mixed layer each time step. Settling of particles does not occur in water depths where waves reach the bottom (taken as 1.5 times wave height). Wave height is calculated from wind speed, duration and fetch (distance upwind to land), using the algorithms in CERC (1984). Wave height is on the scale of centimetres in small rivers and streams, and near lee shorelines; whereas it may increase to metres in open waters under windy conditions.

1.3.6 Emulsification (Mousse Formation)

The formation of water-in-oil emulsions, or mousse, depends on oil composition and turbulence level. Emulsified oil can contain as much as 80% water in the form of micrometre-sized droplets dispersed within a continuous phase of oil (Daling and Brandvik, 1988; Fingas et al., 1997). Viscosities are typically much higher than that of the parent oil. The incorporation of water also dramatically increases the oil/water mixture volume.

The Mackay and Zagorski (1982) emulsification scheme is implemented in SIMAP for floating oil. Water content increases exponentially, with the rate related to the square of wind speed and previous water incorporation. Viscosity is a function of water content. The change in viscosity feeds back in the model to the entrainment rate.

1.3.7 Dissolution

Dissolution is the process by which soluble hydrocarbons enter the water from a surface slick or from entrained oil droplets. The lower molecular weight hydrocarbons tend to be both more volatile and more soluble than those of higher molecular weight. For surface slicks, since the partial pressures tend to exceed the solubilities of these lower molecular weight compounds, evaporation accounts for a larger portion of the mass than dissolution (McAuliffe, 1989), except perhaps under ice. Dissolution and evaporation are competitive processes. The dissolved component concentration of hydrocarbons in water under a surface slick shows an initial increase followed by a rapid decrease after some hours due to the evaporative loss of components. Most soluble components are also volatile and direct evaporation (volatilization) from the water column depletes their concentrations in the water. Dissolution is particularly important where evaporation is low (dispersed oil droplets and ice-covered surfaces). Dissolution can be significant from entrained droplets because of the lack of atmospheric exposure and because of the higher surface area per unit of volume.

The model developed by Mackay and Leinonen (1977) is used in SIMAP for dissolution from a surface slick. The slick (spillet) is treated as a flat plate, with a mass flux (Hines and Maddox, 1985) related to solubility and temperature. It assumes a well-mixed layer with most of the resistance to mass transfer lying in a hypothetical stagnant region close to the oil. For subsurface oil, dissolution is treated as a mass flux across the surface area of a droplet (treated as a sphere) in a calculation analogous to the Mackay and Leinonen (1977) algorithm. The dissolution algorithm was developed in French et al. (1996a).

1.3.8 Volatilization from the Water column

The procedure outlined by Lyman et al. (1982), based on Henry's Law and mass flux (Hines and Maddox, 1985), is followed in the SIMAP fates model. The volatilization depth for dissolved substances is limited to the maximum of one half the wave height. Wave height is computed from the wind speed and fetch (CERC, 1984). The volatilization algorithm was developed in French et al. (1996a).

1.3.9 Adsorption and Sedimentation

Aromatics dissolved in the water column are carried to the sediments primarily by adsorption to suspended particulates, and subsequent settling. The ratio of adsorbed (C_a) to dissolved (C_{dis}) concentrations is computed from standard equilibrium partitioning theory as

$$C_a / C_{dis} = K_{oc} C_{ss}$$

K_{oc} is a dimensionless partition coefficient and C_{ss} is the concentration of suspended particulate matter (SPM) in the water column expressed as mass of particulate per volume of water. As a default, the model uses a mean value of total suspended solids of 10 mg/l (Kullenberg, 1982); alternatively suspended sediment concentration is specified as model input.

Sedimentation of oil droplets occurs when the specific gravity of oil increases over that of the surrounding water. Several processes may act on entrained oil and surface slicks to increase density: weathering (evaporation, dissolution and emulsification), adhesion or sorption onto suspended particles or detrital material, and incorporation of sediment into oil during interaction with suspended particulates, bottom sediments, and shorelines. Rates of sedimentation depend on the concentration of suspended particulates and the rates of particulate flux into and out of an area. In areas with high suspended particulate concentrations, rapid dispersal and removal of oil is found due to sorption and adhesion (Payne and McNabb, 1984).

Kirstein et al. (1987) and Payne et al. (1987) used a reaction term to characterize the water column interactions of oil and suspended particulates. The reaction term represents the collision of oil droplets and suspended matter, and both oiled and unoiled particulates are accounted for. The model formulation developed by Kirstein et al. (1987) is used to calculate the volume of oil adhered to particles. In the case where the oil mass is larger than the adhered sediment (i.e., the sediment has been incorporated into the oil) the buoyancy of the oil droplet will control its settling or rise rate. The Stoke's law formulation is used to adjust vertical position of these particles. If the mass of adhered droplets is small relative to the mass of the sediment it has adhered to, the sediment settling velocity will control the fate of the combined particulate.

1.3.10Degradation

Degradation may occur as the result of photolysis, which is a chemical process energized by ultraviolet light from the sun, and by biological (bacterial) breakdown, termed biodegradation. In the model, degradation occurs on the surface slick, deposited oil on the shore, the entrained oil and aromatics in the water column, and oil in the sediments. A first order decay algorithm is used, with a specified (total) degradation rate for each of surface oil, water column oil and sedimented oil (French et al., 1999).

1.4 Habitat Type

Ecological habitat types (Table 2) are broadly categorized into two zones within SIMAP: shoreline and submerged (or intertidal versus subtidal in estuarine and marine areas, where intertidal habitats are those above spring low water tide level, with subtidal being all water areas below that level). In modelled scenarios, the shoreline habitats may become oiled as surface oil makes contact with these cells. Submerged or subtidal cells are always underwater. Intertidal/shoreline areas may be extensive, such that they are wide enough to be represented by an entire grid cell at the resolution of the grid. These are typically either mud flats or wetlands, and are coded 20 (seaward mudflat), 21 (seaward wetland), 50 (landward mudflat), or 51 (landward wetland). All other intertidal/shoreline habitats are typically much narrower than the size of a grid cell. Thus, these fringing intertidal/shore types (indicated by F in Table 2) have typical (for the region, e.g., French et al., 1996a for estuarine and marine areas) widths associated with them in the model. Boundaries between land and water are fringing habitat types. On the waterside of fringing grid cells, there may be extensive intertidal/shoreline grid cells if the wetlands or mudflats are extensive. Otherwise, subtidal/submerged habitats border the fringing cells.

Table 2. Classification of habitats. seaward (Sw) and landward (Lw) system codes are listed. (fringing types indicated by (F) are only as wide as the intertidal zone or shoreline width where oiling might occur. Others (W = water) are a full grid cell wide and have a fringing type on the land side.)

Habitat Code (Sw,Lw)	Ecological Habitat	F or W
Intertidal / Shore		
1,31	Rocky Shore	F
2,32	Gravel Shore	F
3,33	Sand Beach or Shore	F
4,34	Fringing Mud Flat	F
5,35	Fringing Wetland (Emergent or Forested)	F
6,36	Macroalgal Bed	F

Habitat Code (Sw,Lw)	Ecological Habitat	F or W
7,37	Mollusk Reef	F
8,38	Coral Reef (marine only)	F
Subtidal / Submerged		
9,39	Rock Bottom	W
10,40	Gravel Bottom	W
11,41	Sand Bottom	W
12,42	Silt-mud Bottom	W
13,43	Wetland (submerged areas)	W
14,44	Macroalgal Bed	W
15,45	Mollusk Reef	W
16,46	Coral Reef (marine only)	W
17,47	Submerged Aquatic Vegetation Bed	W
Intertidal / Shore		
18,48	Man-made, Artificial	F
19,49	Ice Edge	F
20,50	Extensive Mud Flat	W
21,51	Extensive Wetland (Emergent or Forested)	W

1.5 References

Aamo, O.M., M. Reed and P. Daling, 1993. A laboratory based weathering model: PC version for coupling to transport models. In Proceedings of the 16th Arctic and Marine Oil Spill Program (AMOP) Technical Seminar, Environmental Protection Service, Emergencies Science Division, Environment Canada, Ottawa, ON, Canada, pp. 617-626.

ASCE Task Committee on Modeling Oil Spills, 1996. State-of-the-art Review of Modeling Transport and Fate of Oil Spills, Water Resources Engineering Division, ASCE, Journal of Hydraulic Engineering 122(11): 594-609.

Coastal Engineering Research Center (CERC), 1984. Shore Protection Manual, Vol. I. Coastal Engineering Research Center, Department of the Army, Waterways Experiment Station, U.S. Army Corps of Engineers, Vicksburg, Mississippi, 1,105p. plus 134p. in appendices.

CSE/ASA/BAT, 1986. Development of a Coastal Oil Spill Smear Model. Phase 1: Analysis of Available and Proposed Models, Prepared for Minerals Management Service by Coastal Science & Engineering, Inc. (CSE) with Applied Science Associates, Inc. (ASA) and Battelle New England Research Laboratory (BAT), 121p.

Daling, P.S. and P.J. Brandvik, 1988. A Study of the Formation and Stability of Water-in-Oil Emulsions. In Proceedings of the 11th Arctic and Marine Oil Spill Program Technical Seminar. Emergencies Science Division, Environment Canada, Ottawa, ON, Canada, pp.153-170.

Daling, P.S., D. Mackay, N. Mackay, and P.J. Brandvik, 1990. Droplet size distributions in chemical dispersion of oil spills: Towards a mathematical model. Oil and Chemical Pollution 7: 173-198.

Daling, P.S. and P.J. Brandvik, 1991. Characterization and prediction of the weathering properties of oils at sea – A manual for the oils investigated in the DIWO project. IKU SINTEF Group report 91.037, DIWO report no. 16 02.0786.00/16/91, 29 May 1991, 140p.

Daling, P.S., O.M. Aamo, A. Lewis, and T. Strom-Kritiansen, 1997. SINTEF/IKU Oil-Weathering Model: Predicting Oil's Properties at Sea. In Proceedings 1997 Oil Spill Conference, Publication No. 4651, American Petroleum Institute, Washington, D.C., pp. 297-307.

Daling, P.S. A.Lewis, S. Ramstad. 1999. The use of colour as a guide to oil film thickness – Main report. SINTEF Report STF66 F99082. 48p., SINTEF, Trondheim, Norway.

Delvigne, G.A.L. and C.E. Sweeney, 1988. Natural Dispersion of Oil. Oil and Chemical Pollution 4: 281-310.

Di Toro, D.M., J.A. McGrath and D.J. Hansen, 2000. Technical basis for narcotic chemicals and polycyclic aromatic hydrocarbon criteria. I. Water and tissue. Environmental Toxicology and Chemistry 19(8): 1951-1970.

Fay, J.A., 1971. Physical processes in the spread of oil on a water surface. In Proceedings, Conference on Prevention and Control of Oil Spills, sponsored by API, EPA, and US Coast Guard, American Petroleum Institute, Washington, D.C., June 15-17, 1971, pp. 463-467.

Fingas, M., 1996. The Evaporation of Crude Oil and Petroleum Products. PhD Dissertation, McGill University, Montreal, Canada, 181p.

Fingas, M., B. Fieldhouse, and J.V. Mullin, 1997. Studies of Water-in-Oil Emulsions: Stability Studies. In Proceedings of 20th Arctic and Marine Oil Spill Program (AMOP) Technical Seminar, Emergencies Science Division, Environment Canada, Ottawa, ON, Canada, pp. 21-42.

Fingas, M., 1997. The Evaporation of Oil Spills: Prediction of Equations Using Distillation Data. In Proceedings of the 20th Arctic and Marine Oil Spill Program (AMOP) Technical Seminar, Emergencies Science Division, Environment Canada, Ottawa, ON, Canada, pp. 1-20.

Fingas, M.F., 1998. Studies on the Evaporation of Crude Oil and Petroleum Products: II. Boundary Layer Regulation. Journal of Hazardous Materials, Vol. 57, pp.41-58.

Fingas, M.F., 1999. The Evaporation of Oil Spills: Development and Implementation of New Prediction Methodology. In Proceedings of the 1999 International Oil Spill Conference, American Petroleum Institute, Washington, D.C., pp. 281-287.

Fingas, M., B. Fieldhouse, and J.V. Mullin, 1997. Studies of Water-in-Oil Emulsions: Stability Studies. In: Proceedings of 20th Arctic and Marine Oil Spill Program (AMOP) Technical Seminar, Emergencies Science Division, Environment Canada, Ottawa, ON, Canada, pp. 21-42.

French, D., M. Reed, K. Jayko, S. Feng, H. Rines, S. Pavignano, T. Isaji, S. Puckett, A. Keller, F. W. French III, D. Gifford, J. McCue, G. Brown, E. MacDonald, J. Quirk, S. Natzke, R. Bishop, M. Welsh, M. Phillips and B.S. Ingram, 1996a. The CERCLA type A natural resource damage assessment model for coastal and marine environments (NRDAM/CME), Technical Documentation, Vol. I - Model Description. Final Report, submitted to the Office of Environmental Policy and Compliance, U.S. Dept. of the Interior, Washington, DC, April, 1996, Contract No. 14-0001-91-C-11.

French, D., M. Reed, S. Feng and S. Pavignano, 1996b. The CERCLA type A natural resource damage assessment model for coastal and marine environments (NRDAM/CME), Technical Documentation, Vol. III - Chemical and Environmental Databases. Final Report, Submitted to the Office of Environmental Policy and Compliance, U.S. Dept. of the Interior, Washington, DC, April, 1996, Contract No. 14-01-0001-91-C-11.

French, D., S. Pavignano, H. Rines, A. Keller, F.W. French III and D. Gifford, 1996c. The CERCLA type A natural resource damage assessment model for coastal and marine environments (NRDAM/CME), Technical Documentation, Vol.IV - Biological Databases. Final Report, Submitted to the Office of Environmental Policy and Compliance, U.S. Dept. of the Interior, Washington, DC, April, 1996, Contract No. 14-01-0001-91-C-11.

French, D.P. and H. Rines, 1997. Validation and use of spill impact modeling for impact assessment. Proceedings, 1997 International Oil Spill Conference, Fort Lauderdale, Florida, American Petroleum Institute Publication No. 4651, Washington, DC, pp-829-834.

French, D.P., H. Rines and P. Masciangioli, 1997. Validation of an Orimulsion spill fates model using observations from field test spills. Proceedings, Twentieth Arctic and Marine Oil Spill Program Technical Seminar, Vancouver, Canada, June 10-13, 1997.

French, D., H. Schuttenberg, and T. Isaji, 1999. Probabilities of Oil Exceeding Thresholds of Concern: Examples from an Evaluation for Florida Power and Light. In Proceedings of the 22nd Arctic and

Marine Oil Spill Program (AMOP) Technical Seminar, June 2-4, 1999, Calgary, Alberta, Environment Canada, pp.243-270.

French McCay, D. and J.R. Payne, 2001. Model of Oil Fate and Water concentrations with and without application of dispersants. In Proceedings of the 24th Arctic and Marine Oil Spill Program (AMOP) Technical Seminar, Emergencies Science Division, Environment Canada, Ottawa, ON, Canada, pp. 601-653.

French McCay, D.P., 2002. Development and Application of an Oil Toxicity and Exposure Model, OilToxEx. Environmental Toxicology and Chemistry 21(10): 2080-2094.

French McCay, D.P., 2003. Development and Application of Damage Assessment Modeling: Example Assessment for the North Cape Oil Spill. Marine Pollution Bulletin, Volume 47, Issues 9-12, September-December 2003, pp. 341-359.

French McCay, D.P., 2004. Oil spill impact modeling: Development and validation. Environmental Toxicology and Chemistry 23(10): 2441-2456.

French McCay, D.P., and J.J. Rowe, 2004. Evaluation of Bird Impacts in Historical Oil Spill Cases Using the SIMAP Oil Spill Model. In Proceedings of the 27th Arctic and Marine Oil Spill Program (AMOP) Technical Seminar, Emergencies Science Division, Environment Canada, Ottawa, ON, Canada, pp. 421-452.

Gundlach, E.R., 1987. Oil Holding Capacities and Removal Coefficients for Different Shoreline Types to Computer Simulate Spills in Coastal Waters. In Proceedings of the 1987 Oil Spill Conference, pp. 451-457.

Hines, A.L. and R.N. Maddox, 1985. Mass Transfer Fundamentals and Application. Prentice-Hall, Inc., Englewood Cliffs, New Jersey, 542p.

Jones, R.K., 1997. A Simplified Pseudo-Component of Oil Evaporation Model. In Proceedings of the 20th Arctic and Marine Oil Spill Program (AMOP) Technical Seminar, Environment Canada, pp. 43-61.

Kirstein, B.E., J.R. Clayton, C. Clary, J.R. Payne, D. McNabb, Jr., G. Fauna and R. Redding, 1987. Integration of Suspended Particulate Matter and Oil Transportation Study. Minerals Management Service, OCS Study MMS87-0083, Anchorage, Alaska, 216p.

Kolluru, V., M.L. Spaulding and E. Anderson, 1994. A three dimensional subsurface oil dispersion model using a particle based approach. In Proceedings of 17th Arctic and Marine Oil Spill Program (AMOP) Technical Seminar, Vancouver, British Columbia, June 8-10, 1994, Emergencies Science Division, Environment Canada, Ottawa, ON, Canada, pp. 867-893.

Kullenberg, G. (ed.), 1982. Pollutant transfer and transport in the sea. Volume I. CRC Press, Boca Raton, Florida. 227 p.

Lehr, W.J., D. Wesley, D. Simecek-Beatty, R. Jones, G. Kachook and J. Lankford, 2000. Algorithm and interface modifications of the NOAA oil spill behavior model. In Proceedings of the 23rd Arctic and

Marine Oil Spill Program (AMOP) Technical Seminar, Vancouver, BC, Environmental Protection Service, Environment Canada, pp. 525-539.

Lunel, T., 1993a. Dispersion: Oil droplet size measurements at sea. In Proceedings of the 16th Arctic Marine Oilspill Program (AMOP) Technical Seminar, Environment Canada, Calgary, Alberta, June 7-9, 1993, pp. 1023-1056.

Lunel, T., 1993b. Dispersion: Oil droplet size measurements at sea. In Proceedings of the 1993 Oil Spill Conference, pp. 794-795.

Lyman, C.J., W.F. Reehl, and D.H. Rosenblatt, 1982. Handbook of Chemical Property Estimation Methods. McGraw-Hill Book Co., New York, 960p.

Mackay, D. and R.M. Matsugu, 1973. Evaporation rates of liquid hydrocarbon spills on land and water. Canadian Journal of Chemical Engineering 51: 434-439.

Mackay, D. and P.J. Leinonen, 1977. Mathematical model of the behavior of oil spills on water with natural and chemical dispersion. Prepared for Fisheries and Environment Canada. Economic and Technical Review Report EPS-3-EC-77-19, 39p.

Mackay, D., S. Paterson and K. Trudel, 1980. A mathematical model of oil spill behavior. Department of Chemical and Applied Chemistry, University of Toronto, Canada, 39p.

Mackay, D., and W. Zagorski, 1982. Water-In-Oil Emulsions. Environment Canada Manuscript Report EE-34, Ottawa, Ontario, Canada, 93p.

Mackay, D, W.Y. Shiu, K. Hossain, W. Stiver, D. McCurdy and S. Peterson, 1982. Development and calibration of an oil spill behavior model. Report No. CG-D-27-83, U.S. Coast Guard, Research and Development Center, Groton, Connecticut, 83p.

Mackay, D., W.Y. Shiu, and K.C. Ma, 1992. Illustrated Handbook of Physical-Chemical Properties and Environmental Fate for Organic Chemicals, Vol. I-IV. Lewis Publishers, Inc, Chelsea, Michigan.

McAuliffe, C.D., 1987. Organism exposure to volatile/soluble hydrocarbons from crude oil spills –a field and laboratory comparison. Proceedings of the 1987 Oil Spill Conference. Washington, D.C.: API. pp. 275-288.

McAuliffe, C.D., 1989. The Weathering of Volatile Hydrocarbons from Crude Oil Slicks on Water. In Proceedings of the 1989 Oil Spill Conference, San Antonio, Texas, American Petroleum Institute, Washington, D.C., pp. 357-364.

Okubo, A. and R.V. Ozmidov, 1970. Empirical dependence of the coefficient of horizontal turbulent diffusion in the ocean on the scale of the phenomenon in question. Atmospheric and Ocean Physics 6(5):534-536.

Okubo, A., 1971. Oceanic diffusion diagrams. Deep-Sea Research 8:789-802.

Payne, J.R. and G.D. McNabb Jr., 1984. Weathering of Petroleum in the Marine Environment. Marine Technology Society Journal 18(3):24-42.

Payne, J.R., B.E. Kirstein, G.D. McNabb, Jr., J.L. Lambach, R. Redding R.E. Jordan, W. Hom, C. deOliveria, G.S. Smith, D.M. Baxter, and R. Gaegel, 1984. Multivariate analysis of petroleum weathering in the marine environment – sub Arctic. Environmental Assessment of the Alaskan Continental Shelf, OCEAP, Final Report of Principal Investigators, Vol. 21 and 22, Feb. 1984, 690p.

Payne, J.R., B.E. Kirstein, J.R. Clayton, Jr., C. Clary, R. Redding, G.D. McNabb, Jr., and G. Farmer, 1987. Integration of suspended particulate matter and oil transportation study. Final Report. Minerals Management Service, Environmental Studies Branch, Anchorage, AK. Contract No. 14-12-0001-30146, 216 p.

Stiver, W. and D. Mackay, 1984. Evaporation rate of oil spills of hydrocarbons and petroleum mixtures. Environmental Science and Technology 18: 834-840.

Thorpe, S.A., 1984. On the Determination of K in the Near Surface Ocean from Acoustic Measurements of Bubbles. Journal of Physical Oceanography 14: 855-863.

Youssef, M. and M.L. Spaulding, 1993. Drift current under the action of wind waves, Proceedings of the 16th Arctic and Marine Oil Spill Program Technical Seminar, Calgary, Alberta, Canada, pp. 587-615.

1.6 References – SIMAP Example Applications and Validations

Copies of theses papers can be provided by sending a request to matt.horn@rpsgroup.com and requesting one or more specific papers.

French, D.P., and H. Rines, 1997. Validation and use of spill impact modeling for impact assessment. In Proceedings, 1997 International Oil Spill Conference, Fort Lauderdale, Florida, American Petroleum Institute Publication No. 4651, Washington, DC, pp-829-834.

French, D. P., 1998a. Estimate of Injuries to Marine Communities Resulting from the North Cape Oil Spill Based on Modeling of Fates and Effects. Report to US Department of

14 Commerce, National Oceanic and Atmospheric Administration (NOAA), Damage Assessment Center, Silver Spring, MD, January 1998.

French, D. P., 1998b. Updated Estimate of Injuries to Marine Communities Resulting from the North Cape Oil Spill Based on Modeling of Fates and Effects. Report to US Department of Commerce, National Oceanic and Atmospheric Administration (NOAA), Damage Assessment Center, Silver Spring, MD, December 1998.

French, D.P., 1998c. Modeling the Impacts of the North Cape, p. 387-430.In Proceedings, 21st Arctic and Marine Oilspill Program (AMOP) Technical Seminar, June 10-12, 1998, West Edmonton Mall Hotel Edmonton, Alberta, Canada, Emergencies Science Division, Environment Canada, Ottawa, ON, Canada.

French McCay, D. and James R. Payne, 2001.Model of Oil Fate and Water concentrations with and with out application of dispersants. In Proceedings of the 2001 24th Arctic and Marine Oil spill Program (AMOP) Technical Seminar, June 12-14, 2001, Environment Canada, pp.611-645.

French, D. P., Jones, M. A., and Coakley, L., 2001. Use of Oil Spill Modeling for Contingency Planning and Impact Assessment: Application for Florida Power and Light. In Proceedings of the 2001 International Oil Spill Conference & Exposition, American Petroleum Institute, March 26-29, 2001, Tampa, Florida.

French, D.P. and H. Schuttenberg, 1999.Evaluation of net environmental benefit using fates and effects modeling. Paper ID #321. In Proceedings, 1999 International Oil Spill Conference, American Petroleum Institute.

French McCay, D. 2002. Modeling Evaluation of Water Concentrations and Impacts Resulting from Oil Spills With and Without the Application of Dispersants. International Marine Environmental Seminar 2001, Journal of Marine Systems, Special Issue 2002.

French McCay, D., N. Whittier, S. Sankaranarayanan, J. Jennings, and D. S. Etkin, 2002.Modeling Fates and Impacts for Bio-Economic Analysis of Hypothetical Oil Spill Scenarios in San Francisco Bay. In Proceedings of the Twenty Fifth Arctic and Marine Oil Spill Program (AMOP) Technical Seminar, Environment Canada, Calgary, AB, Canada, 2002, p. 1051-1074.

French McCay, D., N. Whittier, T. Isaji, and W.Saunders, 2003. Assessment of the Potential Impacts of Oil Spills in the James River, Virginia. In Proceedings of the 26th Arctic and Marine Oil Spill Program (AMOP) Technical Seminar, Emergencies Science Division, Environment Canada, Ottawa, ON, Canada, p. 857-878.

French McCay, D., N. Whittier, S. Sankaranarayanan, J. Jennings, and D. S. Etkin, 2003.Estimation of Potential Impacts and Natural Resource Damages of Oil. J. Hazardous Materials (in press).

French McCay, D. and N. Whittier, 2003.Modeling Assessment of Potential Fates and Exposure for Orimulsion and Heavy Fuel Oil Spills. In: Proceedings, International Oil Spill Conference, April 2003, Paper 157, American Petroleum Institute, Washington, DC.

French McCay, D.P., 2003. Development and Application of Damage Assessment Modeling: Example Assessment for the North Cape Oil Spill. Marine Pollution Bulletin, Volume 47, Issues 9-12, September-December 2003, pp. 341-359.

French McCay, D.P., and J.J. Rowe, 2004.Evaluation of Bird Impacts in Historical Oil Spill Cases Using the SIMAP Oil Spill Model. In Proceedings of the 27th Arctic and Marine Oil Spill Program (AMOP) Technical Seminar, Emergencies Science Division, Environment Canada, Ottawa, ON, Canada, pp. 421-452.

French-McCay, D.P., J.J. Rowe, N. Whittier, S. Sankaranarayanan, D. S. Etkin, and L. Pilkey- Jarvis, 2005. Evaluation of the Consequences of Various Response Options Using Modeling of Fate, Effects and NRDA Costs of Oil Spills into Washington Waters. In: Proceedings, International Oil Spill Conference, May 2005, Paper 395, American Petroleum Institute, Washington, DC.

French-McCay, D.P., N. Whittier, C. Dalton, J.J. Rowe, and S. Sankaranarayanan, 2005.Modeling fates and impacts of hypothetical oil spills in Delaware, Florida, Texas, California, and Alaska waters, varying response options including use of dispersants. In: Proceedings, International Oil Spill Conference, May 2005, Paper 399, American Petroleum Institute, Washington, DC.

French McCay, D., N. Whittier, J.J. Rowe, S. Sankaranarayanan and H.-S.Kim, 2005. Use of Probabilistic Trajectory and Impact Modeling to Assess Consequences of Oil Spills with Various Response Strategies. In Proceedings of the 28th Arctic and Marine Oil Spill Program (AMOP) Technical Seminar, Emergencies Science Division, Environment Canada, Ottawa, ON, Canada, pp. 253-271, 2005.

French-McCay, D.P., M. Horn, Z. Li, K. Jayko, M. Spaulding, D. Crowley, and D. Mendelsohn. 2017. Modeling Distribution, Fate, and Concentrations of Deepwater Horizon Oil in Subsurface Waters of the Gulf of Mexico. In: S.A. Stout and Z. Wang (eds.) Case Studies in Oil Spill Environmental Forensics. Elsevier.

2 OILMAP Deep Model Description

OILMAP Deep was used to characterize the near field blowout conditions for use in the SIMAP model, which characterized the far field effects. OILMAP Deep contains two sub-models, a plume model and a droplet size model. The plume model predicts the evolution of plume position, geometry, centerline velocity, and oil and gas concentrations until the plume either surfaces or reaches a terminal height at which point the plume is trapped. The droplet model predicts the size and volume (mass) distribution of the oil droplets. Provided below is an overview of blowout theory and modeling implementation.

2.1 Blowout Model Theory

RPS ASA's oil blowout model is based on the work of McDougall (gas plume model, 1978), Fanneløp and Sjøen (1980a, plume/free surface interaction), Spaulding (1982, oil concentration model), Kolluru, (1993, World Oil Spill Model implementation), Spaulding et.al. (2000, hydrate formation) and Zheng et.al. (2002, 2003, gas dissolution). A simplified integral jet theory is employed for the vertical as well as for the horizontal motions of the gas-oil plume. The necessary model parameters defining the rates of entrainment and spreading of the jet are obtained from laboratory studies (Fanneløp and Sjøen 1980a). The gas plume analysis is described in McDougall (1978), Spaulding (1982), and Fanneløp and Sjøen (1980a). The hydrate formation and dissociation is formulated based on a unique equilibrium kinetics model developed by R. Bishnoi and colleagues at the University of Calgary. A brief description of the governing equations used in RPS ASA's blowout model and the solution methodology are described in Spaulding et al., 2000. The core components of this model are conservation of water mass, conservation of oil mass, conservation of momentum, and conservation of buoyancy.

Oil droplet size distribution calculations are based on the methodology presented by Yapa and Zheng (2001a&b) and Chen and Yapa (2007), which uses a maximum diameter calculation and the associated volumetric droplet size distribution. The maximum diameter can is determined using Hinze (1955) and coefficients consistent with Chen and Yapa (2007). The droplet size distribution is defined using a Rosin-Rammler (1933) function.

2.2 Blowout Model Implementation

The results of the near-field blowout model provide information to the far field fates model about the plume (the three dimensional extent of the mixture of gas/oil/water) and a characterization of the initial dispersion / mixing of the oil discharged during the blowout. Key factors in this analysis are the volume flux of oil and gas, gas to oil ratio (GOR), depth, exit flow velocity and environmental water column conditions (the profile of water temperature and density), which affect both the trap height and the potential for hydrate formation. Other factors such as duration of the blowout and ambient currents are also included but are less important.

The OILMAP Deep blowout model implementation is done in two parts; the first is the plume model described in the previous section, based on the McDougall bubble plume model; the second is the oil

droplet size distribution and volume fraction calculation. While they are based on the same scenario blowout specifications (e.g. oil type and flow rate, gas oil ratio and depth), the model predictions are treated separately and do not interact. The two parts of the model predictions only come together at the collapse of the near field plume, at the trap height, where the depth and droplet distribution predictions are used for initialization of the far field particle model simulation.

The blowout plume model solves equations for conservation of water mass, momentum, buoyancy, and gas mass as described in Section 2.1 of the OILMAP Deep Technical Documentation, using integral plume theory. An additional equation for the conservation of oil at the plume centerline is also solved.

The plume model prediction is defined externally by a small set of parameters including:

- Blowout release depth
- Oil discharge rate
- Oil density
- Gas : oil ratio (GOR) at the surface
- Atmospheric pressure
- Ambient seawater density profile
- Plume spreading coefficient ( )
- Entrainment parameter (α)
- Slip velocity of gas bubbles in the oil plume
- Ambient current velocity
- Water column profile of temperature and density

The blowout plume models the evolution of the plume within the water column, solving for the position, radius, velocity and oil and gas concentrations along the centerline. The blowout droplet model solves for the distribution of mass within droplet sizes associated with the turbulence of the release. Typically, the near-field model is on the timescale of seconds and length scale of hundreds of metres, where the far-field model is on the scales of hours/days and kilometres. The details of the near field modelling that are passed along to the far field model include the distribution of the release mass in different droplet sizes at the appropriate initial position in the water column.

2.3 References

Chen, F.H. and P.D. Yapa. 2007. Estimating the Oil Droplet Size Distributions in Deepwater Oil Spills. Journal of Hydraulic Engineering, Vol. 133, No. 2, pp. 197-207.

Fanneløp, T.K. and K. Sjoen , 1980a. Hydrodynamics of underwater blowouts, AIAA 8th Aerospace Sciences Meeting, January 14-16, Pasadena, California, AIAA paper, pp. 80- 0219.

Fanneløp, T. K. and K. Sjoen, 1980b. Hydrodynamics of underwater blowouts, Norwegian Maritime Research, No. 4, pp. 17-33.

Hinze, J. O. 1955 Fundamentals of the hydrodynamics mechanisms of splitting in dispersion process. AIChE J. 1, 289–295.

Kolluru, V., M.L. Spaulding and E. Anderson, 1994. A three dimensional subsurface oil dispersion model using a particle based approach. In Proceedings of 17th Arctic and Marine Oil Spill Program (AMOP) Technical Seminar, Vancouver, British Columbia, June 8-10, 1994, Emergencies Science Division, Environment Canada, Ottawa, ON, Canada, pp. 867-893.

McDougall, T.J., 1978. Bubble plumes in stratified environments, Journal of Fluid Mechanics, Vol. 85, Part 4, pp. 655-672.

Rosin, P. and E. Rammler, 1933. The Laws Governing the Fineness of Powdered Coal, Journal of the Institute of Fuel 7: 29–36Seo, I.W. and K.O. Baek, 2004. Estimation of the Longitudinal Dispersion Coefficient Using the Velocity Profile in Natural Streams. Journal of Hydraulic Engineering. March 2004.

Spaulding, M.L., 1982. User's manual for a simple gas blowout plume model, Continental Shelf Institute, Trondheim, Norway.

Spaulding, M.L., 1984. A vertically averaged circulation model using boundary-fitted coordinates. Journal of Physical Oceanography 14: 973-982.

Spaulding, M.L., P.R. Bishnoi, E. Anderson, and T. Isaji, 2000, An Integrated Model for Prediction of Oil Transport from a Deep Water Blowout.

Yapa, P. D., Zheng, L., and Chen, F. H. 2001a. A model for deepwater oil/gas blowouts. Mar. Pollution Bull., 43, 234–241.

Yapa, P. D., Zheng, L., and Chen, F. H. 2001b. Clarkson deepwater oil & gas ~CDOG model. Rep. No. 01–10, Dept. of Civil and Environmental Engineering, Clarkson Univ., Potsdam, N.Y.

Zheng, L. and Yapa, P.D., 2002. Modelling Gas Dissolution in Deepwater Oil/Gas Spills, Journal of Marine Systems, Elsevier, the Netherlands, March, 299-309

Zheng, L., Yapa, P.D. and Chen, F.H., 2003. A Model for Simulating Deepwater Oil and Gas Blowouts - Part I: Theory and Model Formulation, Journal of Hydraulic Research, IAHR, August, Vol. 41(4), 339-351

This page has been intentionally left blank for double-sided printing

Trajectory Modelling in Support of the Nexen Energy ULC Flemish Pass Exploration Drilling Project (2018-2028)

Appendix B: High Resolution Images

Prepared for: Nexen Energy ULC

Project Number:
2017-657

Date Submitted:
1/26/2018

Version:
Final Appendix

Project Manager
Matthew Horn, Ph.D.

RPS
55 Village Square Dr.
South Kingstown, RI USA
02879-8248

Release	File Name	Date Submitted	Notes
Draft	Nexen - RPS Technical Report_20180126 _AppendixB.docx	1/26/2018	RPS final draft version of Appendix B, which includes high resolution figures of model outputs at the request of Wood plc and Nexen Energy ULC.

Summary

This Appendix B is provided as a reference to RPS Technical Report: Trajectory Modelling in Support of the Nexen Energy ULC Flemish Pass Exploration Drilling Project (2018-2028). There are no new figures or modifications to those presented in the Technical Report. However, each figure has been provided at a higher resolution filling a full page per image. Stochastic results include predictions of both probability and minimum time to specific threshold exceedances for the EL 1144 and EL 1150 example well sites. Deterministic results include mass balance information, and cumulative maximum footprints of surface oil thickness, in water concentration, and shoreline and sediment mass per unit area. Deterministic results have been provided for the 95th percentile surface oil and water column, and 99th percentile shoreline exposure cases. In addition, deterministic results have been provided for marine diesel releases of 100 and 1,000 L associated with batch spills and a vessel collision with complete loss of cargo and fuel from a supply vessel.

In addition to the figure legends, additional release information is contained within a banner at the top of each figure. For stochastic figures, the information includes the type of image displayed (e.g. Surface Oil Probability), release site, type of release (e.g. Subsurface Blowout), release rate, season of release, release duration, model duration, and number of simulations presented. For deterministic figures, the information includes the type of image displayed (e.g. Surface Oil Thickness), release site, type of release, release rate, date and time of release, release duration, and model duration.

Table of Contents

List of Figures

1 Stochastic Analysis Results

1.1 EL 1144 Release Site

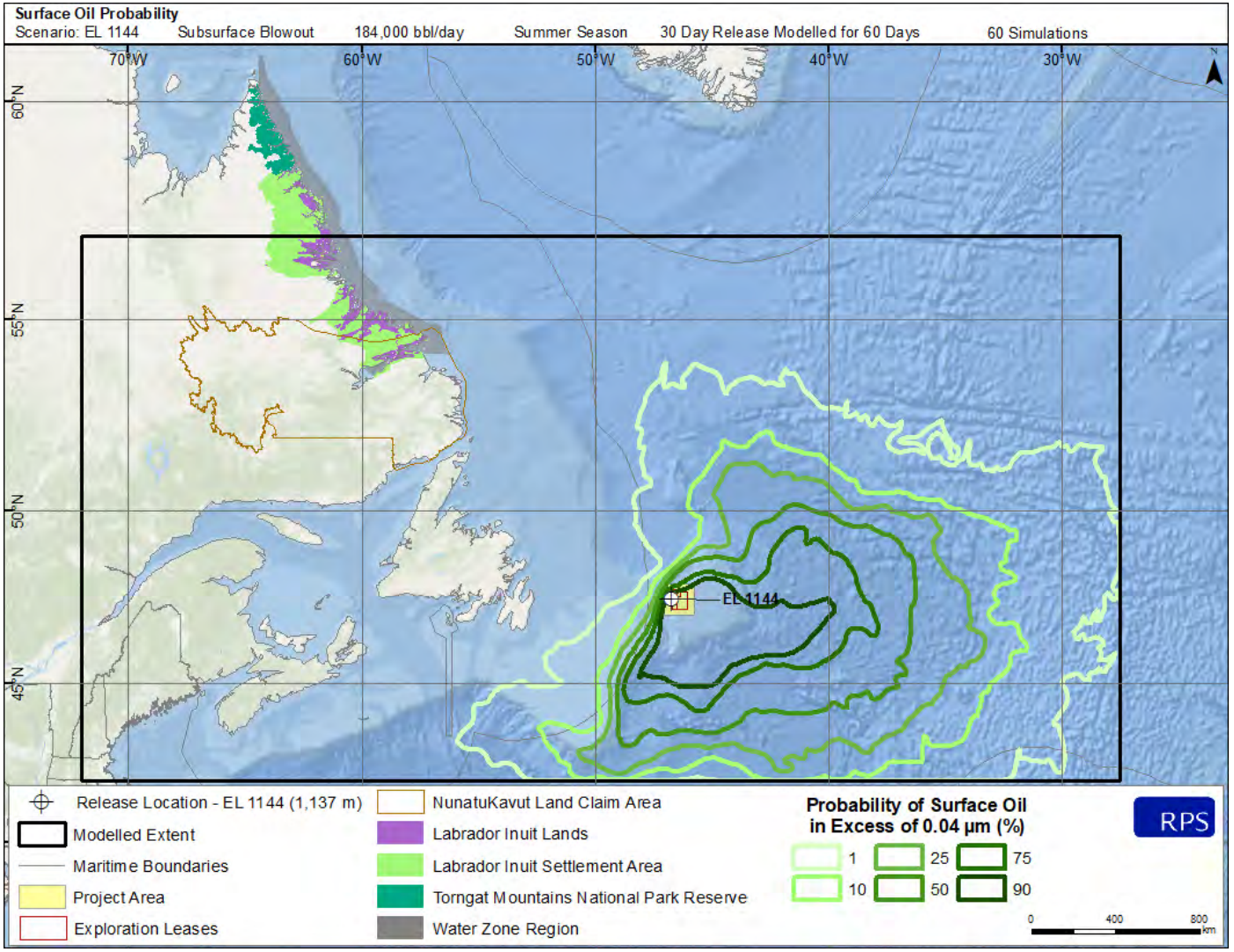

Figure 1-1. Summer probability of average surface oil thickness exceeding 0.04 µm resulting from a subsurface blowout at the EL 1144 example well release site.

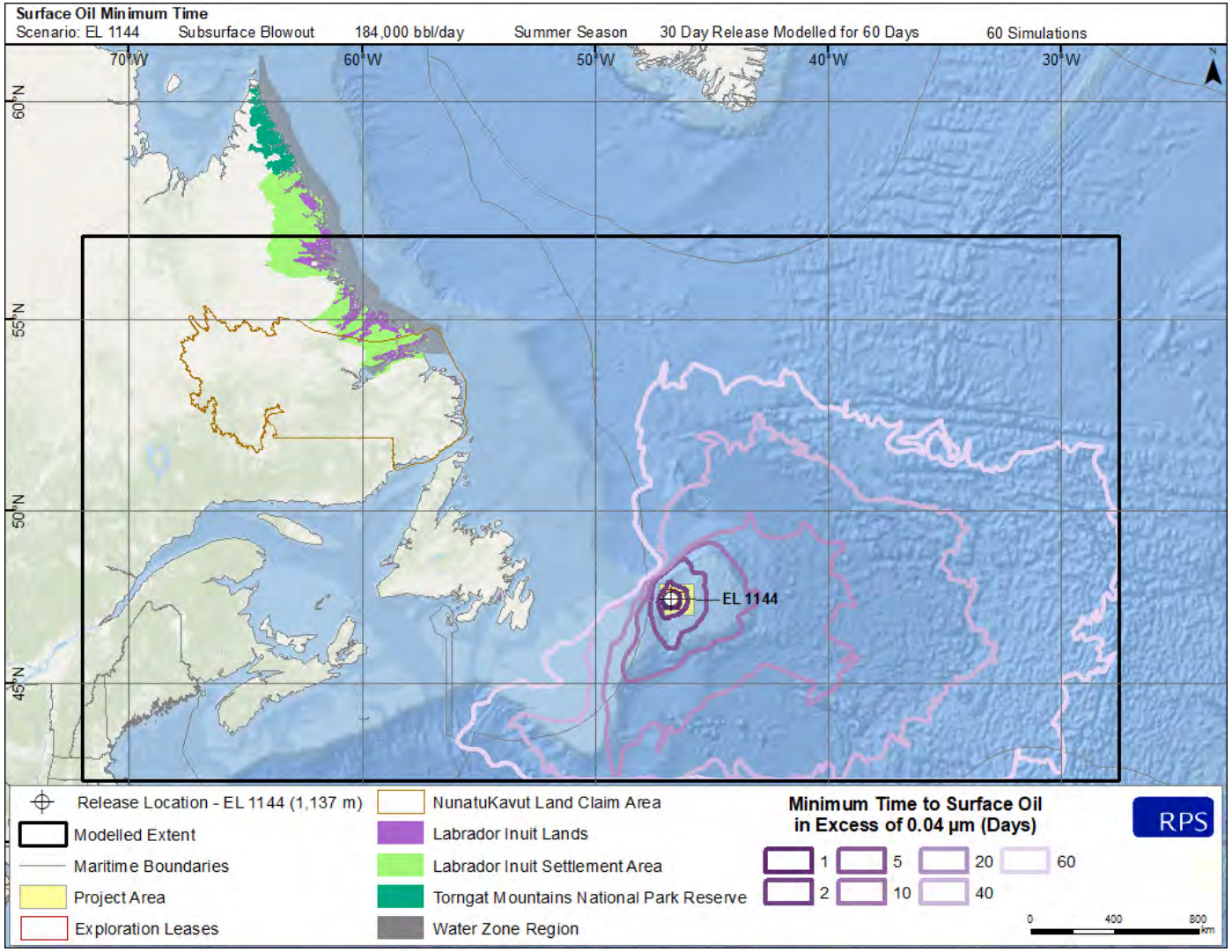

Figure 1-2. Minimum time to threshold exceedance resulting from a subsurface blowout at the EL 1144 example well release site.

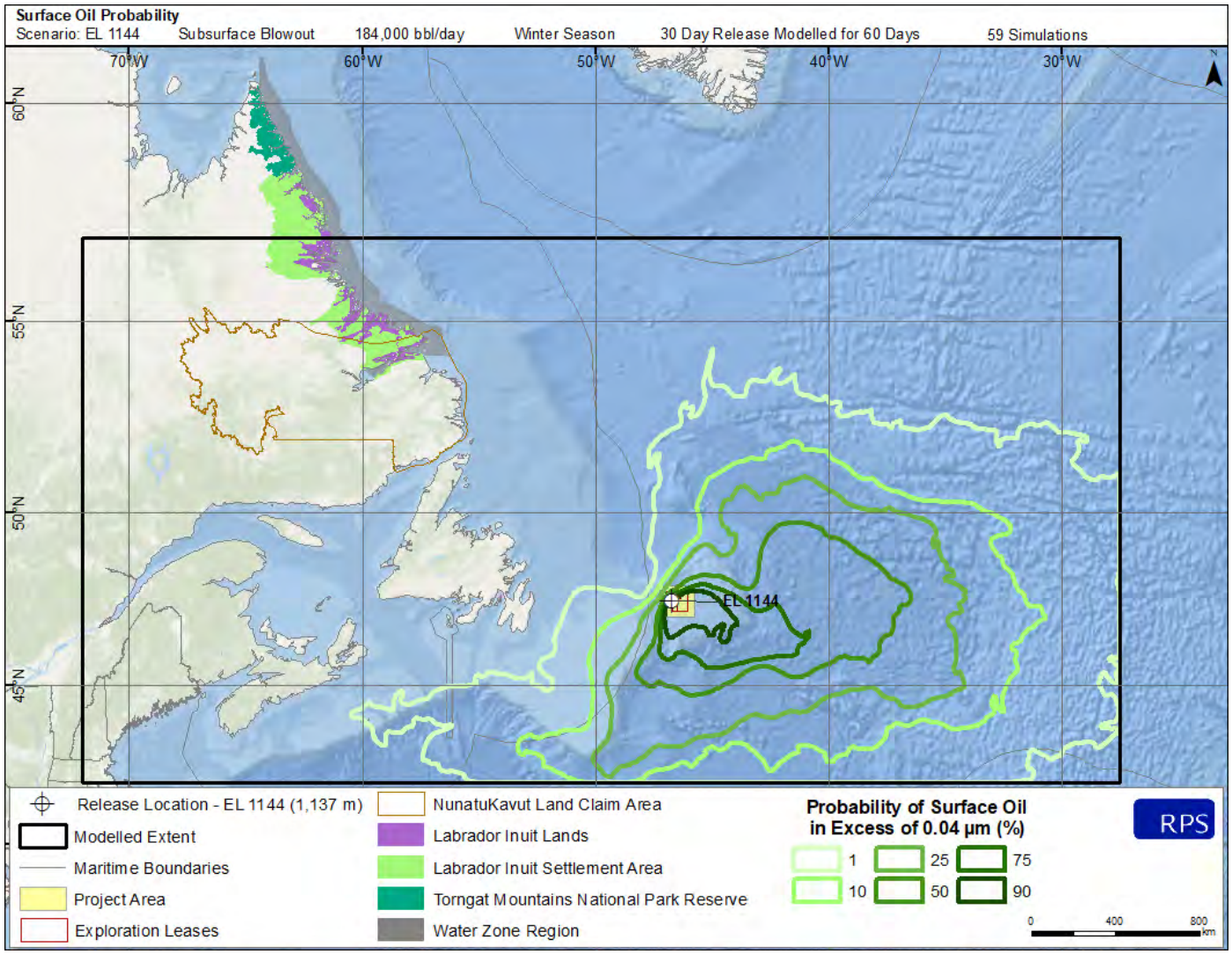

Figure 1-3. Winter probability of surface oil thickness exceeding 0.04 µm resulting from a subsurface blowout at the EL 1144 example well release site.

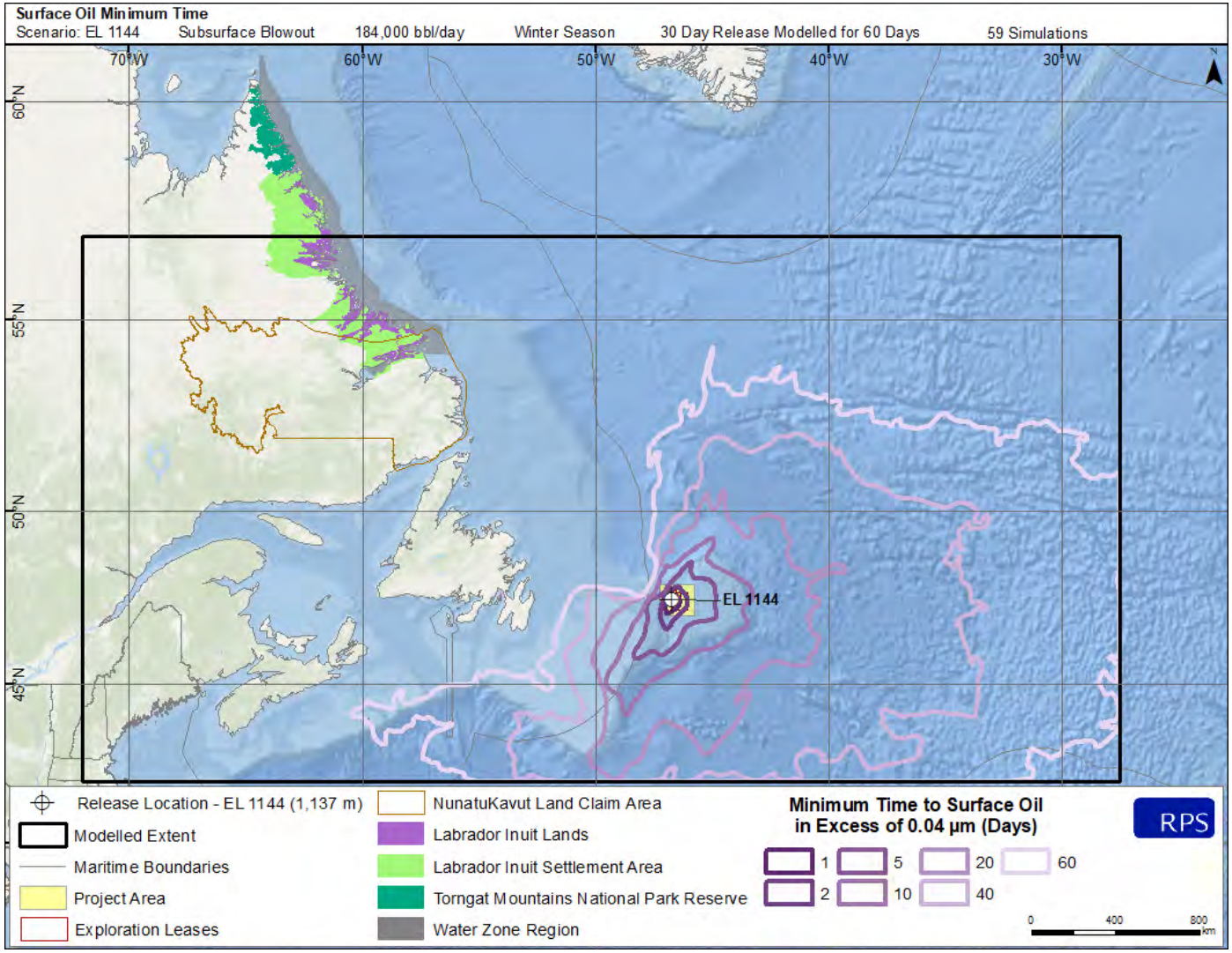

Figure 1-4. Minimum time to threshold exceedance resulting from a subsurface blowout at the EL 1144 example well release site.

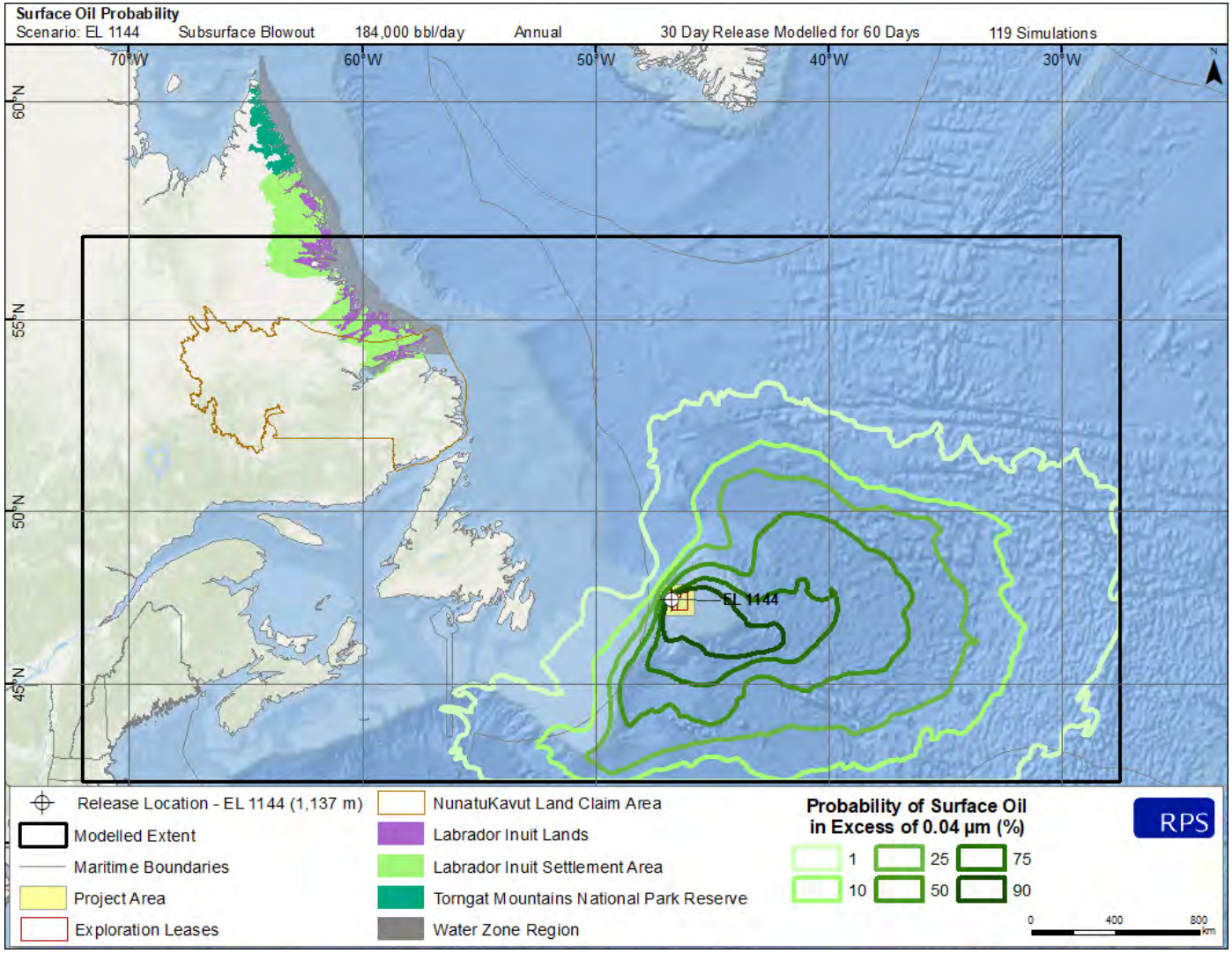

Figure 1-5. Annual probability of surface oil thickness exceeding 0.04 µm resulting from a subsurface blowout at the EL 1144 example well release site.

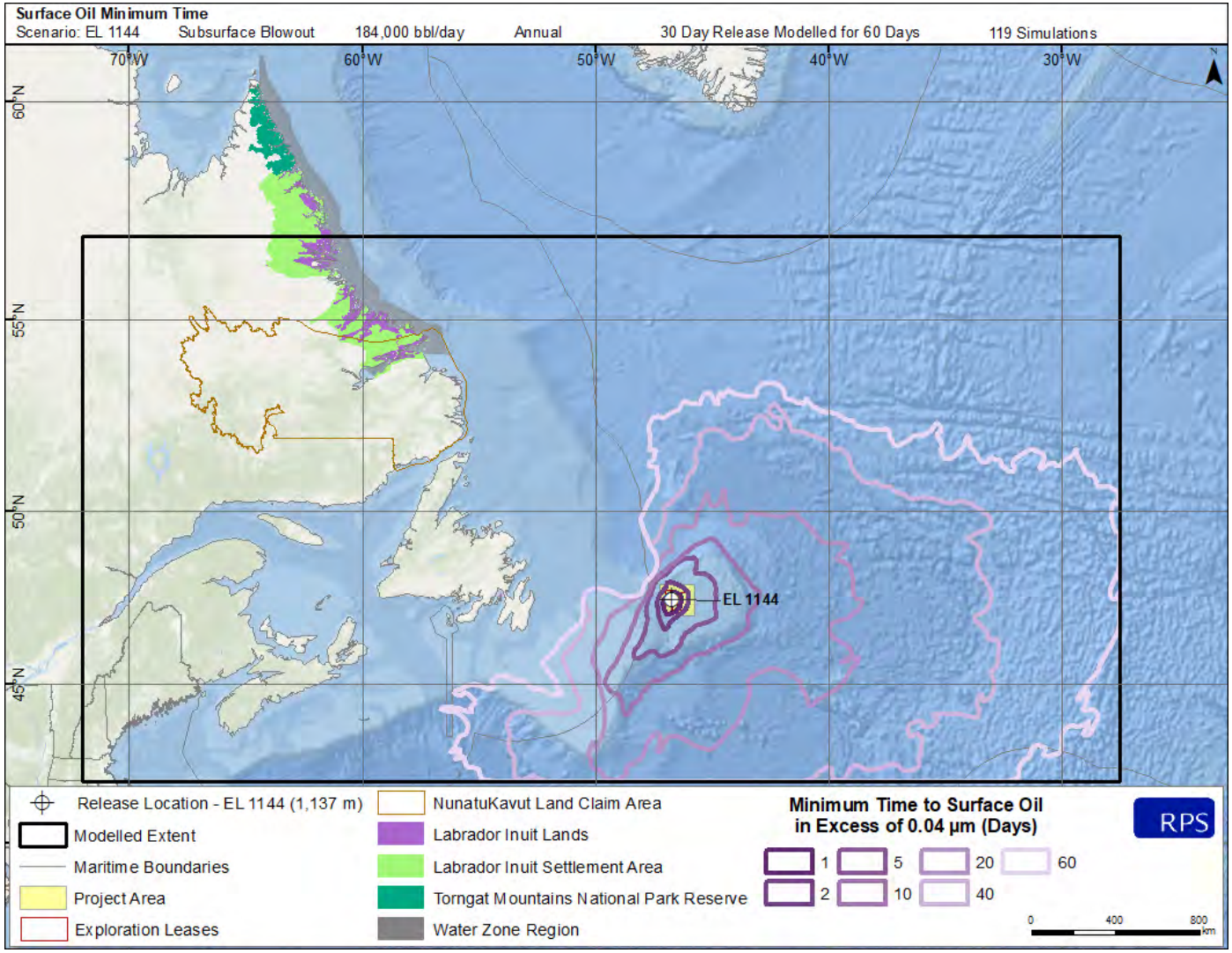

Figure 1-6. Minimum time to threshold exceedance resulting from a subsurface blowout at the EL 1144 example well release site.

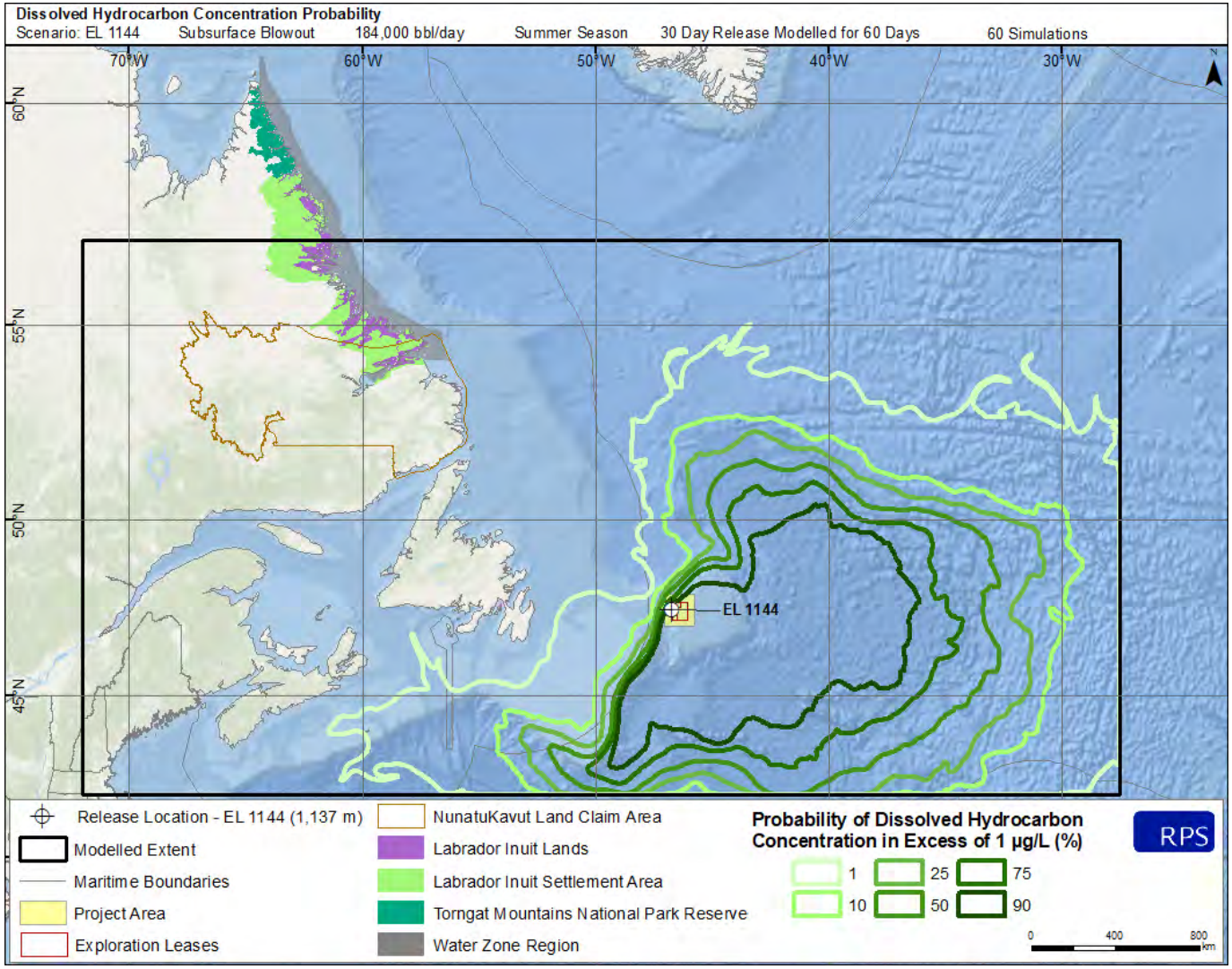

Figure 1-7. Summer probability of dissolved hydrocarbon concentrations exceeding 1 µg/L at some depth in the water column resulting from a subsurface blowout at the EL 1144 example well release site.

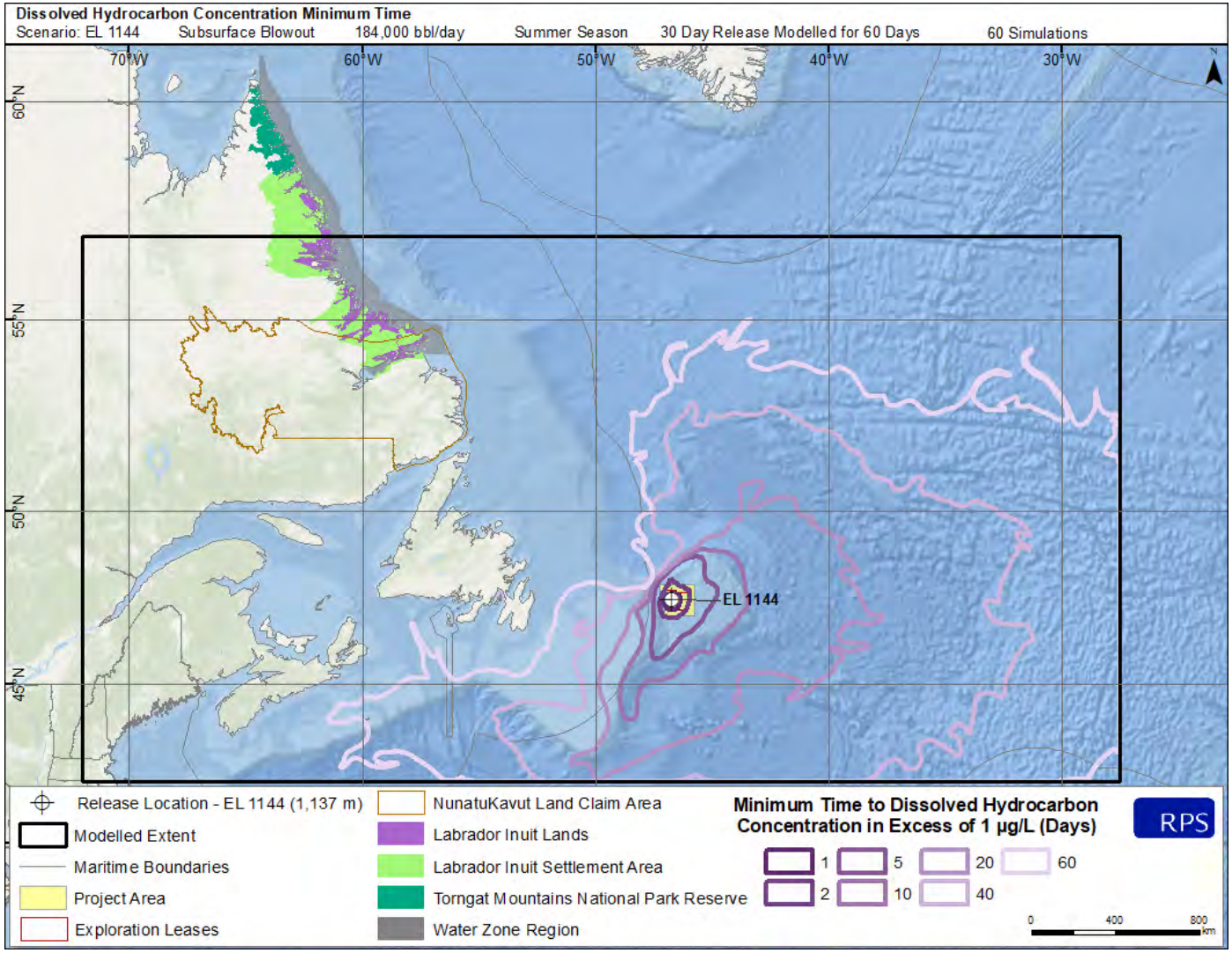

Figure 1-8. Minimum time to threshold exceedance resulting from a subsurface blowout at the EL 1144 example well release site.

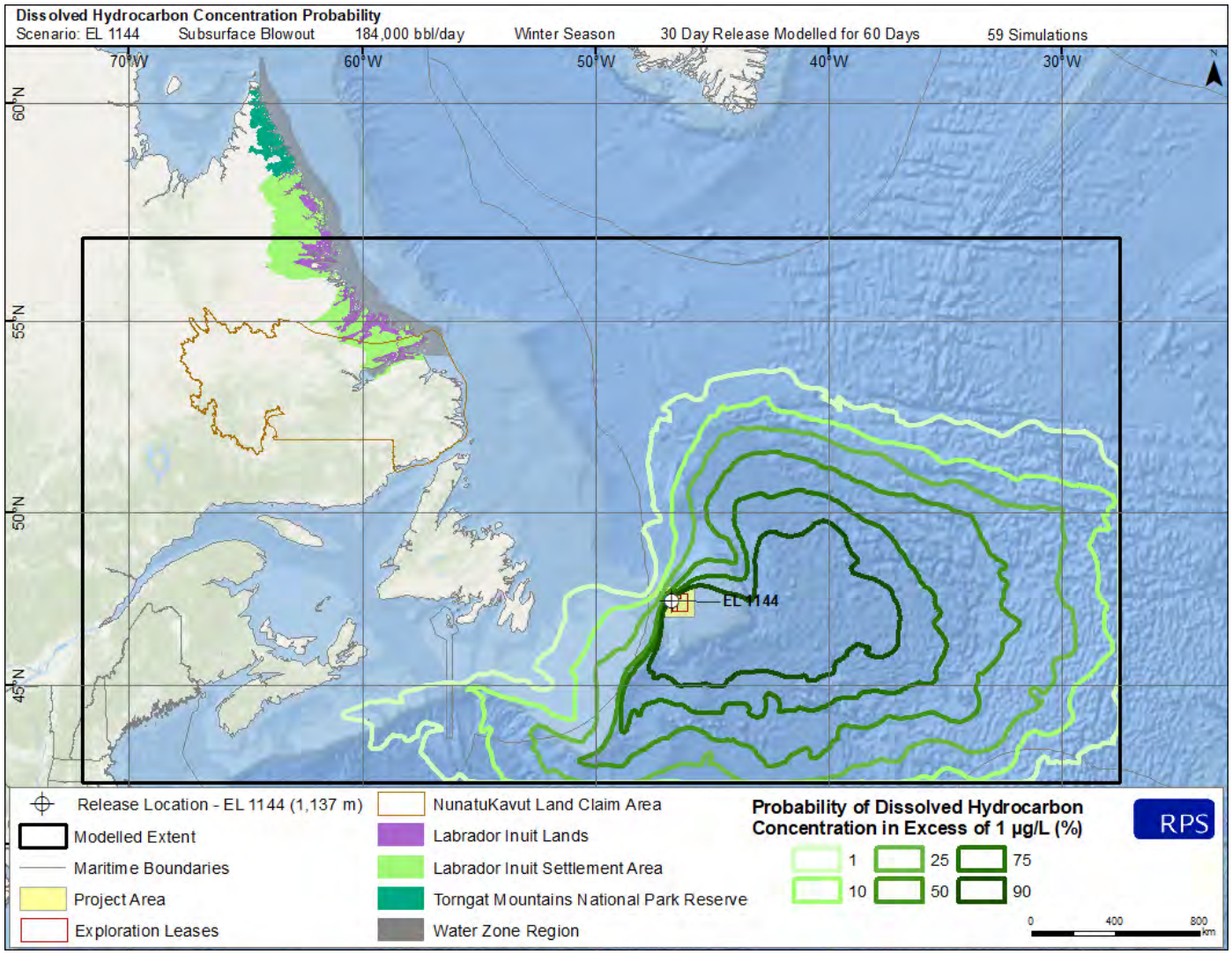

Figure 1-9. Winter probability of dissolved hydrocarbon concentrations exceeding 1 µg/L at some depth in the water column resulting from a subsurface blowout at the EL 1144 example well release site.

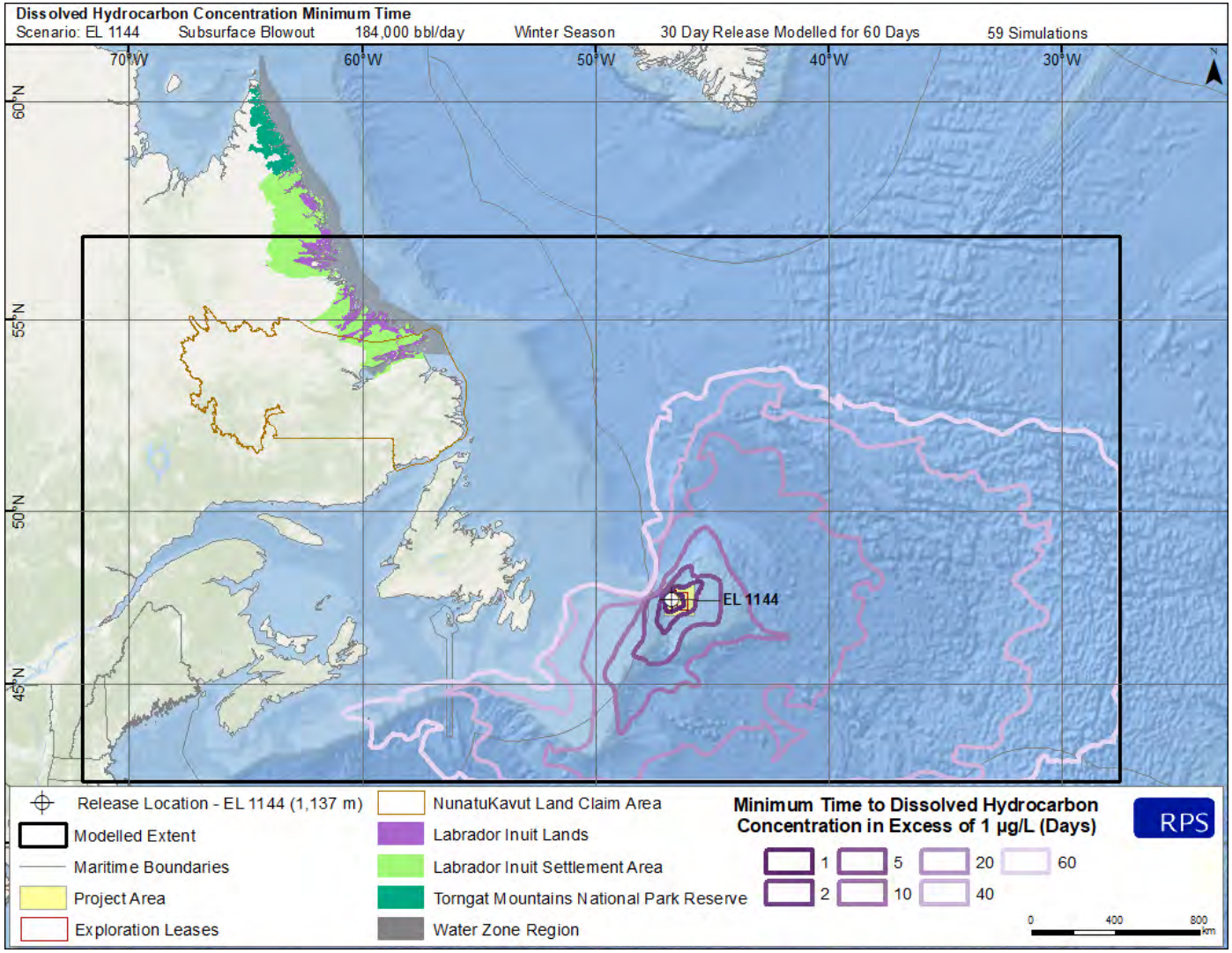

Figure 1-10. Minimum time to threshold exceedance resulting from a subsurface blowout at the EL 1144 example well release site.

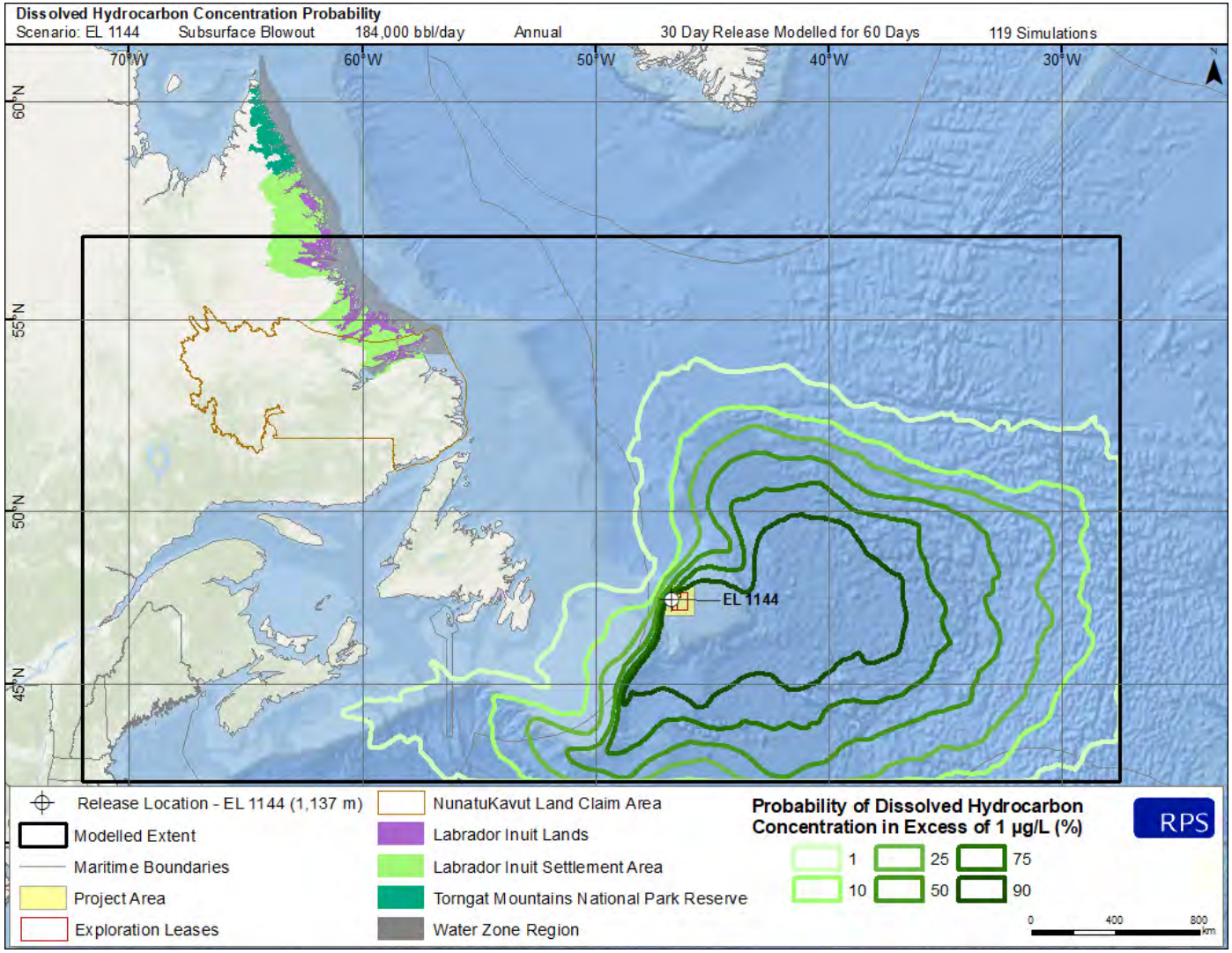

Figure 1-11. Annual probability of dissolved hydrocarbon concentrations exceeding 1 µg/L at some depth in the water column resulting from a subsurface blowout at the EL 1144 example well release site.

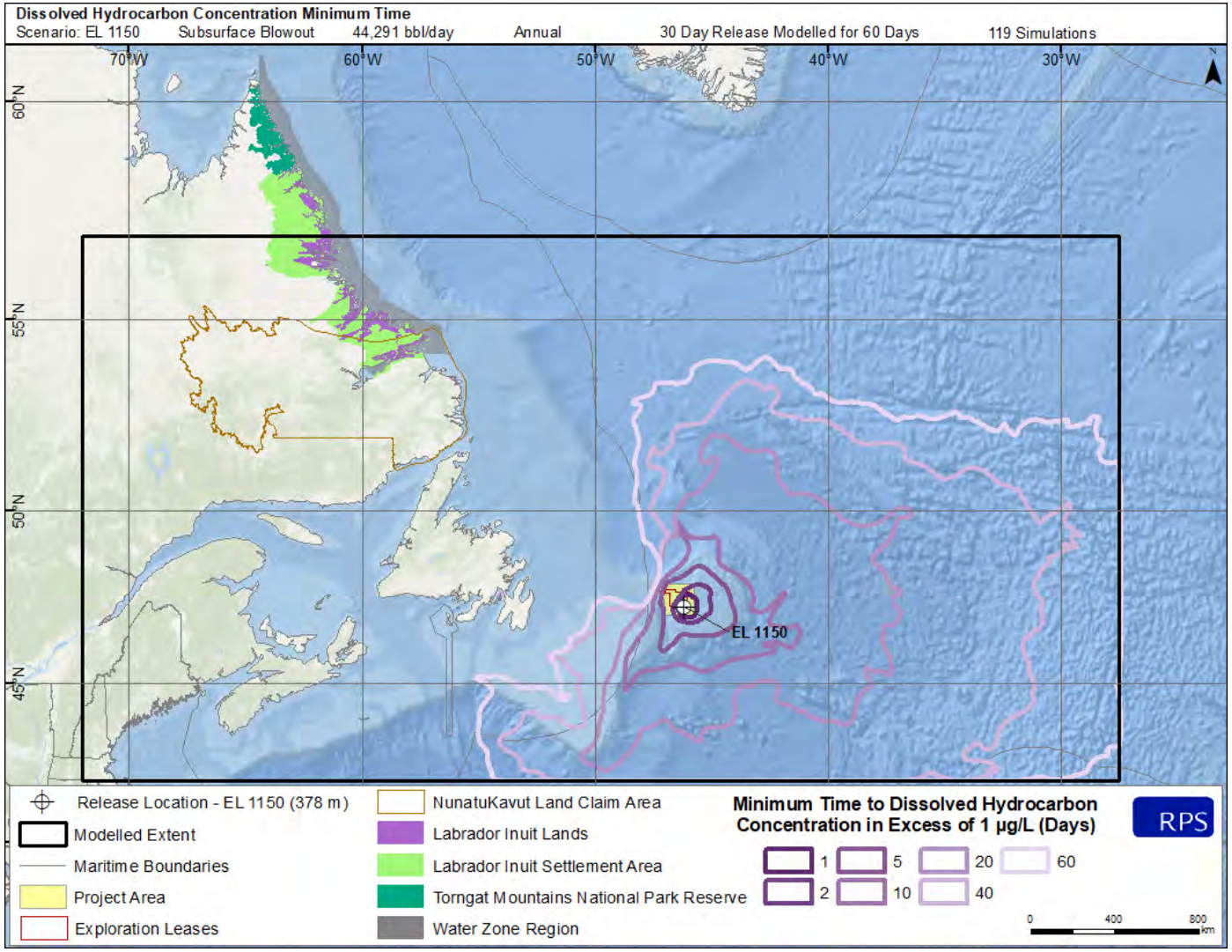

Figure 1-12. Minimum time to threshold exceedance resulting from a subsurface blowout at the EL 1144 example well release site.

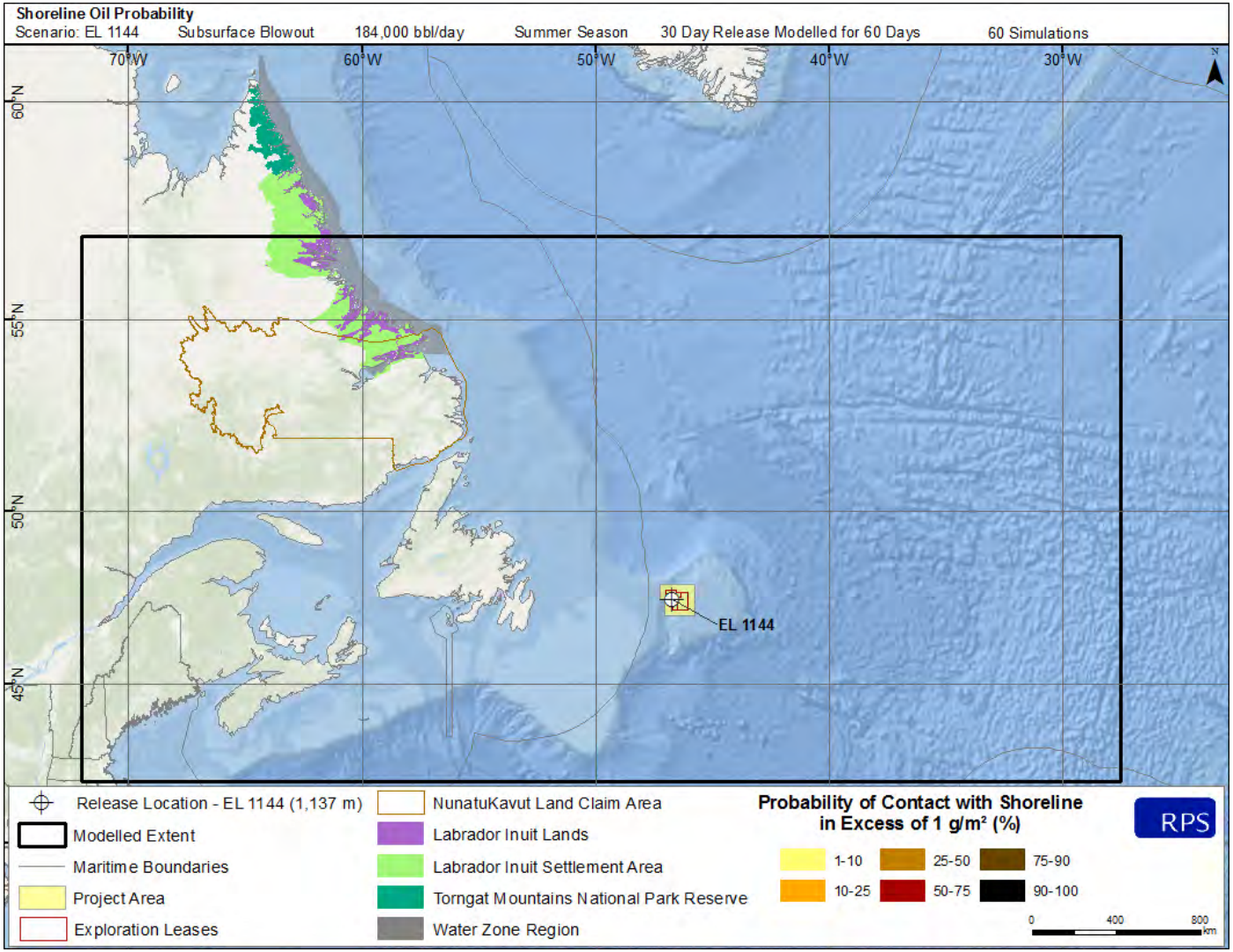

Figure 1-13. Summer probability of shoreline contact exceeding 1 g/m^2 resulting from a subsurface blowout at the EL 1144 example well release site. No shoreline contact was predicted for this scenario.

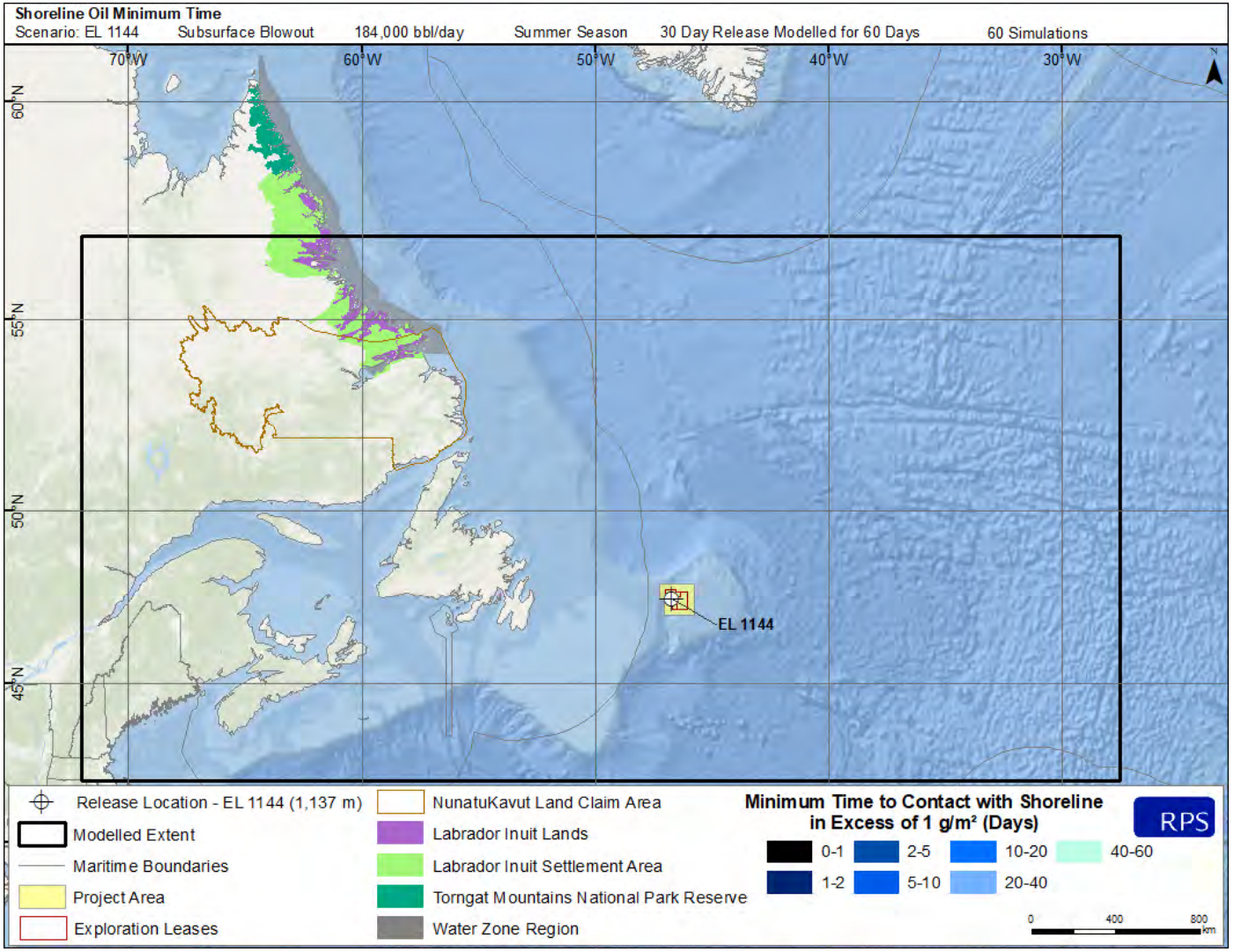

Figure 1-14. Minimum time to threshold exceedance resulting from a subsurface blowout at the EL 1144 example well release site. No shoreline contact was predicted for this scenario.

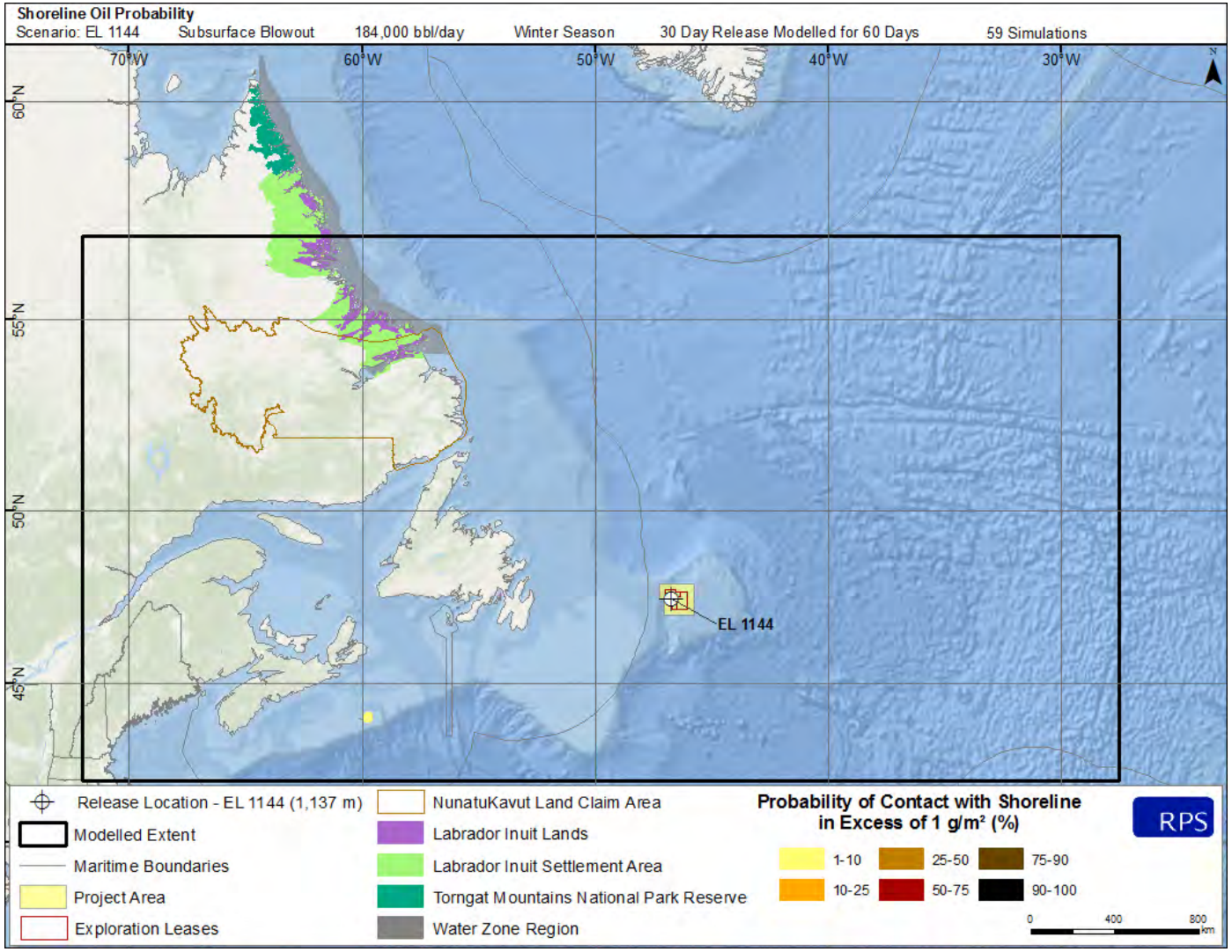

Figure 1-15. Winter probability of shoreline contact exceeding 1 g/m² resulting from a subsurface blowout at the EL 1144 example well release site.

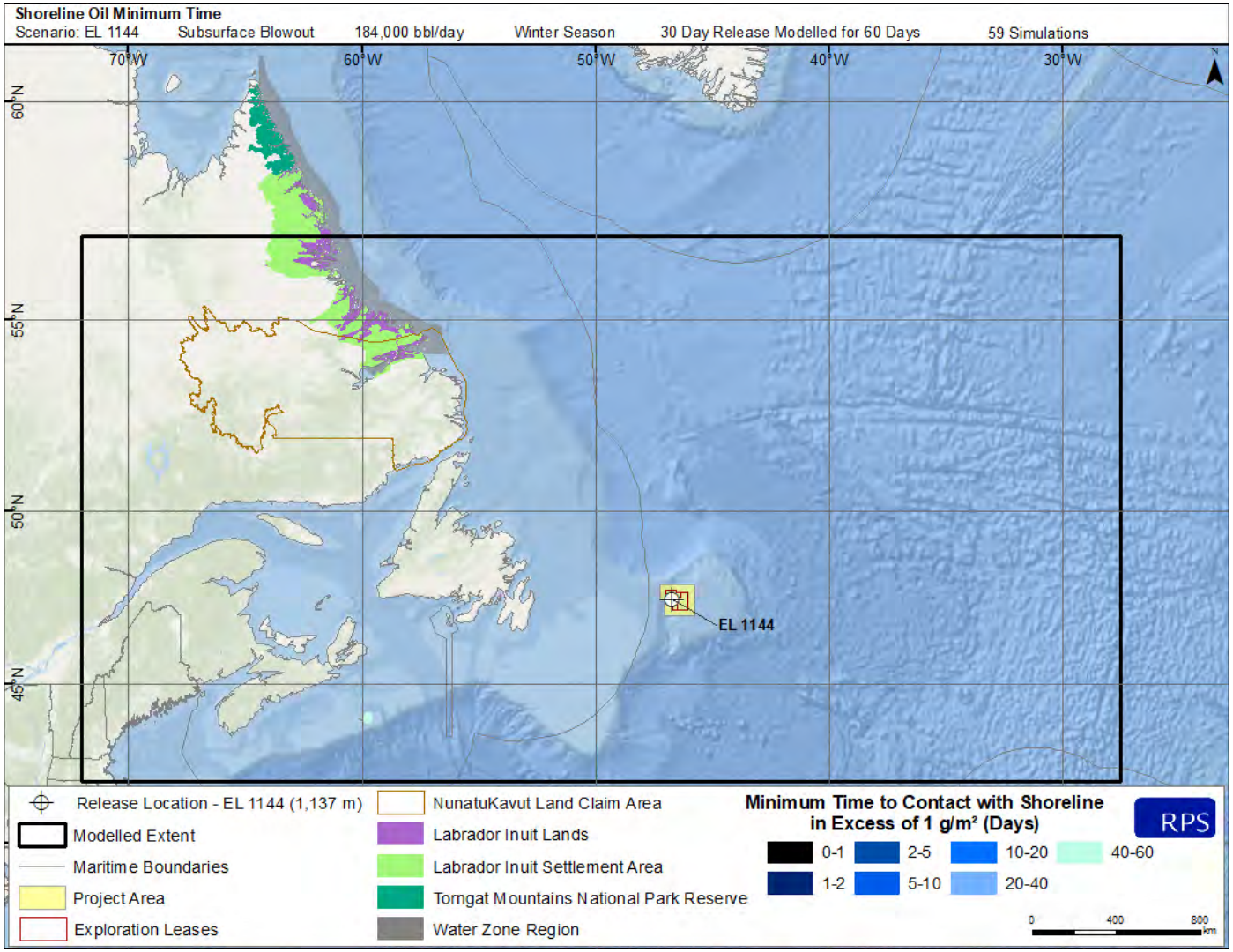

Figure 1-16. Minimum time to threshold exceedance resulting from a subsurface blowout at the EL 1144 example well release site.

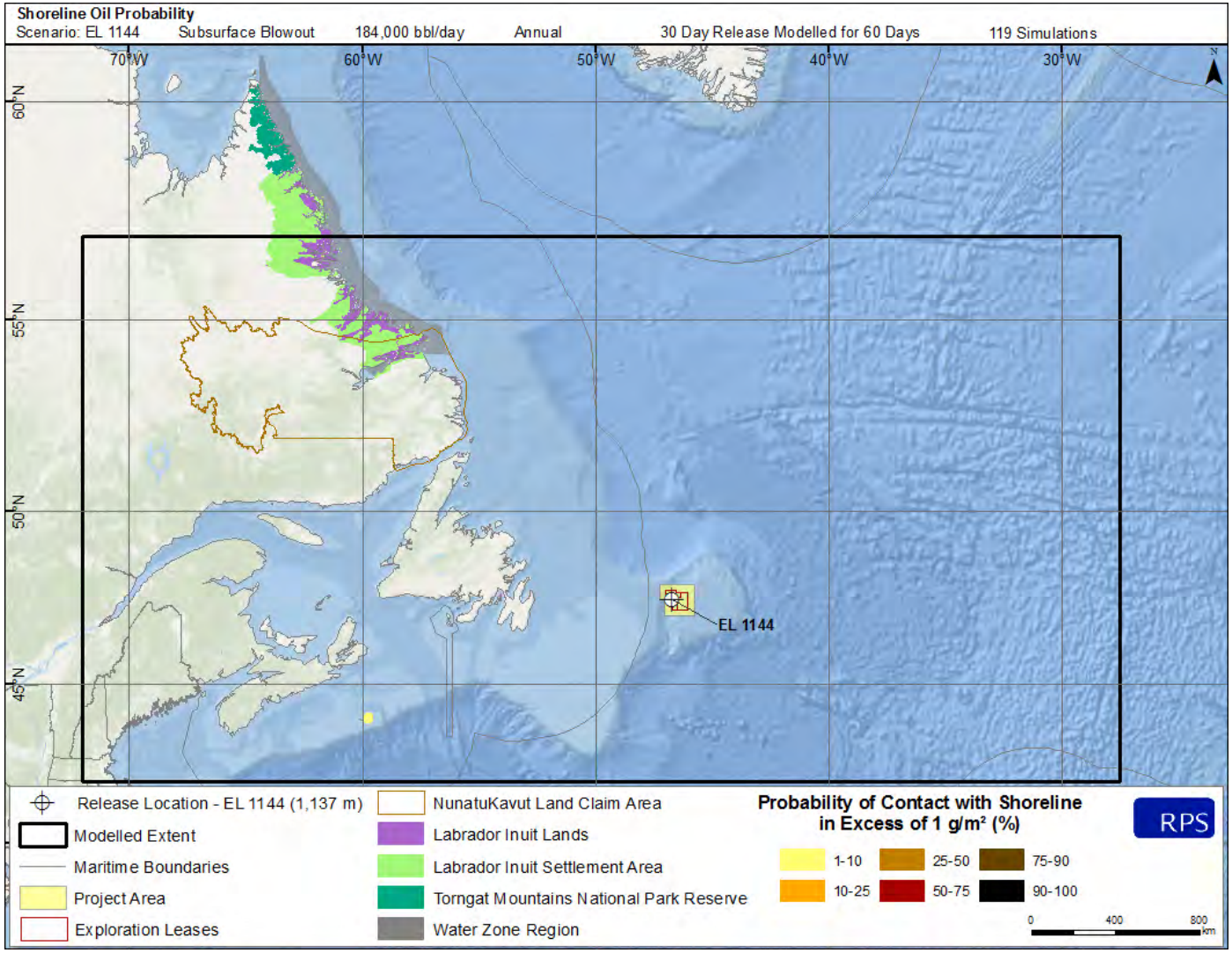

Figure 1-17. Annual probability of shoreline contact exceeding 1 g/m^2 resulting from a subsurface blowout at the EL 1144 example well release site.

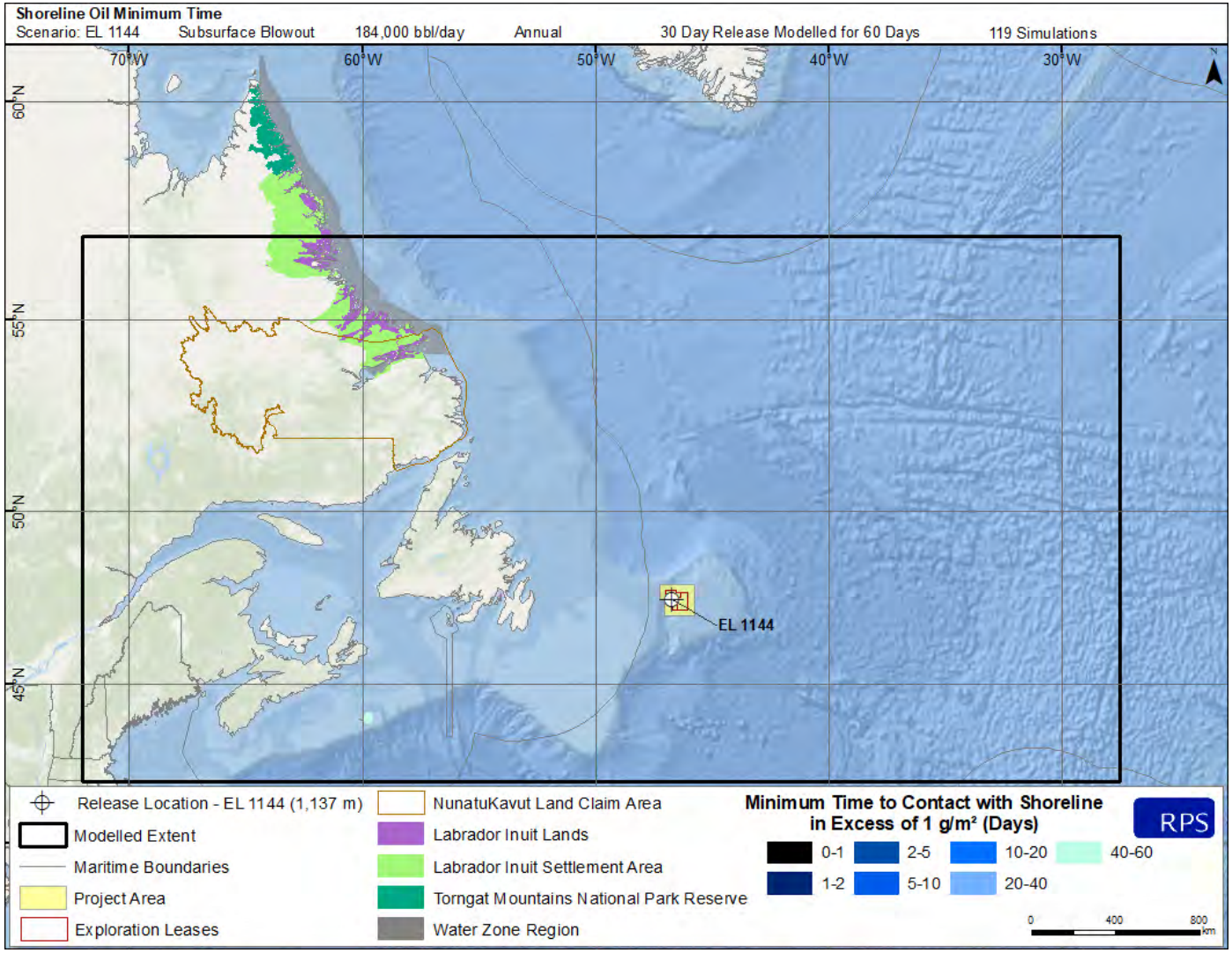

Figure 1-18. Minimum time to threshold exceedance resulting from a subsurface blowout at the EL 1144 example well release site.

1.2 EL 1150 Release Site

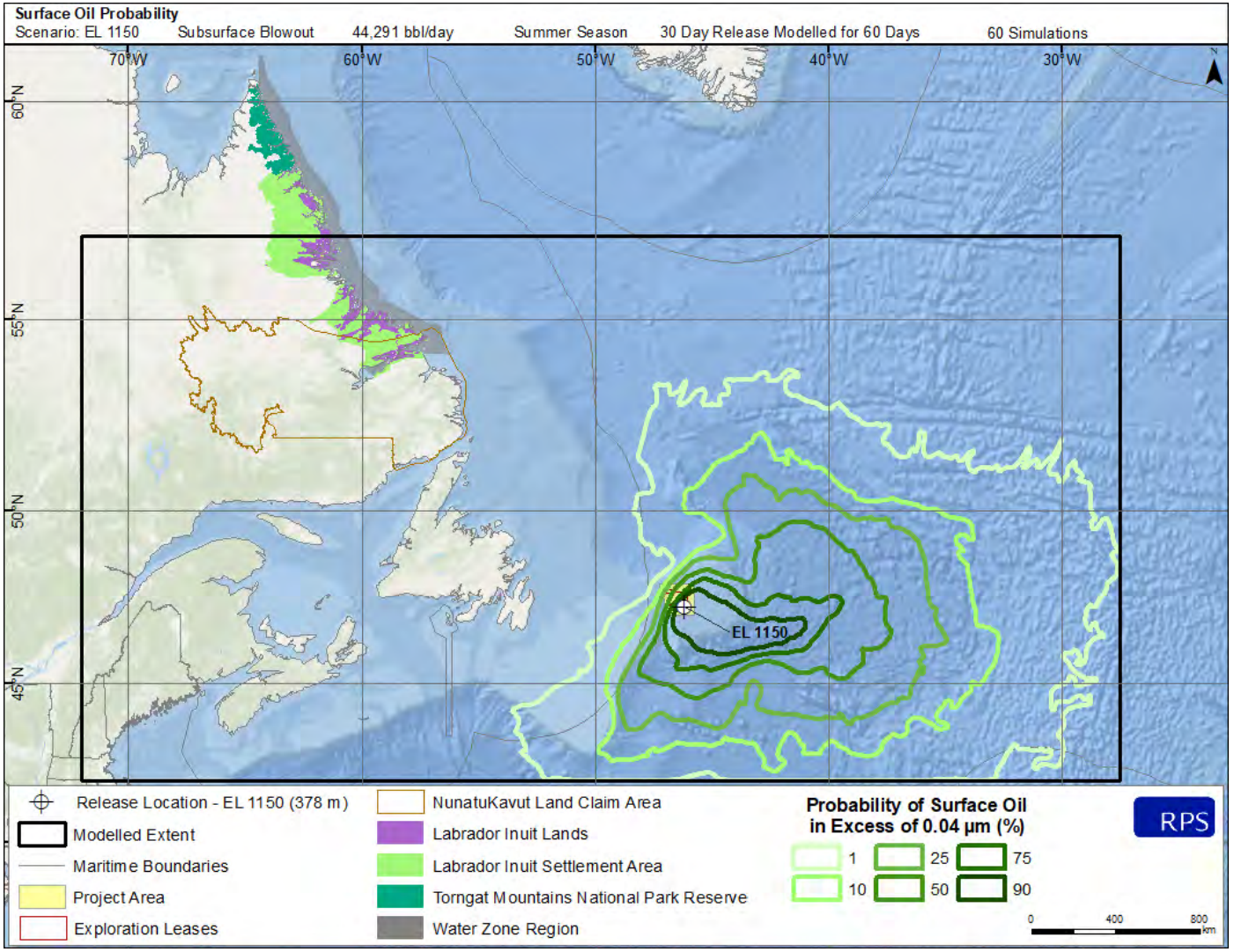

Figure 1-19. Summer probability of average surface oil thickness exceeding 0.04 µm resulting from a subsurface blowout at the EL 1150 example well release site.

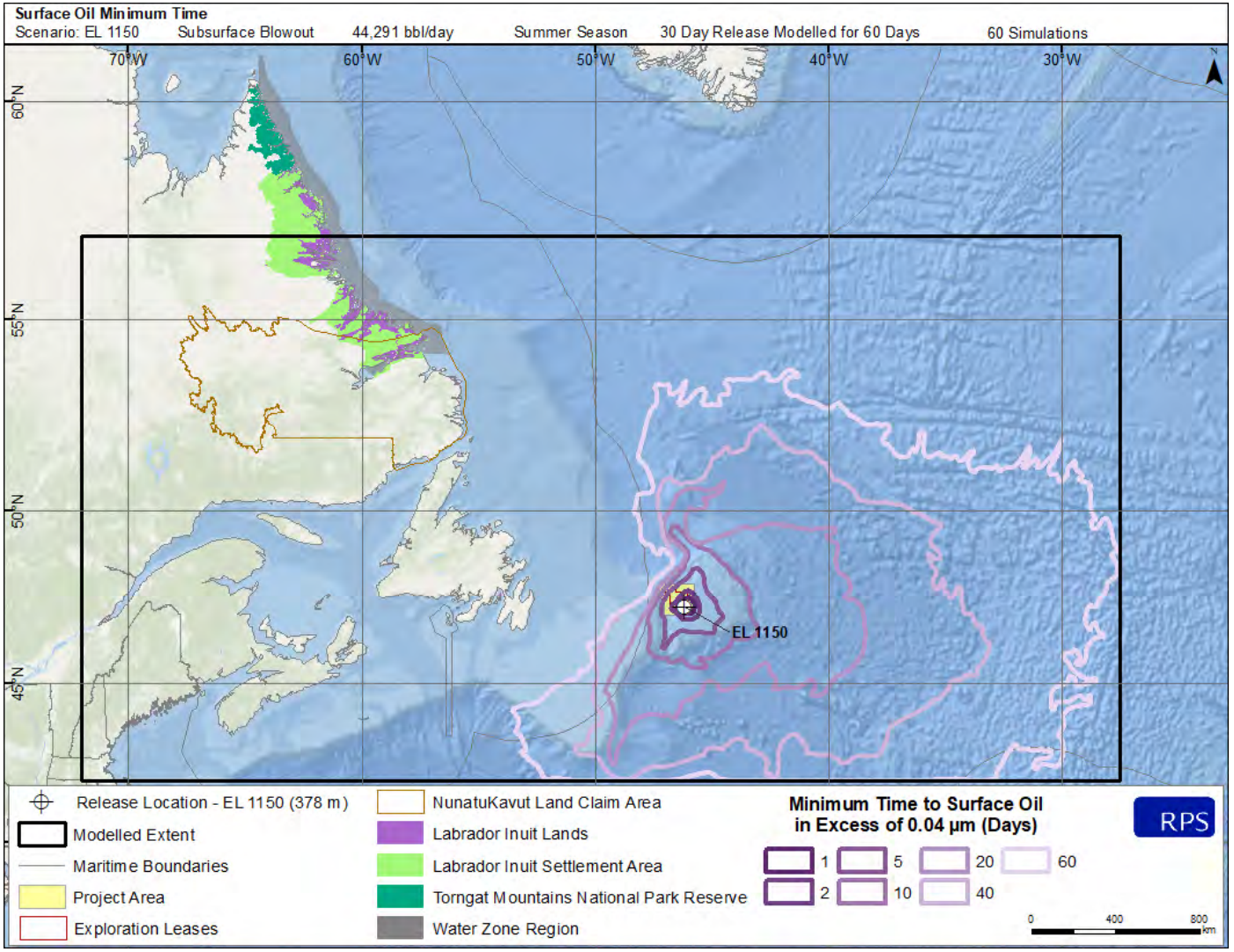

Figure 1-20. Minimum time to threshold exceedance resulting from a subsurface blowout at the EL 1150 example well release site.

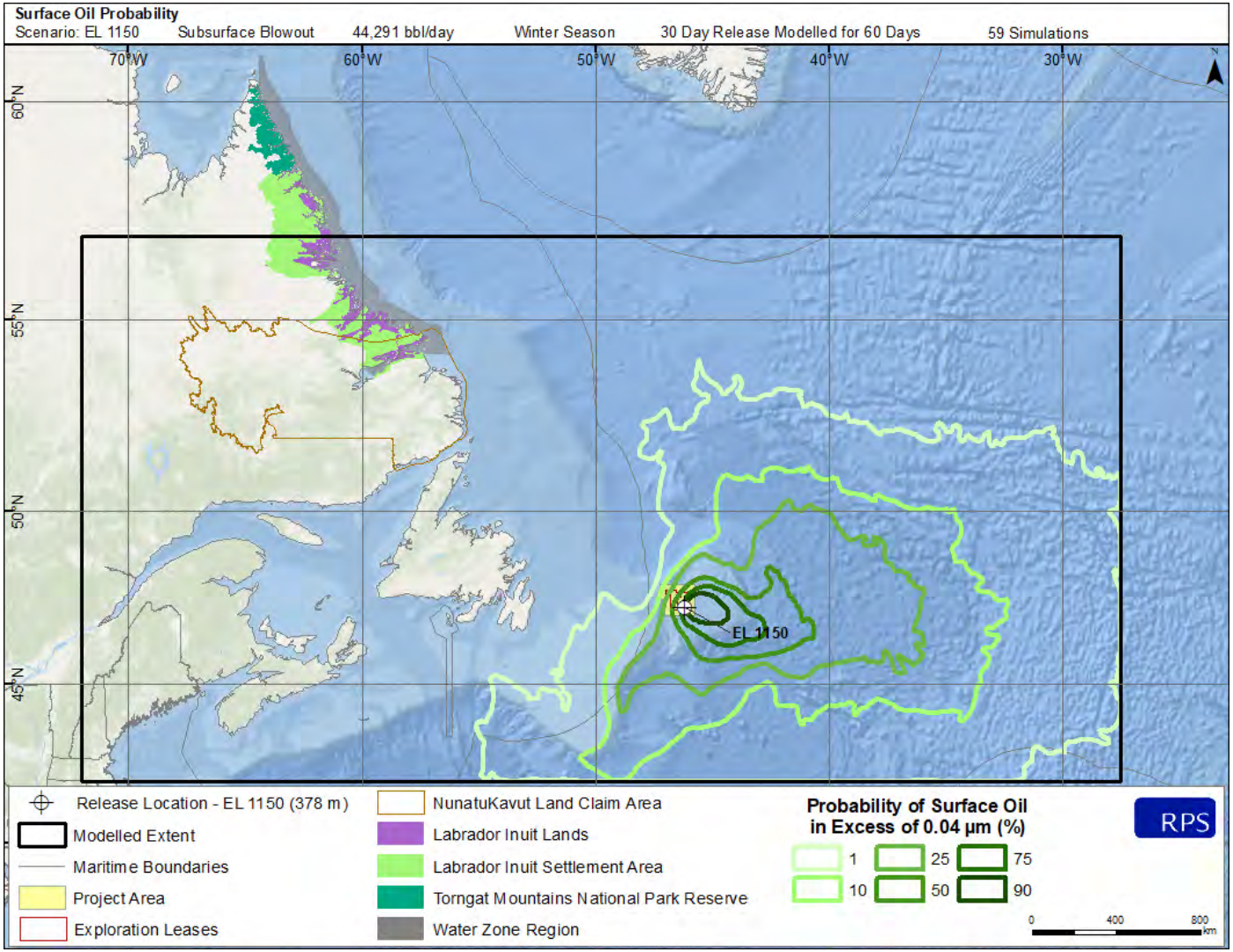

Figure 1-21.Winter probability of average surface oil thickness exceeding 0.04 µm resulting from a subsurface blowout at the EL 1150 example well release site.

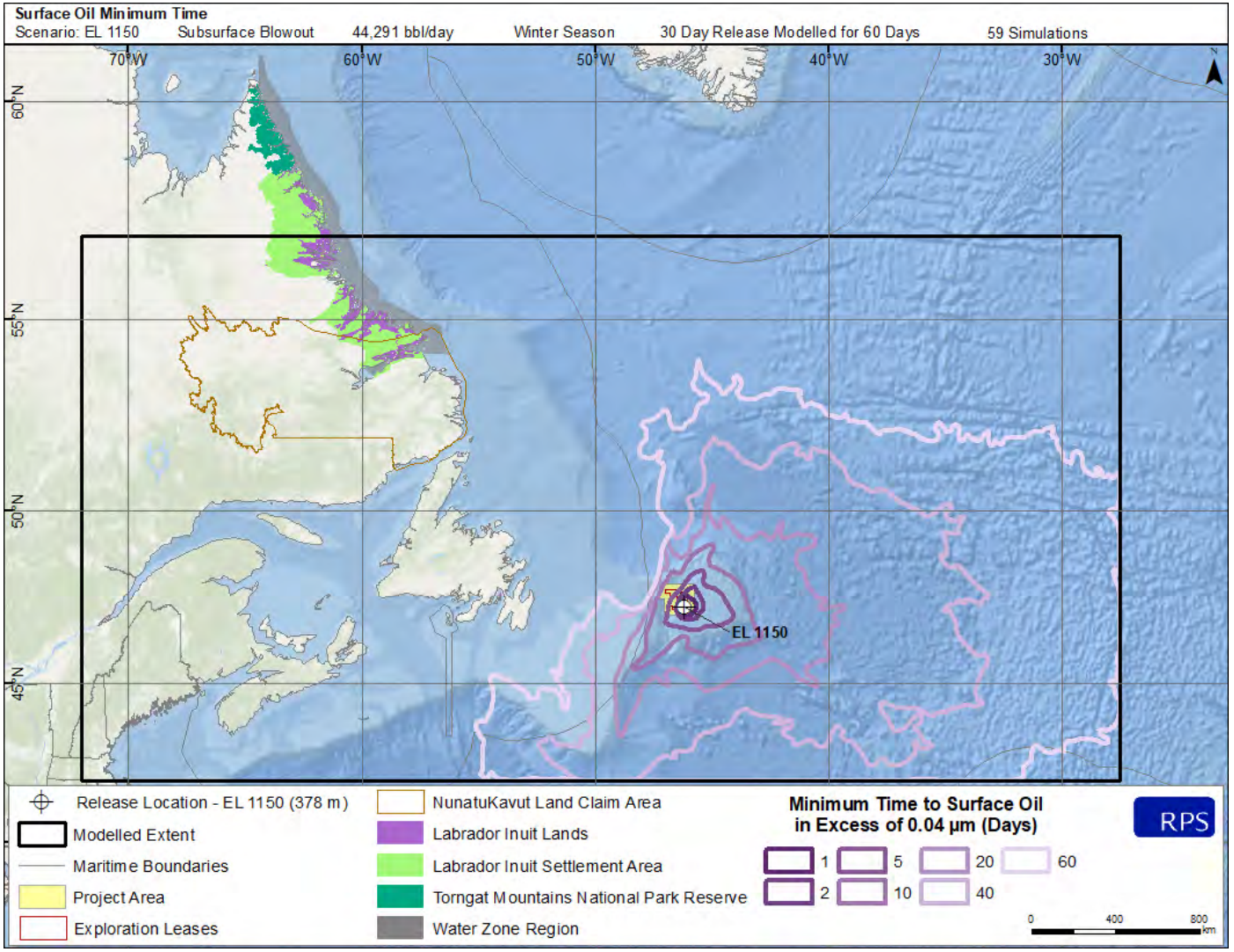

Figure 1-22. Minimum time to threshold exceedance resulting from a subsurface blowout at the EL 1150 example well release site.

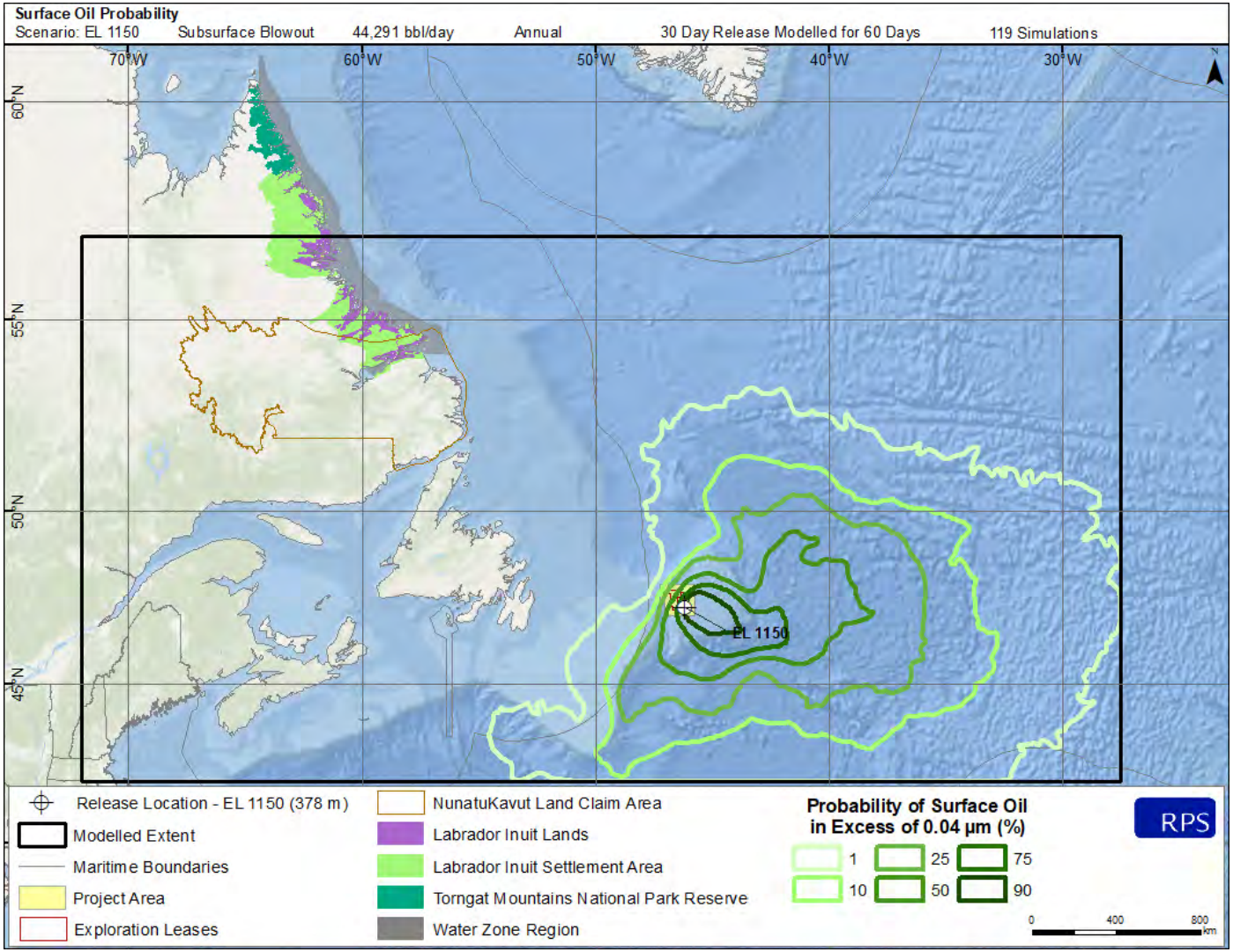

Figure 1-23. Annual probability of average surface oil thickness exceeding 0.04 µm resulting from a subsurface blowout at the EL 1150 example well release site.

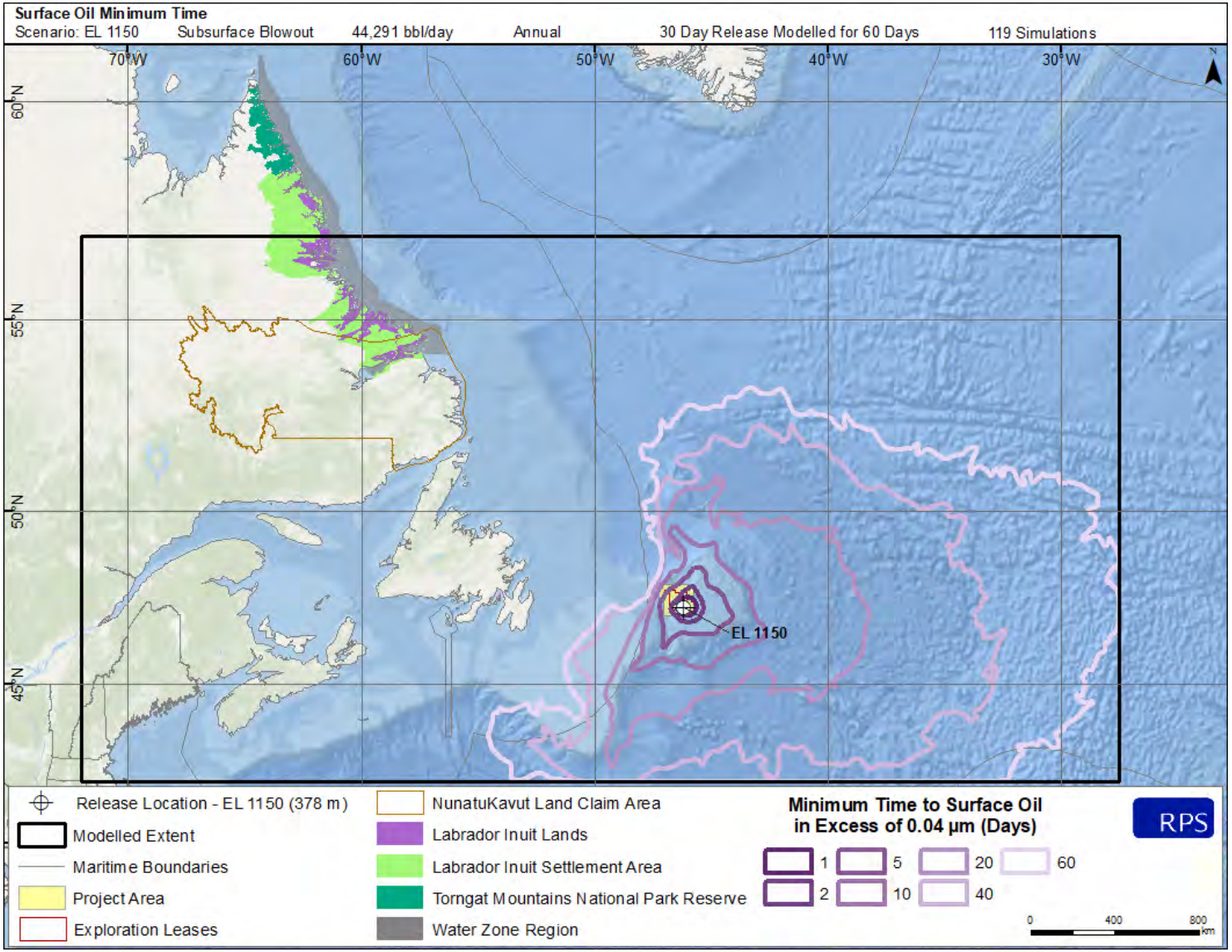

Figure 1-24. Minimum time to threshold exceedance resulting from a subsurface blowout at the EL 1150 example well release site.

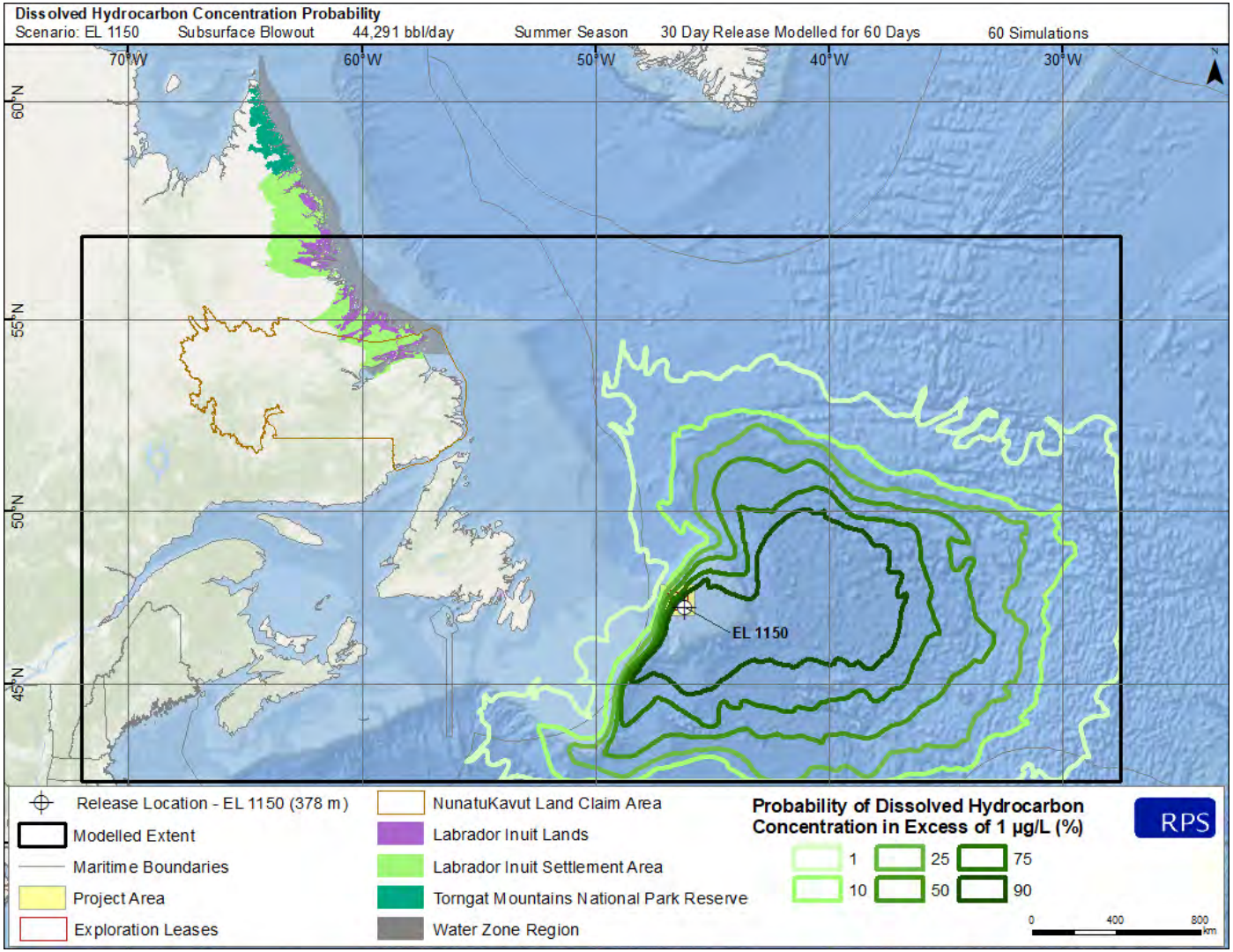

Figure 1-25. Summer probability of dissolved hydrocarbon concentrations exceeding 1 µg/L at some depth in the water column resulting from a subsurface blowout at the EL 1150 example well release site.

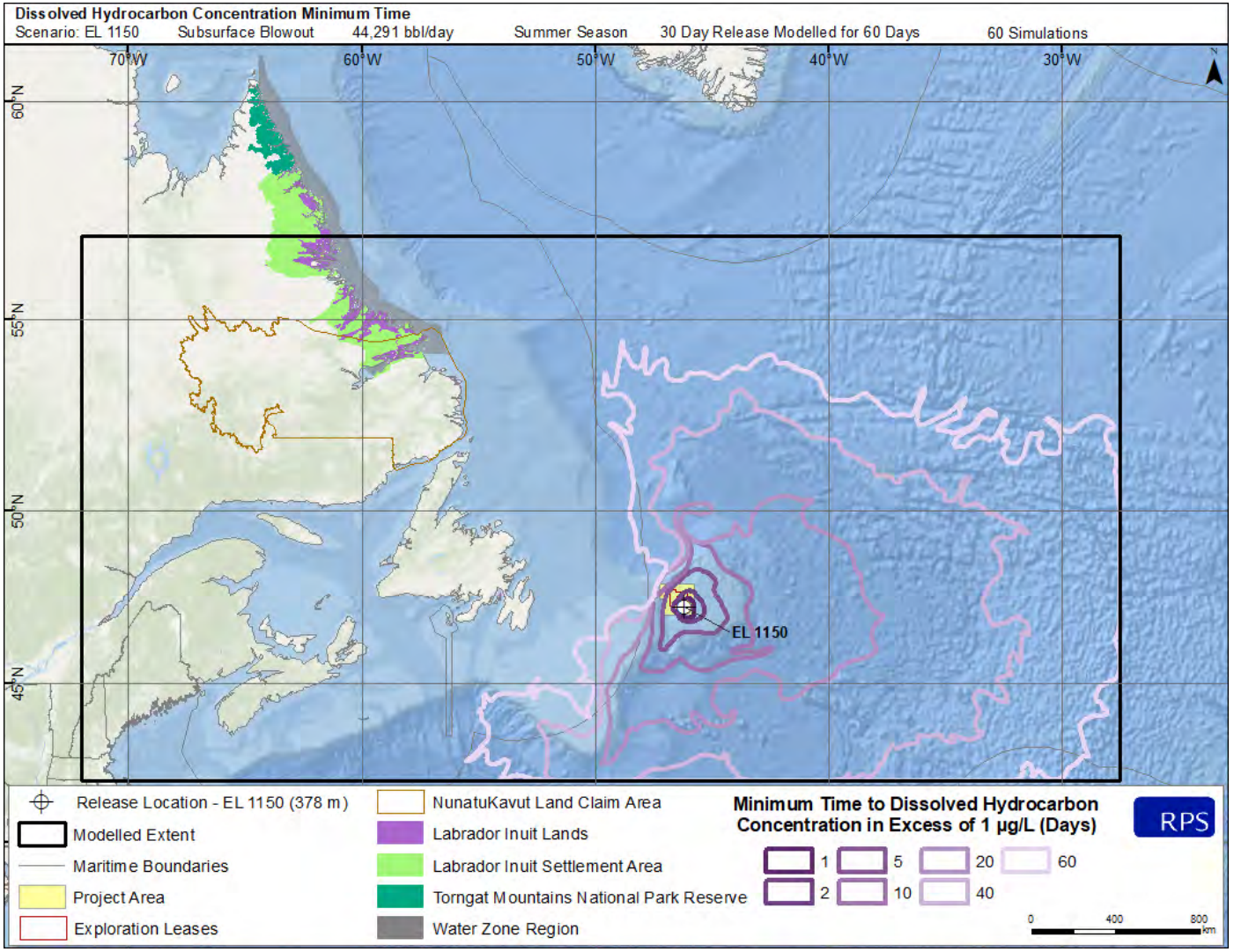

Figure 1-26. Minimum time to threshold exceedance resulting from a subsurface blowout at the EL 1150 example well release site.

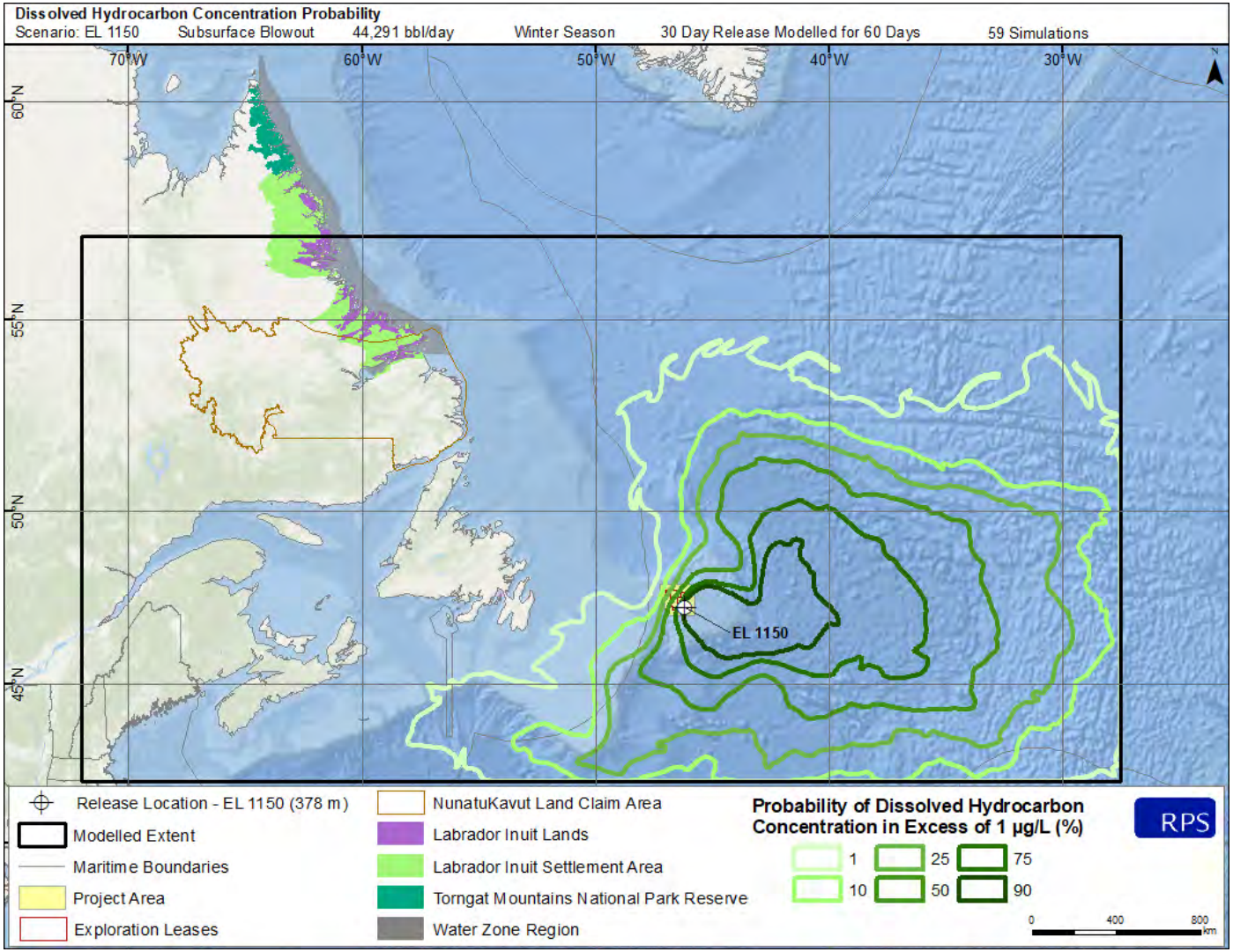

Figure 1-27. Winter probability of dissolved hydrocarbon concentrations exceeding 1 µg/L at some depth in the water column resulting from a subsurface blowout at the EL 1150 example well release site.

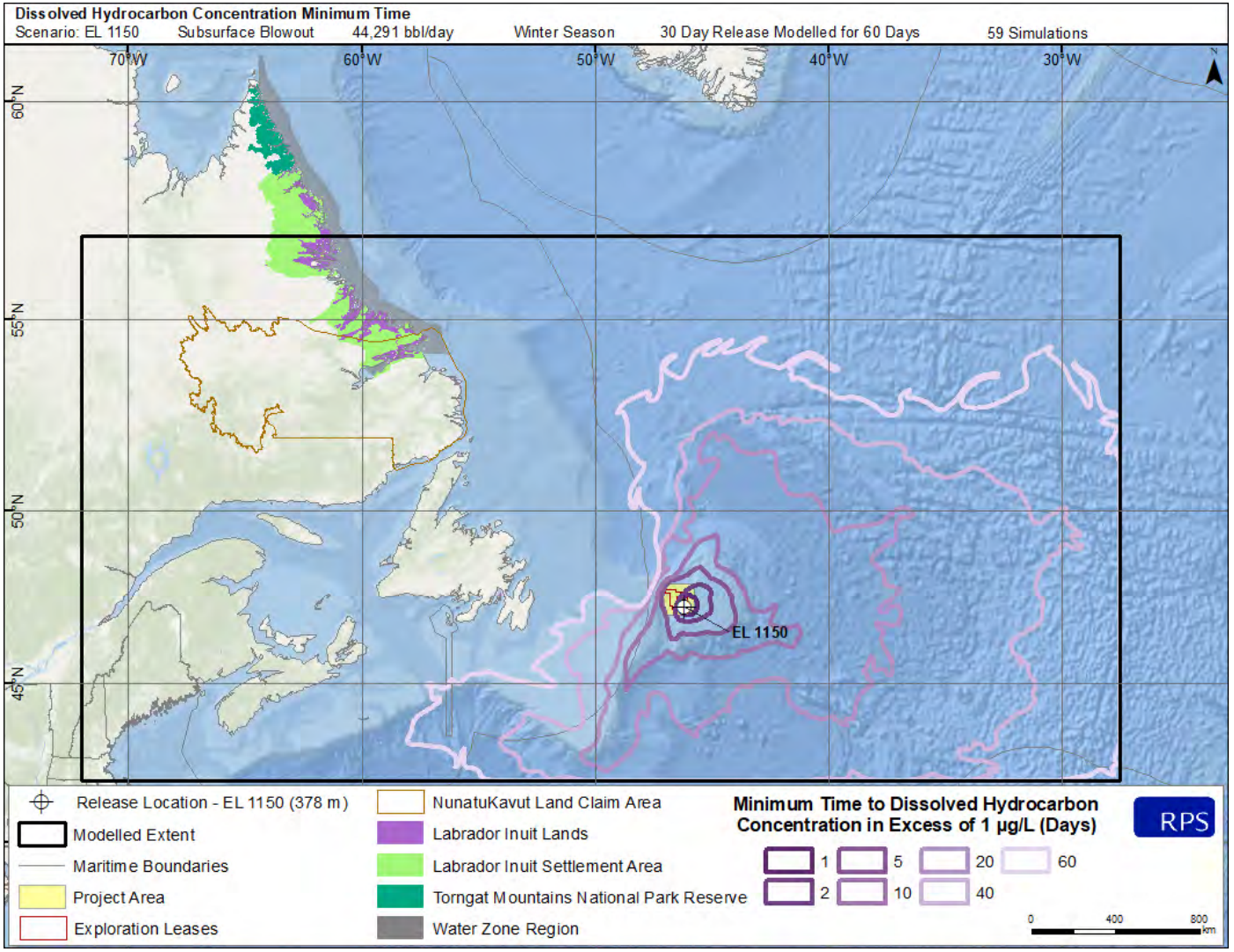

Figure 1-28. Minimum time to threshold exceedance resulting from a subsurface blowout at the EL 1150 example well release site.

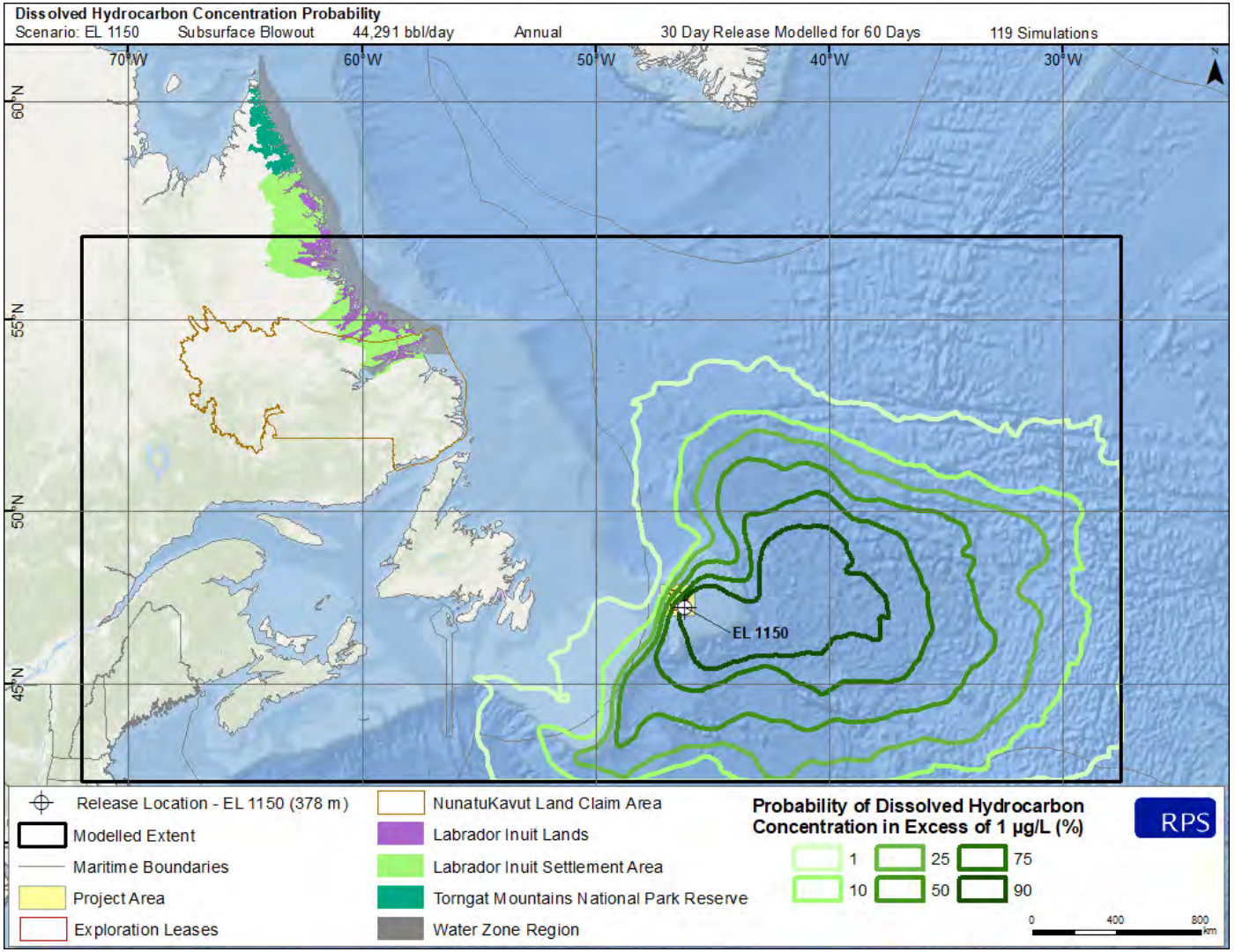

Figure 1-29. Winter probability of dissolved hydrocarbon concentrations exceeding 1 µg/L at some depth in the water column resulting from a subsurface blowout at the EL 1150 example well release site.

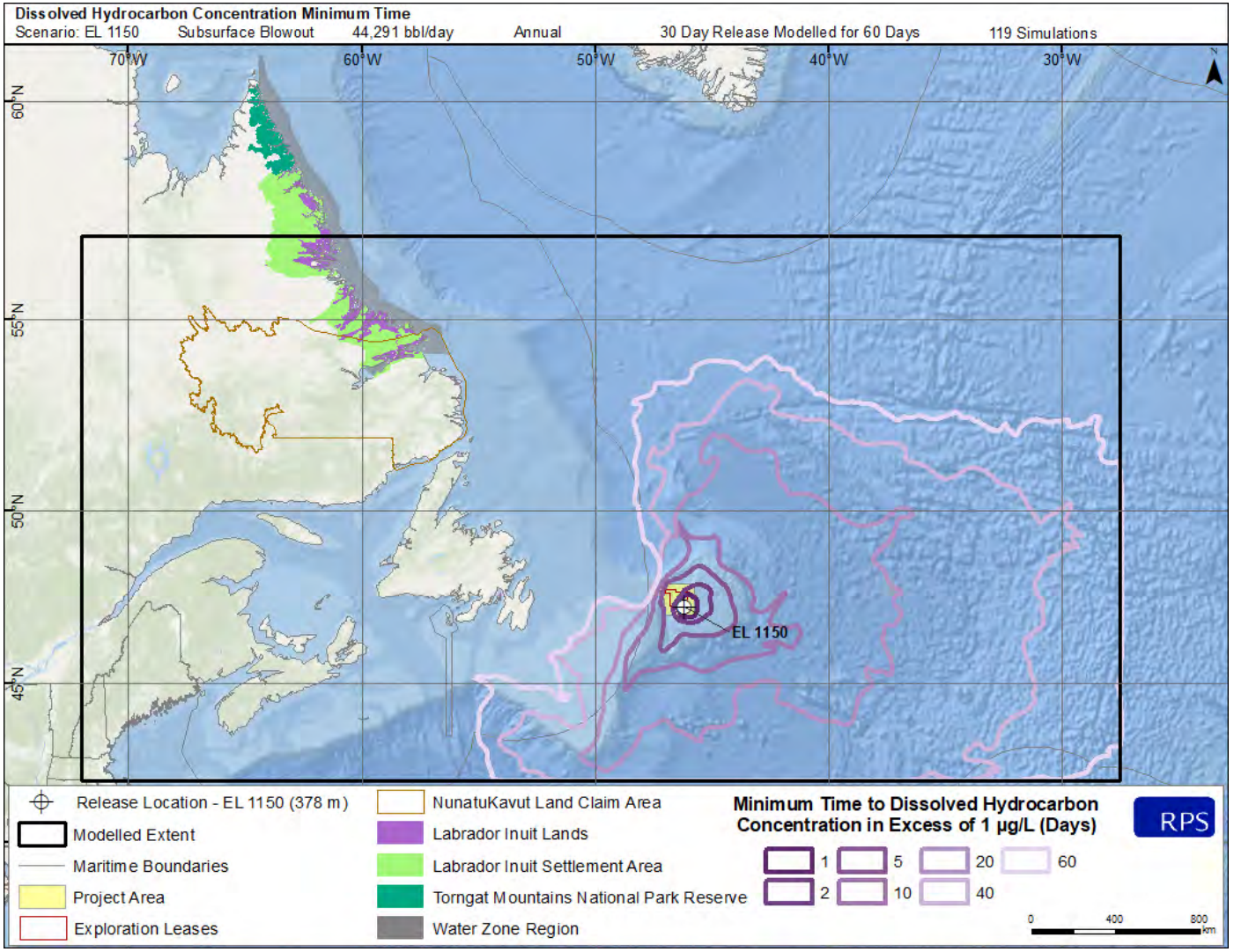

Figure 1-30. Minimum time to threshold exceedance resulting from a subsurface blowout at the EL 1150 example well release site.

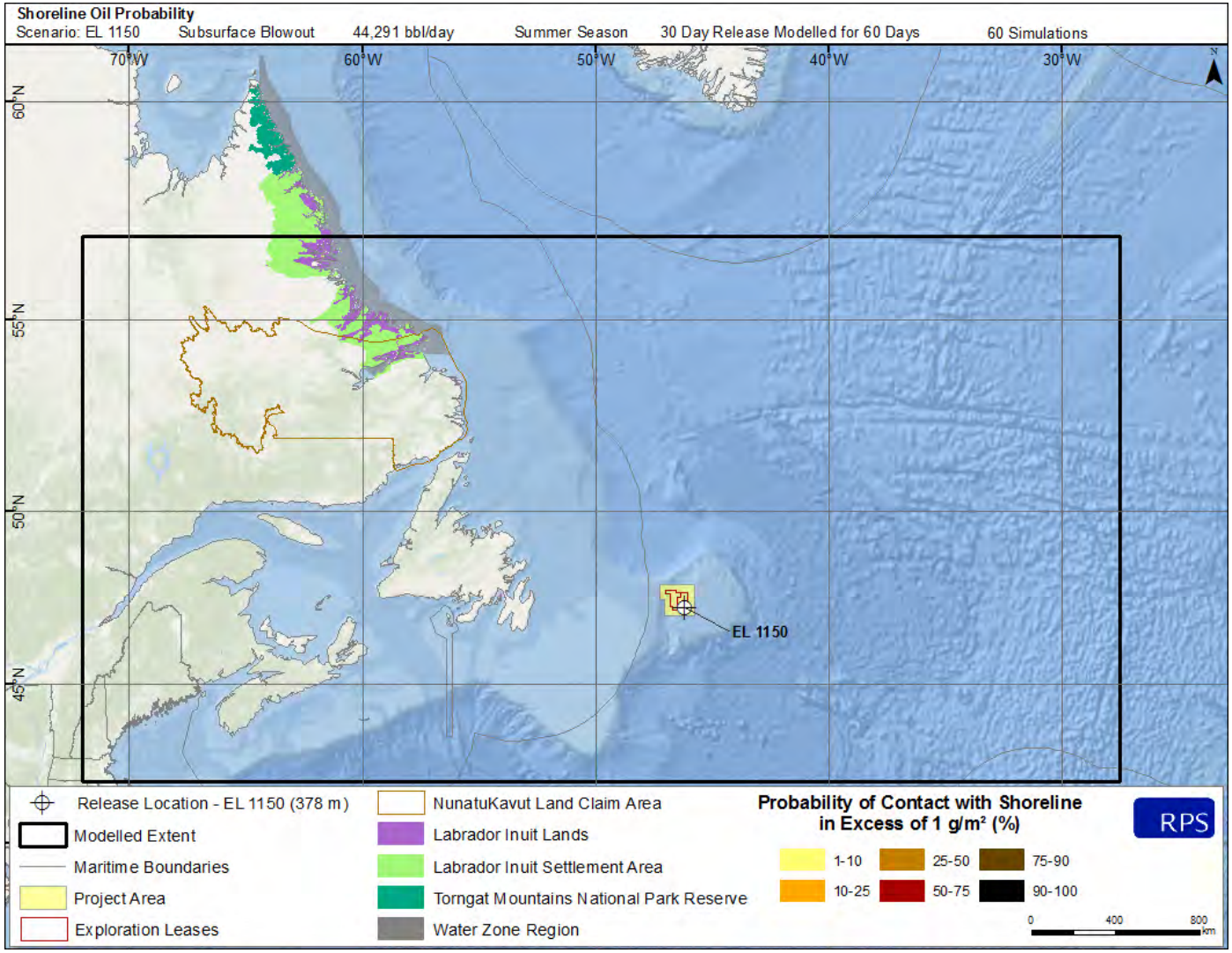

Figure 1-31. Summer probability of shoreline contact exceeding 1 g/m^2 resulting from a subsurface blowout at the EL 1150 example well release site. No shoreline contact was predicted for this scenario.

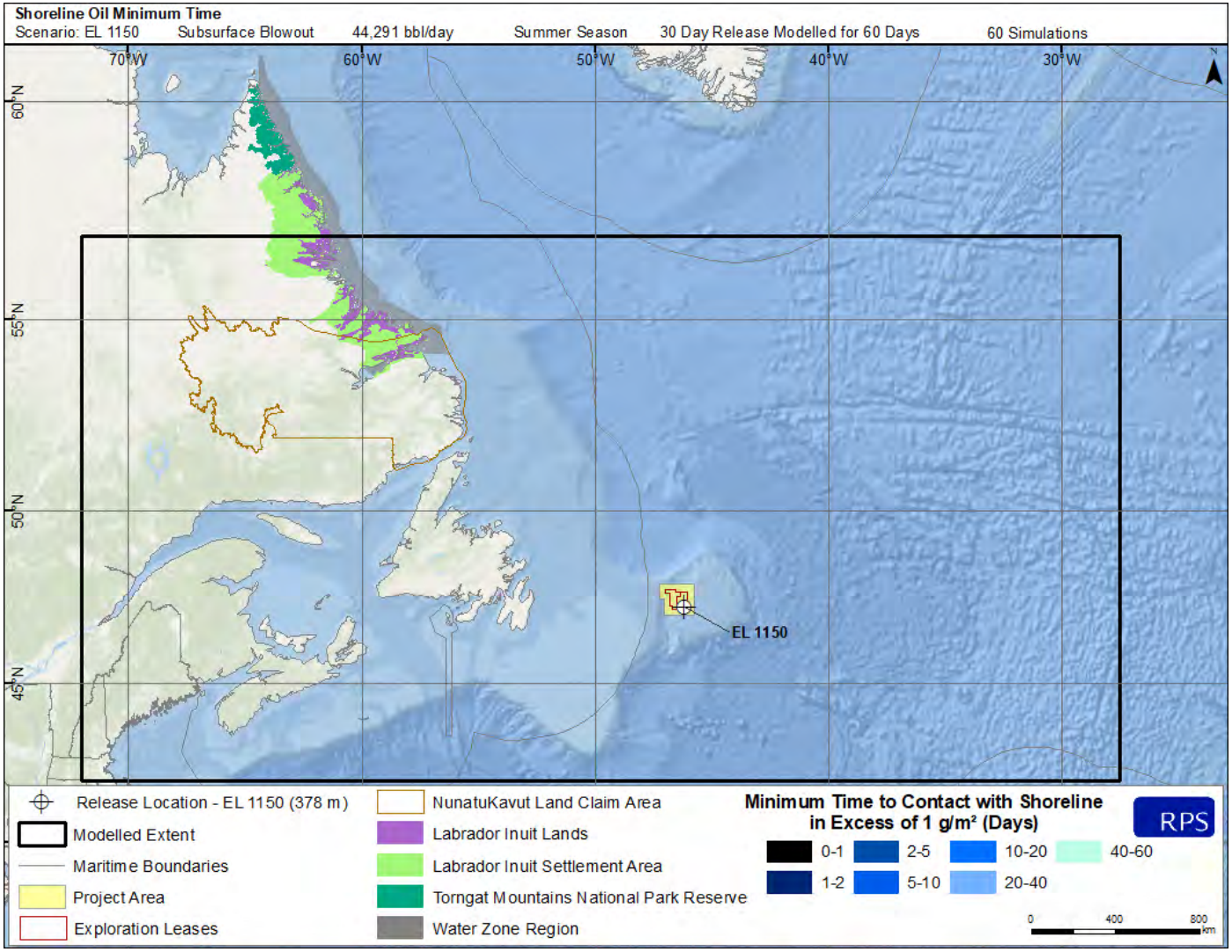

Figure 1-32. Minimum time to threshold exceedance resulting from a subsurface blowout at the EL 1150 example well release site. No shoreline contact was predicted for this scenario.

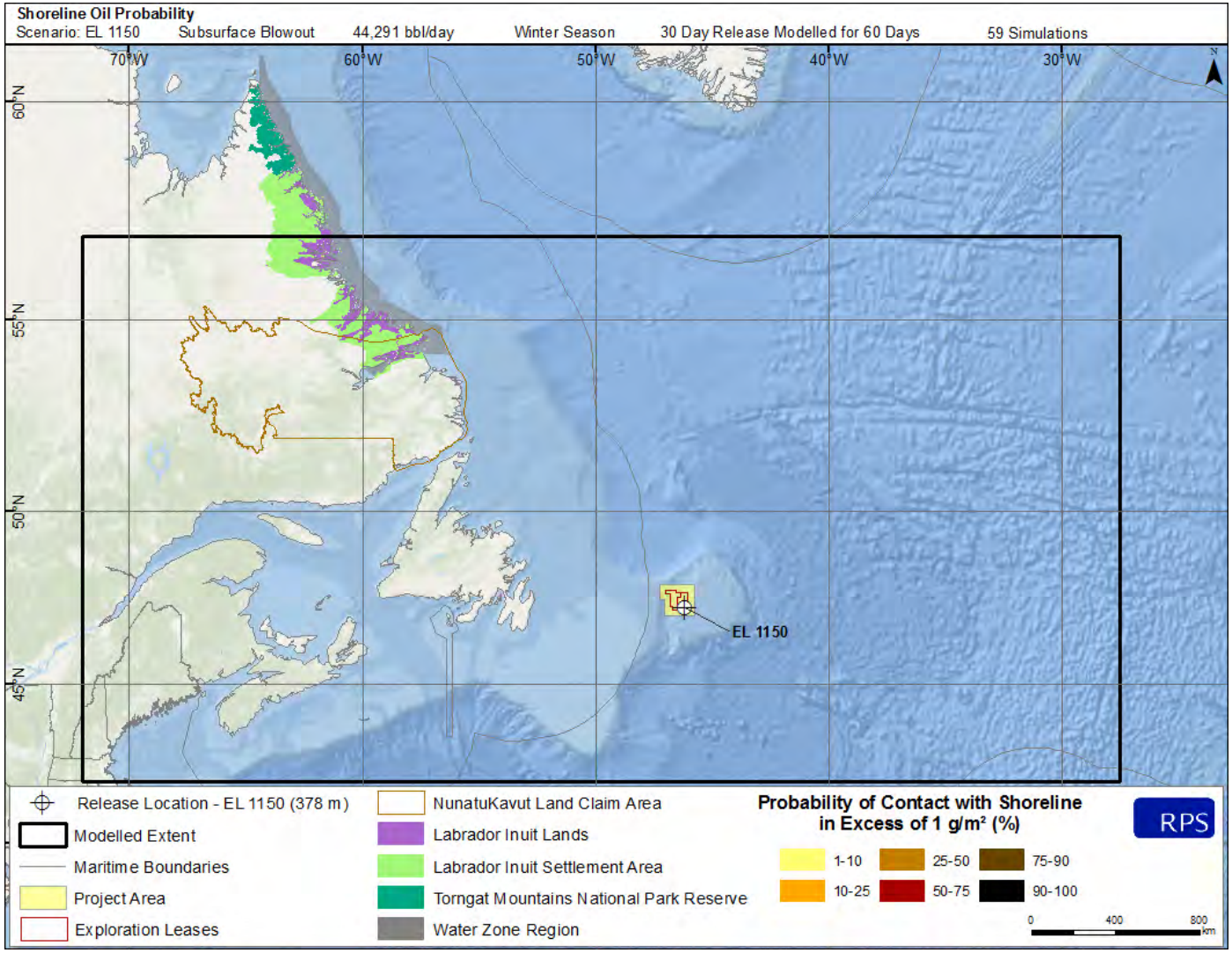

Figure 1-33. Winter probability of shoreline contact exceeding 1 g/m^2 resulting from a subsurface blowout at the EL 1150 example well release site. No shoreline contact was predicted for this scenario.

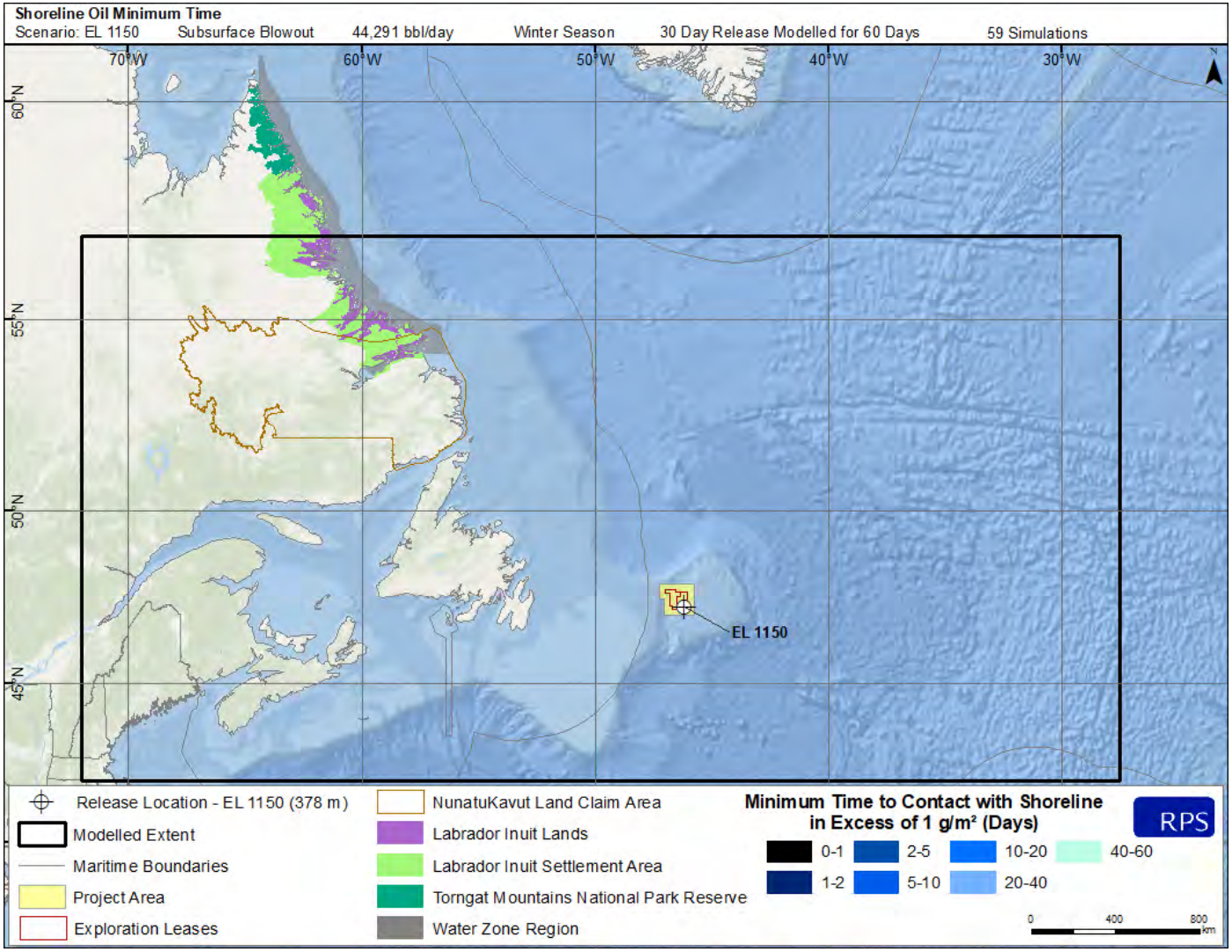

Figure 1-34. Minimum time to threshold exceedance resulting from a subsurface blowout at the EL 1150 example well release site. No shoreline contact was predicted for this scenario.

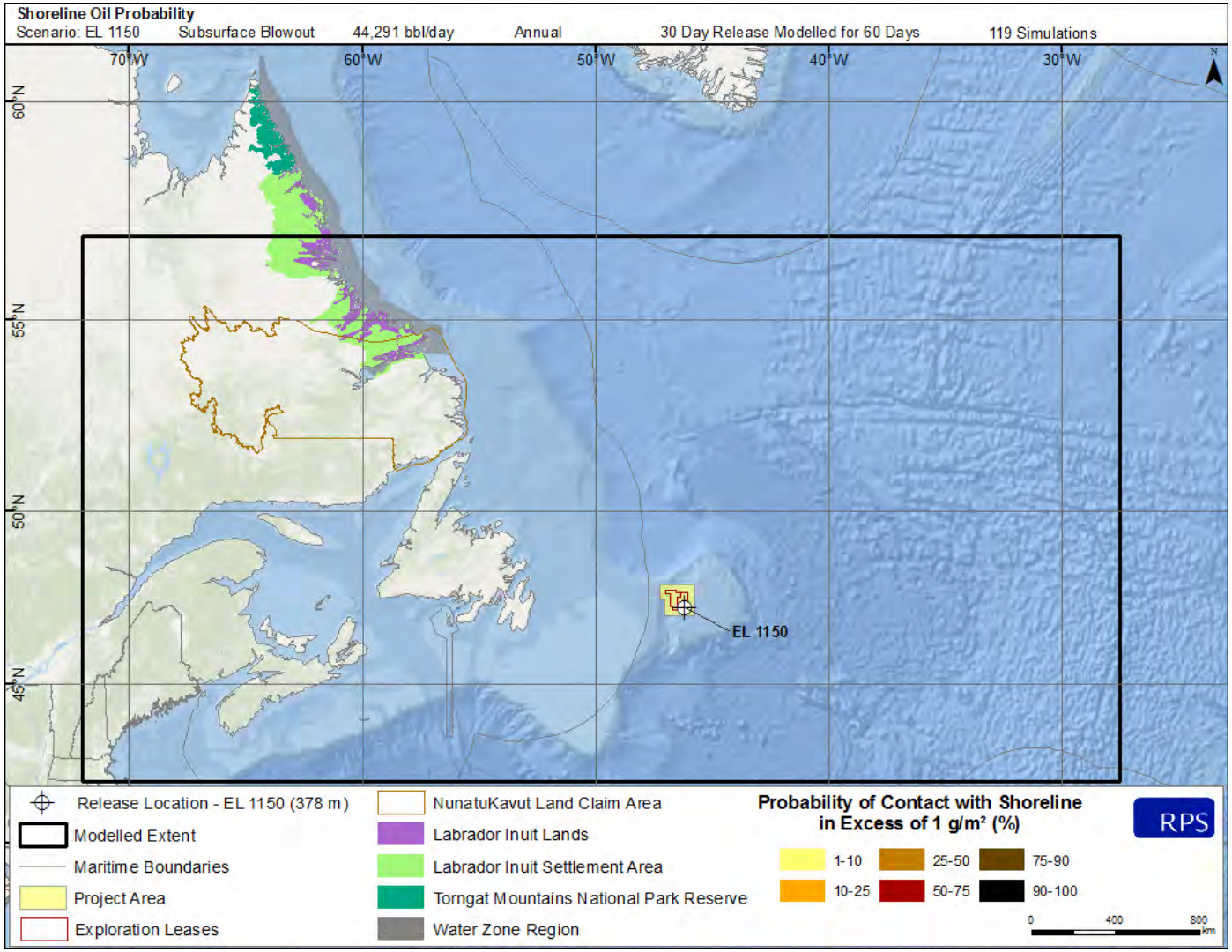

Figure 1-35. Annual probability of shoreline contact exceeding 1 g/m^2 resulting from a subsurface blowout at the EL 1150 example well release site. No shoreline contact was predicted for this scenario.

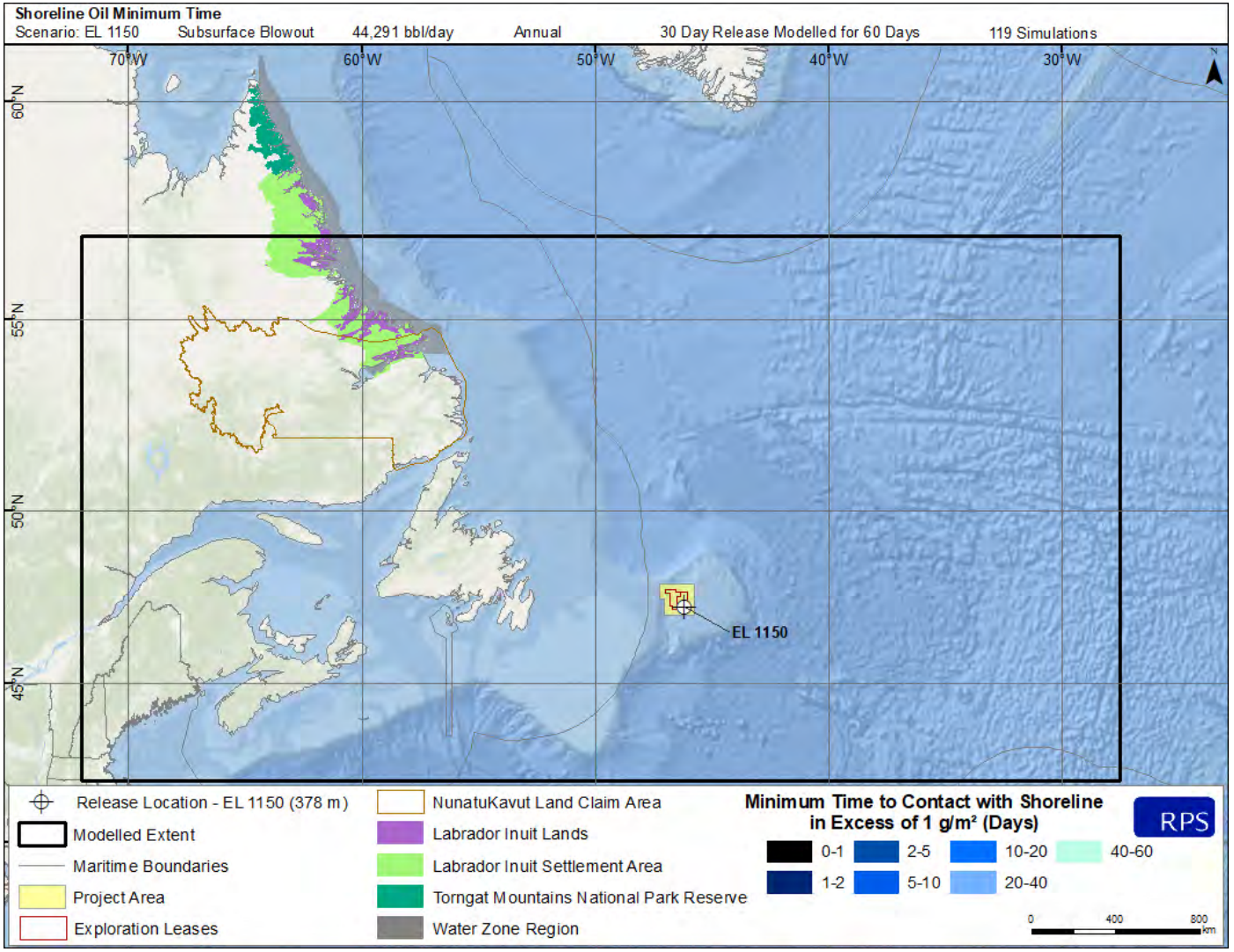

Figure 1-36. Minimum time to threshold exceedance resulting from a subsurface blowout at the EL 1150 example well release site. **No shoreline contact was predicted for this scenario.**

2 Deterministic Analysis Results

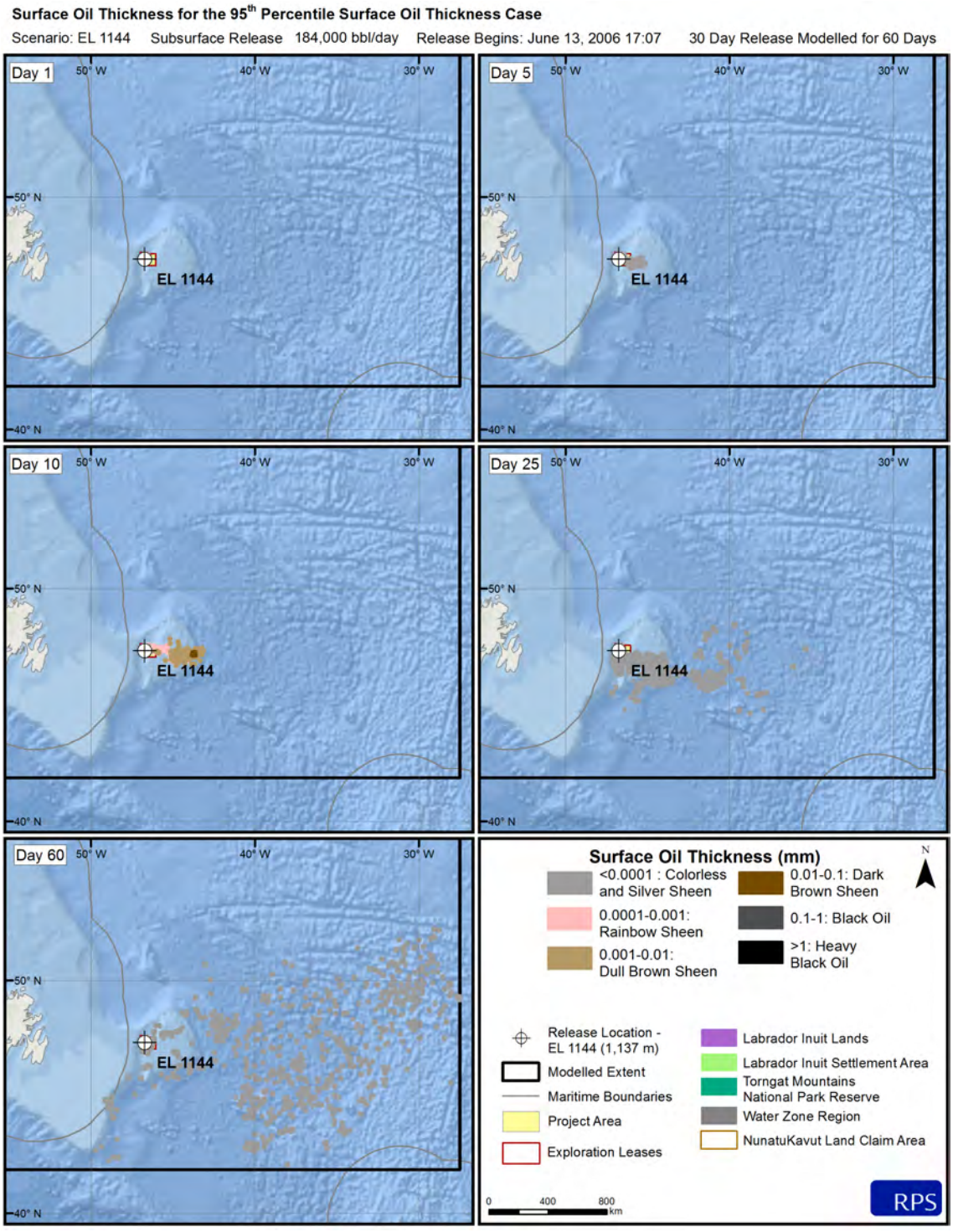

Figure 2-1. Predicted surface oil thickness for the 95th percentile surface oil exposure case at the EL 1144 example well release site at days 1, 5, 10, 25, and 60.

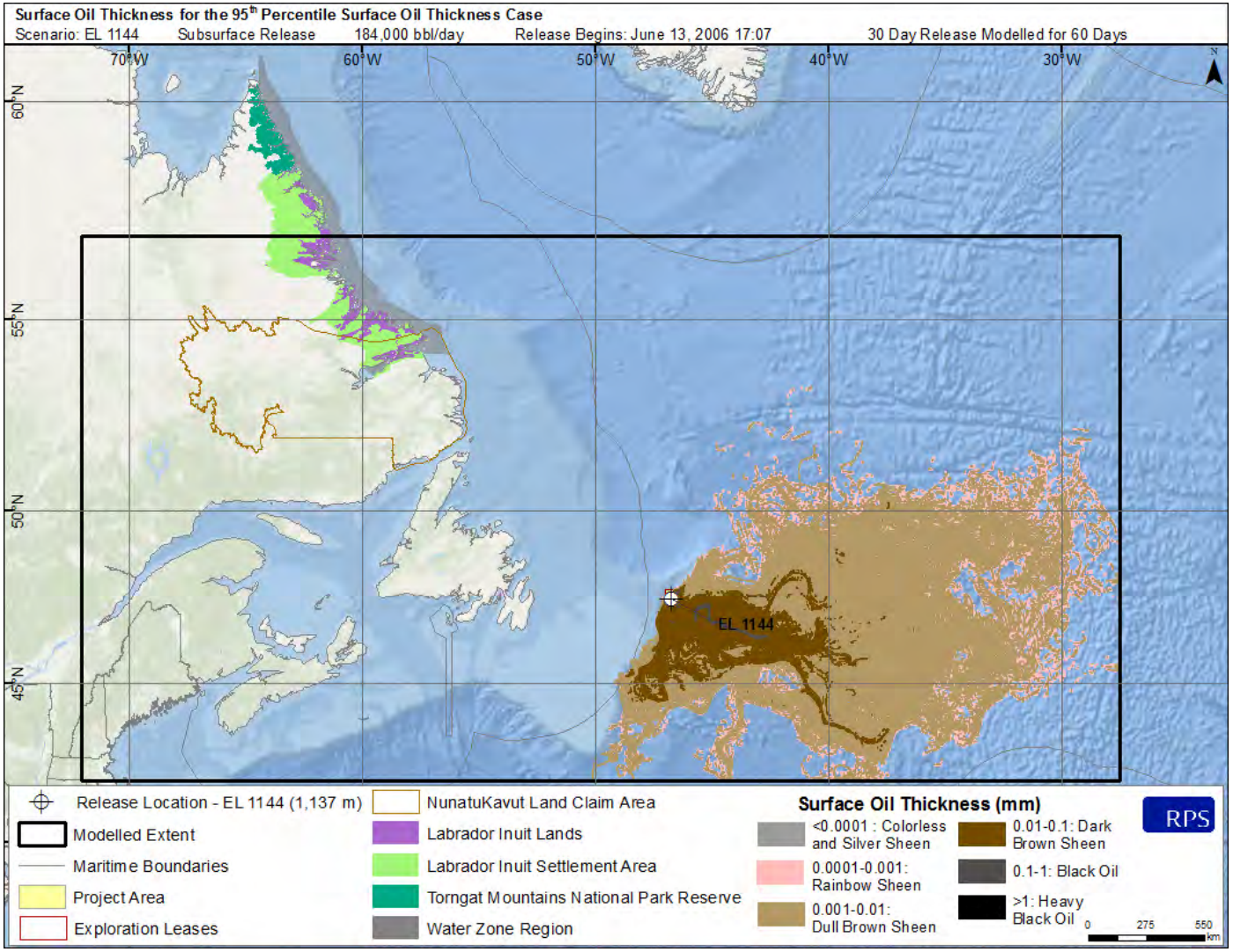

Figure 2-2. Maximum cumulative surface oil thickness for the 95th percentile surface oil exposure case at the EL 1144 example well release site.

2.1 Surface Oil Exposure Cases

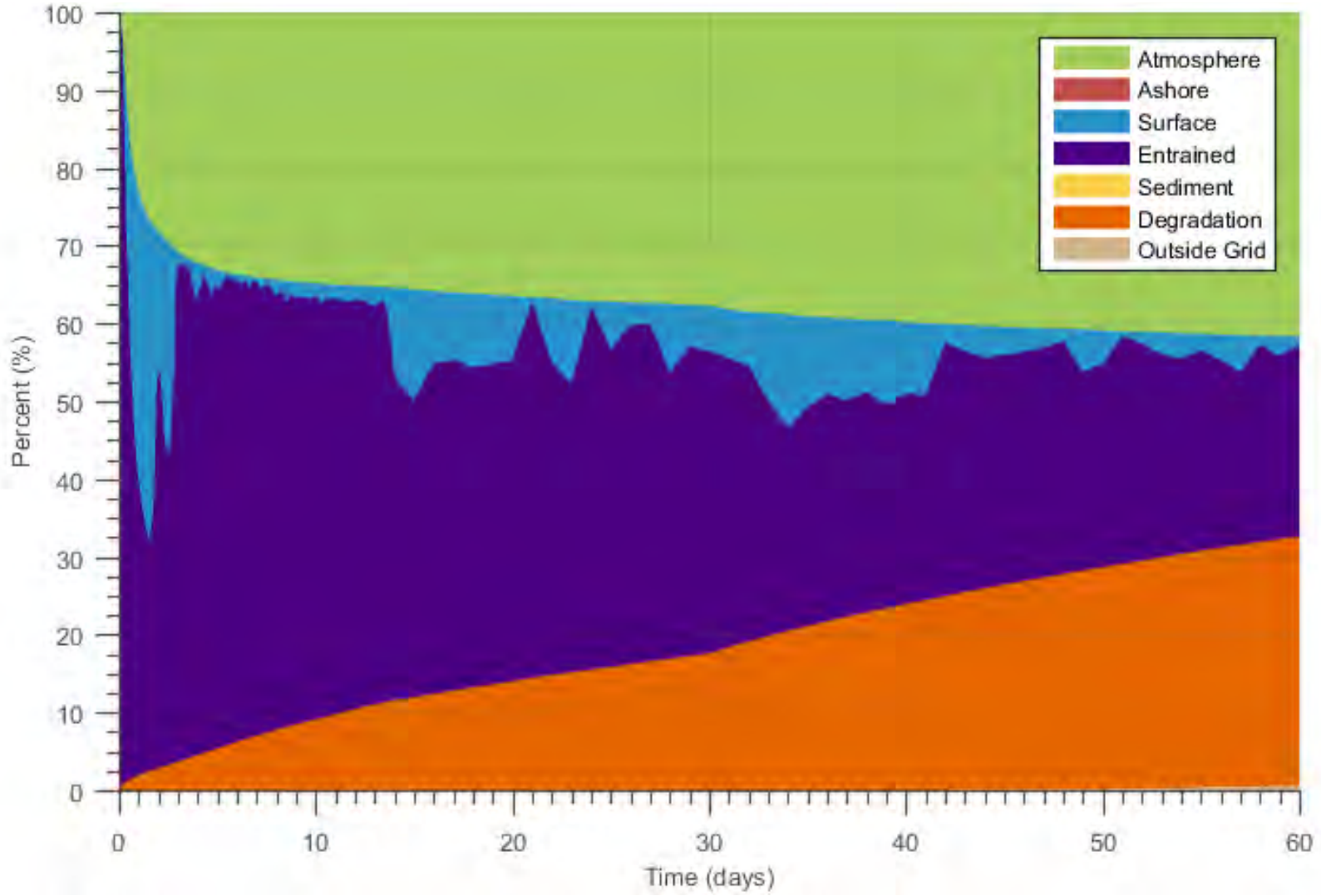

Figure 2-3. Mass balance plots for the 95th percentile surface oil thickness cases at the EL 1144 example well release site.

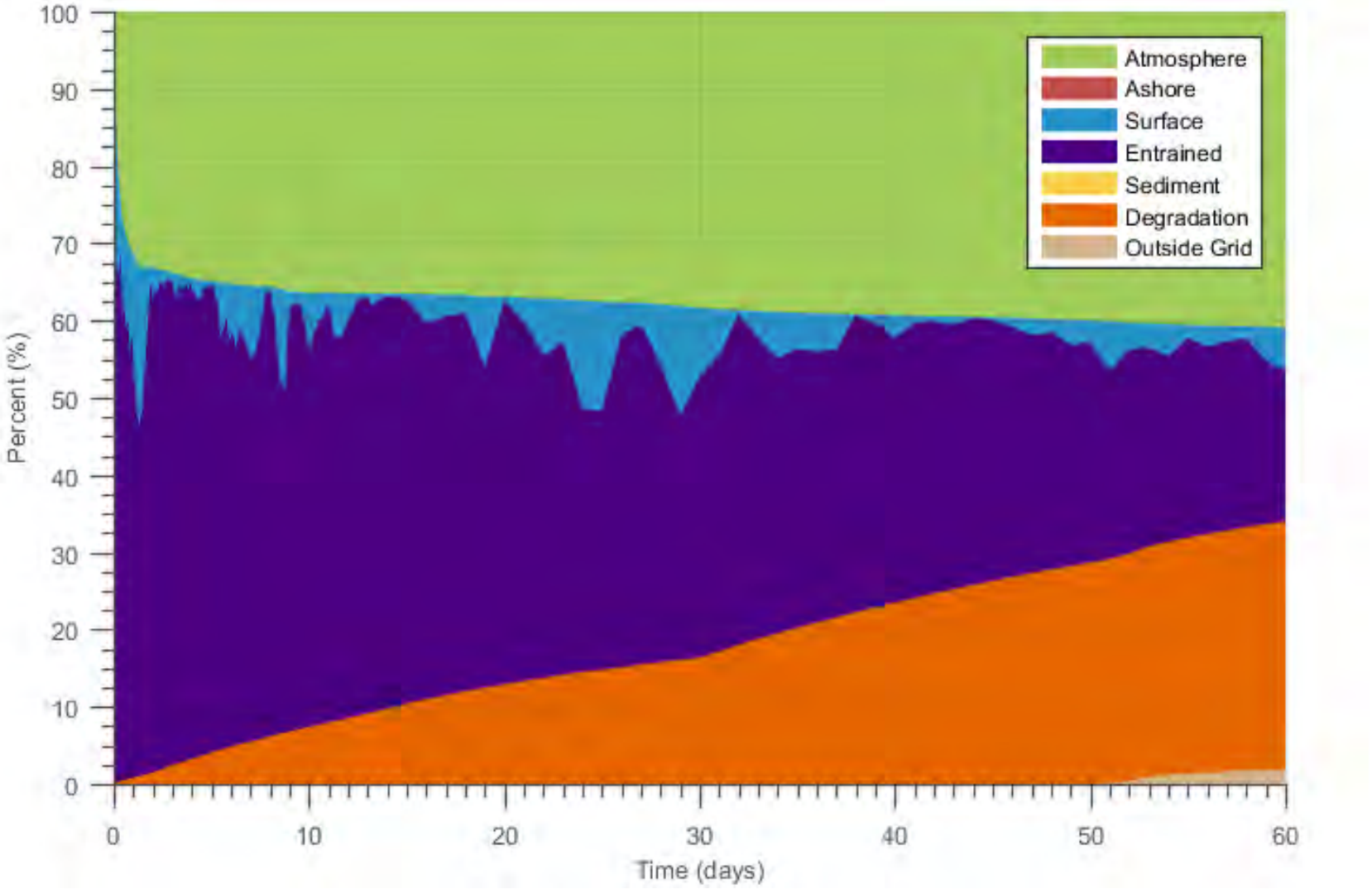

Figure 2-4. Mass balance plots for the 95th percentile surface oil thickness cases at the EL 1150 example well release site.

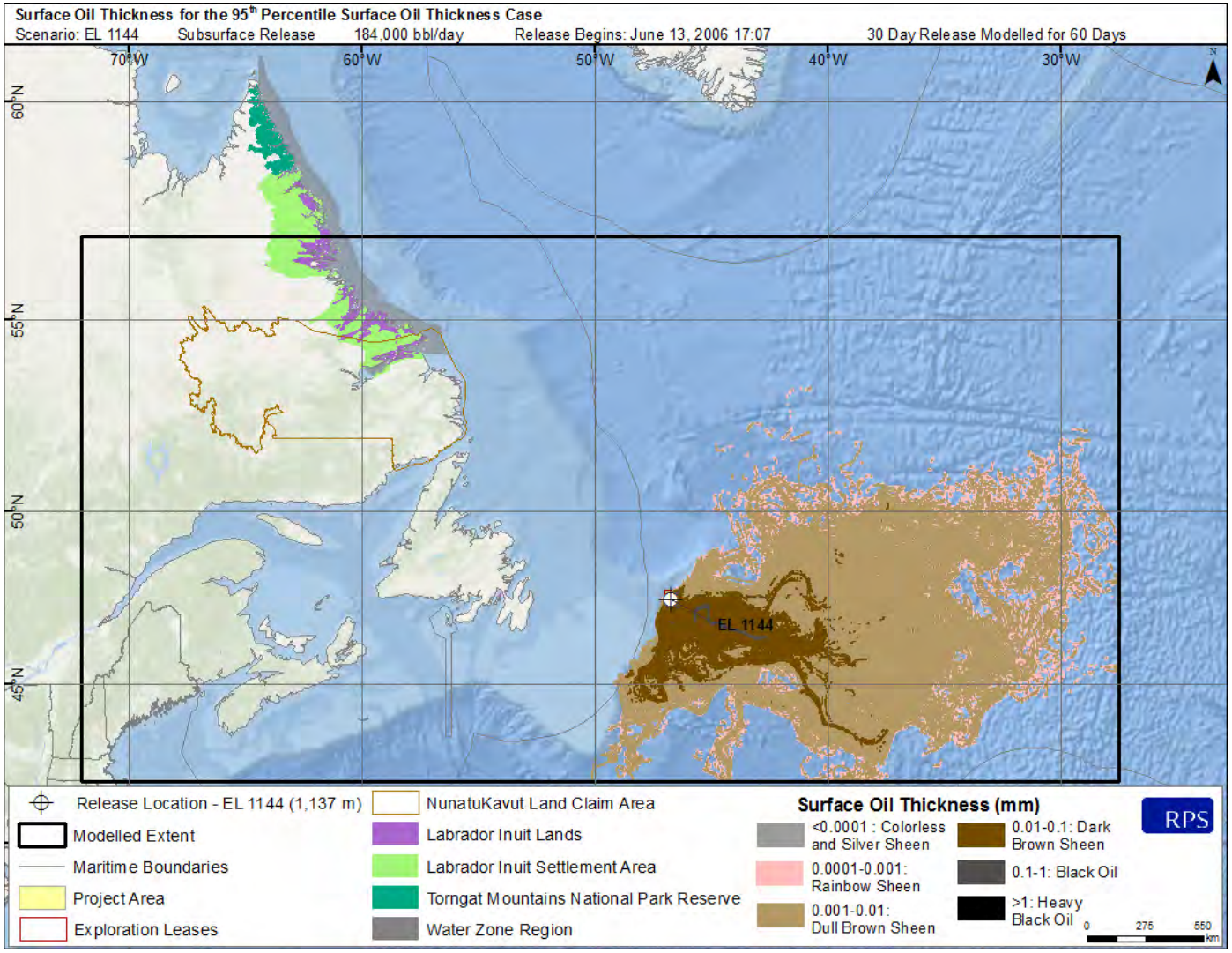

Figure 2-5. Surface oil thickness for the 95th percentile surface oil thickness case at the EL 1144 example well release site.

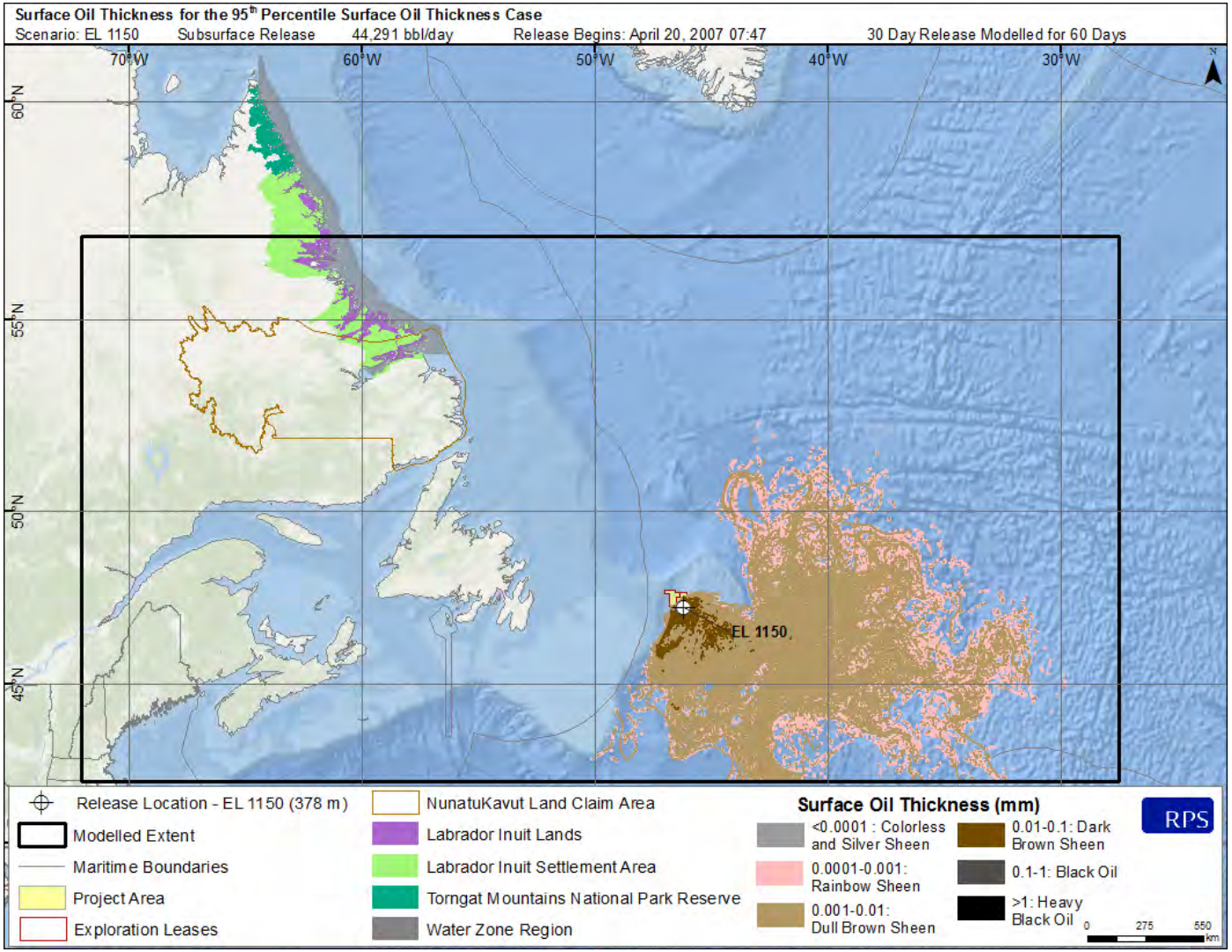

Figure 2-6. Surface oil thickness for the 95th percentile surface oil thickness case at the EL 1150 example well release site.

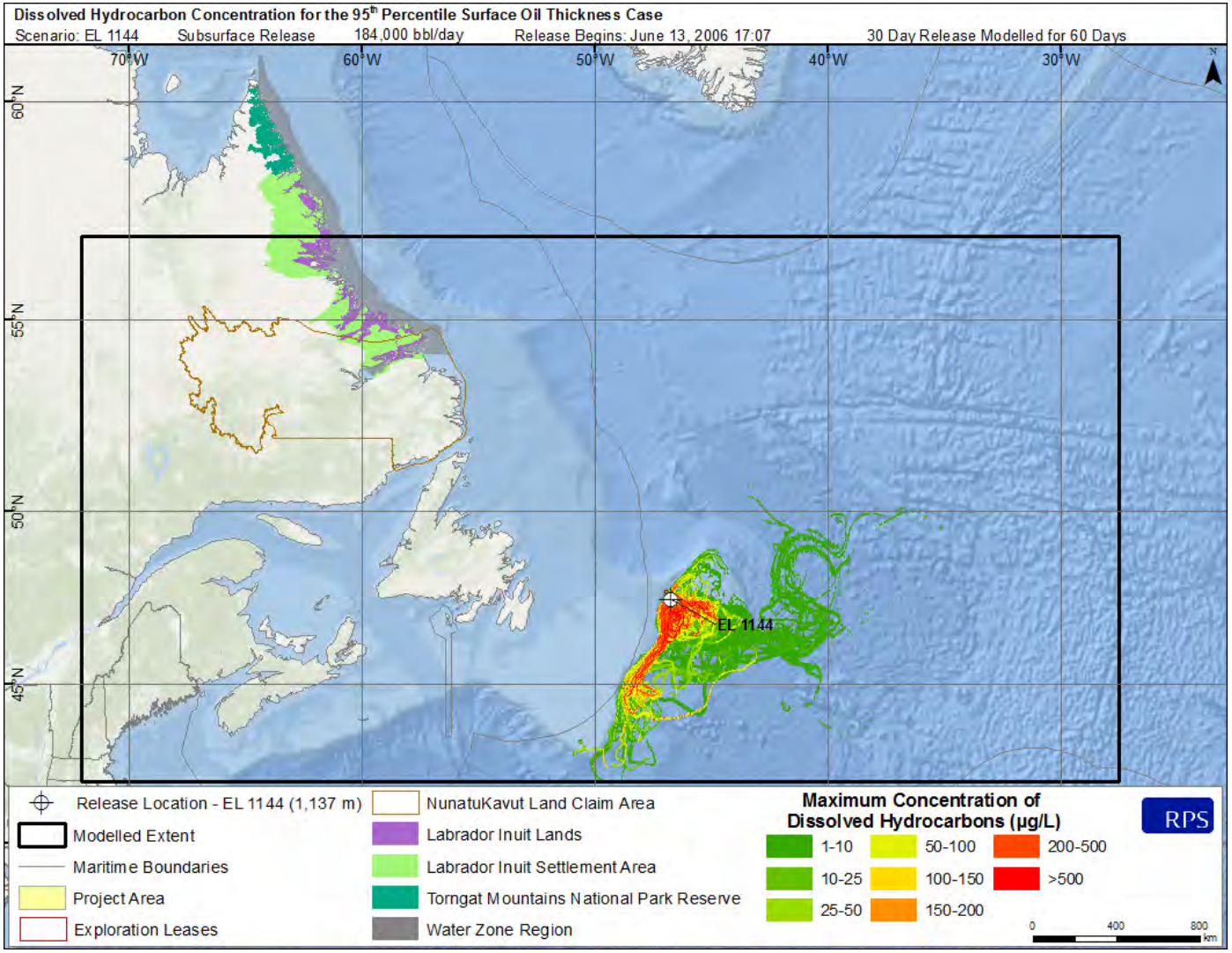

Figure 2-7. Maximum dissolved hydrocarbon concentration at any depth in the water column for the 95th percentile surface oil thickness case at the EL 1144 example well release site.

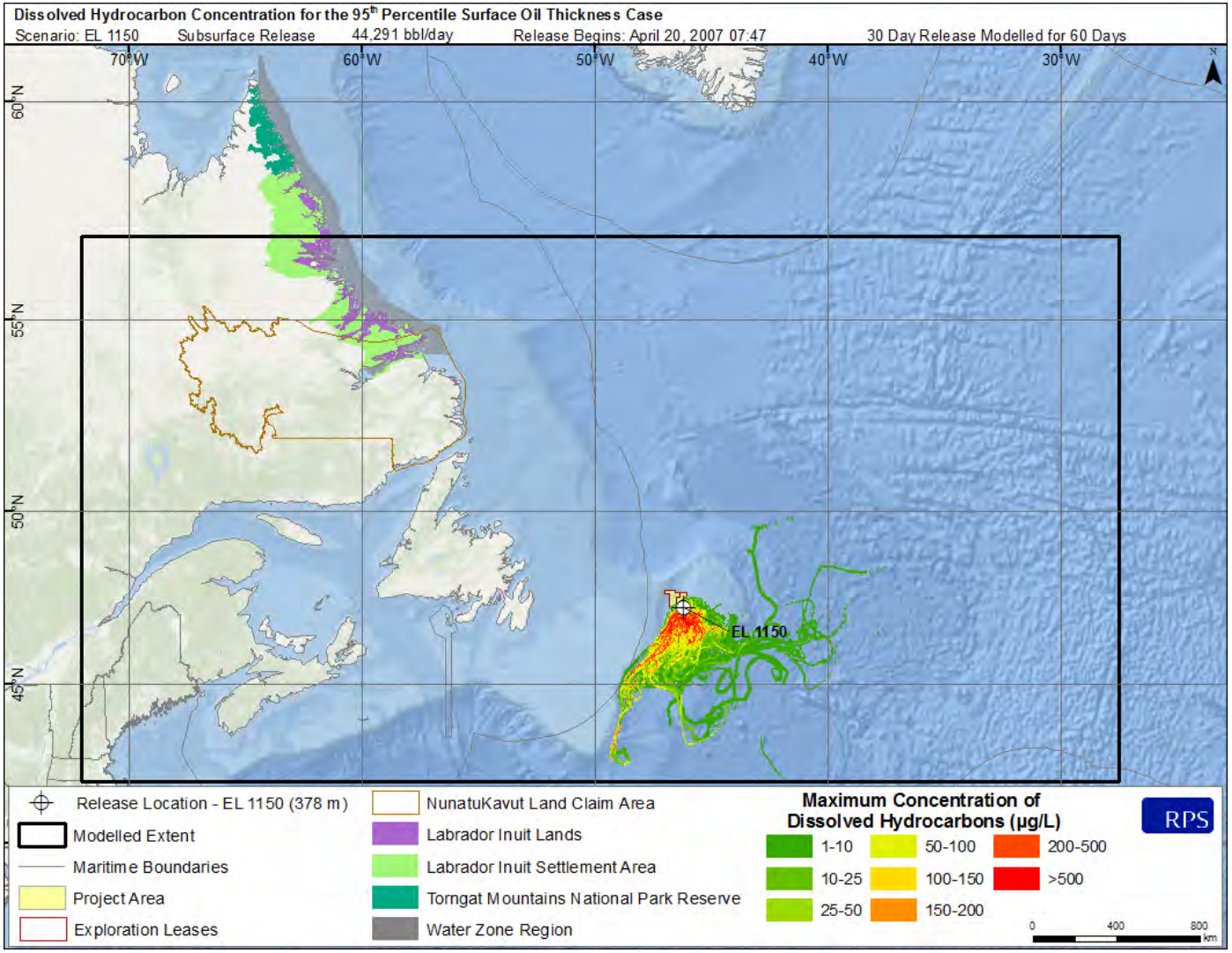

Figure 2-8. Maximum dissolved hydrocarbon concentration at any depth in the water column for the 95th percentile surface oil thickness case at the EL 1150 example well release site.

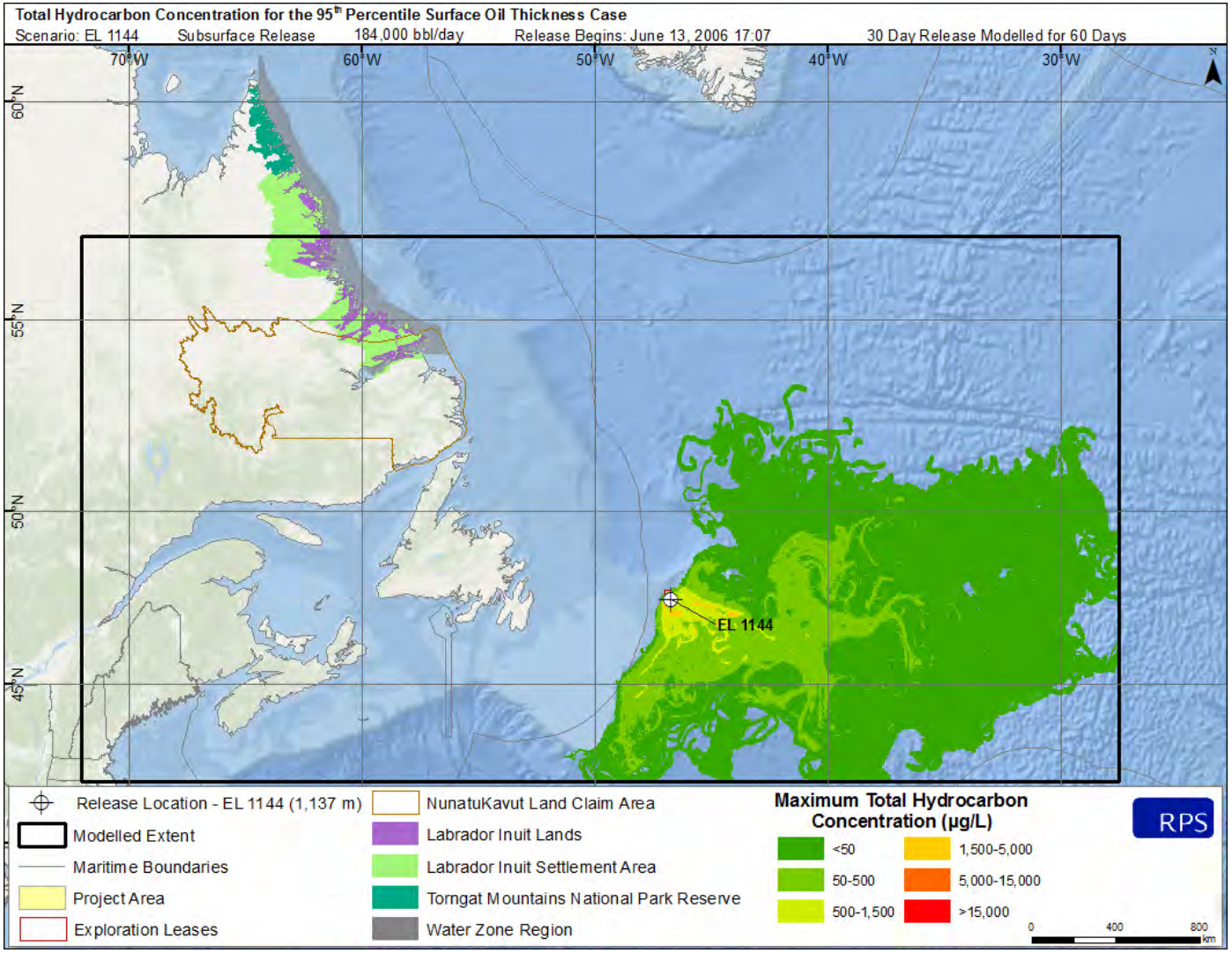

Figure 2-9. Maximum total hydrocarbon concentration (THC) at any depth in the water column for the 95th percentile surface oil thickness case at the EL 1144 example well release site.

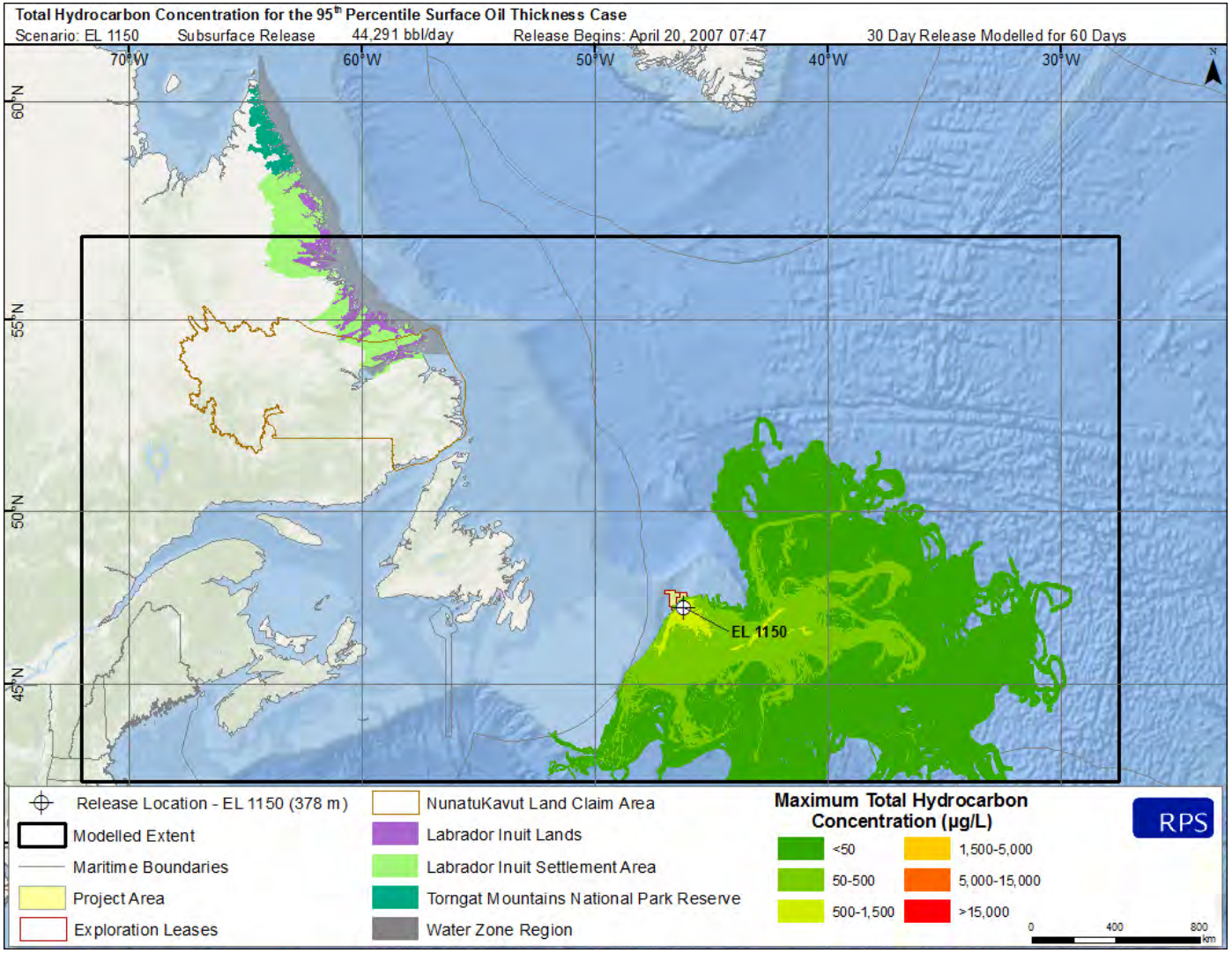

Figure 2-10. Maximum total hydrocarbon concentration (THC) at any depth in the water column for the 95th percentile surface oil thickness case at the EL 1150 example well release site.

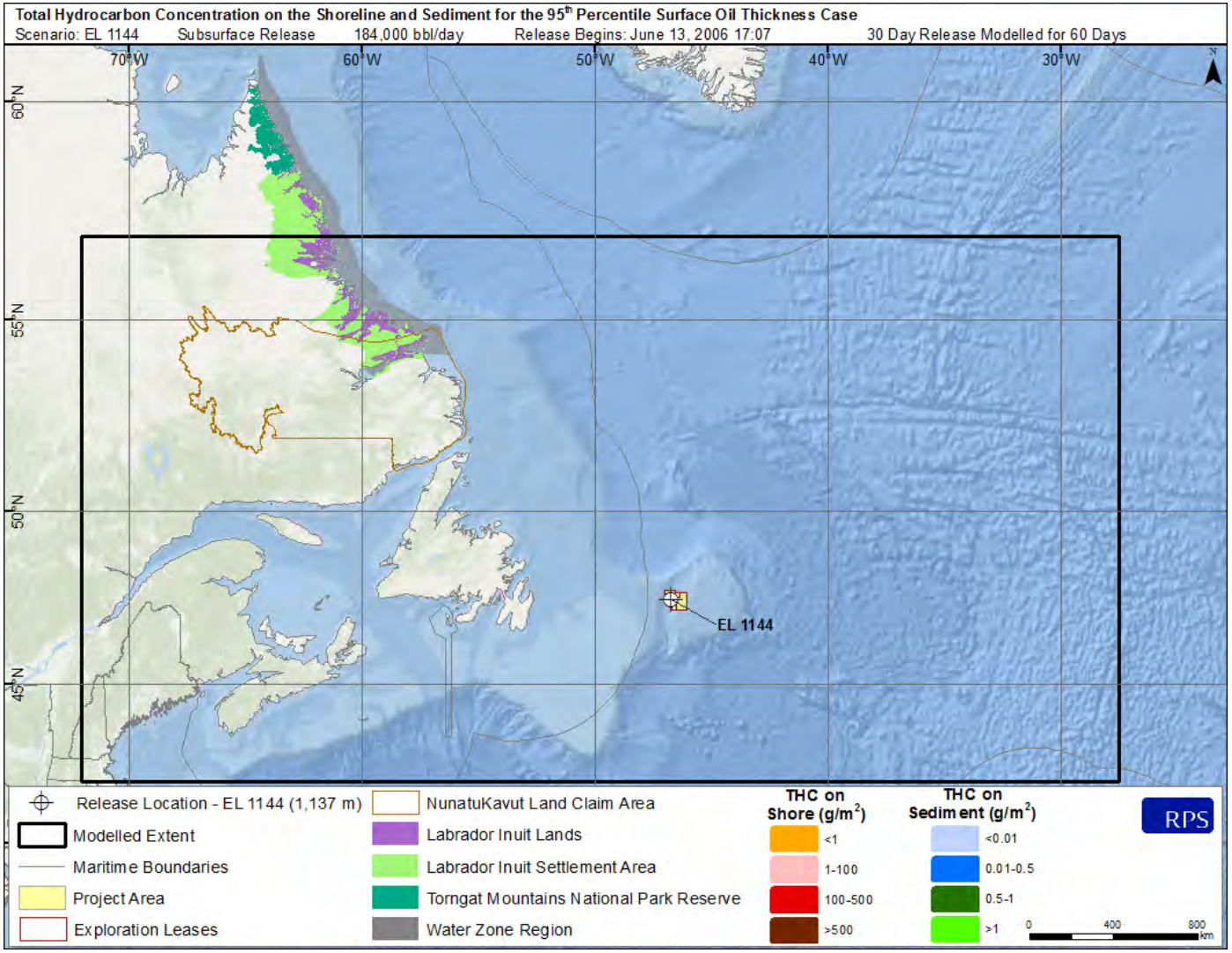

Figure 2-11. Total hydrocarbon concentration (THC) on the shore and sediment for the 95th percentile surface oil thickness case at the EL 1144 example well release site. No shoreline contact was predicted for this scenario.

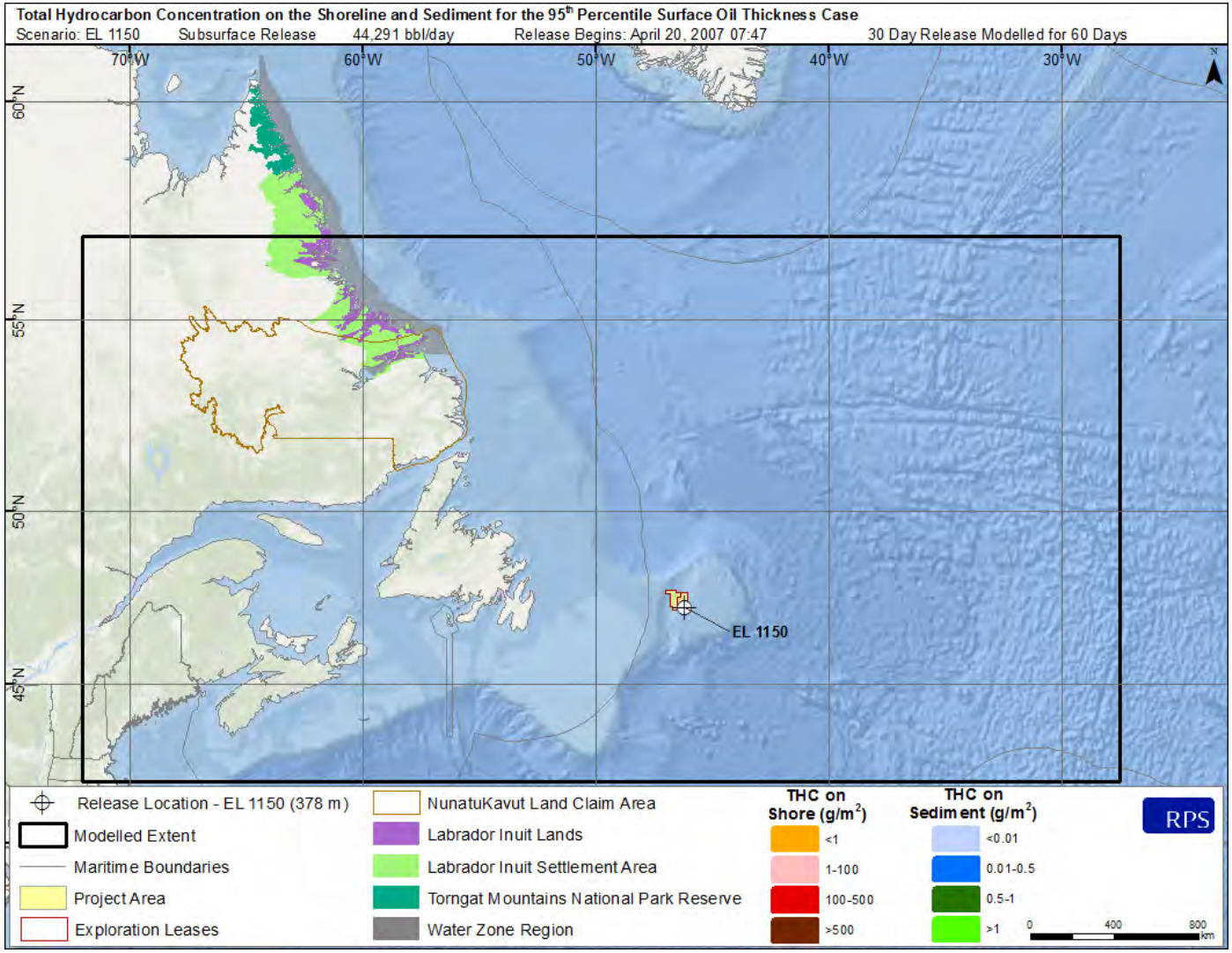

Figure 2-12. Total hydrocarbon concentration (THC) on the shore and sediment for the 95th percentile surface oil thickness case at the EL 1150 example well release site. No shoreline contact was predicted for this scenario.

2.2 Water Column Exposure Cases

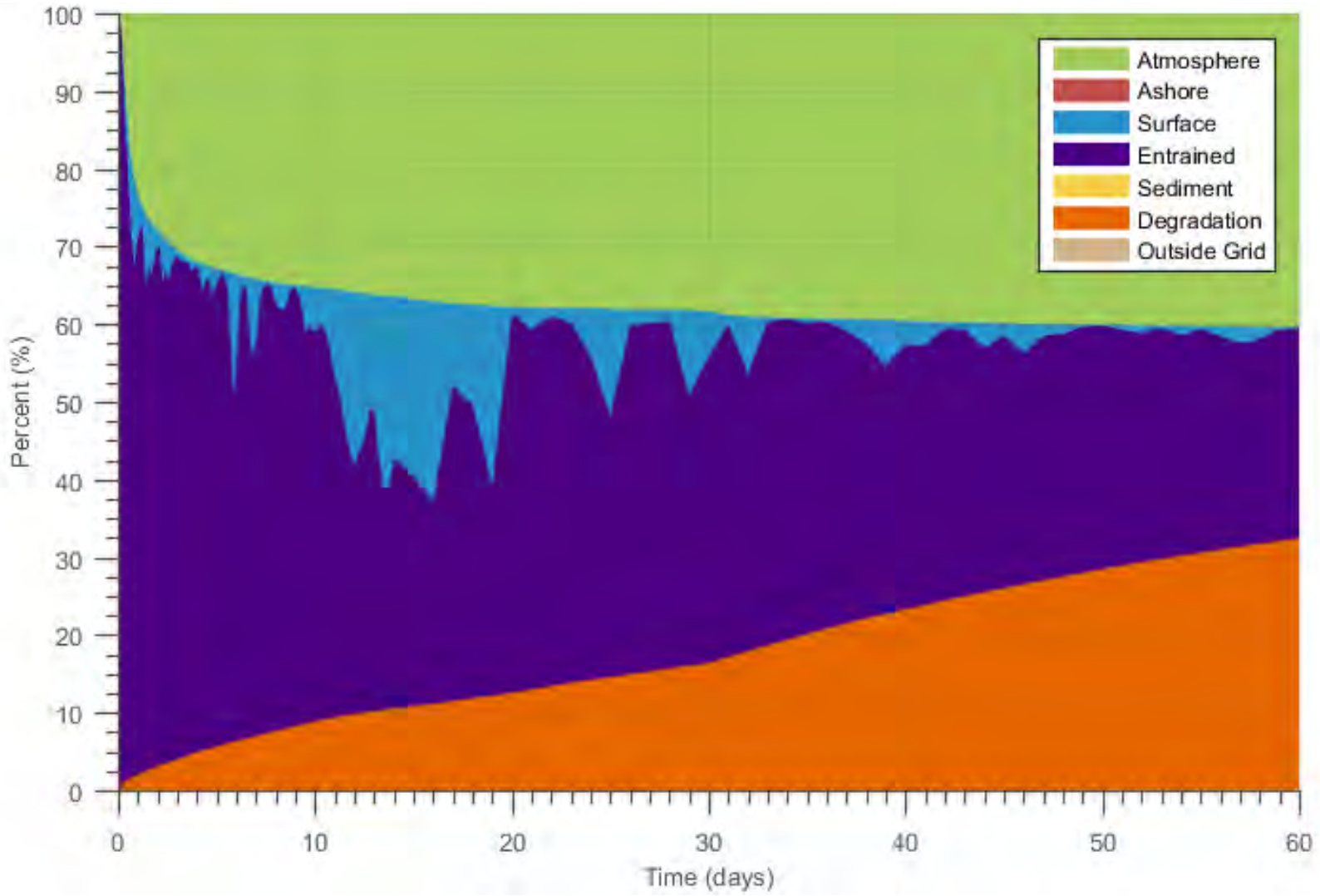

Figure 2-13. Mass balance plots of the 95th percentile water column contamination case at the EL 1144 example well release site.

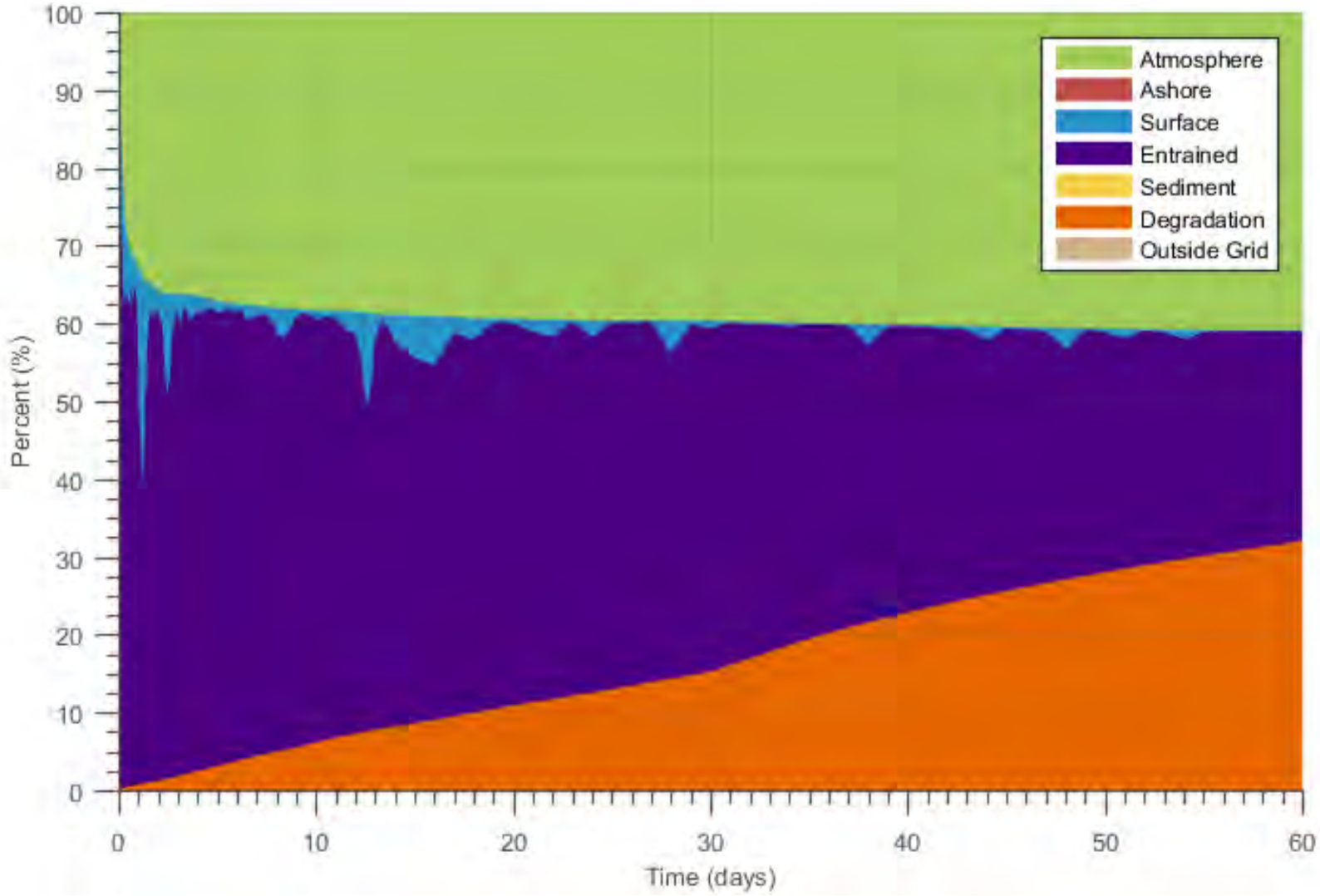

Figure 2-14. Mass balance plots of the 95th percentile water column contamination case at the EL 1150 example well release site.

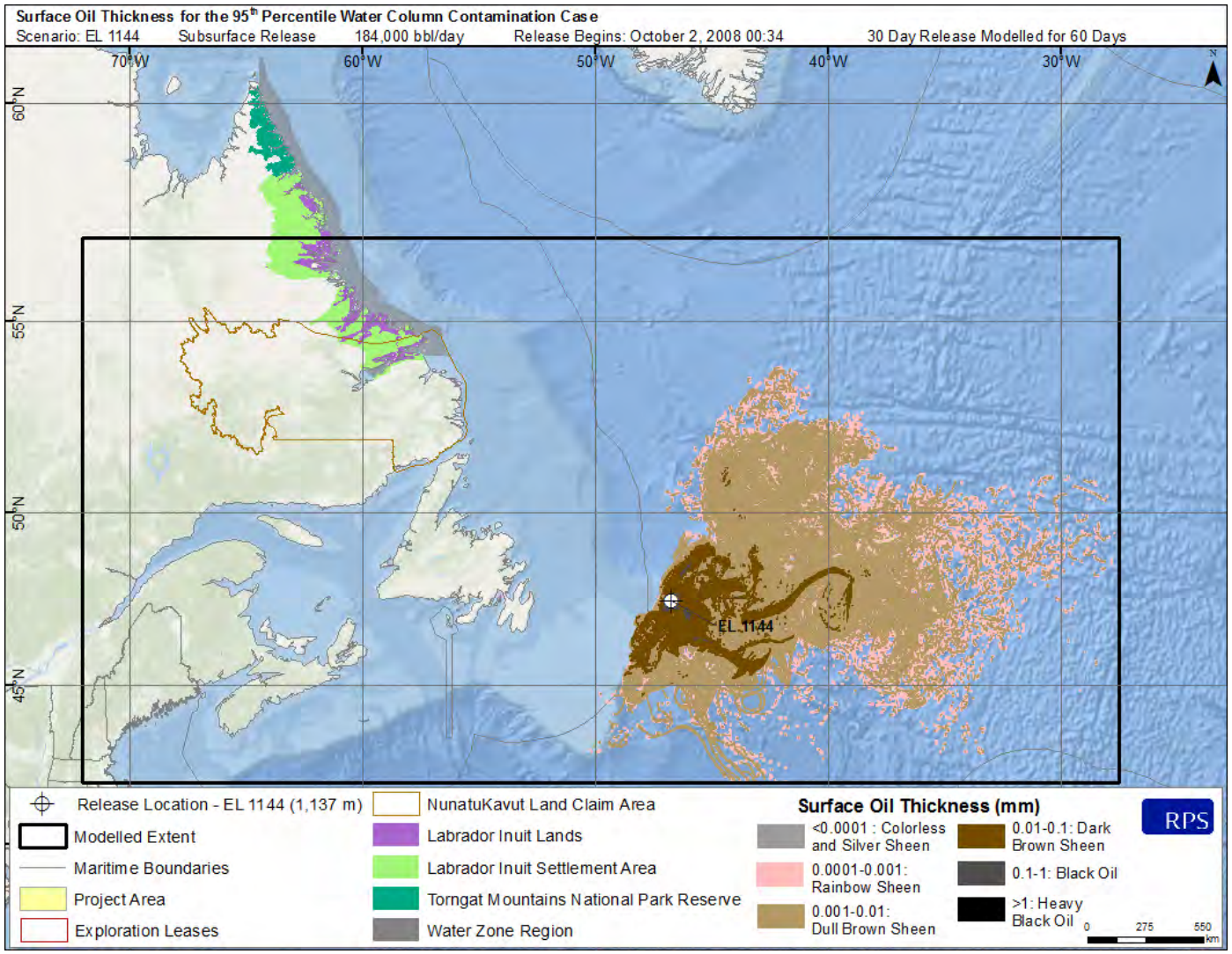

Figure 2-15. Surface oil thickness for the 95th percentile water column contamination case resulting from a subsurface blowout at the EL 1144 example well release site.

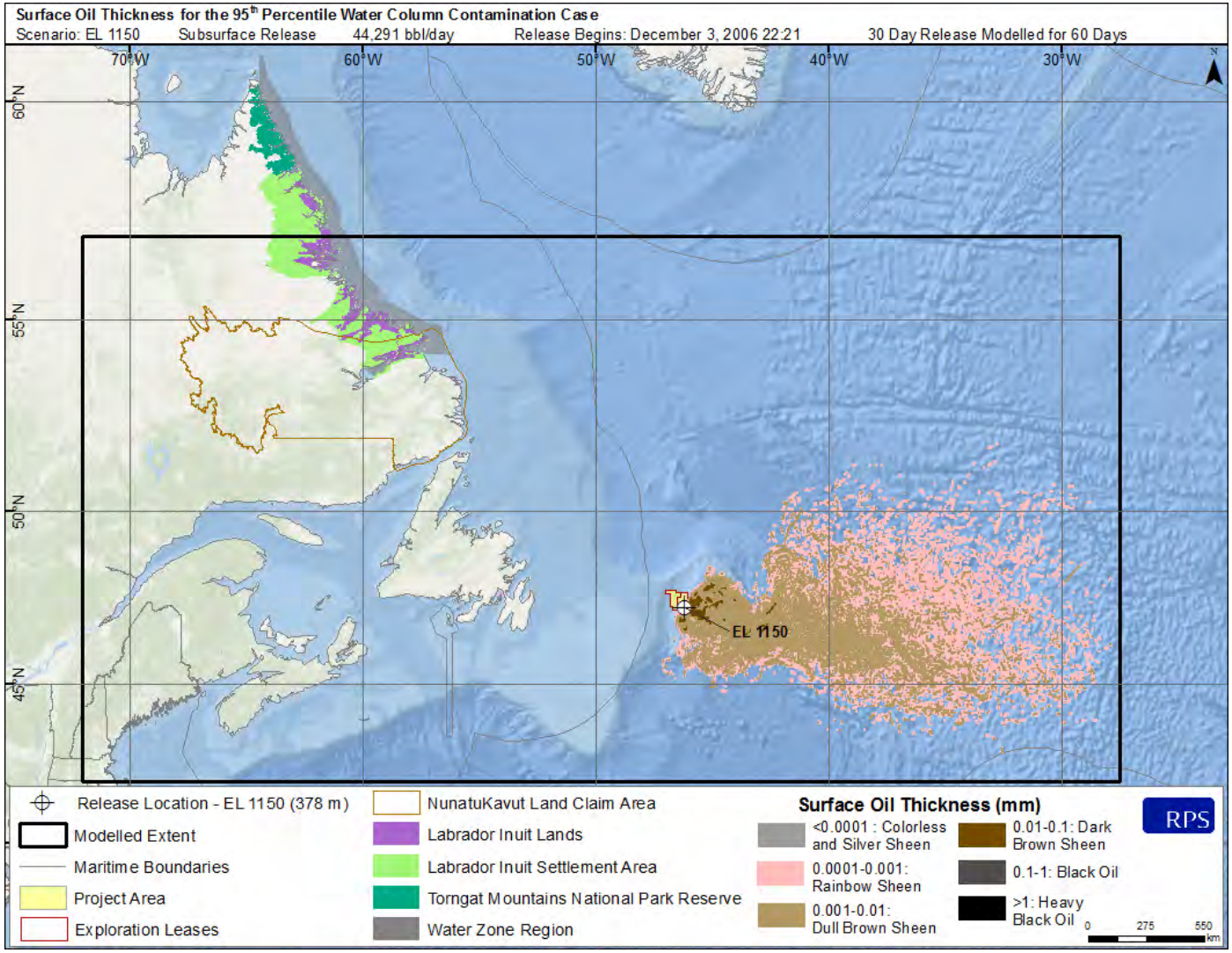

Figure 2-16. Surface oil thickness for the 95th percentile water column contamination case resulting from a subsurface blowout at the EL 1150 example well release site.

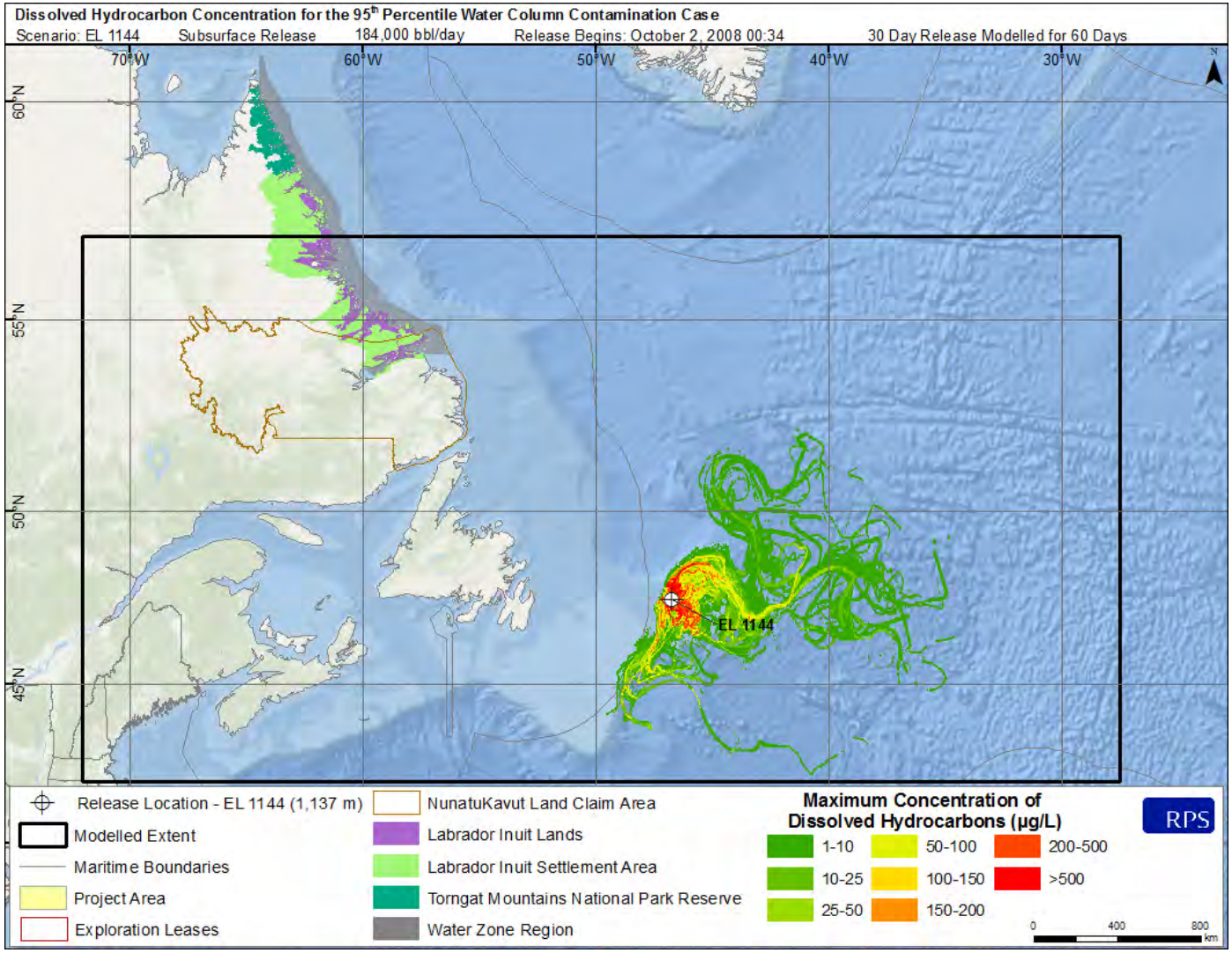

Figure 2-17. Maximum dissolved hydrocarbons at any depth in the water column for the 95th percentile water column contamination case from a subsurface blowout at the EL 1144 example well release site.

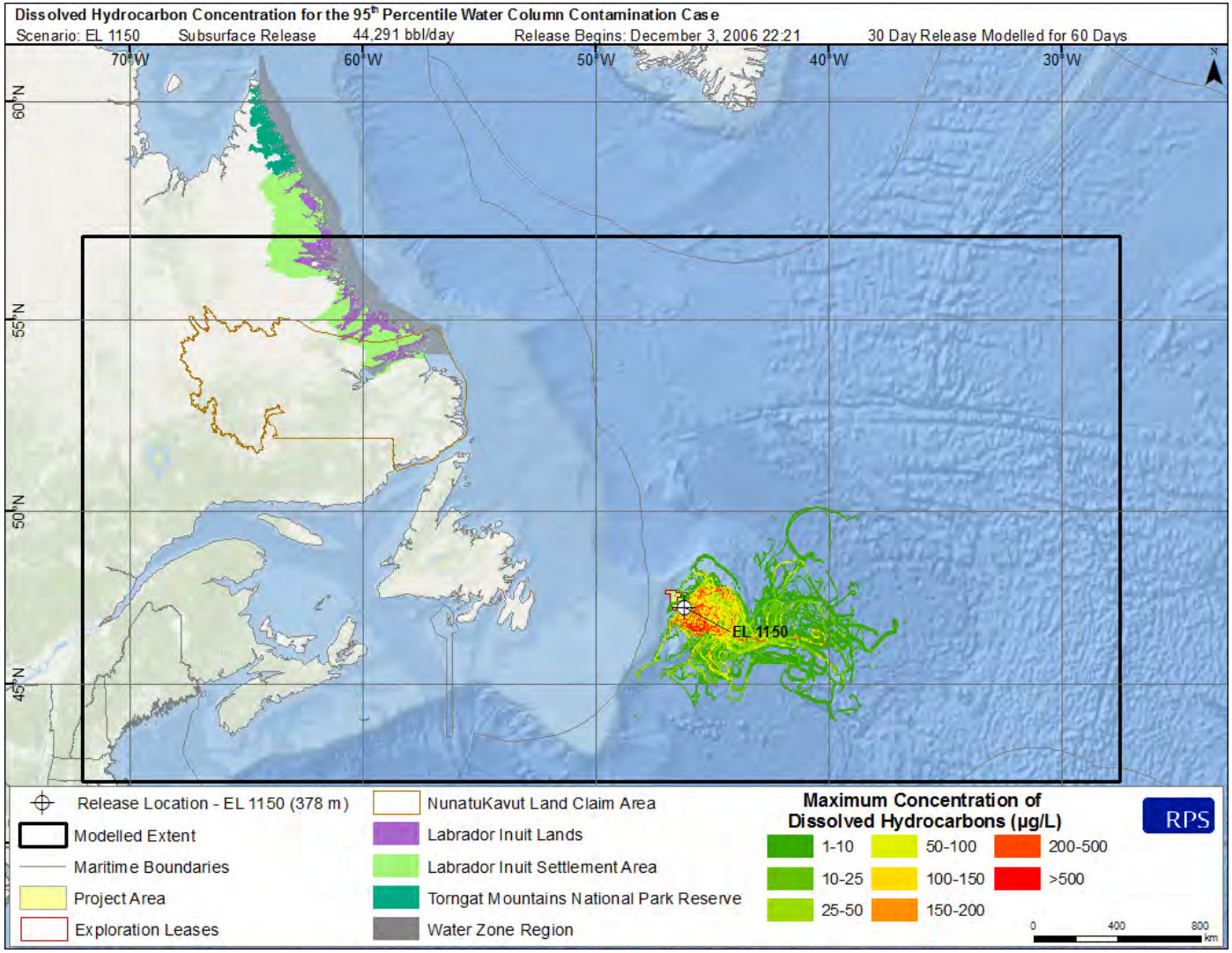

Figure 2-18. Maximum dissolved hydrocarbons at any depth in the water column for the 95th percentile water column contamination case from a subsurface blowout at the EL 1150 example well release site.

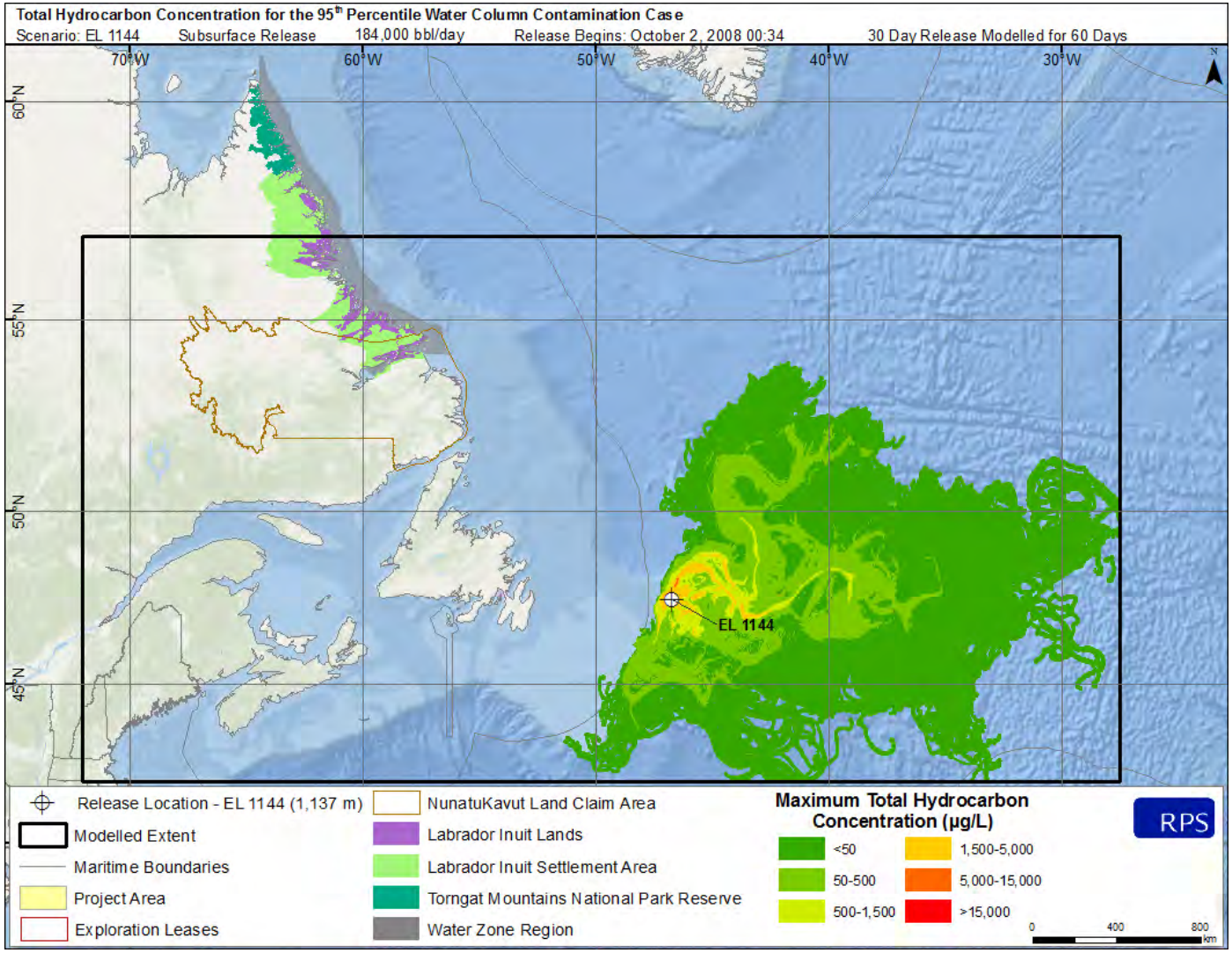

Figure 2-19. Maximum total hydrocarbon concentration (THC) at any depth in the water column for the 95th percentile water column contamination case from a subsurface blowout at the EL 1144 example well release site.

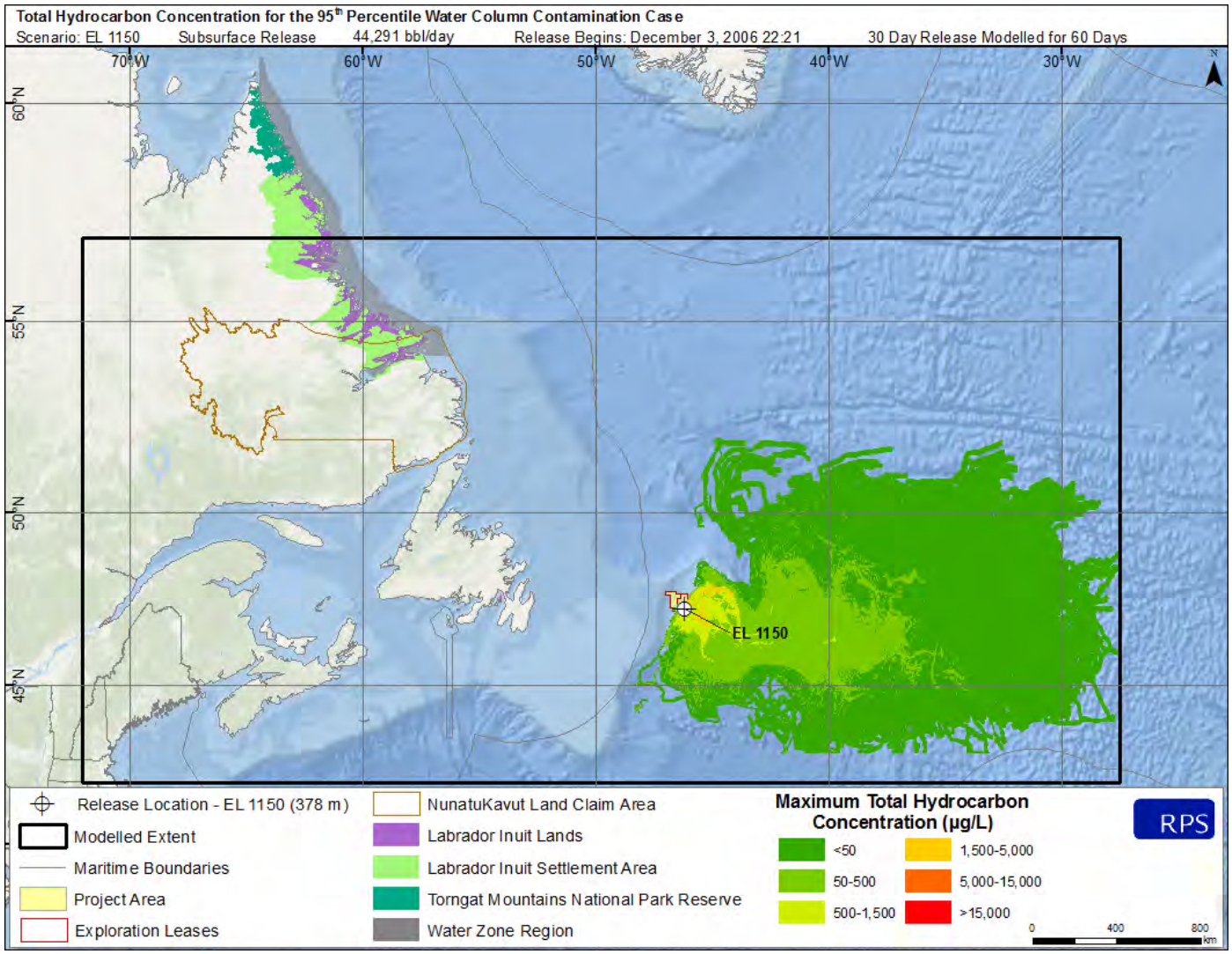

Figure 2-20. Maximum total hydrocarbon concentration (THC) at any depth in the water column for the 95th percentile water column contamination case from a subsurface blowout at the EL 1150 example well release site

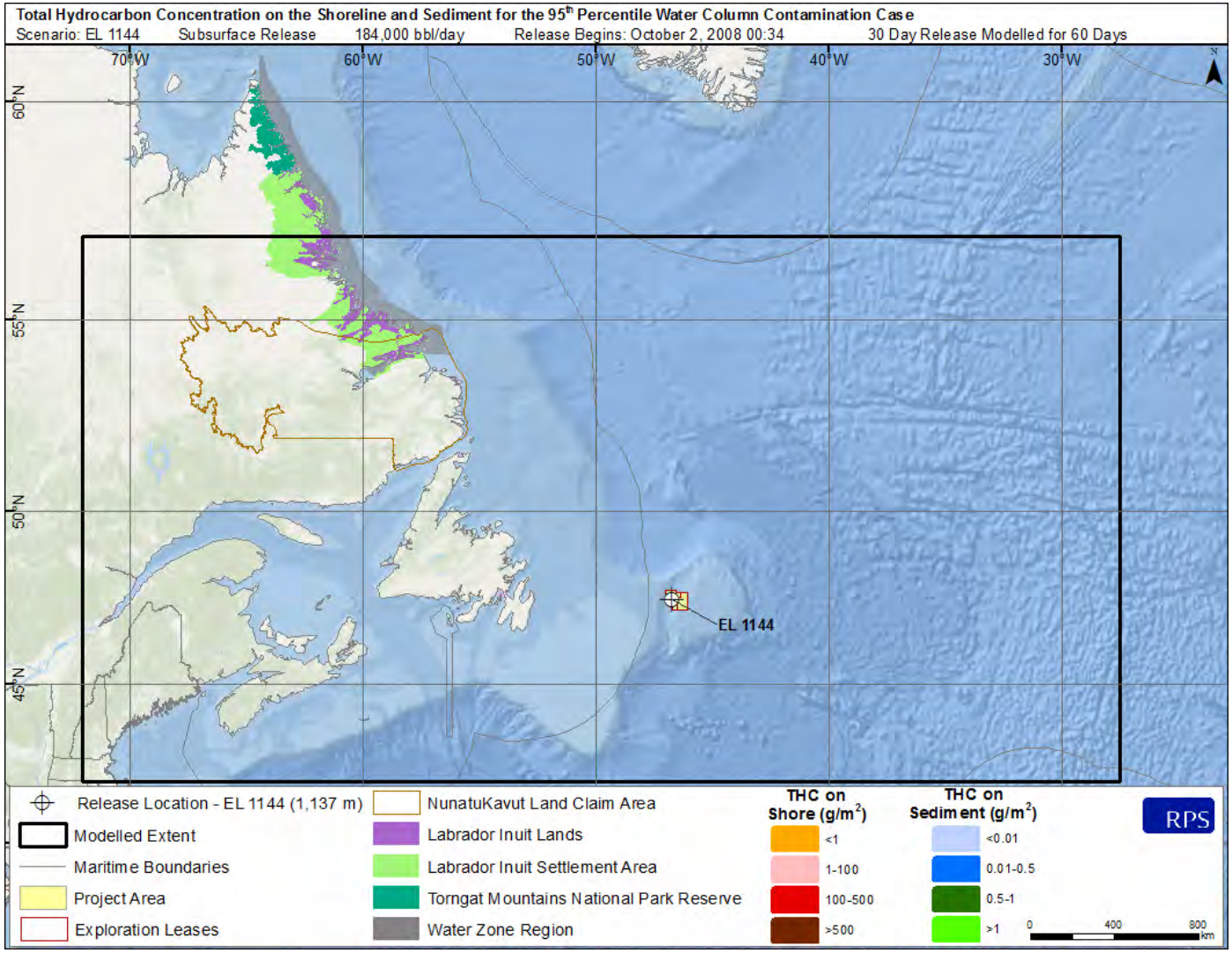

Figure 2-21. Total hydrocarbon concentration (THC) on the shore and sediment for the 95th percentile water column contamination case from a subsurface blowout at the EL 1144 example well release site. No shoreline contact was predicted for this scenario.

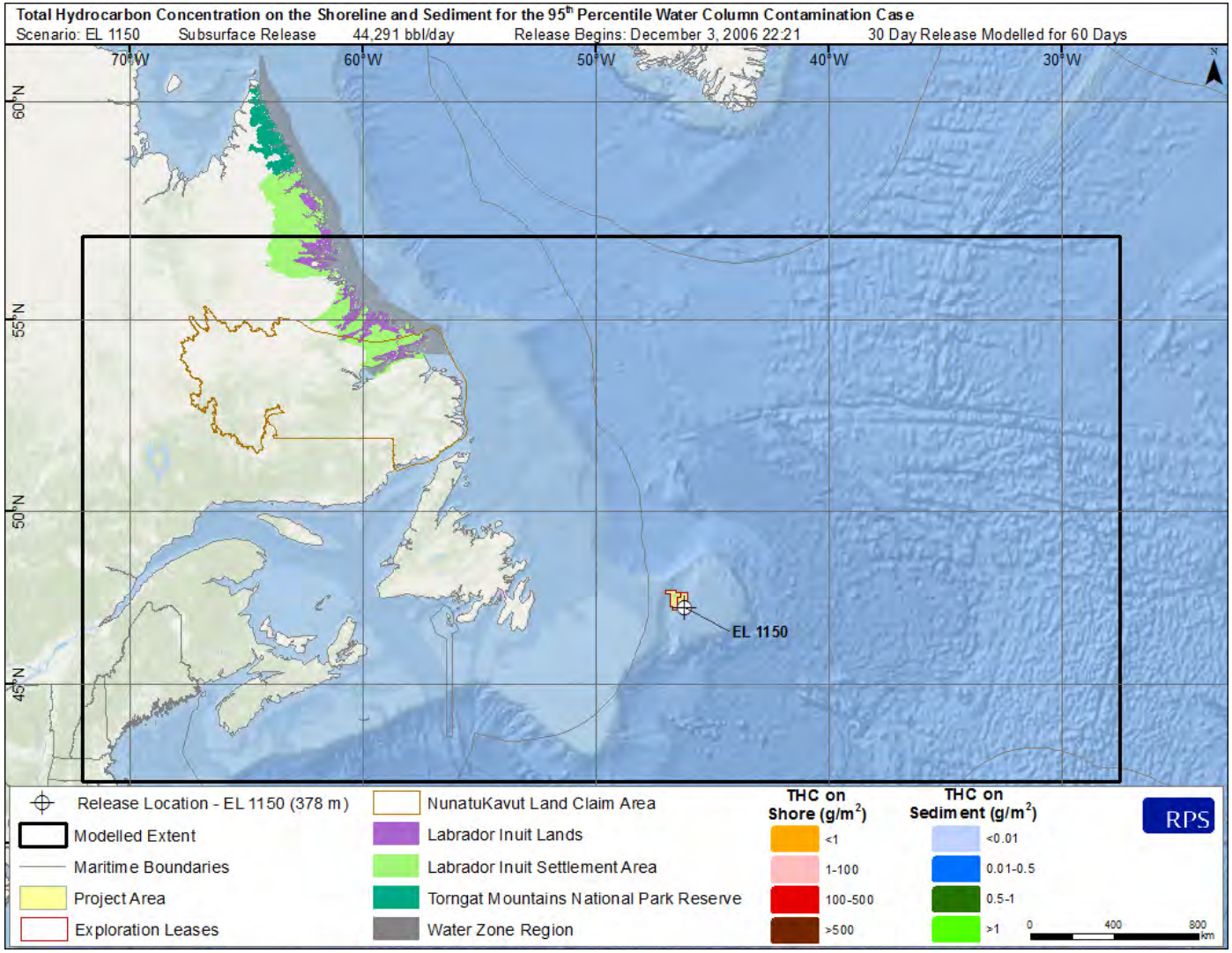

Figure 2-22. Total hydrocarbon concentration (THC) on the shore and sediment for the 95th percentile water column contamination case from a subsurface blowout at the EL 1150 example well release site. No shoreline contact was predicted for this scenario.

2.3 Shoreline Exposure Case

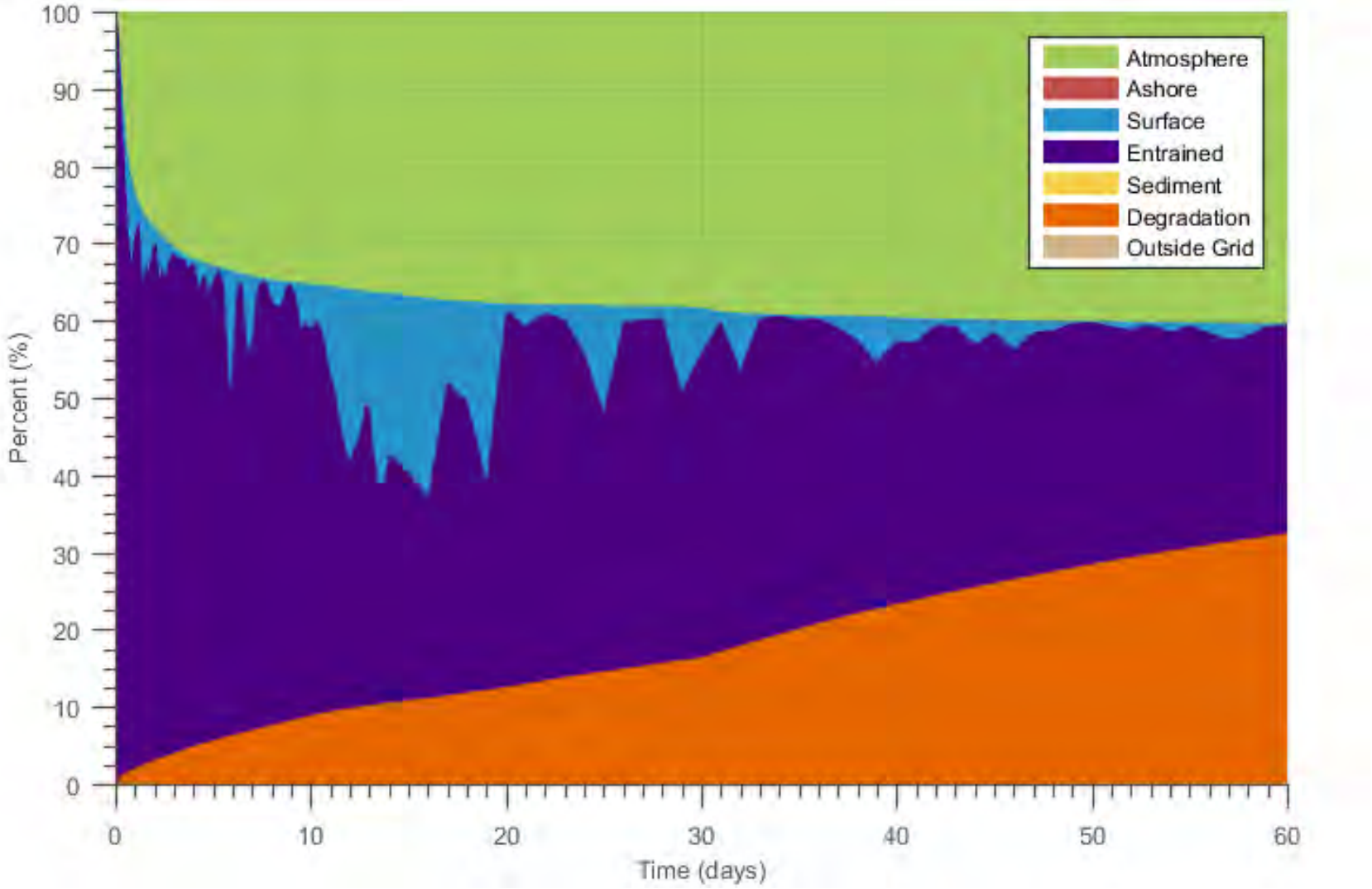

Figure 2-23. Mass balance plot of the 99th percentile contact with shoreline case at the EL 1144 example well release site.

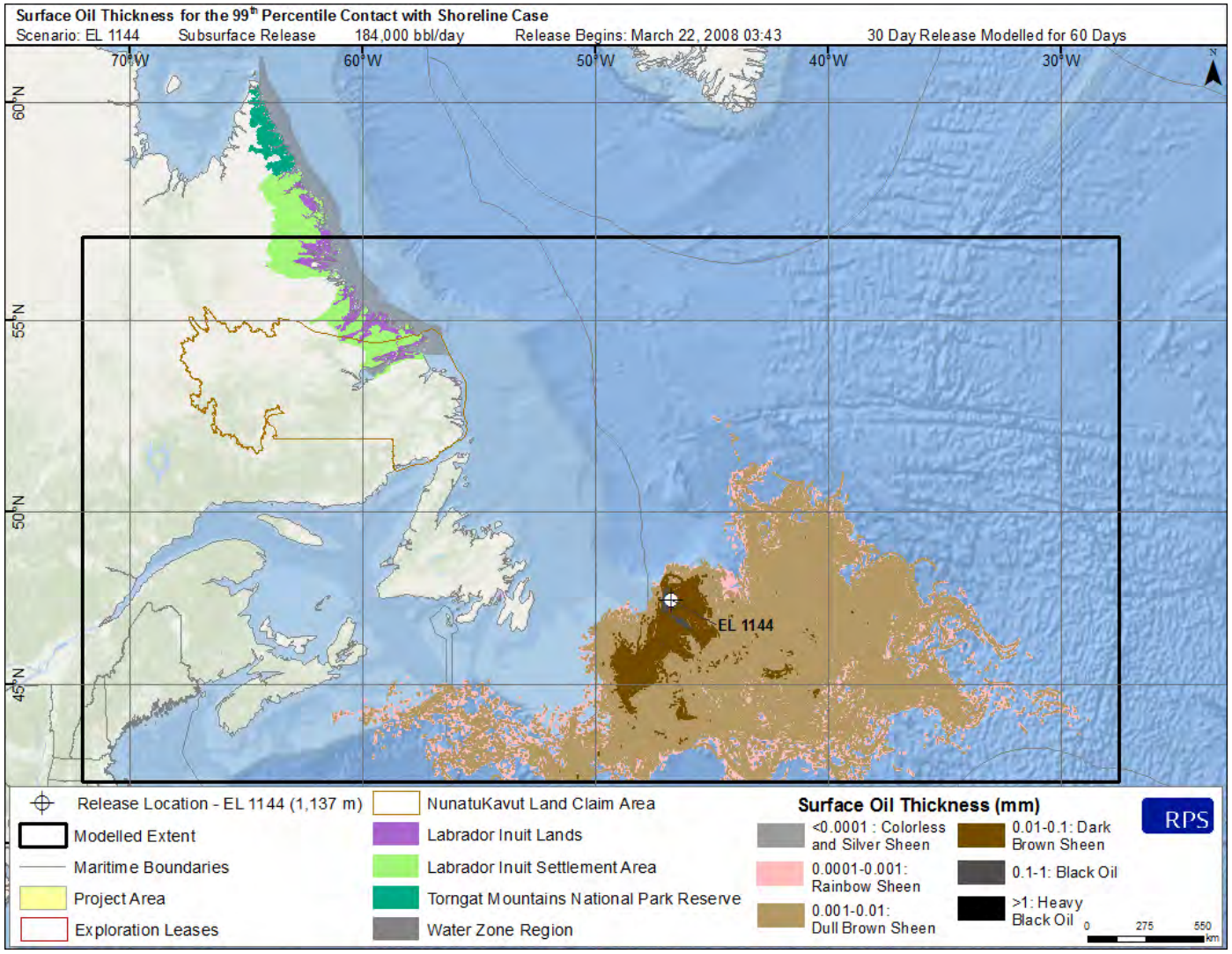

Figure 2-24. Surface oil thickness for the 99th percentile contact with shoreline case at the EL 1144 example well release site.

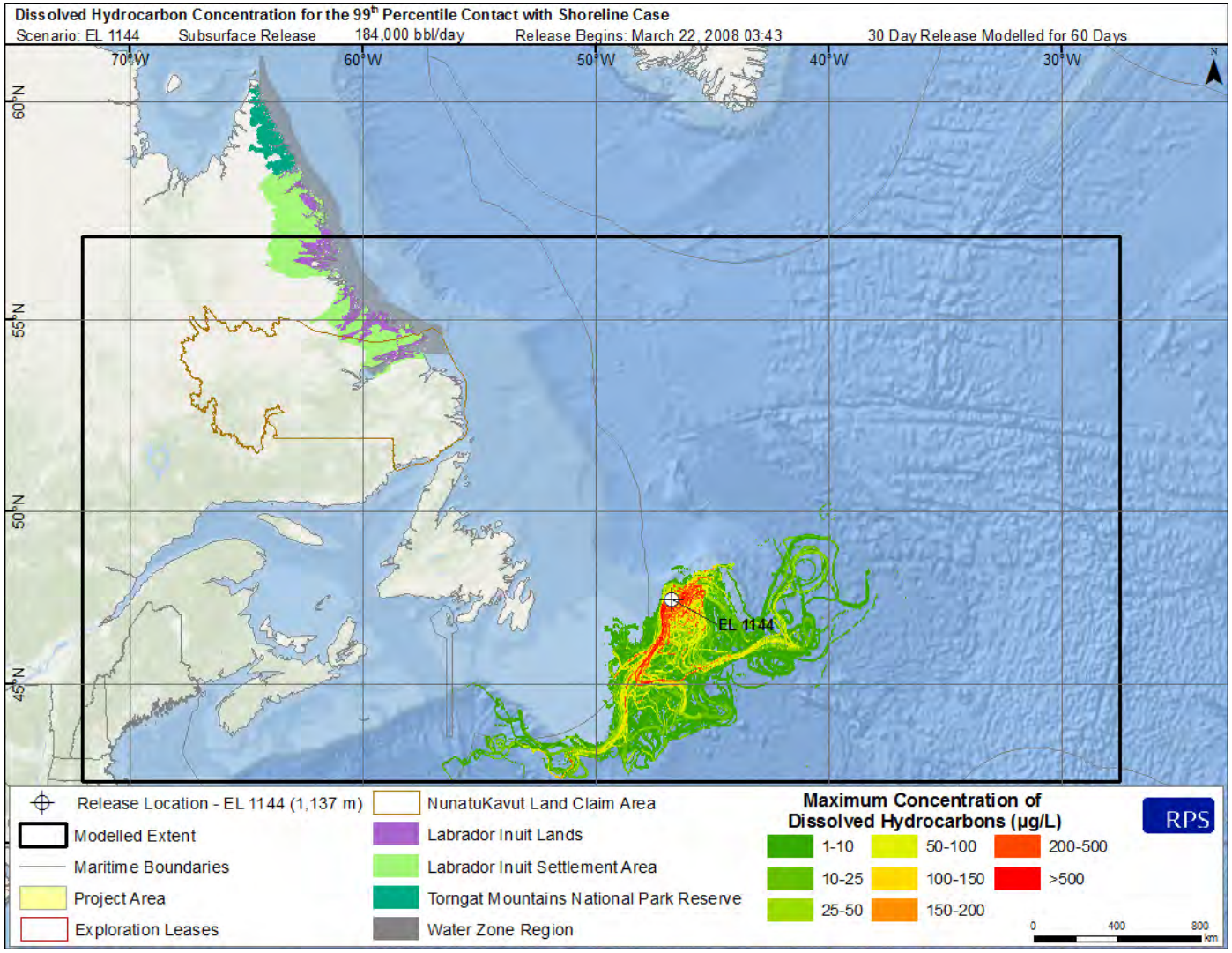

Figure 2-25. Maximum dissolved hydrocarbons at any depth in the water column for the 99th percentile contact with shoreline case at the EL 1144 example well release site.

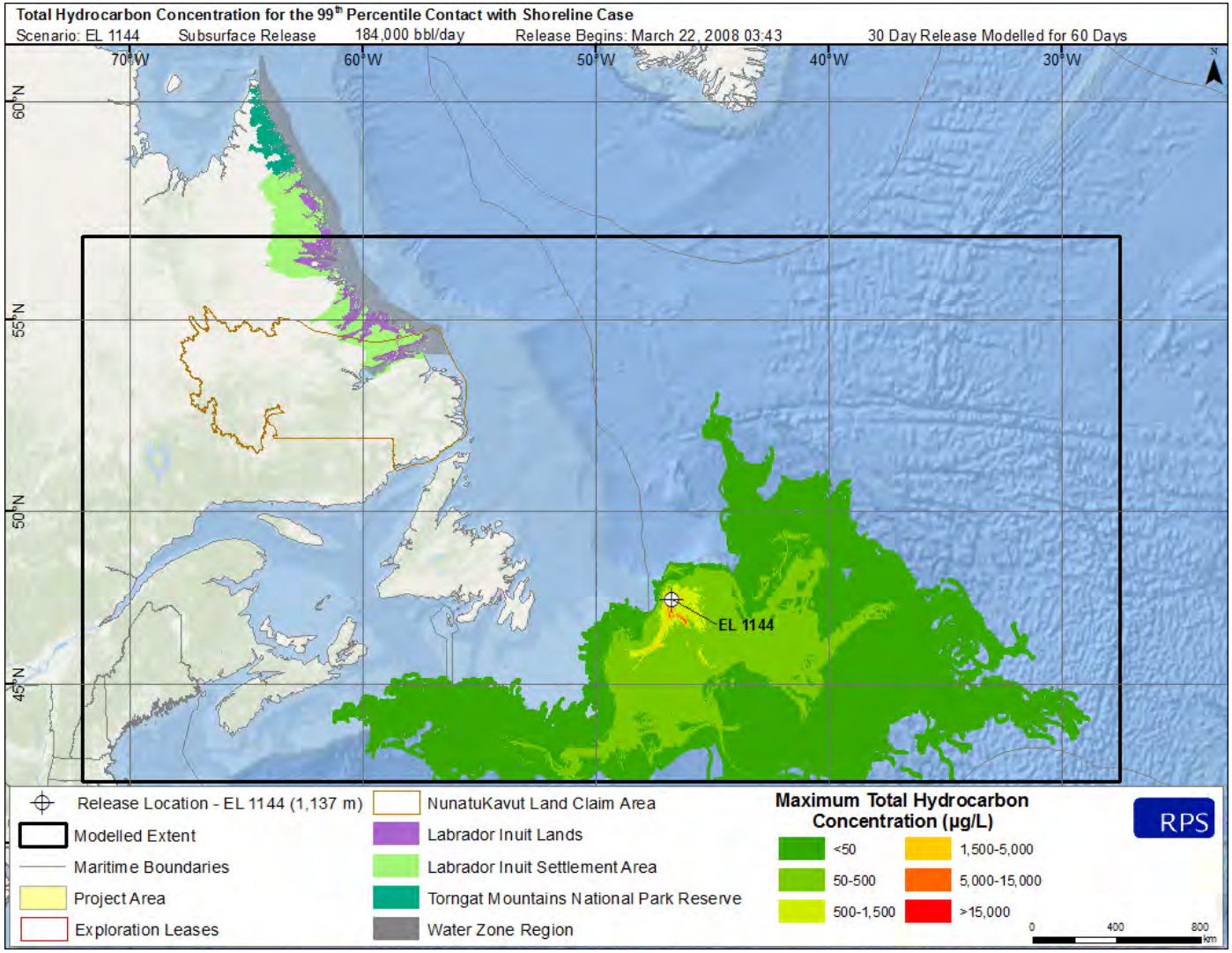

Figure 2-26. Maximum total hydrocarbon concentration (THC) at any depth in the water column for the 99th percentile contact with shoreline case from a subsurface blowout at the EL 1144 example well release site.

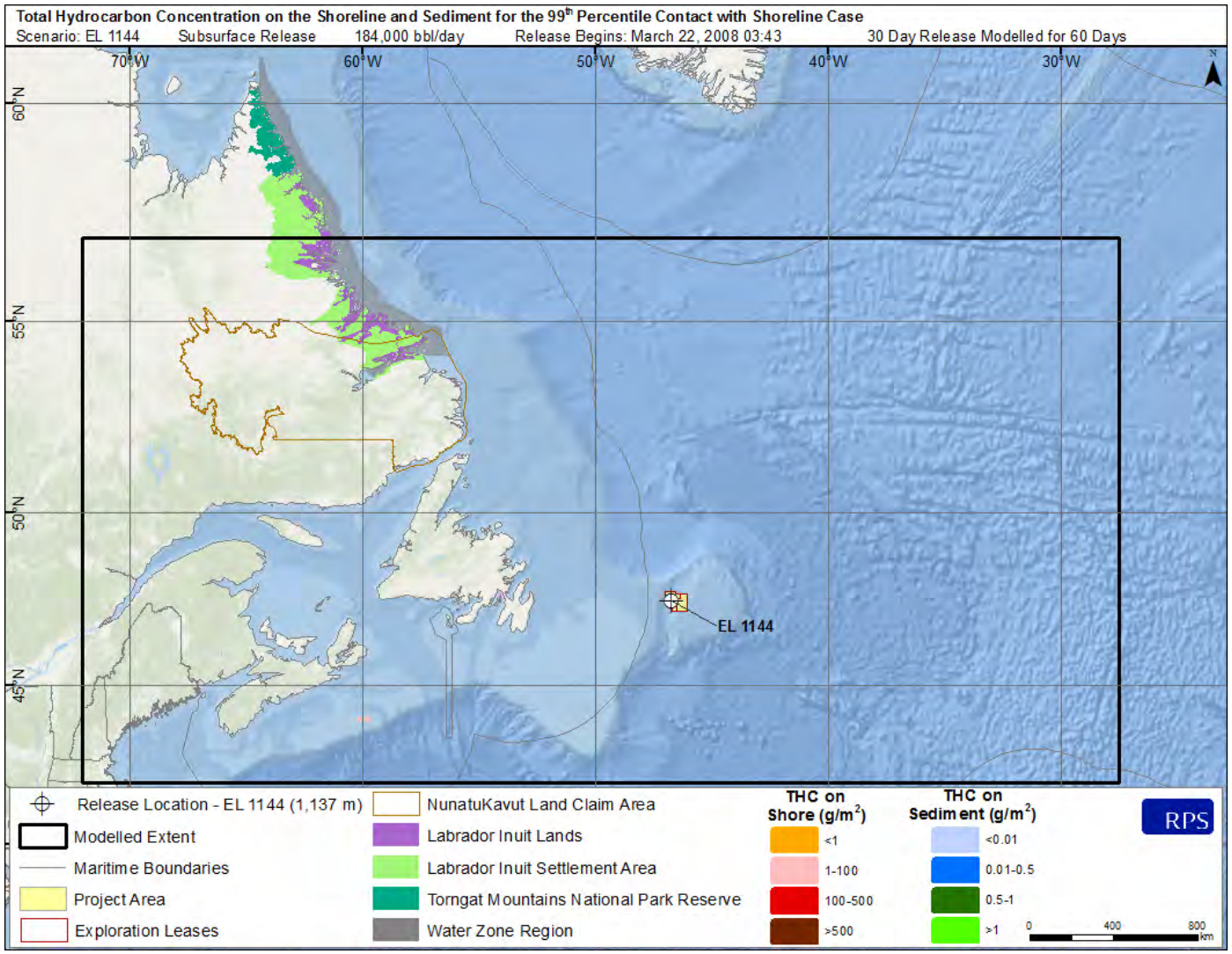

Figure 2-27. Total hydrocarbon concentration (THC) on the shore and sediment for the 99th percentile contact with shoreline case from a subsurface blowout at the EL 1144 example well release site. Only limited shoreline contact was predicted for this scenario at Sable Island.

2.4 Marine Diesel Releases

2.4.1 100 L Release

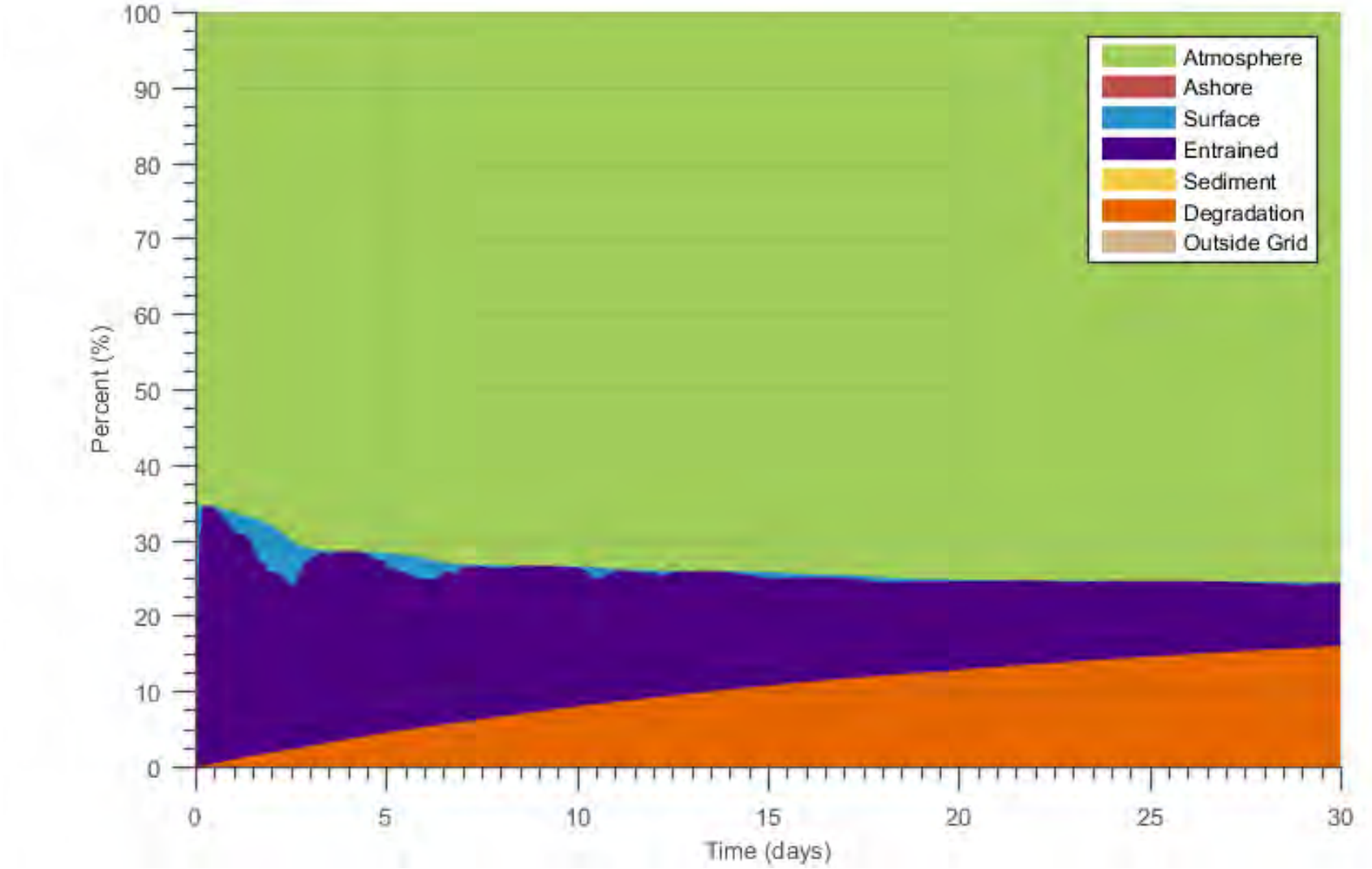

Figure 2-28. Mass balance plots of the release of 100 L of marine diesel from a batch spill at the EL 1144 example well site.

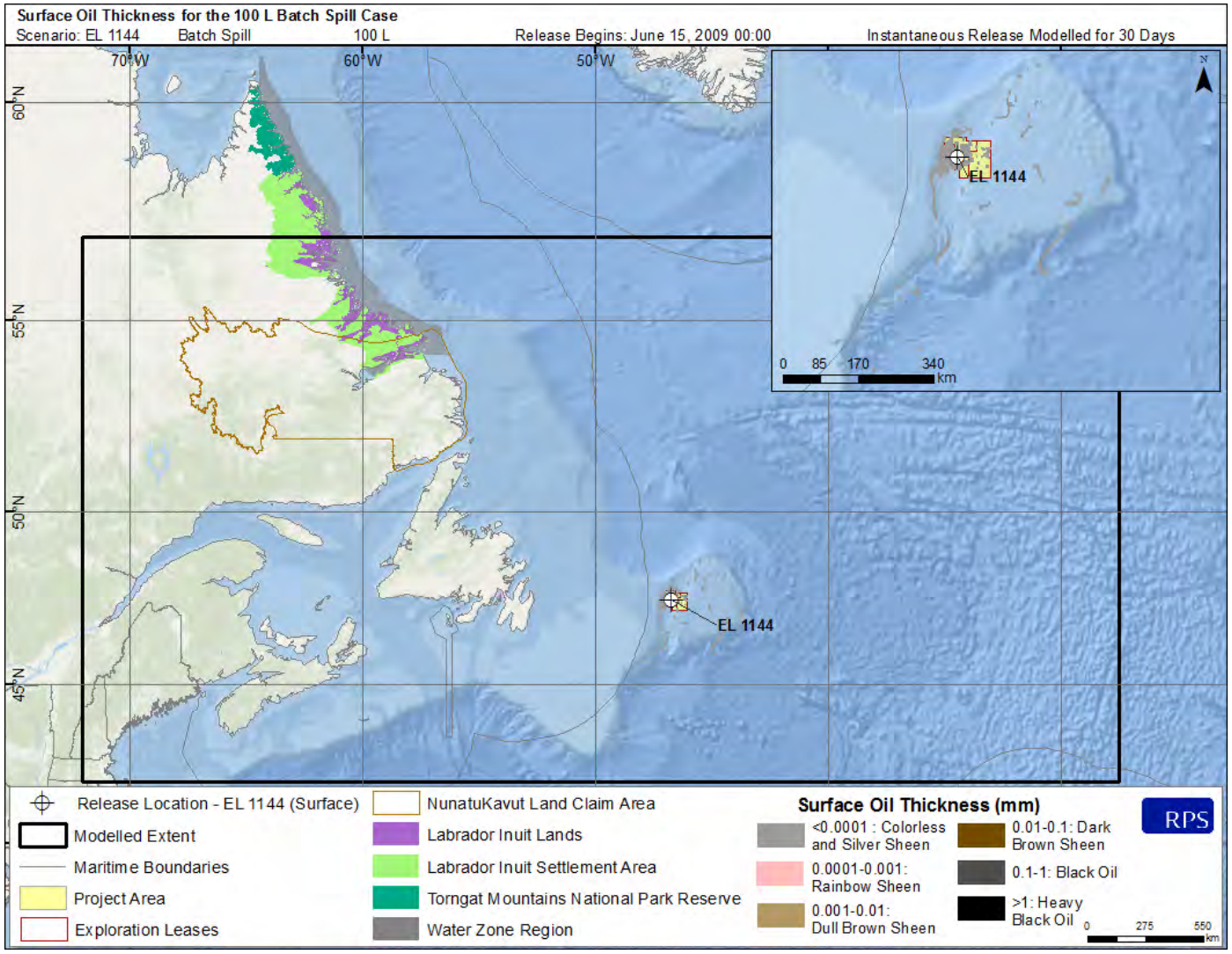

Figure 2-29. Surface oil thickness resulting from the EL 1144 example well site release of marine diesel from a batch spill of 100 L.

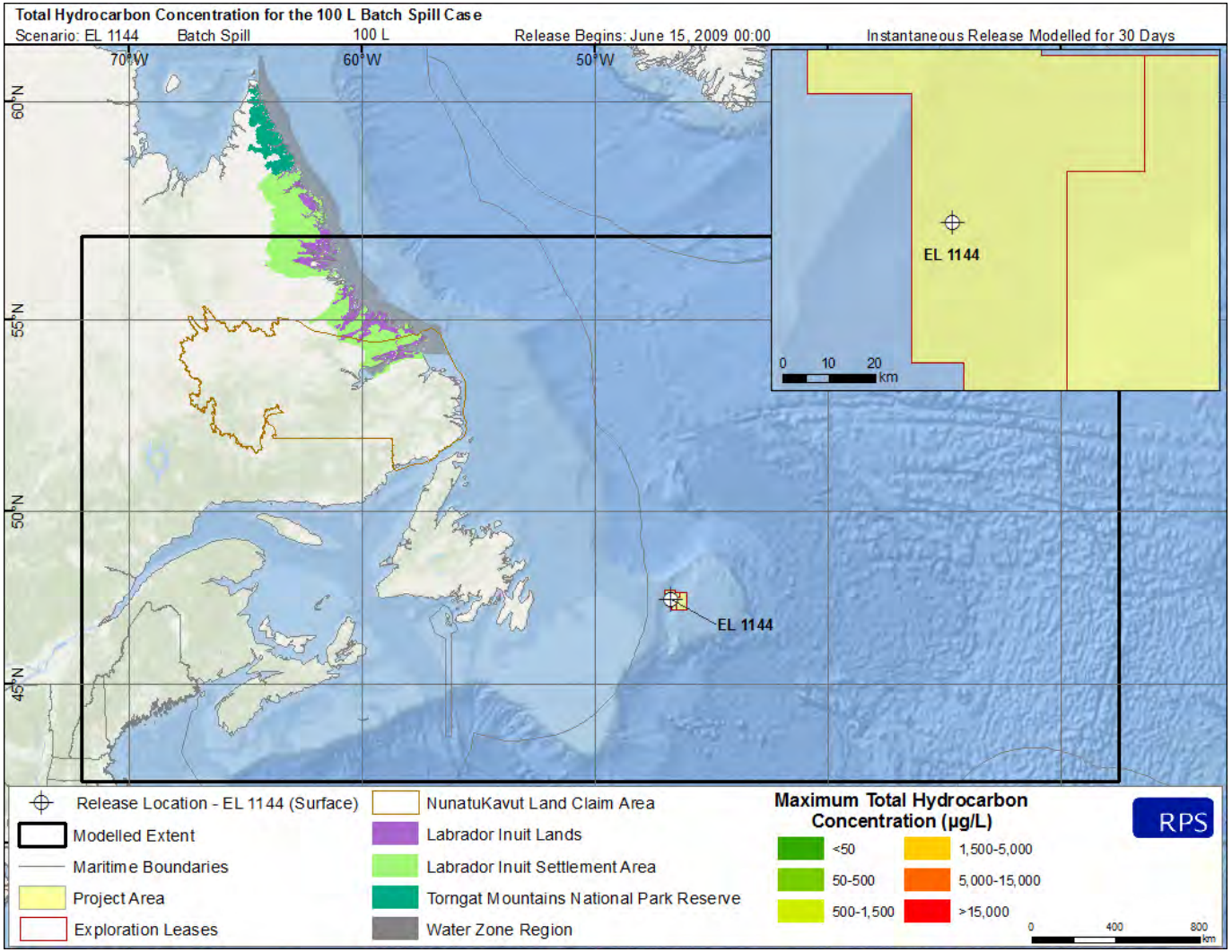

Figure 2-30. Maximum total hydrocarbon concentration (THC) at any depth in the water column resulting from the EL 1144 example well release site of marine diesel from a batch spill of 100 L. Due to the small volume of the release and the concentration gridding, concentrations of THC were not sufficient to produce results.

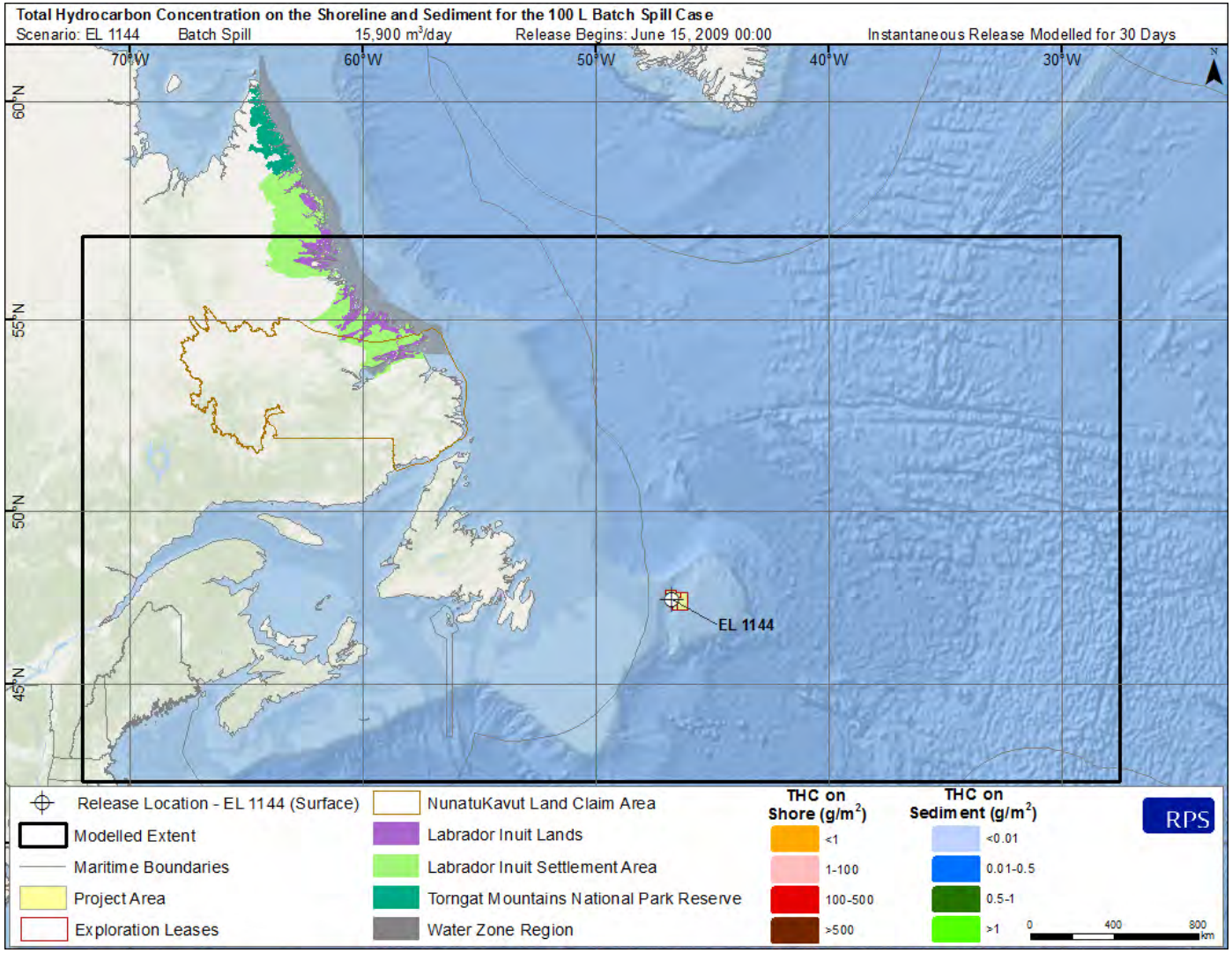

Figure 2-31. Total hydrocarbon concentration (THC) on the shore and sediment resulting from the EL 1144 example well release site of marine diesel from a batch spill of 100 L. No shore or sediment contamination was predicted.

2.4.2 1,000 L Release

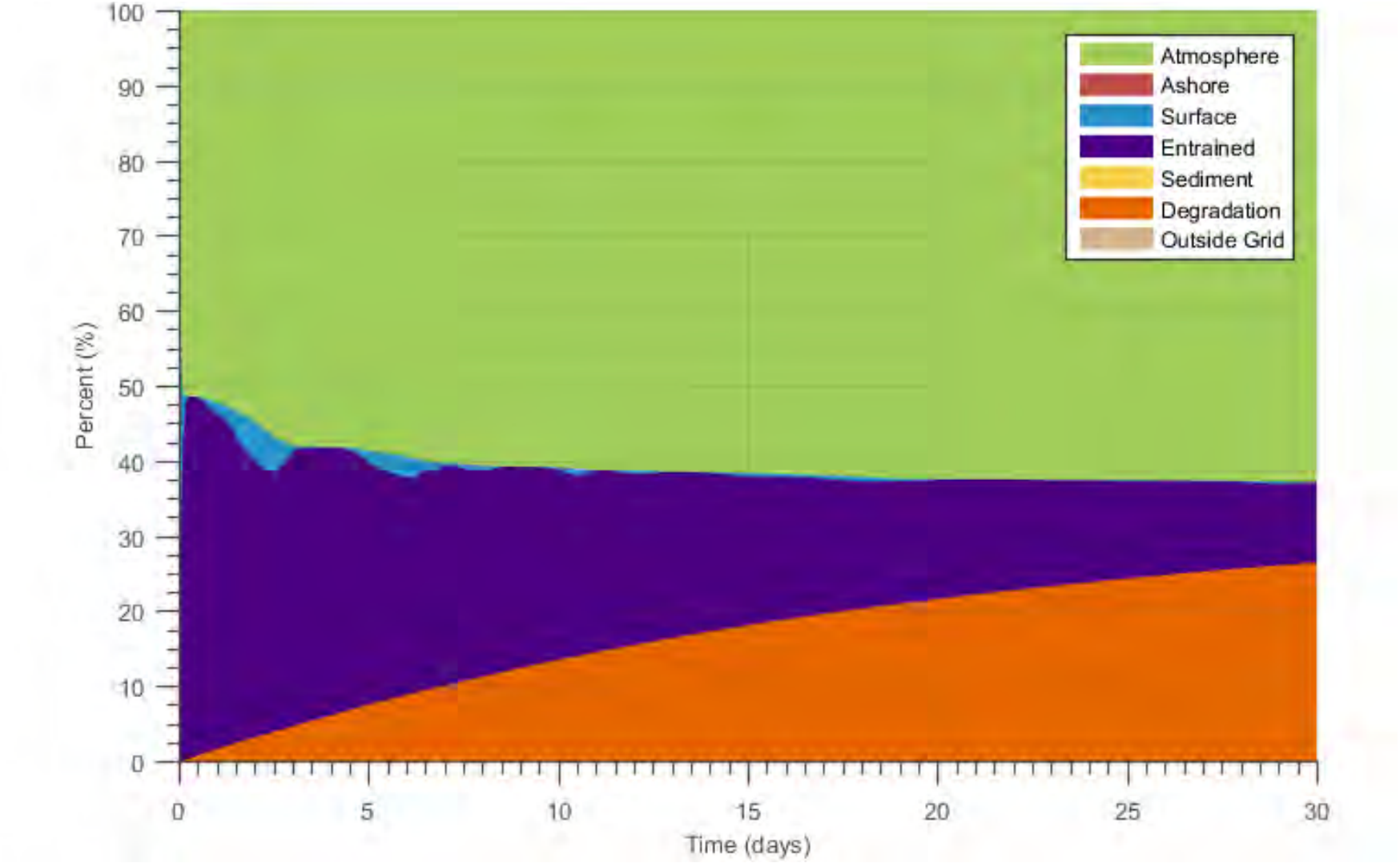

Figure 2-32. Mass balance plots of the release of 1,000 L of marine diesel from a batch spill at the EL 1144 example well site.

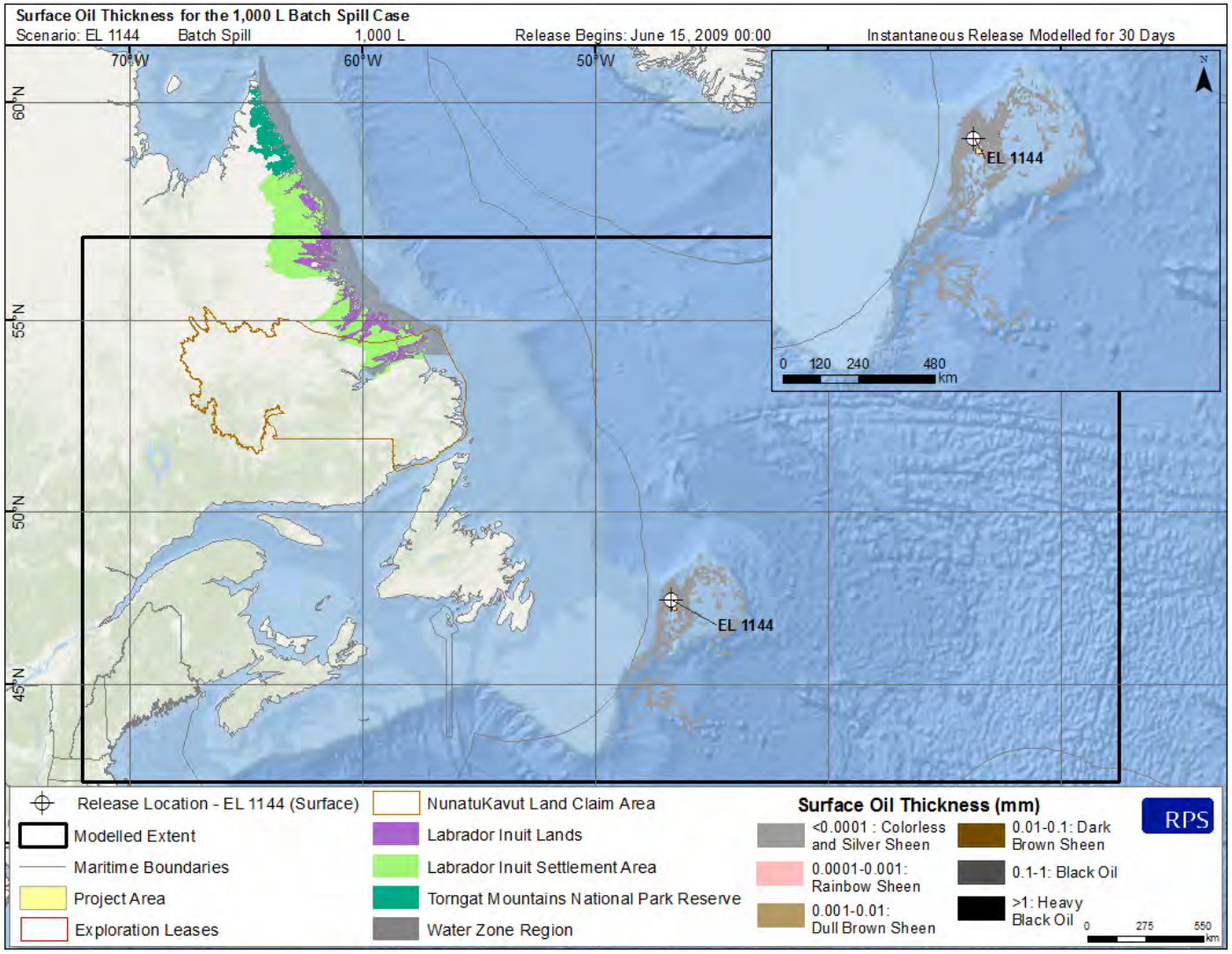

Figure 2-33. Surface oil thickness resulting from the EL 1144 example well site release of marine diesel from a batch spill of 1,000 L.

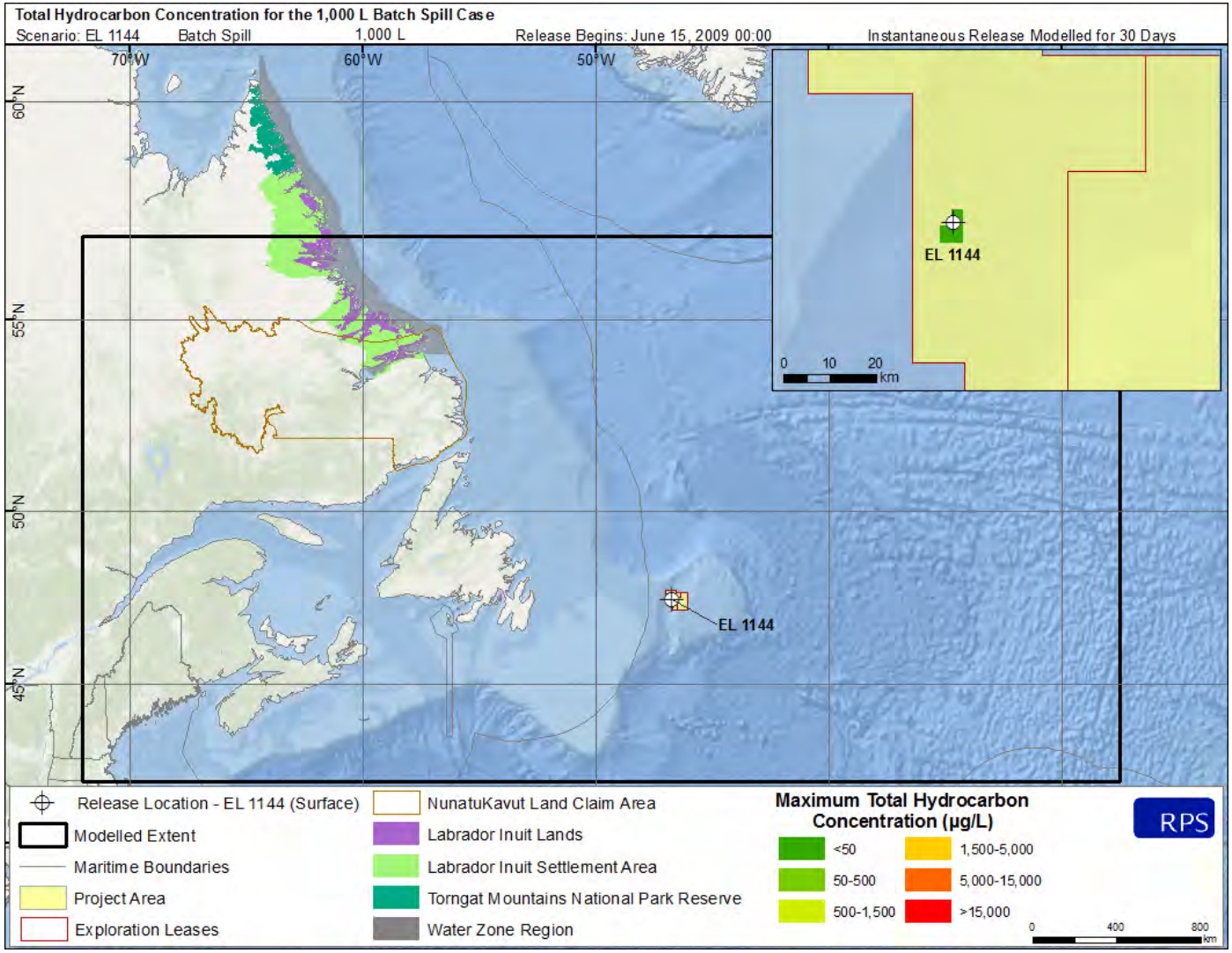

Figure 2-34. Maximum total hydrocarbon concentration (THC) at any depth in the water column resulting from EL 1144 example well site release of marine diesel from a batch spill of 1,000 L.

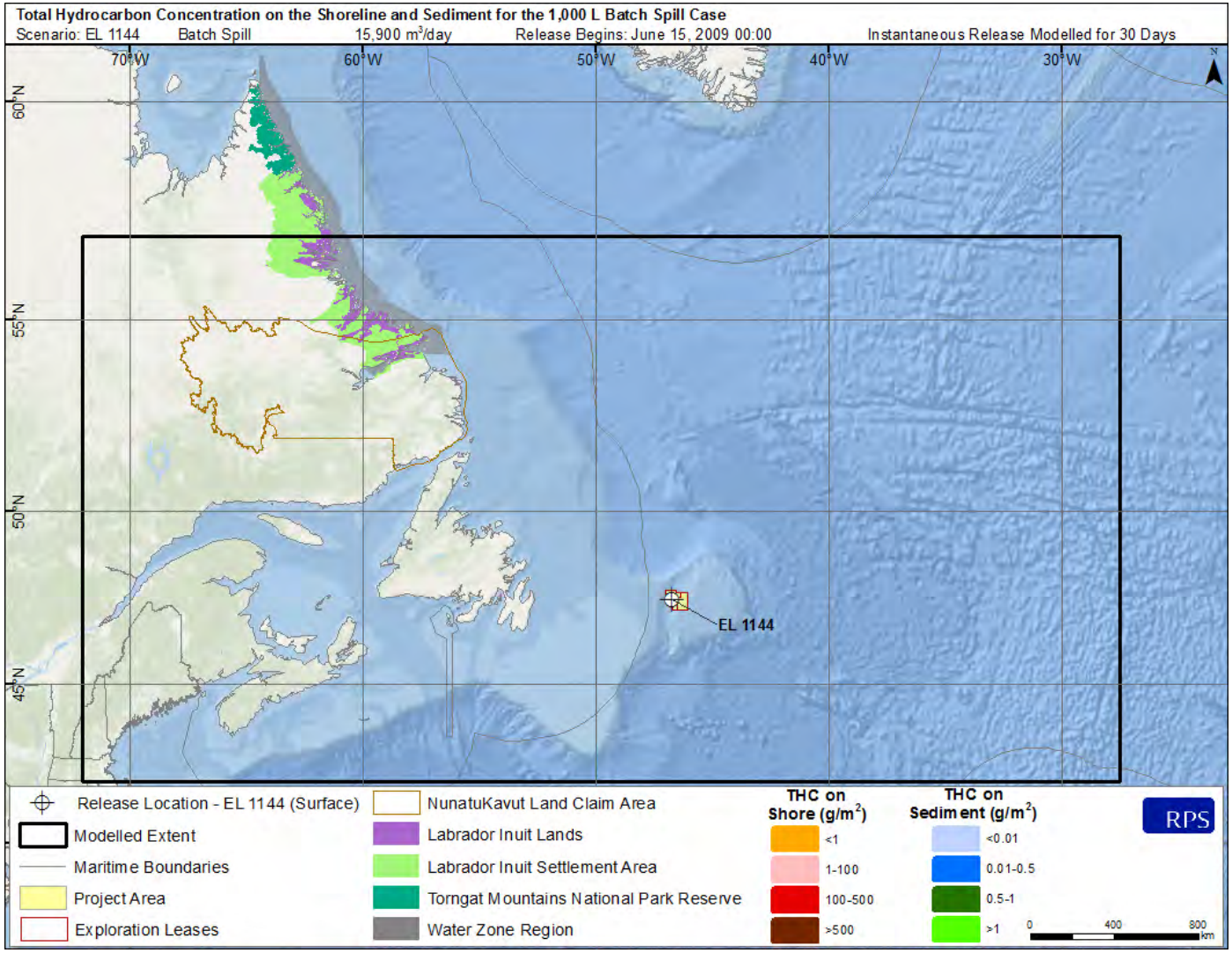

Figure 2-35. Total hydrocarbon concentration (THC) on the shore and sediment resulting from the EL 1144 example well site release of marine diesel from a batch spill of 1,000 L. No shore or sediment contamination was predicted.

2.4.3 Vessel Collision Release

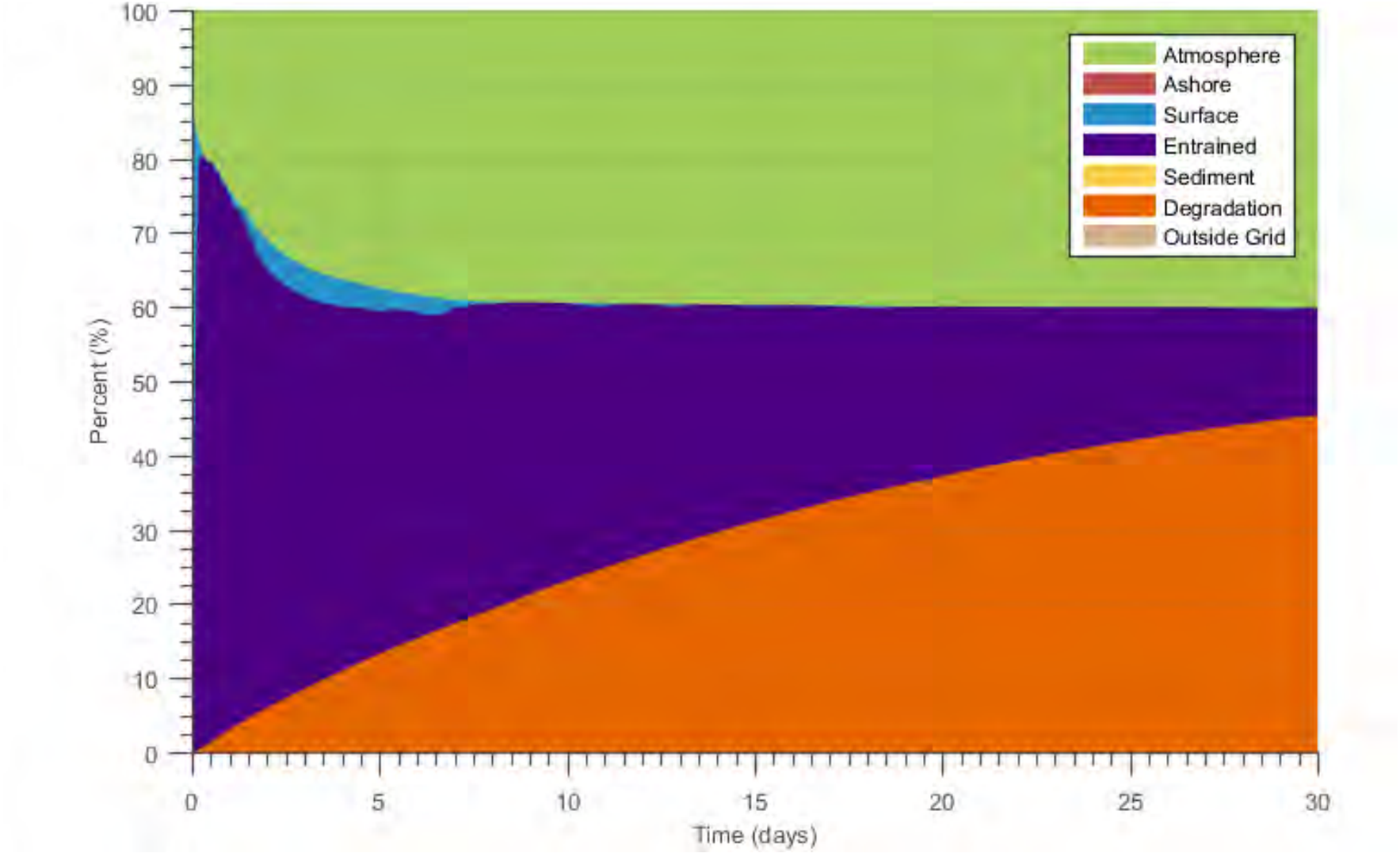

Figure 2-36. Mass balance plots of the VCL release site of marine diesel from the vessel collision release of 750,000 L.

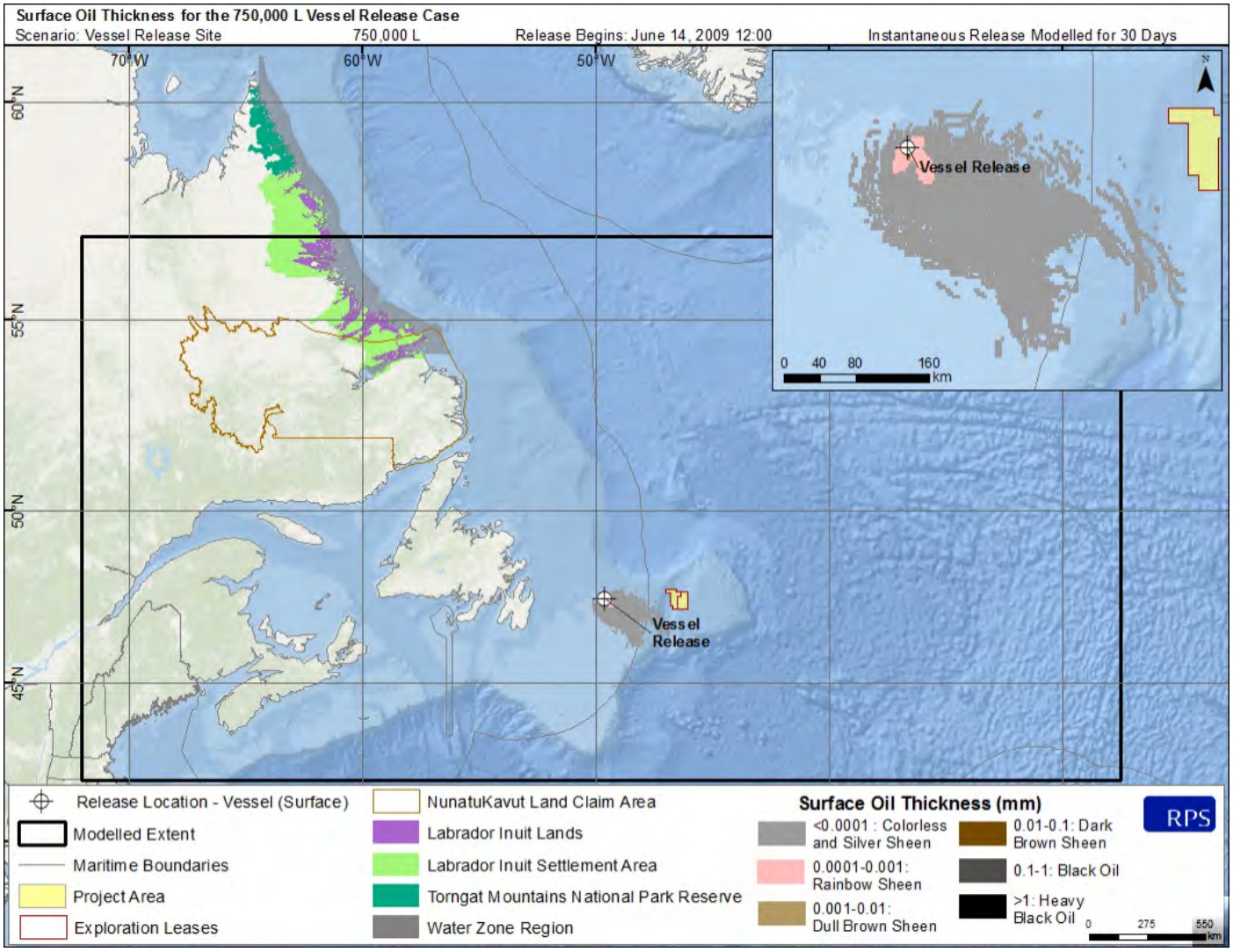

Figure 2-37. Surface oil thickness resulting from the VCL release of marine diesel from the vessel collision release of 750,000 L.

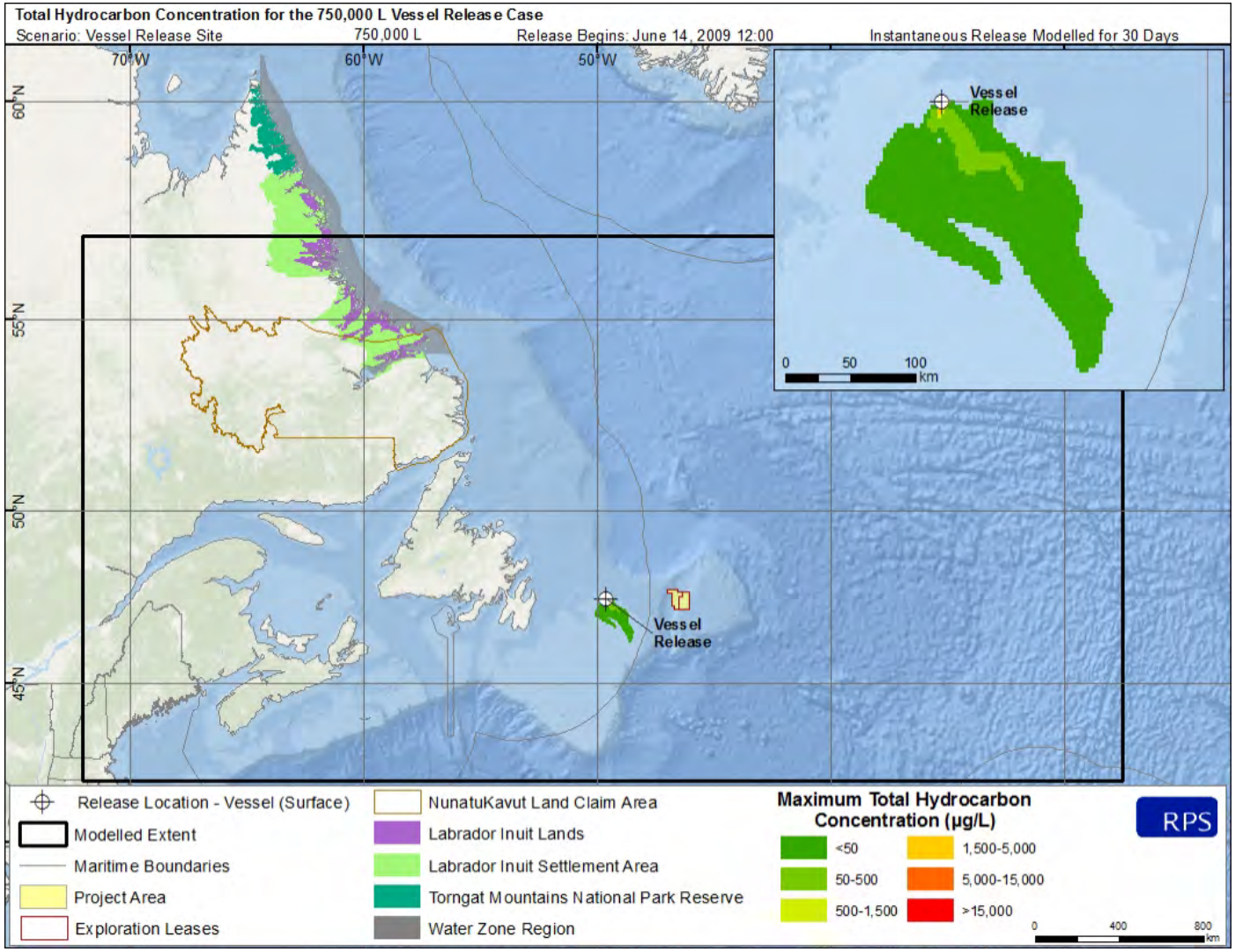

Figure 2-38. Maximum total hydrocarbon concentration (THC) at any depth in the water column resulting from the VCL release of marine diesel from the vessel collision release of 750,000 L.

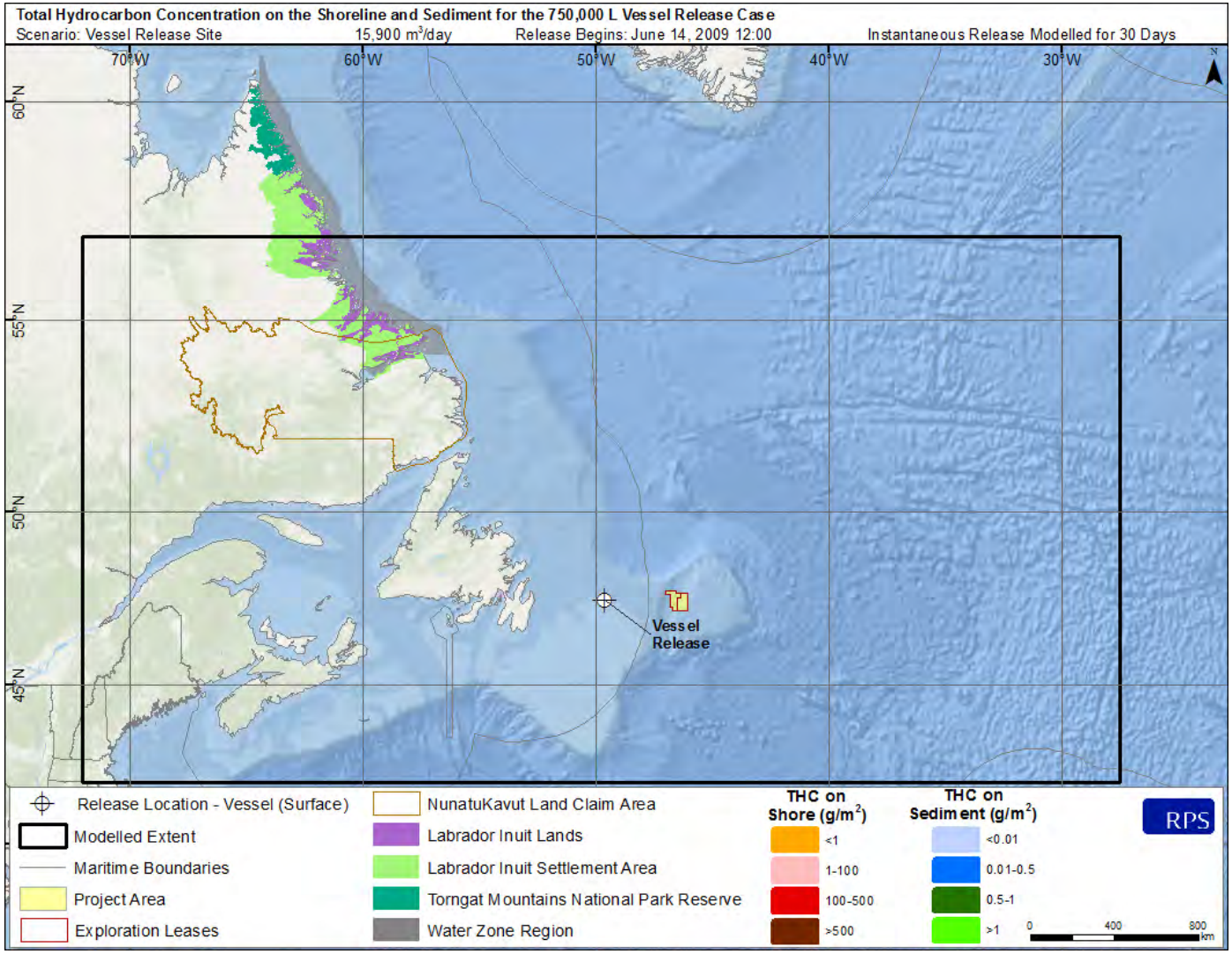

Figure 2-39: Total hydrocarbon concentration (THC) on the shore and sediment resulting from the VCL release of marine diesel from the vessel collision release of 750,000 L. No shore or sediment contamination was predicted.